Downloaded from orbit.dtu.dk on: Apr 18, 2024

DTU Library

Investigation of the molecular level interactions between mucins and food proteins: Spectroscopic, tribological and rheological studies

Celebioglu, Hilal Yilmaz

Publication date:
2017

Document Version
Publisher's PDF, also known as Version of record

Link back to DTU Orbit

Citation (APA):
Celebioglu, H. Y. (2017). *Investigation of the molecular level interactions between mucins and food proteins: Spectroscopic, tribological and rheological studies*. National Food Institute, Technical University of Denmark.

General rights
Copyright and moral rights for the publications made accessible in the public portal are retained by the authors and/or other copyright owners and it is a condition of accessing publications that users recognise and abide by the legal requirements associated with these rights.

- Users may download and print one copy of any publication from the public portal for the purpose of private study or research.
- You may not further distribute the material or use it for any profit-making activity or commercial gain
- You may freely distribute the URL identifying the publication in the public portal

If you believe that this document breaches copyright please contact us providing details, and we will remove access to the work immediately and investigate your claim.

Investigation of the molecular level interactions between mucins and food proteins: Spectroscopic, tribological and rheological studies

PhD Thesis

by

Hilal Yılmaz Çelebioğlu

Submitted: 30.04.2017

National Food Institute

Technical University of Denmark

Kemitorvet 202, 2800 Kongens Lyngby, Denmark

Preface

The work described in this PhD thesis was carried out at Nano-Bio Science Research Group, National Food Institute, Technical University of Denmark, from May 2013 to April 2017. The project was supervised by professor Ioannis S. Chronakis, associate professor Seunghwan Lee, and associate professor María Gudjónsdóttir. The scholarship for the PhD student was co-founded by the Republic of Turkey, Ministry of National Education and the project was founded by the Danish Strategic Research Council (DSF -10-93456, FENAMI Project) and the European Research Council (Funding scheme: ERC Starting Grant 2010, project 261152).

The publications resulting from this PhD study:

Paper I

Çelebioğlu, H. Y., Gudjónsdóttir, M., Meier, S., Duus, J. Ø., Lee, S., & Chronakis, I. S. (2015). Spectroscopic studies of the interactions between β-lactoglobulin and bovine submaxillary mucin. *Food Hydrocolloids*, *50*, 203-210.

Paper II

Çelebioğlu, H. Y., Gudjónsdóttir, M., Chronakis, I. S., & Lee, S. (2016). Investigation of the interaction between mucins and β-lactoglobulin under tribological stress. *Food Hydrocolloids*, *54*, 57-65.

Paper III

Çelebioğlu, H. Y., Kmiecik, J., Lee, S., & Chronakis, I. S. (2017). Interfacial shear rheology of β-lactoglobulin – bovine submaxillary mucin layers adsorbed at air/water interface. *International Journal of Biological Macromolecules,* http://dx.doi.org/10.1016/j.ijbiomac.2017.04.063

Paper IV

Çelebioğlu, H. Y., Gudjónsdóttir, M., Chronakis, I. S., & Lee, S. Spectroscopic studies of the interactions of β-Lactoglobulin (BLG) with bovine submaxillary mucin (BSM) vs. porcine gastric mucin (PGM): the role of hydrophobic and hydrophilic residues as studied by fluorescence and nuclear magnetic resonance (NMR) spectroscopies. *Submitted to Food Chemistry – February 2017.*

Paper V

Çelebioğlu, H. Y., Lee, S. & Chronakis, I. S. Interaction of salivary and gastrointestinal mucus/mucins with proteins as model food ingredient/food emulsion compounds systems: A review. For submission to *Critical Reviews in Food Science and Nutrition.*

Manuscript in preparation resulting from this PhD study

Çelebioğlu, H. Y., Subasi, B. G., Chronakis, I. S., & Lee, S. Lubrication studies of β-lactoglobulin-stabilized emulsions mixed with bovine submaxillary mucin. In preparation.

The abstracts of oral or poster presentations at conferences:

Celebioglu, H. Y., Guðjónsdóttir, M., Chronakis, I. S., Duus, J. Ø., & Lee, S. (2014). Relationship between Beta-Lactoglobulin and Bovine Submaxillary Mucin: Structure and Tribology Studies. In *the 12th International Conference on the Applications of Magnetic Resonance in Food Science: Defining Food by Magnetic Resonance*. Cesena, Italy, 20–23 May, 2014. Poster presentation.

Celebioglu, H. Y., Guðjónsdóttir, M., Chronakis, I. S., Duus, J. Ø., & Lee, S. (2014). Interaction between β-LG & BSM: A structural and tribological approach in relation to oral processing. In *the 3rd International Conference on Food Oral Processing (FOP2014): Physics, physiology and psychology of eating*. Wageningen, The Netherlands, 29 June – 2 July, 2014. Oral presentation.

Celebioglu, H. Y., Guðjónsdóttir, M., Chronakis, I. S., Duus, J. Ø., & Lee, S. (2014). Whey protein β-Lactoglobulin affects the structural and lubrication properties of salivary mucin. In *the 7th*

International Conference and Exhibition on Nutraceuticals and Functional Foods. Istanbul, Turkey, 14–17 October, 2014. Poster presentation.

Celebioglu, H. Y., Guðjónsdóttir, M., Chronakis, I. S., & Lee, S. (2016). Spectroscopic and tribological studies of the interactions between β-lactoglobulin and mucins. In *the 4th International Conference on Food Oral Processing.* Lausanne, Switzerland, 3–6 July, 2016. Poster and selected oral flash presentation.

Celebioglu, H. Y., Chronakis, I. S., & Lee, S. (2016). Investigation of protein-protein interaction under mimic oral and gastric condition using tribology and rheology approach. In *the 3rd International Conference on BioTribology.* London, UK, 11–14 September 2016. Accepted for oral presentation.

Supervisors

Ioannis S. Chronakis, PhD, Professor, Nano-BioScience Research Group, Danish National Food Institute, Technical University of Denmark

Seunghwan Lee, PhD, Associate Professor, Department of Mechanical Engineering, Technical University of Denmark.

María Gudjónsdóttir, PhD, Associate Professor, Faculty of Food Science and Nutrition, University of Iceland.

Assessment committee

Mohammad Amin Mohammadifar, PhD, Associate Professor, Research Group for Food Production Engineering, National Food Institute, Technical University of Denmark

Alan Mackie, PhD, Professor, School of Food Science & Nutrition, University of Leeds, UK

Javier Sotres, PhD, Researcher at Biomedical Sciences Department, Faculty of Health and Society, Malmö University, Sweden

Acknowledgements

I would like to thank to my main supervisor Ioannis S. Chronakis who was guiding me at each part of this project. I am grateful to him not only for precious scientific advices and all the knowledge he shared with me but also his support to have pleasant process of being a PhD student.

I would also thank to my co-supervisor Seunghwan Lee who was guiding me as much as my main supervisor. I am very grateful to him for his critical comments, advices, and technical support during PhD study and for his quick responses regarding any questions and written papers that required corrections.

Many thanks to my co-supervisor María Gudjónsdóttir for her technical support, for very important contribution especially about NMR spectroscopy studies to our papers, for translation of the English summary to Danish, and also her cheerful friendship.

I would like to thank to the whole team of *Nano-Bio Science* under the leadership of Jens Jørgen Sloth for spending nice social and scientific times. Thank you Ana, Adele, Elham, Jorge, Maria T., Mozhdeh, Michele, Maryam Sami, and Fatemeh for your friendship and crazy-crazy good-bye party. I also thank to my colleague Troels Røn in the Department of Mechanical Engineering for all instrument training and help.

I would like to thank to Jens Ø. Duus for his help to perform high field NMR experiments in the Department of Chemistry and his valuable comments and suggestion during data analysis. I am also grateful to Flemming H. Larsen and Åsmund Rinnan for their help during NMR and fluorescence spectroscopy measurements at University of Copenhagen.

I also thank to Joanna Kmiecik-Palczewska for her collaboration for interfacial rheology studies. Moreover, I thank to Anton Paar Nordic AB Malmö, Sweden (Parastoo Salavati and Jan B Petersen) for providing access to the interfacial Physica MCR 302 rheometer and for valuable discussions.

The special thanks to Busra Gultekin for her help especially in experimental process of the emulsion studies and her nonpareil friendship.

The persons deserving an honorable place in these acknowledgements are my family, my loving and patient husband Hasan Ufuk Çelebioğlu, my joy of the legislature son Baris Çelebioğlu, and my suporting and loving mother Pervin, father Ahmet, sisters Hande and Sibel, and brother Alperen who shared our ups and downs.

I wish to thank the Republic of Turkey, Ministry of National Education for the PhD scholarship.

Kongens Lyngby, April 2017

Hilal Y. Çelebioğlu

Table of Contents

Summary 1
Dansk Sammendrag 3
List of Abbreviations 5
Objective of the thesis 7
CHAPTER 1: 9
INTRODUCTION 9
Interaction of salivary and gastrointestinal mucus/mucins with proteins as model food ingredient/food emulsion compounds systems: A review 9
Introduction 11
Mucin/saliva interaction with whey proteins 14
Mucin/saliva interaction with β-lactoglobulin (BLG) 17
Mucin/saliva interaction with Casein 34
Mucin interaction with Lactoferrin 37
Mucin/saliva interaction with gelatin 41
Mucin interaction with galectin/lectin (carbohydrate binding proteins) /proline-rich-proteins . 45
Concluding remarks 50
References 51
CHAPTER 2 64
Spectroscopic studies of the interactions between β-lactoglobulin and bovine submaxillary mucin 64
Appendix: Supplementary data 73
CHAPTER 3 76
Investigation of the Interaction between Mucins and β-Lactoglobulin under Tribological Stress 76
Appendix: Supplementary data 86
CHAPTER 4 90
Interfacial Shear Rheology of β-Lactoglobulin – Bovine Submaxillary Mucin Layers Adsorbed at Air/Water Interface 90
CHAPTER 5 102

Spectroscopic studies of the interactions of β-Lactoglobulin (BLG) with bovine submaxillary mucin (BSM) vs. porcine gastric mucin (PGM): the role of hydrophobic and hydrophilic residues as studied by fluorescence and nuclear magnetic resonance (NMR) spectroscopies 102
Introduction 104
Materials and methods 106
Results and discussion 108
Conclusions 124
References 126
CHAPTER 6 131
Lubrication studies of β-lactoglobulin-stabilized emulsions mixed with bovine submaxillary 131
Introduction 131
Materials and methods 132
Results 136
Summary of the results for future discussion 142
References 143
Tables 145
Figures 146
Appendix 157

Summary

The thesis investigated the structure and molecular-level interaction of β-lactoglobulin (BLG) and mucins, representing major components of the dairy products and saliva/digestion systems, respectively. Mucins are long glycoprotein molecules responsible for the gel nature of the mucous layer covers epithelial surfaces throughout the body. A literature review of the interactions of different mucin types and saliva mucins with several food proteins and food protein emulsions, as well as their functional properties related to the food oral processing is presented at the first chapter of the thesis (Paper V). Most of the studies suggest an electrostatic attraction between positively charged food proteins with negatively charged moieties of mucins (mainly on glycosylated region of mucins).

The structural changes occurring during the interaction between BLG, the major whey protein, and bovine submaxillary mucin (BSM), a major salivary protein, were studied using high and low field Nuclear Magnetic Resonance (NMR), Dynamic Light Scattering (DLS), and Circular Dichroism (CD) spectroscopy. The zeta potentials of the proteins were also measured to provide information on the role of electrostatic forces in the interaction. These spectroscopic results suggested that the interaction between BSM and BLG led to a compact aggregation. The interaction between the two proteins was concluded to be mostly of hydrophilic origin (Paper I). The interaction characteristics between mucins and BLG under tribological stress were investigated by comparing the lubricity of mixed solutions of mucin-BLG with that of neat protein solutions at compliant hydrophobic interfaces. BSM and porcine gastric mucin (PGM) showed distinctly higher adsorbed masses compared to BLG onto polydimethylsiloxane (PDMS) or polystyrene (PS) surfaces. The adsorbed masses of the mixed protein solutions, namely BLG-BSM and BLG-PGM, reduced significantly. The dominant lubrication mechanism of the protein solutions was boundary lubrication. The pH

dependent lubricating properties of BLG-BSM mixed solutions appeared to be determined by competitive adsorption of the two proteins onto the substrates, which suggests that they do not form as strong aggregates as BLG-saliva, especially under tribological stress (Paper II). Moreover, the interfacial rheological properties of solutions of BLG mixed with BSM have been investigated. BLG-BSM protein mixtures exhibited interfacial properties with lower elastic and viscous moduli than BLG, as a result of competitive displacement of BLG proteins with BSMs from the interface. It is suggested that hydrophobic patches of BSM can be imbedded into the BLG monolayer as driven by a strong hydrophobic interaction with air and disrupt the cohesive assembly of BLG, whereas the hydrophilic (negatively charged) parts of the BSM chain are protruding from the interface towards the bulk water (Paper III). To elucidate the interaction mechanisms of BLG and two types of mucins, BSM and PGM, specifically focusing on the role of hydrophobic residues of the proteins at different pH conditions, intrinsic fluorescence spectroscopy, the fluorescent dye ANS techniques and high field NMR spectroscopy were used. Results from intrinsic fluorescence spectroscopy indicated stronger hydrophobic interactions of BLG with PGM than with BSM, which was further supported by extrinsic fluorescence spectroscopy. Stronger interactions of BLG with PGM also suggest a more abundant presence of hydrophobic moieties in PGM than BSM. Furthermore, HF-NMR studies indicated that the hydrophilic interaction also contributed to the interactions with both mucins, especially at acidic conditions (Paper IV). In the final Chapter VI, the tribological and physicochemical properties (emulsion particle size, viscosity, contact angle measurements, microscopy) of a model mucus compound, namely highly concentrated BSM, with the negatively charged BLG-stabilized emulsion (at pH 6.8) were determined as an attempt to understand the physicochemical basis of BLG-stabilized emulsion in the oral environment.

Dansk Sammendrag

Afhandlingen undersøgte strukturen og molekylær interaktion mellem β-lactoglobulin (BLG) og muciner, der repræsenterer hovedkomponenterne i henholdsvis mejeriprodukterne og spyt / fordøjelsessystemerne. Muciner er lange glycoproteinmolekyler, der er ansvarlige for gelens art af slimlaget, dækker epitelflader i hele kroppen. En litteraturoversigt over interaktionerne mellem forskellige mucintyper og spytmuciner med adskillige fødevareproteiner og fødevareproteinemulsioner samt deres funktionelle egenskaber relateret til mundtlig forarbejdning fremgår af første afhandlingens kapitel (Papir V). De fleste af undersøgelserne antyder en elektrostatisk attraktion mellem positivt ladede fødevareproteiner med negativt ladede dele af muciner (hovedsageligt på glycosylerede områder af muciner).

De strukturelle ændringer, som fandt sted under interaktionen mellem BLG, hovedvalleproteinet og bovint submaxillært mucin (BSM), et stort spytprotein, blev undersøgt ved anvendelse af højkernemagnetisk resonans (NMR), Dynamic Light Scattering (DLS) og højfelt Circular Dichroism (CD) spektroskopi. Zeta-potentialerne af proteinerne blev også målt for at tilvejebringe information om elektrostatiske kræfts rolle i interaktionen. Disse spektroskopiske resultater antyder, at interaktionen mellem BSM og BLG førte til en kompakt aggregering. Samspillet mellem de to proteiner blev konkluderet at være for det meste af hydrofil oprindelse (papir I). Interaktionsegenskaberne mellem muciner og BLG under tribologisk stress blev undersøgt ved at sammenligne smøremidlet af blandede opløsninger af mucin-BLG med det for pæne proteinopløsninger ved kompatible hydrofobiske grænseflader. BSM og porcine gastrisk mucin (PGM) viste tydeligt højere adsorberede masser sammenlignet med BLG på polydimethylsiloxan (PDMS) eller polystyren (PS) overflader. De adsorberede masser af de blandede proteinopløsninger, nemlig BLG-BSM og BLG-PGM, reduceres signifikant. Den dominerende

smøremekanisme af proteinopløsningerne var grænsesmøring. De pH-afhængige smøreegenskaber af BLG-BSM-blandede opløsninger syntes at være bestemt ved konkurrencedygtig adsorption af de to proteiner på substraterne, hvilket antyder, at de ikke danner så stærke aggregater som BLG-spyt, især under tribologisk stress (Paper II). Desuden er de gensidige rheologiske egenskaber af BLG-blandinger blandet med BSM blevet undersøgt. BLG-BSM proteinblandinger udviser grænsefladeegenskaber med lavere elastisk og viskøs moduli end BLG som et resultat af konkurrencedygtig forskydning af BLG-proteiner med BSM'er fra grænsefladen. Det foreslås, at hydrofobiske patches af BSM kan indlejres i BLG-monolaget som drevet af en stærk hydrofob interaktion med luft og forstyrre den sammenhængende samling af BLG, medens de hydrofile (negativt ladede) dele af BSM-kæden stikker ud fra grænsefladen mod Bulkvandet (papir III). For at belyse interaktionsmekanismerne af BLG og to typer muciner, BSM og PGM, der specifikt fokuserede på hydrofobiske rester af proteinerne ved forskellige pH-betingelser, blev der anvendt intern fluorescensspektroskopi, fluorescensfarve ANS teknikker og højfelt NMR spektroskopi. Resultater fra indre fluorescensspektroskopi indikerede stærkere hydrofobe interaktioner af BLG med PGM end med BSM, som blev understøttet yderligere af ekstrinsisk fluorescensspektroskopi. Sterkere interaktioner af BLG med PGM foreslår også en mere rigelig tilstedeværelse af hydrofobe dele i PGM end BSM. HF-NMR-undersøgelser viste endvidere, at den hydrofile interaktion også bidrog til interaktionen med begge muciner, især ved sure betingelser (papir IV). I det sidste kapitel VI blev de tribologiske og fysisk-kemiske egenskaber (emulsionspartikelstørrelse, viskositet, kontaktvinkelmålinger, mikroskopi) af en model slimforbindelse, nemlig stærkt koncentreret BSM, med den negativt ladede BLG-stabiliserede emulsion (ved pH 6,8) bestemt Som et forsøg på at forstå det fysisk-kemiske grundlag for BLG-stabiliseret emulsion i det orale miljø.

List of Abbreviations

ANS: 8-anilino-1-naphthalene sulfonate

BCA: bicinchoninic acid

BLG: β-lactoglobulin

BSA: bovine serum albumin

BSM: bovine submaxillary mucin

CD: circular dichroism

COF: coefficient of friction

CPA: cis-parinaric acid

CPP: casein phosphopeptide

DLS: dynamic light scattering

EHL: elastohydrodynamic lubrication

FI: fluorescence intensity

FITC: fluorescein isothiocyanate

GI: gastrointestinal

HDPE: high density polyethylene

HF-NMR: high field nuclear magnetic resonance

HMP: high methoxyl pectin

IEP: isoelectric point

LF: lactoferrin

LMP: low methoxyl pectin

MIX: mixture

MTM: mini traction machine

NMR: nuclear magnetic resonance

ONS: oral nutritional supplement

OSM: ovine submaxillary mucin

PBS: phosphate buffered saline

PDMS: poly(dimethylsiloxane)

PGM: porcine gastric mucin

PoD: pin on disk

POM: polyoxymethlylene

PRODAN: 6-propionyl-2-(N,N dimethylamino)-naphthalene

PRPs: proline rich proteins

PS: polystyrene

SGF: simulated gastric fluid

SRR: slide/roll ratio

WGA: wheat germ agglutinin

WPC: whey protein concentrate

WPI: whey protein isolate

Γ: adsorbed mass

μ: friction coefficient

G_i': interfacial elastic modulus

G_i'': interfacial viscous modulus

η_i: interfacial viscosity

$\tan\delta_i$: interfacial loss factor

D_h: hydrodynamic diameter

D_s: distance between protein molecules on surface

R_q: rout-mean-square roughness

F_{max}: maximum intrinsic fluorescence intensity

λ_{max}: maximum fluorescence emission wavelength

Objective of the thesis

Food oral processing generally involves the lubrication with saliva, water or food slurry. The lubrication of food in the mouth is determined by a variety of factors; these include the concentration and size of oil droplets, the viscosity and protein content of the saliva, the size, shape and hardness of any particle in the oral fluid and the surface property of the oral mucosa and teeth (De Wijk & Prinz, 2006). Food oral processing can be divided in three stages. The first stage, the early part of oral processing, which represents bulk properties such as hardness, brittleness, springiness, etc. The last stage is related to surface and lubrication behavior, such as smoothness, slipperiness, creaminess, etc. There is also a transition stage between them, which is dependent on both bulk rheology and surface tribology factors, such as food thickness, consistency and creaminess. It is believed that the fundamental cause of changing sensory intensity and sensory profile is due to the rheology-tribology transition (Chen & Stokes, 2012). Tribology is about the friction, wear and lubrication of interacting surfaces which are in relative motion and focuses on a mixed layer of food and saliva between tongue and palate sheared and squeezed during eating. Sensed resistance against a moving surface forms an important part of sensory experience. The main parameter for a tribological test is the friction coefficient, calculated as the ratio of the measured friction force against the normal load (Chen & Stokes, 2012). Due to growing interests in the relationship of biomechanical functions and sensory appreciation of foods, tribological approaches, which are conventionally concerned with the friction and lubrication of engineering machinery, started to be employed in food science research. Recently studies based on the combination of rheology and tribology has offered unprecedented findings on the relationship between biomechanical properties and sensory attributes in oral processing of foods. Among many parameters involved in this process, we take a particular note on the role of mucinous proteins,

present in saliva and digestive fluids in gastrointestinal organs, since they are a key component to impart lubricity of these biological fluids.

Aim of the study: To characterize the interaction of salivary and gastrointestinal mucins with model emulsion compounds and food protein ingredient systems and to observe the influence of these interactions on rheological and tribological properties.

Model food systems were employed to simplify sample foods and to readily control the compositional and structural parameters.

CHAPTER 1:

INTRODUCTION

Interaction of salivary and gastrointestinal mucus/mucins with proteins as model food ingredient/food emulsion compounds systems: A review

(Paper V)

Hilal Y. Çelebioğlu,[1] Seunghwan Lee[2], and Ioannis S. Chronakis,[1]*

[1]Nano-BioScience Research Group, DTU-Food, Technical University of Denmark, 2800 Kgs. Lyngby, Denmark.

[2]Department of Mechanical Engineering, Technical University of Denmark, DK-2800 Kgs. Lyngby, Denmark

***Corresponding author**: Ioannis S. Chronakis, e-mail: ioach@food.dtu.dk

Keywords: mucin, β-lactoglobulin, whey, casein, gelatin, lactoferrin, emulsion

For submission to Critical Reviews in Food Science and Nutrition

Abstract

Mucins are long glycoprotein molecules responsible for the gel nature of the mucous layer covers epithelial surfaces throughout the body. Mucin, as the major salivary protein, is an important protein also for the food oral processing and digestion. In the present study, the interactions of different mucin types and saliva mucins with several food proteins and food protein emulsions, as well as their functional properties related to the food oral processing are reviewed. Most of the studies suggest an electrostatic attraction between positively charged food proteins with negatively charged moieties of mucins (mainly on glycosylated region of mucins). Moreover, our recent studies related to the BLG-mucin interactions have clarified the respective contribution of hydrophobic as well as the hydrophilic interactions. The role of such protein-protein interactions in the perception of physicochemical and structural changes of proteins was discussed for the systems mimicking the physiologically active regime.

Introduction

A mucous layer covers epithelial surfaces throughout the body including the gastrointestinal tract and provides protection and lubrication of underlying epithelium.

The main non-water components of the mucous layer are mucins, long glycoprotein molecules that are responsible for the gel nature of the mucous layer (Efremova et al. 2002). Mucin is a glycoprotein consisting of a linear polypeptide core with a highly glycosylated central part accounting for up to 80% of the proteins molecular weight which ranges between 0.5 and 20 MDa (Shi, Ardehali, Caldwell, & Valint, 2000; Bansil & Turner, 2006). Due to the abundance of negatively charged groups, arising mainly from sialic acid residues and sulphated sugars, mucins generally have low isoelectric points, estimated to be between 2 and 3. The presence of many charged groups also results in pH-dependent physicochemical properties of the mucin molecules. Mucin molecules are amphiphilic due to alternating arrays of negatively charged, hydrophilic glycosylated regions (enriched with serine, threonine, and proline residues) and hydrophobic unglycosylated patches (enriched with cysteine residues) (Fig. 1). Monomeric mucin molecules can be linked with each other, such as via disulfide bonds by cysteine residues to form larger aggregates (Durrer, Irache, Duchene, & Ponchel, 1995; Lee, Müller, Rezwan, & Spencer, 2005). Mucin's cysteine residues are capable of forming intermolecular disulfide bonds with other proteins as well (Mehrotra, Thornton, & Sheehan, 1998; Zalewska et al. 2000). Additionally, mucins can also form aggregates with other proteins via non-covalent interactions by involving unglycosylated regions or oligosaccharide side chains.

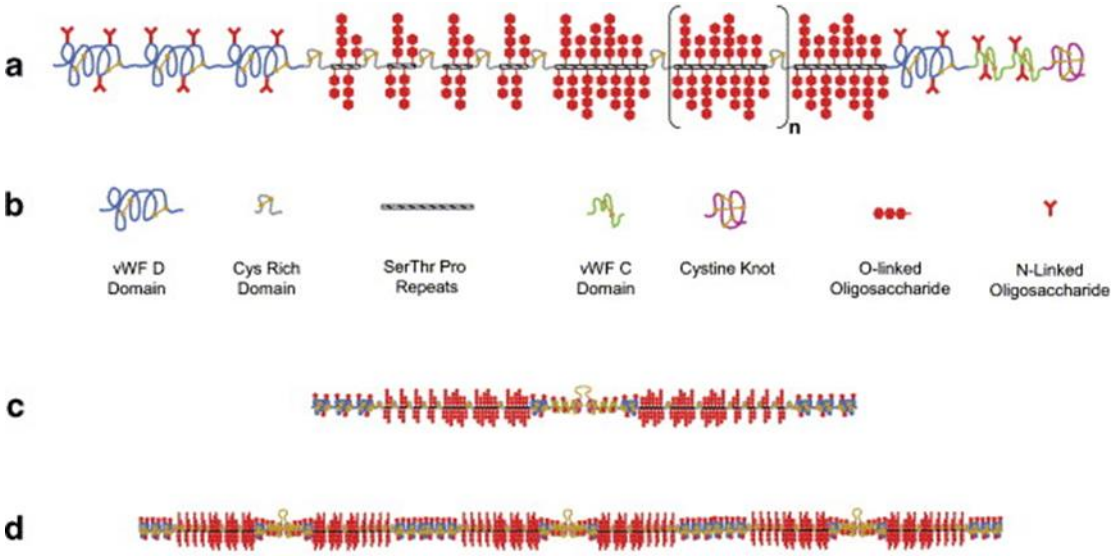

Fig.1. (a) A schematic drawing of the pig gastric mucin (PGM) monomer consisting of glycosylated regions flanked by regions with relatively little glycosylation. (b) The symbols indicate the different domains in the sketch in (a). (This representation is based in part on Figs. 1 and 2 of Dekker et al. (2002)). At the bottom of the figure showing (c) a dimer formed by two monomeric subunits linked via disulfide bonds in the non-glycosylated regions and in (d) dimers that are further disulfide linked to form higher multimers. This gives rise to the high molecular weight and polydispersity of secretory mucins. (Bansil and Turner, 2006).

Furthermore, a first target for oral drug delivery is the mucus layer since it is covering the main target cells. Mucoadhesive drug delivery vehicles and methods to determine mucoadhesive properties have received considerable attention in the last two decades (Lai, Wang & Hanes, 2009; Di Silvio et al. 2015). Mucoadhesive delivery vehicles are designed to exploit the attraction between the mucous layer and the polymer carrier of the drug delivery system. The main advantages of mucoadhesive polymer carriers include the localization of the carriers to a specific site within the body and the prolonged time of delivery. These features greatly enhance the bioavailability of drugs, especially for peptide and protein delivery (Peppas and Robinson 1995:

Lehr, 1994). Moreover, apart from mucin's functions in biological systems, other studies have shown facile adsorption and effective lubrication on various engineering materials (Lee et al. 2005; Nikogeorgos et al 2014; Yakubov et al. 2009).

Mucin, as the major salivary protein, is also an important protein related to the food oral processing and digestion. Through the various stages of oral processing, foods continuously mix with saliva, mucins interact with food components and the humans perceive various sensory and textural attributes. Food oral processing is a complex mechanical process of chewing, mastication, transportation and swallowing by involving various soft and hard tissues such as palate, teeth and tongue in mouth. Therefore, it should be investigated step by step starting with basic components which contribute to the oral processing. In particular, food oral processing can be divided in three stages. The early part of oral processing, representing bulk properties such as hardness, brittleness, springiness, etc., depends on the rheological properties of the compounds. The last stage, relating to surface and lubrication behavior such as smoothness, slipperiness, creaminess, etc, depends on tribological properties of the compounds. There is also a transition stage between them, which is dependent on both bulk rheology and surface tribology factors, such as food thickness, consistency and creaminess. It is believed that the fundamental cause of changing sensory intensity and sensory profile is due to the rheology-tribology transition (Chen & Stokes, 2012). Tribology measurements have been developed to measure friction by mimicking the rubbing contact in oral cavity lubricated by mucin/saliva and/or food protein solution/emulsion. Sotres and Arnebrant (2013) defined the friction as the resistance offered to the sliding of one surface over another and express itself as a (friction) force opposing the sliding. Different factors such as adhesion, interlocking of asperities and surface deformation can cause this resistance (Sotres and Arnebrant, 2013). To analyze the interaction between food and salivary components, environmental conditions, mainly temperature and pH, are also important to consider.

Despite the number of studies addressing the interactions of mucins with polysaccharides (Menchicchi et al., 2014, 2015; Qaqish & Amiji, 1999), studies related to the interaction of mucins with food proteins are much more limited (Senapati, Das, & Batra, 2010). Hence, in the present review, the interactions of different mucin types and mucin/saliva with several food proteins and food protein emulsions, as well as their functional properties related to the food oral processing are reviewed.

Mucin/saliva interaction with whey proteins

Whey proteins include β-lactoglobulin (BLG), bovine serum albumin, α-lactalbumin and immunoglobulins. BLG represents about 50% of the total whey protein in bovine milk. In contrast to caseins, the whey proteins possess high levels of secondary, tertiary and, in most cases, quaternary structures (Edwards, Creamer, & Jameson, 2009; Kinsella & Whitehead, 1989). The important functional properties of protein products include water binding, emulsification, foaming and whipping, gelation and nutritional properties (Singh, 2011). Emulsion-type products, e.g. coffee whiteners, whipped toppings, cream liqueurs, dietary formulations, liquid nutritional products and medical foods, are an important application of caseinates and whey proteins in the food industry.

Beecher et al (2008) using trained panelists and viscosity measurements, showed that electrostatic interaction between positively charged whey proteins and negatively charged saliva proteins caused astringency. Similarly, Jobstl et al. (2004) proposed that the perception of astringency describes the complexation and precipitation of the astringent compounds with salivary proline-rich proteins, which increase friction in the mouth.

Sano et al. (2005) also showed that whey protein isolate was more astringent at pH 3.5 than gelatin based on trained panelists and taste sensors. They attributed this difference to that the whey proteins

are more positively charged at pH 3.5 than gelatin. Moreover, they suggested that astringency was due to that the whey proteins (pH 3.5) mixed with saliva (pH 7.0) form a slightly acidic solution (pH 5.0) in which whey proteins precipitate. They have explained the formation of aggregates, as indicated by an increased turbidity of whey protein-saliva mixtures, based on two possible mechanisms. First, as proposed by Sano et al. (2005), mixing of whey proteins at acidic pH with saliva at neutral pH could result in a beverage-saliva solution at a pH close to the pI of whey proteins, favoring aggregation as observed by an increase in turbidity. In this case, the whey protein aggregates are the main source of the astringency. Alternatively, it could be due to the interactions between the positively charged whey proteins and negatively charged saliva proteins. If salivary proteins have isoelectric points below the isoelectric points of whey proteins, there will be a pH range that results in a net electrostatic attraction causing aggregation. Guo et al. (2006) sequenced 5,338 distinct peptides, representing 1,381 distinct proteins, from human saliva. Approximately 3,400 of the 5,338 peptides where identified as having mean isoelectric points below 5.0. These proteins are likely to be involved in interactions with whey proteins in acidic beverages due to electrostatic attraction. At pH 6.8, the salivary and whey proteins are highly negative and less likely to aggregate. In contrast, at pH 3.4, the net attraction between salivary and whey proteins appears to be the strongest, resulting in the highest level of astringency.

Mucin/saliva interaction with whey protein stabilized emulsion

An understanding of the oral processing of an emulsion is critical for a successful manipulation of the physical and sensorial attributes of colloidal food systems, such as emulsion stability, creaminess and rate of flavor release. Food emulsions are exposed to a range of processing steps during consumption such as mixing with saliva, heating or cooling to the body temperature. In

addition, air is introduced, and the emulsions come into contact with oral surfaces and are exposed to complicated saliva flow profiles. It is anticipated that saliva-emulsion interactions play an important role in understanding emulsion perception, however, little is known about the oral behavior of food emulsions (Aken, Vingerhoeds, & de Hoog, 2007). Previous studies in literature dealing with the interaction between emulsions and saliva was focused on, firstly, sensory analysis of emulsions in relation to the saliva flow (Engelen, de Wijk, Prinz, & Bosman, 2003) and composition (Engelen et al., submitted for publication), secondly with the physicochemical properties of emulsions *in vitro* (Barylko-Pikielna, Martin, & Mela, 1994; Kilcast & Clegg, 2002; Metcalf & Vickers, 2002; de Wijk, van Gemert, Terpstra, & Wilkinson, 2003) and then the flavor release from emulsions (de Roos, 2003) as measured in mouth models (Doyen, Carey, Linforth, Marin, & Taylor, 2001; van Ruth, King, & Giannouli, 2002; van Ruth & Roozen, 2000a,b) and *in vivo via* e.g. electronic noses (Miettinen et al., 2002).

van Aken et al. (2003) reported a strong aggregating effect of saliva on both protein (milk protein – including both caseinate and whey protein) - and surfactant-stabilized emulsions. In addition, explorative experiments were carried out to gain insight in the oral behavior of commercial emulsions (van Aken et al., 2007). They have further investigated the observed aggregation phenomena to elucidate the physicochemical effects of saliva on protein-stabilized food emulsions, with emphasis on the role of high molecular weight mucins. They observed that mixing emulsions with saliva or mucin can induce droplet aggregation and suggested that the observed behavior affects the texture and rheological properties of emulsions and thus the sensory perception of emulsions. For instance, saliva-induced droplet flocculation leads to an increase in low-shear viscosity which is related with product viscosity with mouthfeel (van Aken et al. 2007).

The high molecular weight salivary component mucin was also modeled by porcine gastric mucin (PGM), which consists of both MUC5AC and MUC6 (Nordman et al., 2002). MUC5AC has

particularly large similarities to the high molecular weight human salivary mucins (MUC5B) (van Klinken, Einerhand, Buller, & Dekker, 1998; Offner, Nunes, Keates, Afdhal, & Troxler, 1998). In the study of Vingerhoeds et al. (2005), the rheological behavior of WPI emulsions upon addition of PGM was determined. Aggregation of the emulsions was clearly observed and the results suggested that mucin as the main component in saliva is responsible for the observed aggregation, but also indicated that other salivary components could play a role. They have observed a reversible aggregation upon dilution with water, indicating that the bonds between the emulsion droplets were relatively weak and coalescence was negligible. Hence, they concluded that the aggregation might not be due to covalent bonds or to a precipitation mechanism such as an antigenic reaction. The particle size of the emulsions was not altered by the addition of PGM, meaning that droplet flocculation can arise from a depletion or a bridging mechanism (Blijdenstein, Hendriks et al., 2003; Blijdenstein, van Vliet et al., 2003; Dickinson & Pawlowsky, 1997). The mechanism of droplet flocculation was determined by the nature of the interaction between the surfactant and the polymer, in the absence of which emulsion droplets can lead to depletion flocculation, whereas attractive interactions between polymer and emulsion droplets can impose bridging flocculation (Healy & Lamer, 1964). To elucidate the mechanism behind the observed mucin-induced aggregation, Vingerhoeds et al. (2005) performed demixing experiments as a function of the concentration of PGM. Removal of excess BLG by washing the emulsion before mixing with PGM had no effect on the occurrence of flocculation as observed by light microscopy. This indicates that the dissolved protein emulsifier is not involved in the flocculation. Overall, those observations are indicative for depletion flocculation as the leading mechanism in the case of mucin/saliva interaction with protein-stabilized emulsion.

Mucin/saliva interaction with β-lactoglobulin (BLG)

β-lactoglobulin (BLG) is one of the most important and extensively studied proteins of dairy food systems. BLG is the major whey protein constituting of >50% of the total whey proteins in bovine milk. BLG is a typical globular protein with molecular weight of 18.3 kDa and a radius of approximately 2 nm (Zúniga, Tolkach, Kulozik, & Aguilera, 2010). According to its amino acid sequence and three-dimensional structure, BLG belongs to the lipocalin family, which can bind to small hydrophobic ligands and may thus act as specific transporters (Kontopidis, Holt, & Sawyer, 2004). It is a predominantly β-sheet protein. The β-barrel, or so-called calyx, is conical and is made of two β-sheets: the B–D strands and N-terminal half of the A strand (denoted AN) form one sheet, and the E–H strands and C-terminal half of the A strand (denoted AC) form the other (Fig. 2). On the outer surface of the β-barrel, between the G and H strands, is the 3-turn α-helix. The loops that connect the β-strands at the closed end of the calyx, BC, DE, and FG, are generally quite short, whereas those at the open end, AB, CD, EF, and GH, are significantly longer and more flexible (Brownlow et al. 1997). In the calyx, there is a large central cavity which is surrounded by hydrophobic residues and is accessible to solvent. This cavity provides the principal ligand-binding site. BLG contains two tryptophan residues, Trp 19 on the A strand and Trp 61 on the C strand. The former is buried in the hydrophobic core whereas the latter is exposed to the solvent in the native structure, making them useful probes for monitoring site-specific conformational changes. BLG contains many charged groups and its structure and properties therefore depend strongly on the pH and ionic strength (Fang & Dalgleish, 1997). Taulier and Chalikian (2001) mentioned six pH-dependent structural states of BLG depending on solution conditions and characterized the acid- and base-induced conformational transitions between these structural states over the pH range from 1 to 13. This pH-dependent system may indicate that one of BLG functions is to bind to non-polar molecules and transport them through the acidic environment (stomach) into the basic environment (intestine). This strong pH dependency suggests that electrostatic interactions could play a

significant role in the interactions of BLG with other molecules. The electrostatic attractions even enhance the protein aggregation due to BLG-BLG interaction (Majhi et al., 2006). An association between peptides and BLG due to electrostatic attraction was recently observed in the study of Kosters, Wierenga, de Vries, and Gruppen (2013). They have also observed stronger binding or even the formation of a covalent interaction between the free sulfhydryl group of the peptides and a cysteine residue of the BLG.

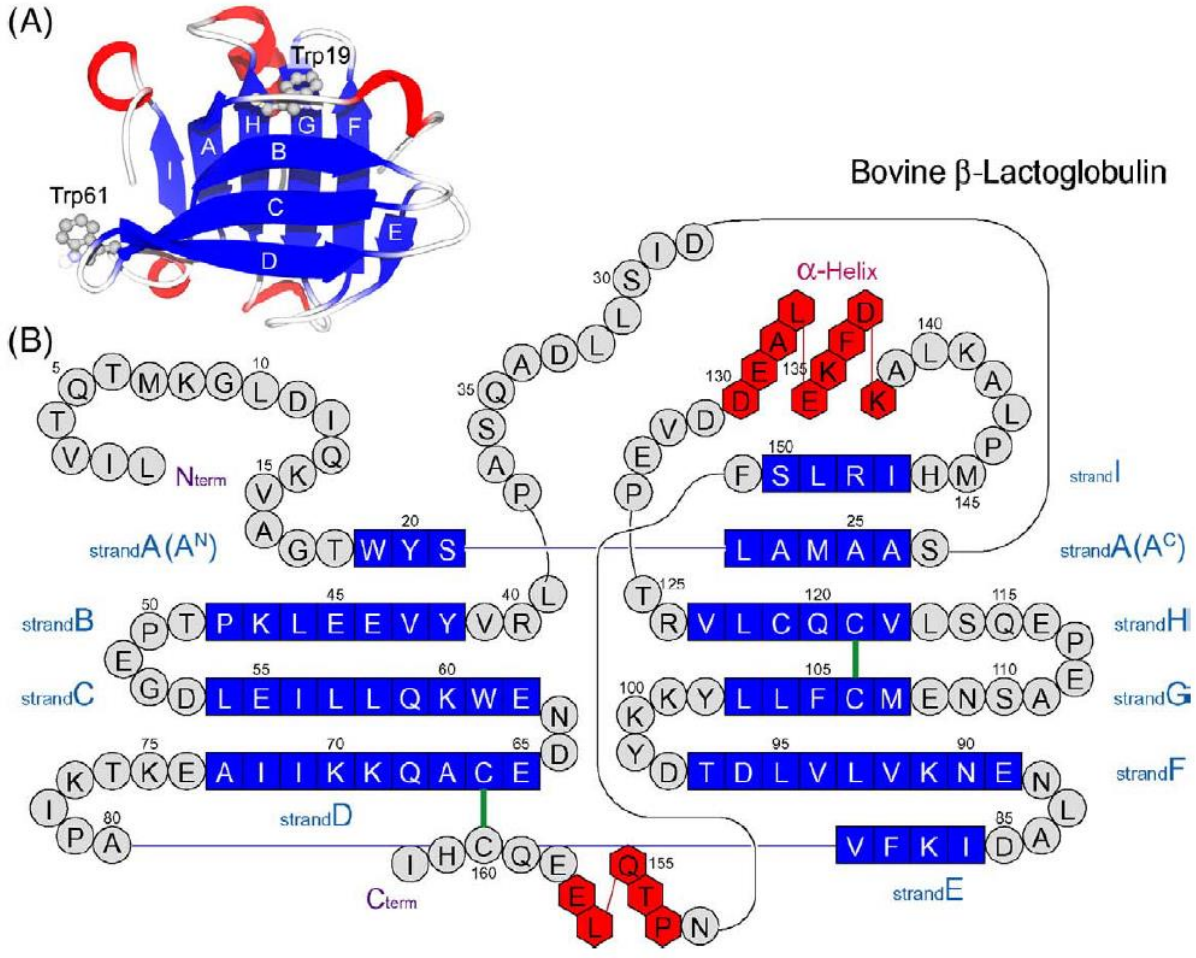

Fig. 2. The 3D structure and amino acid sequence of bovine BLG. (A) Ribbon diagram of a single subunit of bovine BLG lattice X, whose pdb code is 1BEB. The β-strands are labeled. Trp residues are represented as balls and sticks. The diagram was produced using the program MolFeat (FiatLux, Tokyo, Japan). (B) A schematic representation of the amino acid residues of the BLG sequence. Residues making up the α-helix, β-sheet, and loop are represented by hexagons in red, squares in blue, and circles in grey, respectively. Green lines indicate the positions of disulfide bonds. It is

seen that BLG has two β-sheets; The B–D strands and N-terminal half of the A strand (denoted AN) consist of one and the E–H strands and C-terminal half of the A strand (denoted AC) consist of the other. (Sakurai et al. 2009)

The three-dimensional structure of a protein may facilitate interactions with other components found in foods or the gastrointestinal (GI) tract lumen, thus altering their stability to proteolysis which is related with gastric digestion (Moreno, Mackie, & Mills, 2005). It has been also reported that the effects of physiological surfactants on the simulated GI proteolysis of bovine BLG, showing that under certain conditions BLG is almost completely protected from simulated digestion (Mandalari, Mackie, Rigby, Wickham, & Mills, 2009).

BLG is critical protein for the nutritional intake during digestion, as well as for a successful manipulation of the physical and sensorial attributes of colloidal food systems (such as emulsion stability, creaminess and rate of flavor release). However, both emulsions and saliva are complex systems. For instance, human saliva consists mainly of water (99.5%), various proteins (0.3%), small organic compounds and inorganic salts and has a pH of around 6.8 (Zalewska, Zwierz, Zolkowski, & Gindzienski, 2000). Therefore, many scientists preferred to focus on the major protein component of saliva, highly-glycosylated mucin, and its interaction with various food proteins used as emulsifier in order to understand protein-protein interaction mechanisms and the effect of protein charge on the emulsion-saliva interaction. Thus, one of the most commonly used proteins to investigate the interaction with saliva/mucin is BLG.

Saliva interaction with BLG

Kelly et al. (2010) studied the interaction between BLG and salivary proteins and investigated the effects of protein concentration on astringency. Due to the high number of samples, they divided

sensory evaluation into three studies. The first study investigated the effect of protein concentrations ranging from 0.25 to 4%. Protein concentrations in the second study ranged from 4 to 13%. In the third study, samples were selected to cover the whole range of concentrations, and time-intensity analysis was chosen to provide more comprehensive data (i.e., time to reach maximum astringency, astringency duration). They found that the changes in the astringency with varying the concentration of protein, is depended on the pH. At pH 3.5, astringency was significantly increased with the protein concentration from 0.25 to 4% (wt/wt) and then remained constant from 4 to 13% (wt/wt). Conversely, at pH 2.6, astringency was decreased with an increase in protein concentration [0.5–10% (wt/wt)]. This suggests a complex relationship that includes pH and buffering capacity of the beverages. Furthermore, saliva flow rates increased with increasing protein concentrations, showing that the physiological conditions in the mouth changed with the protein concentration. Maximum turbidity of whey protein–saliva mixtures was observed between pH 4.6 and 5.2. Both sensory evaluation and in vitro study of the interactions between BLG and saliva indicate that the astringency of whey proteins is a complex process determined by the extent of aggregation occurring in the mouth, which depends on the pH of the whey protein beverage and buffering capacity in addition to the flow rate of the saliva. This trend was not same with the study of Beecher et al. (2008) in which maximum astringency was found at pH 3.4 and a decrease in astringency was observed when the pH was lowered to 2.6. The difference may be due to the type of protein used and the processing parameters. Beecher et al. (2008) used whey protein isolates [6% (wt/vol) protein] and heated the whey protein beverages. However, Kelly et al. (2010) used BLG because of its higher purity. The samples were unheated to reduce the degree of protein aggregation. These factors may have contributed to the different results.

Peak turbidities resulting from polyphenols and mucin interactions were correlated with maximum astringency (Monteleone et al., 2004; Condelli et al., 2006). Nevertheless, such a linear correlation

with protein-based astringency was not observed by Kelly et al. (2010), who explained this by the differences between intermolecular binding mechanisms of proteins and polyphenols. Interactions between polyphenols and salivary proteins are a result of hydrogen bonding (Haslam, 1974) or hydrophobic interactions (Hagerman and Butler, 1980). These interactions have a minor pH dependence. In contrast, as protein charge is pH dependent, interactions between saliva and whey proteins will be pH dependent. Thus Kelly et al. (2010) suggested a dynamic model to explain the astringency of proteins as pH will depend on the amounts and buffering capacities of saliva and protein beverage, coupled with changes in saliva flow.

Vardhanabhuti et al. (2011) investigated the perception of astringency in relation to the effect of BLG at pH 3.5 and 7.0 by studying the lubrication properties of saliva using tribology. They have used fresh stimulated whole saliva without any treatment in all experiments. Saliva was adsorbed onto surfaces of a rotating poly(dimethylsiloxane) (PDMS) ball and disc to form a film under conditions that mimic the rubbing contacts in the oral cavity (Bongaerts, Rossetti, & Stokes, 2007) and the lubricity of saliva films upon exposure to astringent compounds was measured. While addition of non-astringent BLG at pH 7.0 slowly increased the friction of saliva films between tribopair surfaces, BLG at pH 3.5 rapidly increased the friction coefficients of saliva, similar to other astringent compounds (epigallocatechin gallate and alum). This supports the hypothesis that astringency of BLG arises from the loss of lubrication of saliva which is in agreement with the well-accepted astringency model of polyphenols. They concluded that aggregation and/or precipitation of whey proteins at their pI's, as well as charged interactions between whey proteins and salivary proteins, can contribute to the astringency of whey proteins at low pH. A number of studies already provided evidences that support the role of charged interactions in milk protein astringency (Malone et al., 2003; Vardhanabhuti & Foegeding, 2010; Vardhanabhuti, Kelly, Luck, Drake, & Foegeding, 2010). However, Vardnahabhuti et al, (2011) showed that these interactions lead to the loss of

lubrication properties of saliva. Increasing BLG concentration at pH 3.5 (0.5-10% w/w) caused a rapid increase in friction coefficient; however, at the highest protein concentration, the friction coefficient, although higher than observed for water, was below the values observed for the lower protein concentrations. This clearly supports the hypothesis that precipitation of whey proteins when mixed with saliva or interactions between positively charged whey proteins and salivary proteins leads to an increase in friction and/or the loss of saliva lubrication, and thus contributes to astringency of whey proteins at low pH. After all, Vardhanabhuti et al. (2011) suggested that static tribology testing is different from the dynamic in-mouth system such that a simple relationship between friction and sensory astringency cannot be found for all conditions.

Mucin interaction with BLG

Recently, our group has focused on the interactions of bovine submaxillary mucin (BSM) with BLG at different pH values in order to understand the protein-protein interactions in a food-saliva model system. Among several mucin types involved, submaxillary mucin is the one most related to oral processing. BSM, used as a model mucin in this study, is a glycoprotein consisting of a linear polypeptide core with a highly glycosylated central part accounting for up to 80% of the proteins molecular weight (Shi, Ardehali, Caldwell, & Valint, 2000), which ranges between 0.5 and 20 MDa (Bansil & Turner, 2006). Due to the abundance of negatively charged groups, arising mainly from sialic acid residues and sulphated sugars, mucins generally have low isoelectric points, estimated to be between 2 and 3 (Durrer, Irache, Duchene, & Ponchel, 1995; Lee, Müller, Rezwan, & Spencer, 2005). In order to establish a basis to understand food oral processing of the two proteins on the molecular level, we have selected 1:1 ratio in the present study. Dynamic light scattering (DLS) was employed to investigate the changes in hydrodynamic radius of proteins. High and low field

Nuclear Magnetic Resonance (NMR) techniques were employed to characterize interactions by monitoring changes on the chemical shifts of proteins residues. Finally, secondary and tertiary structures of proteins were studied using circular dichroism (CD) spectroscopy (Çelebioğlu et al. 2015). The zeta potentials of the proteins showed that the surface charge characteristics of the BLG-BSM mixture were dominated by the BSM. Results from DLS measurements suggested that the interaction between the proteins caused a more compact conformation of BSM as the BLG integrated into the BSM. Far UV and near UV CD spectroscopy studies of the mixture of the two proteins showed intermediate spectra compared to each protein alone for both secondary and tertiary structure of the proteins, which may support the interaction theory proposed between them. High field NMR measurements are consistent with polar interactions at pH 5 and pH 3, whereas no significant interaction was detected at pH 7.4. Longer T2 relation times were observed for the BLG-BSM mixture, especially at acidic pH, attributing to higher water mobility. The higher water mobility may indicate that fewer charged groups on the proteins surfaces were available for protein-water interaction due to interactions between the hydrophilic parts of BLG and BSM compared to BSM alone. The overall conclusion is that the higher hydrophilic interaction between the proteins at lower pH supported the pH dependent activity of both BLG and BSM. Furthermore, the positively charged groups of BLG, especially at acidic pHs, neutralized negatively charged groups of BSM and caused the BSM to coil or contract into a smaller hydrodynamic volume (Fig. 3), as suggested by Shrivastava & Nair (2003) as well. In fact, even a weak hydrogen bonding between BLG and BSM brings about aggregation of mucins into a more compact structure at pH 7.4. The NMR results also implied that negatively charged BLG has a tendency to interact with negatively charged mucin via secondary interactions (hydrogen bonding and hydrophobic effects), where the electrostatic interactions are unlikely to be the main reason of the binding.

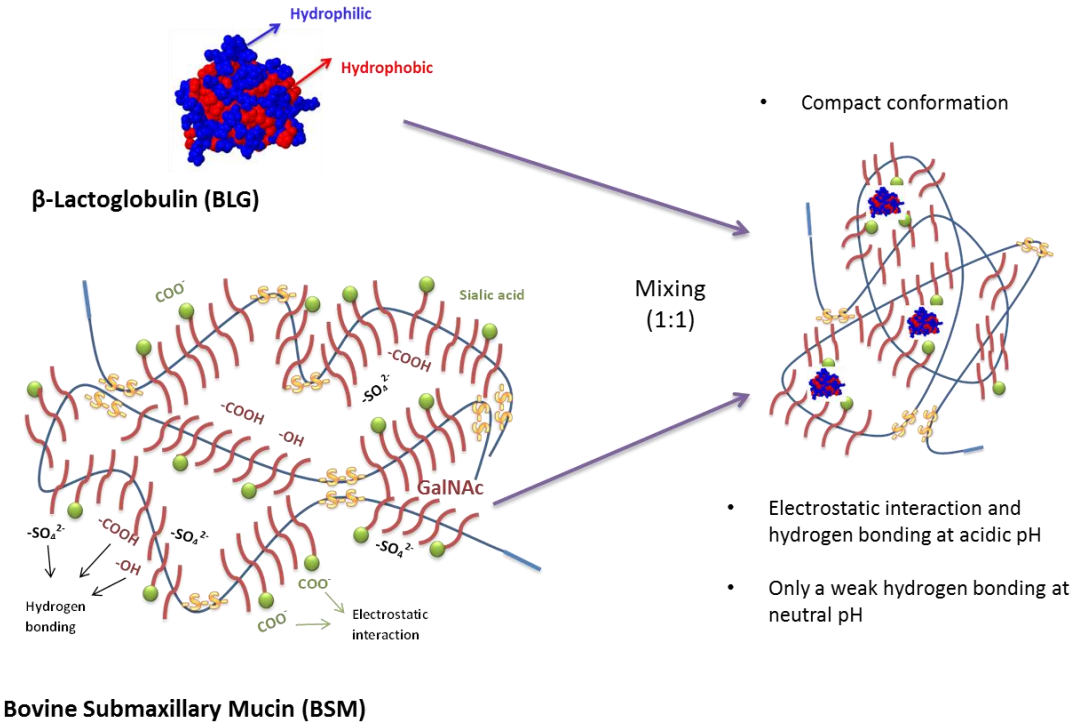

Fig. 3. Illustration of the interaction between β-lactoglobulin and bovine submaxillary mucin.

Since the BSM and the BLG showed an interesting interaction, the interfacial properties of BLG, BSM, and their mixtures at air/liquid interface also draw attention. It is important to understand the interfacial rheological properties of adsorbed BLG and mucin layers and their network formation at the liquid surface that are relevant in a wide range of applications such as foam and emulsion stability or multiphase fluids processing. In our other recent study, the interfacial rheological properties of solutions of BLG (as a model food compound) with a salivary mucin protein, BSM, at different pHs, were investigated (Çelebioğlu et al. submitted). The results showed that all protein layers (BSM, BLG, and BLG-BSM mixtures) formed at air/water interface has some similarities such as a rapidly developed elastic interfacial network, low frequency dependence of the interfacial modulus. The high molecular weight BSM formed a weak viscoelastic interfacial network (lower modulus) compared to BLG at all pHs, which is destroyed even at low strain (0.003 %). The pH has

a significant effect on the surface density of adsorbed BLG proteins, as it determines the net charges and the modulus of the interfacial network. At pH close to pI, electrostatic repulsions between the adsorbed BLG molecules are minimized at the interface, and it promotes the formation of stable adsorbed layer with a high elastic modulus. Furthermore, BLG molecules move faster due to their smaller size/mass than mucins, and dominate the surface adsorption and the network formation for the BLG-BSM mixtures. However, BLG-BSM protein mixtures exhibited interfacial properties with lower elastic and viscous moduli than BLG, as a result of competitive displacement of BLG proteins with BSM molecules from the interface. We propose that BSMs decreased the surface viscoelasticity and the rigidity of the BLG layers through the penetration of the hydrophobic parts of BSM between the adsorbed BLG molecules and disorder their cohesive assembly, which was most pronounced at pH 5 (Fig. 4). Moreover, it is important to stress that facile attraction of BSM molecules towards BLG layer within water phase is not sufficient to activate this mechanism. At pH 3, for example, despite electrostatic attraction between oppositely charged BSMs and BLG layer, the reduction in viscoelasticity and rigidity is weaker compared to at pH 5. This can be explained by that overall hydrophilic nature of the interaction between them hinders the hydrophobic parts of BSM to disrupt the assembled layer of BLG and extend its interaction with air.

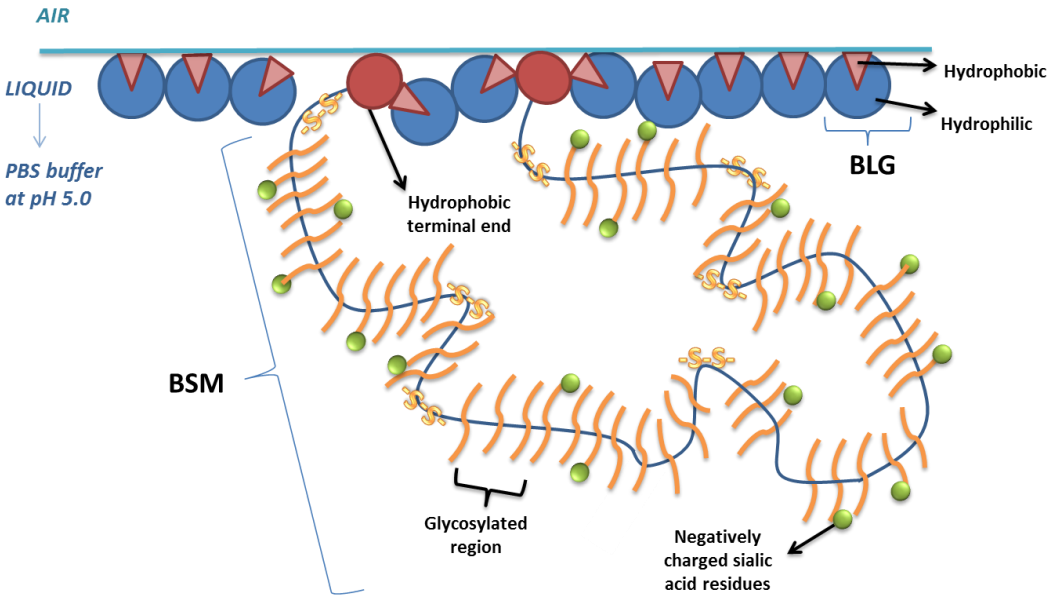

Fig. 4. Interfacial layer of BLG-BSM mixture showing the penetration of the hydrophobic parts of BSM between the adsorbed BLG molecules and disorder their cohesive assembly, which is most pronounced at pH 5.

We have also studied the surface adsorption of BLG, BSM and their mixture at the solid/liquid interface (Çelebioğlu et al. 2016). The study based on bicinchoninic acid (BCA) protein qualification assay showed that mucins were not only higher than BLG in the adsorbed masses onto the solid hydrophobic surface, but also adsorb in a more compact conformation due to a high flexibility to accommodate themselves in a narrow space and/or a possibility to form multilayers (Çelebioğlu et al. 2016). However, BLG can readily dominate the initial stage of surface adsorption at the solid/water interface in the mixture solution of BSM and BLG due to the ability of the smaller and lighter BLG molecules to reach the surface faster than mucins. In the adsorption of the BLG-BSM mixture onto hydrophobic solid surfaces, it was assumed that there is a large portion of "free" BLG molecules in the mixed protein solutions, and that they participate in the surface adsorption process in competition with the mucins. In addition to the BSM, porcine gastric mucin (PGM) was also used for interaction studies with BLG. The fact that both mucins are highly relevant to food

digestion process, yet to different organs, is the first reason for comparing them. Additionally, in parallel with common structural features of the two mucins (Bansil et al., 1995; Sandberg, Blom, & Caldwell, 2009), reported differences in their biophysical properties, especially the lubricating properties (Lee et al., 2005; Nikogeorgos et al., 2014), may lead to different interaction with BLG and alteration in the lubricating properties. The surface adsorption results showed that the net effect of mixing BLG and PGM is featured with substantially decreased adsorbed masses compared to the neat PGM solutions. Thus, it was suggested that BLG dominates the solid/water interface for BLG-PGM mixture.

Another novel approach was to apply tribological techniques to investigate the interaction of BLG with mucins under tribological stress and how it affects their lubricating properties (Çelebioğlu et al. 2016). Recently, tribology has emerged as a new instrumental approach to investigate oral processing of food emulsions in simulated oral environment (Meyer, Vermulst, Tromp, & de Hoog, 2011; Vardhanabhuti, Cox, Norton, & Foegeding, 2011; Chojnicka- Paszun, de Jongh, & de Kruif, 2012; Chen & Stokes, 2012; Van Aken, 2013; Selway & Stokes, 2013; Prakash, Tan, & Chen, 2013; Chen, Liu, & Prakash, 2014; Joyner Melito, Pernell, & Daubert, 2014). In turn, this is often correlated with food's sensory perception (Meyer et al. 2011; Vardhanabhuti et al. 2011; Chojnicka-Paszun et al., 2012; Selway & Stokes, 2013; Prakash et al., 2013). Tribology is particularly useful for understanding the behavior of thin films formed between two opposing surfaces where rheological and structural/mechanical properties of food may no longer explain their behavior sufficiently. Recent applications of tribological techniques allowed for quantitative characterization of the lubricating properties of the fluids involving saliva and BLG or other astringents. For example, Vardhanabhuti et al. (2011) showed that addition of BLG into a soft tribological interface increased the interfacial friction forces, yet at varying rates depending on pH. Aggregation of

macromolecules (BLG) with hydrogel (saliva) is, however, a complex process influenced by a number of parameters.

Recently, we have investigated the molecular-level interaction between mucins and BLG by means of tribological approaches according to mucin type, solution pH, and protein concentration. Hydrophobic interfaces, namely PDMS-PDMS and POM-PDMS, were employed for feasible adsorption of the proteins and consequent possibility of assessment of the boundary lubricating properties. The structural and mechanical properties of thin films generated from two types of mucins, namely, BSM and PGM in aqueous environment were also investigated by Madsen et al. (2016) who showed that both mucins generated hydrated films on hydrophobic polydimethylsiloxane (PDMS) surfaces from spontaneous adsorption arising from their amphiphilic characteristic.

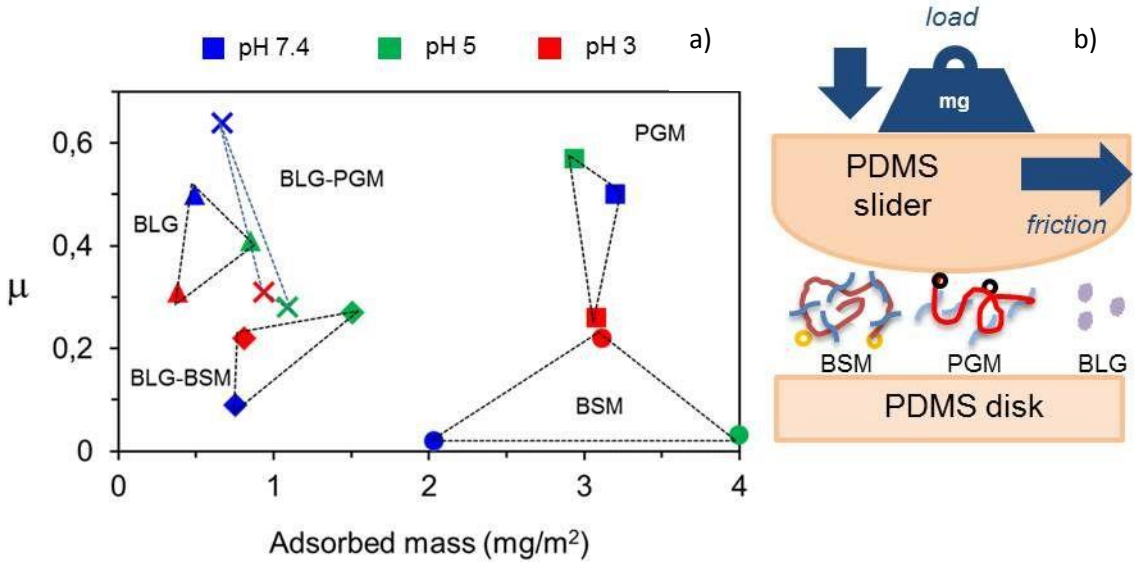

Fig. 5. (a) Coefficient of friction, μ (PDMS-PDMS pair) vs. adsorbed mass, Γ (PDMS surface) of the protein solutions (1 mg/mL concentrations only). The color codes are for different pHs: red for pH = 3, green for pH = 5, and blue for pH = 7.4. Different symbols represent different protein or mixed protein solutions. (For interpretation of the references to color in this figure legend, the reader is referred to the web version of this article. (Çelebioğlu et al. 2016)). (b) Schematic presentation of protein molecules under tribological stress using pin-on-disk tribometer with PDMS-PDMS tribopair.

Overall, we have observed that mucins have effective lubricating properties, in particular BSM, compared to BLG. Nevertheless, nearly ignorable lubricating effect by PGM, despite its facile surface adsorption, suggests that other parameters than adsorbed masses play a significant role to impart superior lubricity of BSM to PGM or BLG (Fig. 5). While both pin-on-disk tribometry and MTM were employed to provide the tribological contacts with different contact pressure, speed range, and slide/roll ratio, the dominating lubrication mechanism by the protein solution was boundary lubrication. Surface adsorption and lubricating properties of mixed protein solutions, such as BLG-BSM and BLG-PGM, with respect to neat protein solutions were of prime interest as it can be compared with the well-known role of BLG as astringency to form a complex with saliva and rapidly deplete from the tribological interface at acidic pH (3.5, for example). Even in the absence of tribostress, the adsorbed masses of the mixed protein solutions reduced significantly, and BLG appeared to dominate the surface adsorption event, presumably due to the reduced concentration of mucins as well as the Vroman effect. Nevertheless, excellent lubricity was still observed at pH 7.4 and BSM apparently dominated the tribological interface, which highlights the excellent lubricating capabilities of BSM. Although being still relatively more lubricious than the other proteins, the BLG-BSM mixture showed the highest level of degradation in the lubricity of BSM at pH 5, which contrasts the case of BLG-saliva interaction. This is due to that instead of strong aggregation, as in BLG-saliva, the lubricating properties of BLG-BSM are determined by competitive adsorption of the two proteins onto substrates. Most importantly, these observations further suggest that BLG and BSM molecules do not form strong aggregates, especially under tribological stress. PGM's intrinsically weaker lubricity remained largely unchanged even in the interaction with BLG.

Consequently, the mucin and the BLG showed an interesting interaction and different surface adsorption behavior at solid/liquid or liquid/air interfaces. However, there has been no study specifically designed to probe hydrophobic interaction between the BLG and mucins or any role of

hydrophobic residues of these proteins. Hence, in another study, we aimed to elucidate the interaction mechanisms of BLG and two types of mucins, namely BSM and PGM, specifically focusing on the role of hydrophobic residues of the proteins at different pH conditions in the context of understanding the food digestion process along the gastrointestinal organs (Çelebioğlu et al. submitted-2017). Intrinsic fluorescence spectroscopy and the fluorescent dye ANS techniques were used to assay conformal modifications of the proteins, as induced by binding interactions between the proteins, by focusing on changes in their hydrophobic residues. As recently shown by Brandão et al. (2017), fluorescence quenching and NMR are two complementary techniques, by together providing information about the modification of protein structure induced by binding and the structural features of the ligand involved in the interaction. Hence, HF-NMR spectroscopy was also used to obtain further details about the structural differences between the two mucins and their interaction properties, both hydrophobic and hydrophilic, with BLG. It can be concluded from the fluorescence analysis that the presence of mucins surrounding BLG tends to enhance the solvent exposure of Trp residues in BLG. More enhanced reduction in FI, together with the red shift of peak maximum of BLG upon mixing with PGM than BSM, suggested that hydrophobic moieties, which can effectively interact with BLG, are more abundantly present in PGM than BSM. This may explain that even at pH 7.4, mixing of BLG with PGM led to a reduction in fluorescence intensity (FI), in contrast to the case of mixing with BSM. In this sense, a quenching effect of mucins on the fluorescence emission of Trp residues of BLG is suggested, chiefly based on hydrophobic interaction, with generally stronger effects by PGM than BSM. Even though the initial interaction between BLG and the mucin molecules can occur via hydrophobic interaction, the results indicated that the interaction can also be facilitated by electrostatic attraction, which was especially evident at pH 3 where BLG and the mucins are oppositely charged.

Mucin/saliva interaction with BLG-stabilized emulsion

Various attempts have been reported in literature to explore the effect of mixing saliva/mucin with the milk proteins, especially by using the BLG-stabilized emulsions (Sarkar, Goh, & Singh, 2009; Sarkar, Goh, & Singh, 2010; Silletti, Vingerhoeds, Norde, & van Aken, 2007; Vingerhoeds, Blijdenstein, Zoet, & van Aken, 2005). Sarkar et al. (2009) determined the physicochemical effects of the porcine gastric mucin (Type II) on negatively charged BLG stabilized emulsion. They showed that the BLG stabilized emulsions remained homogeneous in the presence of low mucin concentrations. However, the emulsions showed network-like flocculation at 1.0 wt% added mucin. These emulsion–saliva mixtures (containing added 1.0 wt% mucin) reverted back to homogenous dispersions after dilution with water, which indicated that the flocculation was reversible. Moreover, Sarkar et al. (2009) mentioned that for the BLG-coated droplets, the presence of some positive patches along the adsorbed BLG molecules probably resulted in some electrostatic interactions with the negatively charged mucin molecules. Moreover, there is also possibility of hydrophobic interactions between unfolded BLG at the adsorbed layer and mucin at low ionic strengths of artificial saliva.

Silletti et al. (2007) also hypothesized that depletion flocculation was responsible for the observed flocculation. To further unravel the mechanism, they investigated the role of electrostatics on the behavior of emulsion/saliva mixtures. Emulsions stabilized with differently charged surfactants and proteins were mixed with saliva. Strongly negatively charged emulsions (SDS and Panodan) did not flocculate, and this could be due to the electrostatic repulsion between the droplets overcomes the attractive depletion and van der Waals interactions. However, reversible flocculation was observed for neutral and weakly negatively charged emulsions (Tween 20 and BLG pH 6.7). Silletti et al. (2007) suggested that this is probably due to depletion interactions, induced by large salivary protein like mucins, in combination with the van der Waals interactions and the sufficiently low

electrostatic repulsion between the droplets. Positively charged emulsions (CTAB, lysozyme and BLG pH 3.0) show irreversible flocculation leading to rapid phase separation. These findings point to a role of electrostatic attraction between the negatively charged proteins present in saliva and the positively charged surfaces of the emulsion droplets. Certainly, these results indicate that the sign and the density of the charge on the surface of the droplets contribute significantly to the behavior of an emulsion when mixed with saliva. Depending on the charge, saliva-induced emulsion flocculation is driven by two different main mechanisms: depletion flocculation and electrostatic attraction.

By employing mucin and BLG-stabilized emulsions, Silletti et al. (2010) investigated the interactions between BLG-stabilized emulsion droplets and salivary proteins (mucin), by means of different techniques, i.e. infrared spectroscopy, Western blotting, PAS staining and SDS-PAGE coupled to MS. They showed that adsorption/association of mucin onto the emulsion droplets is related to the type of emulsifying proteins at the oil-water interfaces and it is driven by the overall net charge at the droplet's oil-water interfaces, i.e. negative for BLG-stabilized emulsion at neutral pH. Sarkar et al. (2010) also mentioned that the presence of a low level of mucin appears to promote the flocculation of BLG-stabilised emulsions, possibly through a bridging mechanism. Broadly, neutral and negatively charged emulsions undergo reversible depletion flocculation whereas cationic emulsions show irreversible associative electrostatic interactions with mucin and salivary salts. Similarly, Teng et al. (2016) found that cationic polymers interact highly with mucin and exhibited better mucoadhesion properties than unmodified BLG. Moreover, Singh and Ye (2013) showed depletion flocculation of a BLG-stabilized emulsion (20 wt% soybean oil, 1.0 wt% BLG) when mixed with an artificial saliva composition containing pig gastric mucin. This flocculation was largely dependent on the mucin concentration (a critical mucin concentration of 0.4 wt%) present in the saliva.

Mucin/saliva interaction with Casein

Caseins evolve from members of a group of secreted calcium (phosphate)-binding phosphoproteins (Kawasaki and Weiss, 2003; Rijnkels et al., 2003; Kawasaki et al., 2004, 2011; Lemay et al., 2009). In eutherian milks, at least three and normally four gene products are found; namely, αS1-, αS2-, β-, and κ-CN, but in some species two quite different αS2-CN-like genes are active, raising the total number of gene products to as many as five. (Holt et al. 2013).

Caseins which constitute about 80% of the proteins of bovine milk contain high numbers of proline residues evenly distributed throughout their amino acid sequences and have relatively open structural features (like the salivary proline rich proteins). For this reason, isolated caseins have often been used as model proteins in various polyphenol–protein studies (Jobstyl, O'Connell, Fairclough, & Williamson, 2004; Pascal, Poncet-Legrand, Cabane, & Vernhet, 2008; Yan et al., 2009).

Withers et al. (2013) recently investigated the potential adhesion of milk proteins to porcine oral mucosa in vitro. This study aimed to evaluate the retention of milk proteins (casein and BLG) on the oral epithelial surfaces including buccal and tongue tissues. The hypothesis of this study was that the adhesion of milk proteins to the oral epithelium may be related to the mouth drying in dairy products. Purified casein and BLG were fluorescently labelled, placed on porcine oral mucosal tissues and their resistance to wash out with simulated saliva was monitored using fluorescence microscopy (Fig. 6). Fluorescein isothiocyanate (FITC)-dextran was used as a negative control in these experiments because it is not expected to provide substantial retention effects as a non-ionic poorly mucoadhesive polymer. Unlabelled samples showed no fluorescence at this wavelength, indicating that no intrinsic fluorescence would be demonstrated by the proteins alone. Therefore, all

fluorescence observed originated from the FITC-bound proteins, with casein exhibiting greater fluorescence than BLG in this study. Dynamic light scattering indicated that the labelling process did not destroy the micellar structure of casein in solution. The presence of BLG on the mucosal surface was detected even after 30 washes, which confirms its stronger ability to adhere to buccal membrane compared to FITC-dextran. Thus, Withers et al. (2013) suggested that although BLG interacted with the cheek mucosal surface, the salivary washes were able to eventually remove this protein. Casein was found to retain on the mucosal surface in substantial quantities even after 50 washes indicating that this protein also strongly interacts with mucosal surface. Moreover, thiol content measurements showed that the level of thiols in BLG was found to be significantly higher than in casein ($p < 0.001$). Both casein and BLG were found to be negatively charged at pH 9.0 as expected. The greater zeta-potential of BLG implies a greater stability of the protein in solution, relative to casein. On the other hand, the viscosity of casein solution was 2.3 times higher than BLG, which is likely related to the ability of casein to form naturally self-assembled micellar structures (Hagerstrom and Edsman, 2003). Overall the results supported that the presence of an interaction between BLG and mucin present in the saliva, but not for casein. This may be a result of the markedly different rheological properties of casein, in part a result of its micellar nature (Withers et al. 2013). In addition, Withers et al. (2013) proposed that electrostatic interactions are unlikely to be the main cause of mucoadhesion due to the overall negative charge of both proteins in the near-neutral pH of the oral cavity. However, the less charged casein should feel a weaker repulsion from the negatively charged mucosal surface compared to BLG.

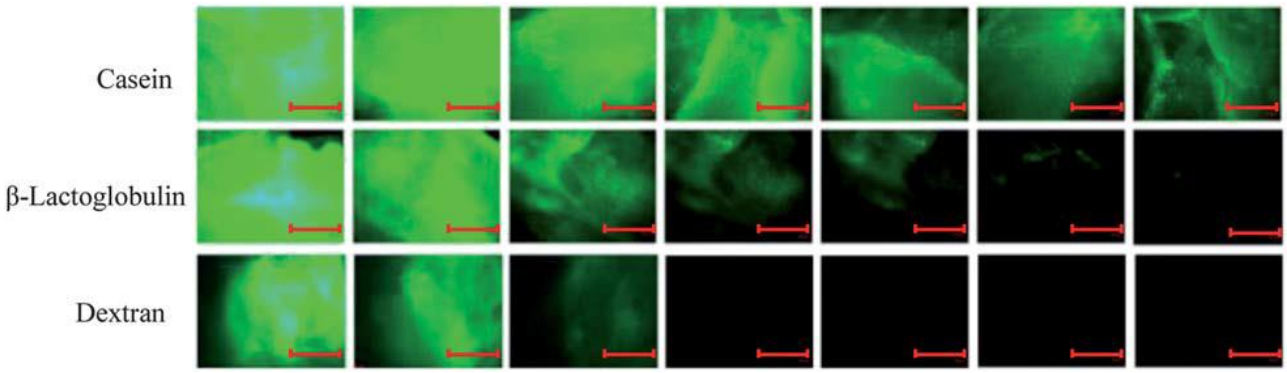

Fig. 6. Exemplary fluorescent microphotographs, showing the retention of casein, β-lactoglobulin and dextran on buccal mucosa against the number of washes with artificial saliva. Scale bars indicate 500 mm at image magnification (Wither et al. 2013)

Another recent study by Withers et al. (2014) aimed to test the hypothesis that casein within protein-fortified beverages of neutral pH could contribute to perceived mouth drying. Sequential profiling found that the whey protein concentrate (WPC75; containing 75% wt/wt protein) and sodium caseinate (NaCas; containing 85% wt/wt protein) samples were not significantly different for mouth drying or chalkiness. Previously, it was suggested by several authors that mouth drying was an attribute found to build substantially during the consumption of oral nutritional supplement (ONS) dairy-based beverages, and it could originate from whey or casein sources (Methven et al., 2010). Previously, whey-based dairy beverages have found to be astringent, especially at reduced pHs; it has been proposed that the negatively charged salivary proteins bind electrostatically to positively charged whey proteins to precipitate around the oral cavity (Sano et al., 2005; Ye et al., 2011) or bind to oral epithelial cells (Ye et al., 2012). Similarly, Withers et al. (2014) found that ONS mouth drying appears to originate predominantly from whey proteins, and that masking mouth drying is not a simple task. However, the potential for casein to contribute to mouth drying was also demonstrated. Whether casein-derived mouth drying is due to the presence of γ-CN remains

unanswered, and further investigation, including the use of HPLC to quantify γ-CN in heat-treated, protein-fortified beverages over shelf life, was recommended.

In a different point of view, Hug et al. (2016) also studied the interaction between casein and saliva using adhesion, SDS-PAGE, and ELISA techniques. Their aim was to demonstrate the repair of early dental caries lesions by the application of the remineralisation technology based on casein phosphopeptide-stabilised amorphous calcium phosphate complexes (CPP–ACP). Hug et al. (2016) showed that the two predominant peptides of the casein phosphopeptide (CPP) have the ability to interact with selected salivary proteins and peptides found as components of the enamel pellicle. The sequences of both αS1-CN (59–79) and β-CN (1–25) peptides have hydrophobic and hydrophilic regions. This enables them to bind to a range of proteins through hydrophobic or electrostatic interactions. Nevertheless, it is evident that the CPP are not promiscuous binders of salivary proteins, but display selectivity (Hug et al. 2016). After all, they attributed the non-covalent interactions between specific salivary proteins and peptides and the CPP, to the concomitant retention of mineral ions and peptides derived from the CPP–ACP complexes within plaque on the enamel surface. In summary, Hug et al. (2016) elucidated the mechanism of anticariogenicity displayed by the CPP–ACP nanocomplexes involving several molecular interactions between organic and inorganic molecules. These interactions include the binding of the CPP to specific salivary proteins and peptides.

Mucin interaction with Lactoferrin

Globular proteins derived from milk are widely used as natural emulsifiers to enhance the formation and stability of oil-in-water emulsions, e.g., whey protein, BLG, α-lactalbumin, and bovine serum albumin (Dickinson, 2003; Kralova & Sjoblom, 2009; Livney, 2010; McClements, 2004; Raikos,

2010). Recently, there has been increasing interest in the utilization of lactoferrin (LF) as an emulsifier (Sarkar, Goh, & Singh, 2009; Sarkar, Horne, & Singh, 2010). Lactoferrin is a globular glycoprotein derived from milk and other mammalian fluids that has an unusually high isoelectric point (pI> 8), and thus cationic at neutral pH whereas most other major dairy globular proteins are anionic (Steijns & van Hooijdonk, 2000). The ability of lactoferrin to form positively charged droplets at neutral pH could have a number of important practical implications. Since cationic droplets do not attract positively charged transition metal ions that catalyze oxidation to the droplet surfaces, they are more stable to lipid oxidation than anionic droplets (Mei, McClements, & Decker, 1999; Mei, McClements, Wu, & Decker, 1998). On the other hand, cationic droplets may interact with other anionic ingredients in foods resulting in the formation of undesirable precipitates (Guzey & McClements, 2006). They may also interact with anionic mucin molecules in the mouth causing astringency (Beecher, Drake, Luck, & Foegeding, 2008; Vardhanabhuti, Kelly, Luck, Drake, & Foegeding, 2010).

In order to compare cationic and anionic emulsions, BLG-stabilized emulsions, lactoferrin-stabilized emulsions with mucin/saliva have been investigated. When these emulsions were mixed with artificial saliva, contained a range of mucin concentrations and salts, negatively charged mucin was shown to interact readily with the positively charged lactoferrin-stabilized emulsion droplets to provide a mucin coverage of approximately 1 mg/m^2 (Sarkar et al. 2009). The higher mucin coverage in the lactoferrin-stabilized emulsion was attributed to the electrostatic attraction between mutually oppositely charged mucin molecules (negative) and lactoferrin molecules (positive) adsorbed at the droplet surface. At low levels of mucin addition (0.1–0.2 wt%) to the lactoferrin-stabilized emulsions, the size of the droplet aggregates appeared to decrease and the emulsions appeared to be rather monodisperse at intermediate mucin concentrations (0.5 wt%). However, at higher mucin concentrations (2.0 wt%), the lactoferrin-stabilized emulsions showed aggregation of

the oil droplets. To monitor the difference between anionic and cationic emulsions in the physiological condition, the mechanisms of interaction for both BLG-stabilized and lactoferrin-stabilized emulsions in the presence of artificial saliva containing different levels of mucin was illustrated by Sarkar et al. (2009) (Fig. 7).

Sarkar et al. (2009) suggested that lactoferrin-stabilised emulsion droplets interacted with mucin via electrostatic interactions. They showed that some bridging type flocculation occurred when there was insufficient mucin to form a complete secondary layer around the lactoferrin-stabilised droplets. On the other hand, depletion type flocculation as well more complex aggregations involving the self-association of mucin molecules increased due to excessive mucin concentration in the continuous phase. These kinds of emulsion–saliva electrostatic interactions might occur upon consumption of emulsions in real situations and could result in different sensorial and textural perceptions in vivo (Sarkar et al. 2009; Singh and Sarkar, 2011; Singh and Ye, 2013).

In the view of emulsion stability, Tokle et al. (2010) studied the effects of three anionic polysaccharides (low methoxyl pectin (LMP), high methoxyl pectin (HMP) and alginate) on the physicochemical properties and stability of lactoferrin (LF)-coated lipid droplets. LMP, HMP and alginate were shown to adsorb to the surfaces of LF-coated droplets at neutral pH, which was primarily attributed to the electrostatic attraction between anionic groups on the polysaccharide molecules and cationic patches on the protein surfaces. The study of Tokle et al. (2010) further supports the electrostatic interaction between negatively charged glycosylated regions of mucin with positively charged lactoferrin. Similarly, Vardhanabhuti et al. (2010) showed that lactoferrin was astringent at pH 7.0 where no acid was added, when comparing among various whey proteins isolates (WPI) and lactoferrin at pH 3.5, 4.5, and 7.0. In contrast, astringency of all WPI decreased at pH 7.0. Vardhanabhuti et al. (2010) explained this as a result of that lactoferrin remained positively charged at pH 7.0.

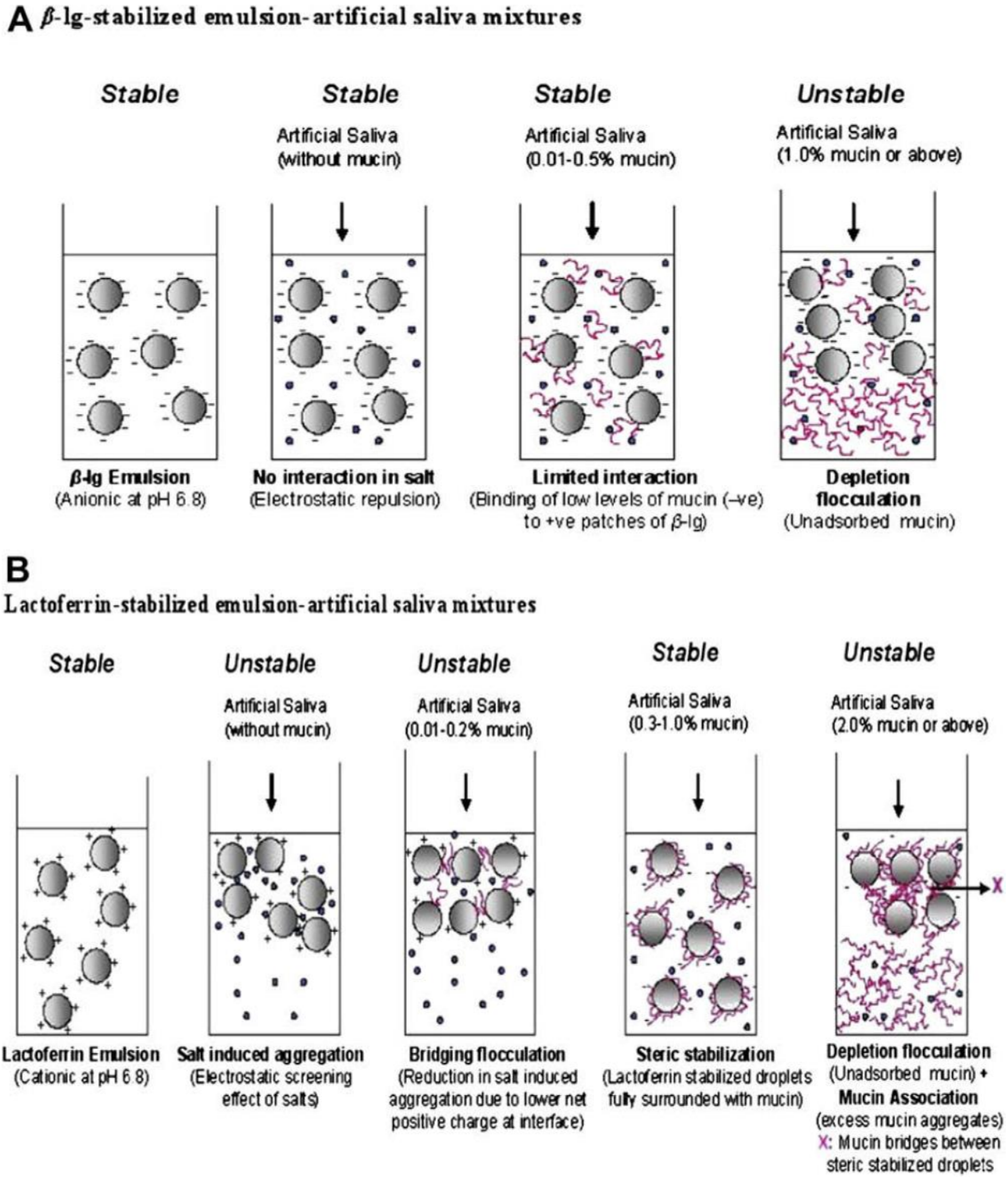

Fig. 7. Mechanisms of interaction in emulsion–saliva mixtures. Big shaded circle represents emulsion droplets; small solid dot represents salivary salts and coil structure represents mucin molecules. (a) BLG-stabilized emulsion interacting with artificial saliva (b) lactoferrin-stabilized emulsion interacting with artificial saliva. (Sarkar et al. 2009)

Moreover, lactoferrin was able to interact with negatively charged saliva proteins, whereas the negatively charged WPI would not interact. Charge interactions were further supported by BLG or lactoferrin and salivary proteins precipitated when mixed at conditions where BLG, lactoferrin, or saliva themselves did not precipitate.

Moreover, Zhang et al. (2015) hypothesized that the presence of mucin in the simulated saliva fluids altered the charge characteristics of the protein-stabilized emulsion systems. Presumably, anionic mucin molecules adsorbed to the surfaces of cationic protein-coated lipid droplets making the net charge negative. To support this hypothesis, they have measured the electric charge of emulsions after exposure to simulated gastric fluids with and without mucin. In the absence of mucin, the zeta-potentials of emulsions stabilized by caseinate and lactoferrin were 4.5 and 5.7 mV, respectively. These results suggest that the negative charge of the protein-coated droplets observed in the stomach phase is due to adsorption of mucin molecules to their surfaces.

Mucin/saliva interaction with gelatin

Gelatin, one of the most commonly used hydrocolloids in the food products, is commercially derived from collagen extracted from the bone, skin or tendons of animals. It contains glycine, proline and hydroxyproline, and is used as a thickening agent in dessert jellies, confectionery jellies and gums (Johnston-Banks, 1990). Gelatin is also used as mucoadhesive materials due to its ability to adhere to the mucus layer and release the loaded drug in a sustained manner. Wang et al. (2000) demonstrated that aminated gelatin microspheres, with high primary amino group content, showed a sustained amoxicillin release characteristic and a considerable gastric mucoadhesive property in vitro. Mucoadhesion involves different kinds of interaction forces between mucoadhesive materials and mucus surface, such as electrostatic attraction, hydrogen bonding, van der Waals forces and

mechanical interpenetration and entanglement. Of the in vitro test, commercial mucin is frequently used as a substitute for fresh mucin because of its reproducible quality and easy availability, although it does not possess the same viscoelastic properties as freshly isolated mucus gel (Madsen et al. 1996). Nevertheless, it is still proved to be effective to provide preliminary information about the interaction with mucoadhesive materials (He, Davis, & Illum, 1998; Rossi et al. 2000).

Wang et al. (2001) utilized two kinds of commonly used commercial mucins with different content of sialic acid (mucin type III from porcine stomach – 1% sialic acid and mucin type I-S from porcine pancreas – 12% sialic acid) to evaluate their interaction with gelatin by measuring absorbance via spectrophotometer. They showed that the interaction between gelatin and mucin changed dramatically in varying environmental conditions. In purified water, gelatin (IEP=9.0) is positively charged, a strong interaction with mucin was observed as a result of the electrostatic attraction with mucin that is negatively charged under this condition. However, aminated gelatin, with a higher positive charge density (higher amino group content) than gelatin, showed a lower interaction with mucin at a low mucin concentration. This could be due to higher solubility of aminated gelatin in water than the gelatin. Moreover, Wang et al. (2001) observed a strong interaction at a higher mucin concentration even when the aminated gelatin concentration was relatively very low. In contrast, gelatin (IEP=5.0) did not show any interaction with mucin in purified water because it carried a net negative charge as mucin did. In the case of PBS, gelatin (IEP=9.0), as well as gelatin (IEP=5.0), showed no interaction with mucin, although gelatin (IEP=9.0) was expected to reveal an electrostatic attraction with mucin as in the case of purified water (Fig. 8) (Wang et al. 2001).

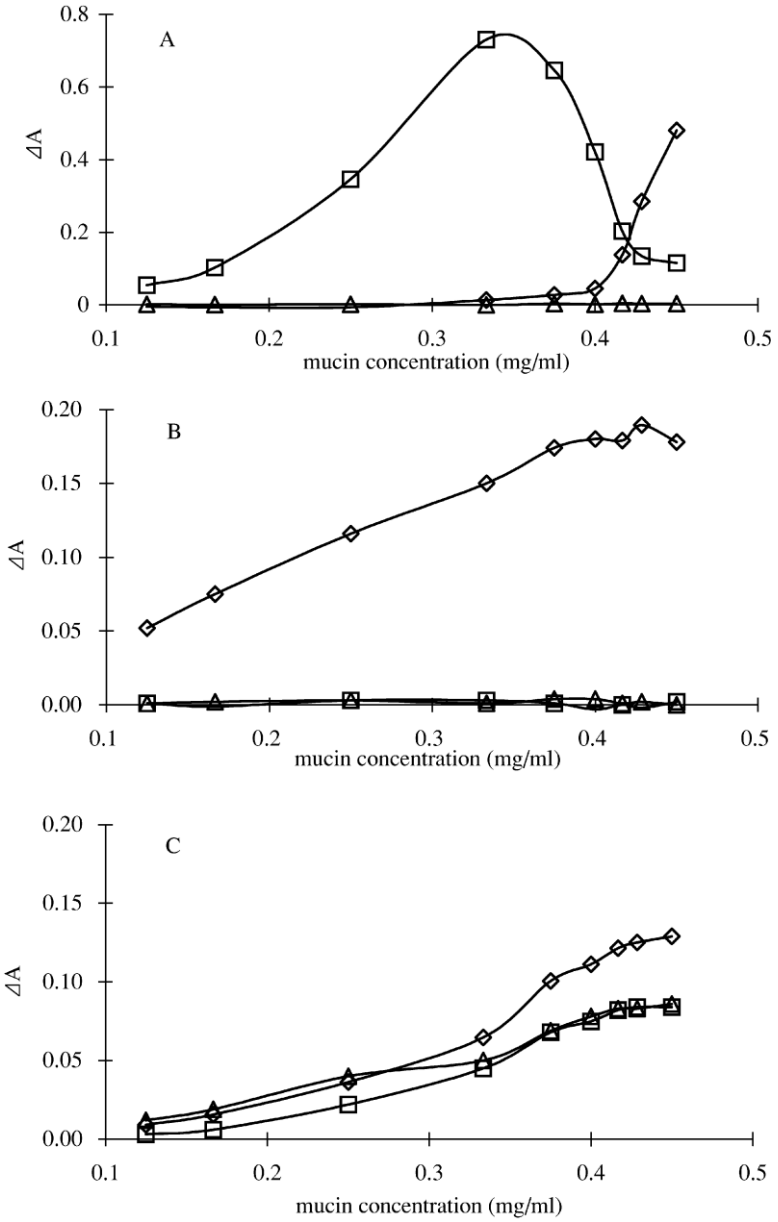

Fig. 8. Turbidimetric measurement of the interactions of gelatin and aminated gelatin with mucin (type III) in (A) purified water, (B) phosphate-buffered saline (PBS) and (C) simulated gastric fluid (SGF). Mucin solution (0.5 mg/ml) and gelatin solution (1 mg/ml) were mixed at volume ratios between 1:3 to 9:1. Δ*A* represents the difference between the experimental and theoretical absorbances of the mixed solution. Each point represents the mean of three experiments. Key: (△) gelatin (IEP=5.0); (□) gelatin (IEP=9.0); (◇)aminated gelatin. (Wang et al. 2001)

This result was ascribed to the unfavorable biopolymer conformation in the presence of high electrolyte concentration where the gelatin was dehydrated, thus shielding the free amino group

content and reducing the available positive charge. Furthermore, due to the existent electrolyte, the ionization of sialic acid residues of mucin was greatly reduced, the electrostatic attraction between mucin and gelatins decreased, hence resulting in a weakened interaction for all kinds of gelatins (Wang et al. 2001). A strong interaction between pig gastric mucins and polymer solutions of gelatin and chitosan at pH 5.5 was also described by Silletti et al. (2007).

Mucin was identified by van Ruth et al. (1995) as the key component in saliva to affect flavour release, by binding to and reducing the release of hydrophobic compounds. Saliva/mucin has been shown to influence both the thermodynamic and kinetic components of flavour release from the gel systems by Boland et al. (2003). The largest effect was seen with the most rigid gel, the gelatin gel, where saliva caused large increases in flavour release, due to an increased surface area for diffusion of flavour compounds. Saliva has ability to enhance the water content of the system, thereby increased the surface area available for the diffusion of flavour compounds. This effect was found for the gelatin gel since it was a rigid gel and the addition of saliva seems to level out the influence of the gel rigidity (Boland et al. 2003).

The reported interaction of mucin with many biologically important entities including biopolymers prompted the preparation of microspheres from admixtures of mucin and gelatin (a widely used pharmaceutical adjuvant). Ofokansi et al. (2007), therefore, aimed to prepare microspheres from admixtures of gelatin and mucin and to evaluate the in vitro and in vivo delivery of ceftriaxone sodium from these microspheres. They observed that microspheres prepared from admixtures of gelatin and S-mucin adsorbed greater amounts of ceftriaxone ($p=0.05$) in comparison with those prepared from gelatin alone. Thus, they have concluded that in the presence of mucin, the intermolecular network and, possibly other characteristics of gelatin, were modified. The water sorption behavior in the two media further confirmed a modification of the gelatin microspheres by the mucin (Ofokansi et al. 2007). A possible enhancement of the mucoadhesive properties of gelatin

microspheres by the soluble portion of porcine mucin due to the modified intermolecular network and possibly other characteristics of gelatin in the presence of mucin was suggested in another study by Ofokansi et al. (2009).

Mucin interaction with galectin/lectin (carbohydrate binding proteins) /proline-rich-proteins

Although mucin plays a key role in the function and properties of mucus, it is the synergistic interaction of mucin with smaller proteins, salts, immunoglobulins, and water, which gives mucus its characteristic slimy, viscoelastic property that is responsible for the exceptional lubricating ability of saliva (Feilier et al. 2007). A number of studies have shown that the rheological properties of mucins vary enormously depending on the type (membrane or secreted) and source (human or animal) and the level of purification, and inclusion of other proteins as well as solution conditions (Bansil et al. 1995; Pearson, Allen, & Hutton, 200; Taylor et al., 2005).

An understanding of the biochemistry behind the known interactions between mucins and other proteins, coupled with an appreciation of their pathophysiological significance, can lend insight into the development of novel therapeutic agents. For instance, cancer-associated alteration in the peripheral carbohydrates of colonic mucins can serve as ligands for galactoside-binding protein galectin-3, which is expressed at higher levels in colon cancer than normal colon, binds to colon cancer mucin. Therefore, binding of galectin-3 to mucin may show therapeutic or preventative promise for colon cancer (Byrd et al. 2004). The binding of galectin-3 is carbohydrate-dependent, but is also influenced by the N-terminal domain, since phosphorylation of serine residue 6 reversibly inhibits binding of galectin-3 to colon cancer mucin (Cooper, 2002).

Wirth et al. (2002) investigated both binding rate and specificity of the mucus–lectin interaction; the binding of fluorescent-labelled analogues of plant lectins with different carbohydrate specificity to the pig gastric mucin coated microplates was studied. Even though the viscoelastic properties of the gastointestinal mucus were not mimicked by this assay, the qualitative composition of pig gastric mucin reflects that of the human one. At neutral pH, the lectin-binding capacity of mucin followed the order wheat germ agglutinin (WGA) (sialic acid and N-acetyl-Dglucosamine) >> Ulex europaeus isoagglutinin I (alpha- L-fucose) >> lentil lectin (alpha mannose) = potato lectin (N-acetyl-D-glucosamine) > peanut lectin (galactosamine) > Dolichos biflorus agglutinin (N-acetyl-galactosamine). This ranking rather reflects the steric accessibility of the mucus proteins than the molar composition of mucins. As sialic acids often operate as chain terminators at the linear or branched glycoproteins, the WGA-binding was highest. The mucin–lectin interaction is characterised by pH-dependence, specificity, and reversibility (Wirth et al. 2002). At pH 2.0 only 15% WGA, and at pH 6.0–7.0, 60–70% WGA were bound to pig gastric mucin as compared to the maximum binding rate at pH 5.0. Overall, it is expected that the strong and specific interaction between mucin and lectin-decorated formulations will result in anchoring of the drug delivery system at the site of absorption (Gabor et al. 2004).

Moreover, Dam et al. (2007) indicated that the longer polypeptide chain forms of porcine submaxillary gland mucins bind with higher affinities to the lectins, and that the total numbers of free GalNAc residues in porcine submaxillary gland mucins are important for binding to the lectins. They also proposed the internal diffusion model of a lectin jumping from carbohydrate epitope to epitope in a mucin chain is similar to that for a variety of ligands binding to DNA in which binding and sliding occur along the DNA backbone (von Hippel, 2007; Dam et al. 2007).

Argueso et al. (2009) investigated a new role for the carbohydrate-binding protein galectin-3 in stabilizing mucosal barriers through its interaction with mucins on the apical glycocalyx. Using the

surface of the eye as a model system, they found that galectin-3 colocalized with two distinct membrane-associated mucins, MUC1 and MUC16, on the apical surface of epithelial cells and that both mucins bound to galectin-3 affinity columns in a galactose dependent manner. These results suggest that galectin-3 plays a key role in maintaining mucosal barrier function through carbohydrate-dependent interactions with cell surface mucins. Regarding the mechanism by which the mucin-galectin-3 interaction contributes to the integrity of the mucosal barrier, they proposed that mucins, which are defined by the presence of amino acid tandem repeat domains with multiple O-glycan chains, form strong complexes with multivalent galectin-3 at the epithelial cell surface, as shown in the model in Fig. 9.

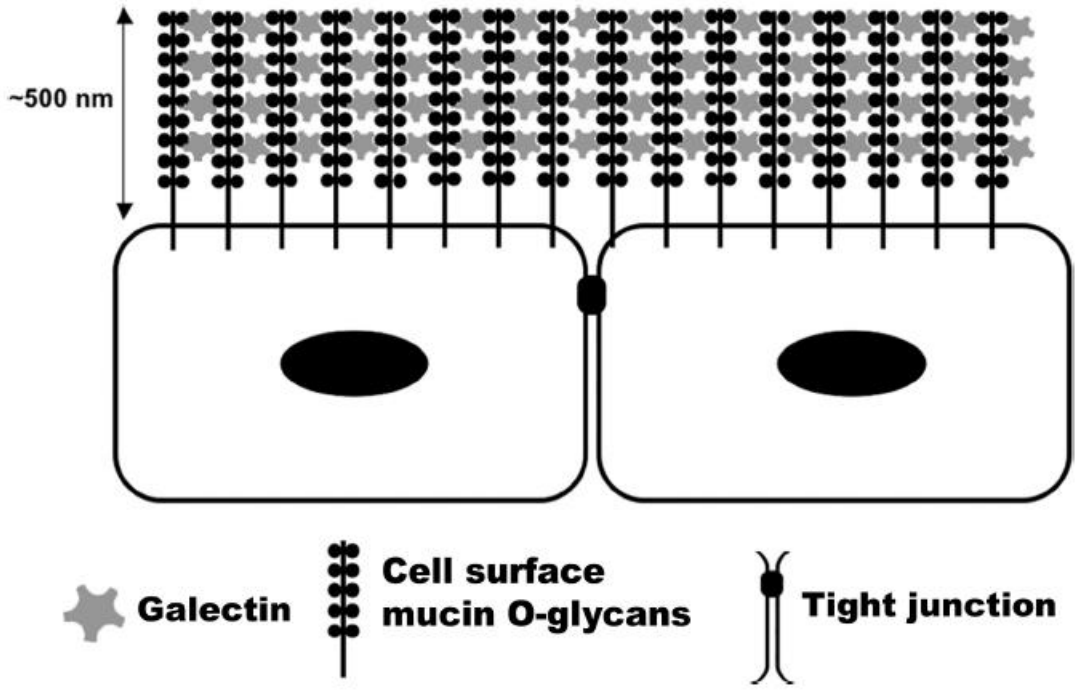

Fig. 9. Proposed model of galectin-mucin barrier formation on epithelial surfaces. (Argueso et al. 2009)

Furthermore, Zhao et al. (2010) have shown that the transmembrane mucin protein MUC1 is an endogenous ligand of galectin-3 in human colon cancer cells and that the interaction between MUC1 and galectin-3 occurs via binding of galectin-3 to the oncofetal Thomsen-Friedenreich carbohydrate (Galβ1,3GalNAcα-, T or TF) antigen on MUC1. They mentioned that the galectin-3-MUC1 interaction induces MUC1 cell surface polarization and exposure of the cell surface adhesion molecules (Fig. 10).

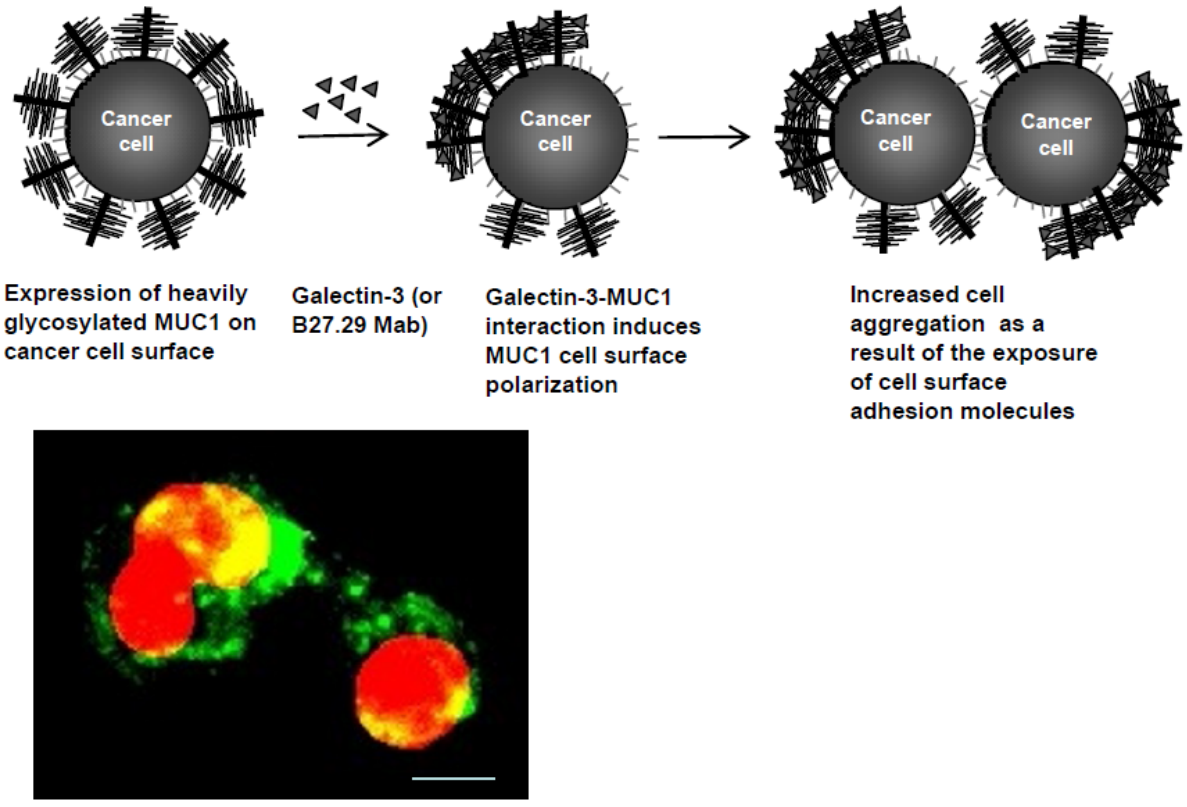

Fig. 10. Representative images of the MUC1 localization in cell aggregates are shown (top). Localization of the cell aggregates-associated MUC1 (green) after treatment of the cells with 1 μg/ml galectin-3 for 48 hr under suspension (red: cell nucleuses) (bottom). Bar = 10 μm. (Zhao et al. 2010)

Overall, it is shown that carbohydrate structures present in the highly glycosylated region of mucins make them potential candidates to interact with the galectin family of carbohydrate binding proteins (b-galactoside-specific lectins). In addition, immunological evidence demonstrates that MUC5B interacts with histatin and proline rich proteins (PRPs) in human salivary fluid (Iontcheva et al. 1997). The MUC5B–histatin interaction is a direct protein–protein interaction; mediated by the MUC5B Cys1, Cys2, and Cys8a (Iontcheva et al. 2000). By contrast, the interaction sites for PRPs remain uncharacterized. Another secretory mucin, MUC7 also interacts directly with PRP2, an acidic PRP via its N-terminal region (Bruno et al. 2005). In human saliva, a-amylase (a glycoside hydrolase) also interacts with MUC5B and MUC7 (Iontcheva et al. 1997; Bruno et al. 2005). The N-terminal region of MUC7 participates in the direct interaction between these two proteins. However, the nature of the α-amylase–MUC5B interaction, which was suggested to be non-covalent, remains incompletely characterized. Like histatins, statherin, another salivary protein, interacts directly with MUC5B; the MUC5B Cys8a-subdomain forms the binding site for statherin. The involvement of the MUC5B Cys1-, Cys2- and Cys8a-subdomains in directing interactions with statherin and histatins suggests that these proteins undergo a glycosylation-independent interaction (Senapati et al.2010). Soares et al. (2003) demonstrated that lactoferrin, an iron-binding protein, interacts directly with MUC7 in a glycosylation-independent manner. Interactions between secretory mucins and the aforementioned salivary proteins seem to be very important in the maintenance of oral physiology (Senapati et al. 2010). Experimental evidence indicates that PRP and statherin promote salivary calcium homeostasis. Statherins are also believed to promote the binding of helpful bacteria to the enamel surface. By contrast, the antimicrobial activities of histatins and lactoferins represent a major component of the non-immune host-defense system in the human oral cavity. Therefore, interactions between salivary mucins and various salivary proteins might help to enhance their stability and function.

Concluding remarks

Despite the fact that the physiology of the oral cavity is well studied, little is known about the oral behavior of food proteins and food-protein-stabilized emulsions. Thus in last decade there is a growing interest on mucin-protein interaction relating the food oral processing and digestion. For this purpose a number of experimental methods have been utilized and developed. For instance, sensory analysis with trained panelist, taste sensors, and viscoelastic measurements were used to observe changes in the taste perception after mucin/saliva interaction with food proteins due to the protein aggregation. Tribology tests were developed to measure friction by mimicking the rubbing contact in oral cavity lubricated by mucin/saliva and/or food protein solution/emulsion. Moreover, several spectroscopies were used to understand in detail the molecular level interaction and the structural changes of proteins. On the other hand, especially for drug delivery purposes, mucoadhesion properties of protein-mucin system via turbimetric measurements and surface adsorption techniques were commonly used.

Furthermore, most of the studies suggest an electrostatic attraction between positively charged proteins with negatively charged moieties of mucin (mainly on glycosylated region of mucin). However, our recent studies related to the BLG-mucin interactions, were the first to clearly suggest the importance of hydrophobic as well as the hydrophilic interactions. Important aspects such as of hydrophobic surface adsorption, structural and functional changes due to hydrophobic attraction in addition to the hydrophilic ones, were proposed. Overall, further studies are required to address in detail the hydrophobic and hydrophilic interactions attraction between mucin and (food) proteins. Moreover, despite the similar interaction mechanisms of mucin with other proteins and peptides, the conformation of the mucin and the other proteins, after the interaction take place, mostly determine their functional properties.

References

Argüeso, P., Guzman-Aranguez, A., Mantelli, F., Cao, Z., Ricciuto, J., & Panjwani, N. (2009). Association of cell surface mucins with galectin-3 contributes to the ocular surface epithelial barrier. *Journal of Biological Chemistry*, 284(34), 23037-23045.

Bansil, R., & Turner, B. S. (2006). Mucin structure, aggregation, physiological functions and biomedical applications. *Current Opinion in Colloid & Interface Science*, *11*(2-3), 164–170.

Bansil, R., Stanley, E., & LaMont, J. T. (1995). Mucin biophysics. *Annual Review of Physiology*, 57, 635–657.

Barylko-Pikielna, N., Martin, A., & Mela, D. J. (1994). Perception of taste and viscosity of oil-in-water and water-in-oil emulsions. *Journal of Food Science*, 59(6), 1318–1321.

Beecher, J. W., Drake, M. A., Luck, P. J., & Foegeding, E. A. (2008). Factors regulating astringency of whey protein beverages. *Journal of dairy science*, 91(7), 2553-2560.

Blijdenstein, T. B. J., Hendriks, W. P. G., van der Linden, E., van Vliet, T., & van Aken, G. A. (2003). Control of strength and stability of emulsion gels by a combination of long- and short-range interactions. *Langmuir*, 19(17), 6657–6663.

Blijdenstein, T. B. J., van Vliet, T., van der Linden, E., & van Aken, G. A. (2003). Suppression of depletion flocculation in oil in water emulsions: a kinetic effect of beta-lactoglobulin. *Food Hydrocolloids*, 17(5), 661–669.

Boland, A. B., Buhr, K., Giannouli, P., & Van Ruth, S. M. (2004). Influence of gelatin, starch, pectin and artificial saliva on the release of 11 flavour compounds from model gel systems. *Food Chemistry*, 86(3), 401-411.

Brandão, E., Silva, M. S., García-Estévez, I., Mateus, N., de Freitas, V., & Soares, S. (2017). Molecular study of mucin-procyanidin interaction by fluorescence quenching and Saturation Transfer Difference (STD)-NMR. *Food Chemistry*, 228, 427-434

Brownlow, S., Cabral, J. H. M., Cooper, R., Flower, D. R., Yewdall, S. J., Polikarpov, I., ... & Sawyer, L. (1997). Bovine β-lactoglobulin at 1.8 Å resolution—still an enigmatic lipocalin. *Structure*, 5(4), 481-495.

Bruno, L. S., Li, X., Wang, L., Soares, R. V., Siqueira, C. C., Oppenheim, F. G., ... & Offner, G. D. (2005). Two-hybrid analysis of human salivary mucin MUC7 interactions. *Biochimica et Biophysica Acta (BBA)-Molecular Cell Research*, 1746(1), 65-72.

Byrd, J. C., & Bresalier, R. S. (2004). Mucins and mucin binding proteins in colorectal cancer. *Cancer and Metastasis Reviews*, 23(1-2), 77-99.

Çelebioğlu, H. Y., Gudjónsdóttir, M., Chronakis, I. S., & Lee, S. (2016). Investigation of the interaction between mucins and β-lactoglobulin under tribological stress. *Food Hydrocolloids*, 54, 57–65.

Çelebioğlu, H. Y., Gudjónsdóttir, M., Meier, S., Duus, J. Ø., Lee, S., & Chronakis, I. S. (2015). Spectroscopic studies of the interactions between β-lactoglobulin and bovine submaxillary mucin. *Food Hydrocolloids*, 50, 203–210.

Chen, J., & Stokes, J. R. (2012). Rheology and tribology: Two distinctive regimes of food texture sensation. *Trends in Food Science & Technology*, 25(1), 4–12.

Chen, J., & Stokes, J. R. (2012). Rheology and tribology: Two distinctive regimes of food texture sensation. *Trends in Food Science & Technology*, 25(1), 4–12.

Chen, J., Liu, Z., & Prakash, S. (2014). Lubrication studies of fluid food using a simple experimental set up. *Food Hydrocolloids*, 42, 100–105.

Chojnicka-Paszun, A., de Jongh, H. H. J., & de Kruif, C. G. (2012). Sensory perception and lubrication properties of milk: Influence of fat content. *International Dairy Journal*, 26, 15–22.

Condelli, N., Dinnella, C., Cerone, A., Monteleone, E., & Bertuccioli, M. (2006). Prediction of perceived astringency induced by phenolic compounds II: Criteria for panel selection and preliminary application on wine samples. *Food Quality and Preference*, *17*(1), 96-107.

Cooper, D. N. (2002). Galectinomics: finding themes in complexity. *Biochimica et Biophysica Acta (BBA)-General Subjects*, 1572(2), 209-231.

Dam, T. K., Gerken, T. A., Cavada, B. S., Nascimento, K. S., Moura, T. R., & Brewer, C. F. (2007). Binding studies of α-GalNAc-specific lectins to the α-GalNAc (Tn-antigen) form of porcine submaxillary mucin and its smaller fragments. *Journal of Biological Chemistry*, 282(38), 28256-28263.

de Roos, K. B. (2003). Effect of texture and microstructure on flavour retention and release. *International Dairy Journal*, 13(8), 593–605.

de Wijk, R. A., van Gemert, L. J., Terpstra, M. E. J., & Wilkinson, C. L. S. O. (2003). Texture of semi-solids; sensory and instrumental measurements on vanilla custard desserts. *Food Quality and Preference*, 14(4), 305–317.

Dekker, J., Rossen, J. W., Büller, H. A., & Einerhand, A. W. (2002). The MUC family: an obituary. *Trends in biochemical sciences*, 27(3), 126-131.

Di Silvio, D., Rigby, N., Bajka, B., Mayes, A., Mackie, A., & Bombelli, F. B. (2015). Technical tip: high-resolution isolation of nanoparticle–protein corona complexes from physiological fluids. *Nanoscale*, 7(28), 11980-11990.

Dickinson, E. (2003). Hydrocolloids at interfaces and the influence on the properties of dispersed systems. *Food Hydrocolloids*, 17(1), 25-39.

Dickinson, E., & Pawlowsky, K. (1997). Influence of iota-carrageenan on flocculation, creaming and rheology of a protein-stabilized emulsion. *Journal of Agriculture and Food Chemistry*, 45, 3799–3806.

Doyen, K., Carey, M., Linforth, R. S. T., Marin, M., & Taylor, A. J. (2001). Volatile release from an emulsion: headspace and in-mouth studies. *Journal of Agriculture and Food Chemistry*, 49(2), 804–810.

Durrer, C., Irache, J. M., Duchene, D., & Ponchel, G. (1995). Mucin Interactions with Functionalized Polystyrene Latexes. *Journal of Colloid and Interface Science*, *170*(2), 555–561.

Edwards, P. B., Creamer, L. K., & Jameson, G. B. (2009). Structure and stability of whey proteins. In A. Thompson, M. Boland, & H. Singh (Eds.), Milk proteins: From expression to food (pp. 163–203). New York: Academic Press.

Efremova, N. V., Huang, Y., Peppas, N. A., & Leckband, D. E. (2002). Direct Measurement of Interactions between Tethered Poly (ethylene glycol) Chains and Adsorbed Mucin Layers. *Langmuir*, *18*(3), 836–845.

Engelen, L., de Wijk, R. A., Prinz, J. F., & Bosman, F. (2003). The relation between saliva flow after different stimulations and the perception of flavor and texture attributes in custard desserts. *Physiology and Behavior*, 78, 165–169.

Engelen, L., van den Keybus, P. A., de Wijk, R. A., Veerman, E. C., Amerongen, A. V. N., Bosman, F., ... & van der Bilt, A. (2007). The effect of saliva composition on texture perception of semi-solids. *Archives of Oral Biology*, 52(6), 518-525.

Fang, Y., & Dalgleish, D. (1997). Conformation of beta-Lactoglobulin Studied by FTIR: Effect of pH, Temperature, and Adsorption to the Oil-Water Interface. *Journal of Colloid and Interface Science*, 196(2), 292–298.

Feiler, A. A., Sahlholm, A., Sandberg, T., & Caldwell, K. D. (2007). Adsorption and viscoelastic properties of fractionated mucin (BSM) and bovine serum albumin (BSA) studied with quartz crystal microbalance (QCM-D). *Journal of colloid and interface science*, 315(2), 475-481.

Gabor, F., Bogner, E., Weissenboeck, A., & Wirth, M. (2004). The lectin–cell interaction and its implications to intestinal lectin-mediated drug delivery. *Advanced drug delivery reviews*, 56(4), 459-480.

Guo, T., Rudnick, P. A., Wang, W., Lee, C. S., DeVoe, D. L., & Balgley, B. M. (2006). Characterization of the human salivary proteome by capillary isoelectric focusing/nanoreversed-phase liquid chromatography coupled with ESI-tandem MS. Journal of proteome research, 5(6), 1469-1478.

Guzey, D., & McClements, D. J. (2006). Formation, stability and properties of multilayer emulsions for application in the food industry. *Advances in Colloid and Interface Science*, 128, 227-248.

Hagerman, A. E., and L. G. Butler. (1980). Determination of protein in tannin-protein precipitates. *Journal of Agricultural Food Chemistry*, 28:944–947.

Haslam, E. (1974). Polyphenol-protein interactions. *Biochemical Journal*, 139:285–288

He, P., Davis, S.S., Illum, L. (1998). In vitro evaluation of the mucoadhesive properties of chitosan microspheres. *International Journal of Pharmaceutics*, 166, 75–88.

Healy, T. W., & Lamer, V. K. (1964). Energetics of flocculation and redispersion by polymers. *Journal of Colloid Science*, 19(4), 323–332.

Holt, C., Carver, J. A., Ecroyd, H., & Thorn, D. C. (2013). Invited review: Caseins and the casein micelle: their biological functions, structures, and behavior in foods. *Journal of Dairy Science*, 96(10), 6127-6146.

Huq, N. L., Myroforidis, H., Cross, K. J., Stanton, D. P., Veith, P. D., Ward, B. R., & Reynolds, E. C. (2016). The Interactions of CPP–ACP with Saliva. *International Journal of Molecular Sciences*, 17(6), 915.

Hägerström, H., & Edsman, K. (2003). Limitations of the rheological mucoadhesion method: the effect of the choice of conditions and the rheological synergism parameter. *European Journal of Pharmaceutical Sciences*, 18(5), 349-357.

Iontcheva, I., Oppenheim, F. G., & Troxler, R. F. (1997). Human salivary mucin MG1 selectively forms heterotypic complexes with amylase, proline-rich proteins, statherin, and histatins. *Journal of Dental Research*, 76(3), 734-743.

Iontcheva, I., Oppenheim, F. G., Offner, G. D., & Troxler, R. F. (2000). Molecular mapping of statherin-and histatin-binding domains in human salivary mucin MG1 (MUC5B) by the yeast two-hybrid system. *Journal of Dental Research*, 79(2), 732-739.

Jobstyl, E., O'Connell, J., Fairclough, J. P. A., & Williamson, M. P. (2004). Molecular model for astringency produced by polyphenol/protein interactions. *Biomacromolecules*, 5(3), 942–949.

Johnston-Banks, F. A. (1990). Gelatine. In P. Harris (Ed.), Food gels (pp. 233–289). London: Elsevier Science.

Joyner Melito, H. S., Pernell, C. W., & Daubert, C. R. (2014). Impact of formulation and saliva on acid milk gel friction behavior. *Journal of Food Science*, 79, 67–80.

Kawasaki, K., & Weiss, K. M. (2003). Mineralized tissue and vertebrate evolution: the secretory calcium-binding phosphoprotein gene cluster. *Proceedings of the National Academy of Sciences*, 100(7), 4060-4065.

Kawasaki, K., Lafont, A. G., & Sire, J. Y. (2011). The evolution of milk casein genes from tooth genes before the origin of mammals. *Molecular Biology and Evolution*, 28(7), 2053-2061.

Kawasaki, K., Suzuki, T., & Weiss, K. M. (2004). Genetic basis for the evolution of vertebrate mineralized tissue. *Proceedings of the National Academy of Sciences of the United States of America*, 101(31), 11356-11361.

Kelly, M., Vardhanabhuti, B., Luck, P., Drake, M. A., Osborne, J., & Foegeding, E. A. (2010). Role of protein concentration and protein–saliva interactions in the astringency of whey proteins at low pH. *Journal of Dairy Science*, 93(5), 1900-1909.

Kilcast, D., & Clegg, S. (2002). Sensory perception of creaminess and its relationship with food structure. *Food Quality and Preference*, 13, 609–623.

Kinsella, J. E., & Whitehead, D. M. (1989). Proteins in whey: chemical, physical, and functional properties. *Advances in Food and Nutrition Research*, 33, 343-438.

Kontopidis, G., Holt, C., & Sawyer, L. (2004). Invited review: beta-lactoglobulin: binding properties, structure, and function. *Journal of Dairy Science*, 87(4), 785–96.

Kosters, H. A., Wierenga, P. A., de Vries, R., & Gruppen, H. (2013). Protein-peptide interaction: study of heat-induced aggregation and gelation of β-lactoglobulin in the presence of two peptides from its own hydrolysate. *Journal of Agricultural and Food Chemistry*, 61, 4218–4225.

Kralova, I., & Sjoblom, J. (2009). Surfactants used in food industry: a review. *Journal of Dispersion Science and Technology*, 30(9), 1363-1383.

Lai, S. K., Wang, Y. Y., & Hanes, J. (2009). Mucus-penetrating nanoparticles for drug and gene delivery to mucosal tissues. *Advanced Drug Delivery Reviews*, 61(2), 158-171.

Lee, S., Müller, M., Rezwan, K., & Spencer, N. D. (2005). Porcine gastric mucin (PGM) at the water/poly(dimethylsiloxane) (PDMS) interface: influence of pH and ionic strength on its conformation, adsorption, and aqueous lubrication properties. *Langmuir : The ACS Journal of Surfaces and Colloids*, *21*, 8344–8353.

Lehr, C. M. (1994). Bioadhesion technologies for the delivery of peptide and protein drugs to the gastrointestinal tract. *Critical Reviews in Therapeutic Drug Carrier Systems*, 11(2), 119-160.

Lemay, D. G., Lynn, D. J., Martin, W. F., Neville, M. C., Casey, T. M., Rincon, G., ... & Pollard, K. S. (2009). The bovine lactation genome: insights into the evolution of mammalian milk. *Genome Biology*, 10(4), R43.

Livney, Y. D. (2010). Milk proteins as vehicles for bioactives. *Current Opinion in Colloid & Interface Science*, 15(1-2), 73-83.

Madsen, F., Eberth, K., & Smart, J.D. (1996). A rheological evaluation of various mucus gels for use in in vitro mucoadhesion testing. *Pharmaceutical Science*, 2, 563–566.

Madsen, J. B., Sotres, J., Pakkanen, K. I., Efler, P., Svensson, B., Abou Hachem, M., ... & Lee, S. (2016). Structural and Mechanical Properties of Thin Films of Bovine Submaxillary Mucin versus Porcine Gastric Mucin on a Hydrophobic Surface in Aqueous Solutions. *Langmuir*, 32(38), 9687-9696.

Majhi, P. R., Ganta, R. R., Vanam, R. P., Seyrek, E., Giger, K., & Dubin, P. L. (2006). Electrostatically Driven Protein Aggregation : β-Lactoglobulin at Low Ionic Strength. *Langmuir*, 22(22), 9150–9159.

Malone, M. E., Appelqvist, I. A. M., & Norton, I. T. (2003). Oral behaviour of food hydrocolloids and emulsions. Part 1. Lubrication and deposition considerations. *Food Hydrocolloids*, 17(6), 763-773.

Mandalari, G., Mackie, A. M., Rigby, N. M., Wickham, M. S., & Mills, E. N. (2009). Physiological phosphatidylcholine protects bovine beta-lactoglobulin from simulated gastrointestinal proteolysis. *Molecular Nutrition & Food Research*, 53(1), 131–139.

McClements, D. J. (2004). Protein-stabilized emulsions. *Current Opinion in Colloid & Interface Science*, 9(5), 305-313.

Mehrotra, R., Thornton, D., & Sheehan, J. (1998). Isolation and physical characterization of the MUC7 (MG2) mucin from saliva: evidence for self-association. *Biochemical Journal*, *334*, 415–422.

Mei, L. Y., McClements, D. J., & Decker, E. A. (1999). Lipid oxidation in emulsions as affected by charge status of antioxidants and emulsion droplets. *Journal of Agricultural and Food Chemistry*, 47(6), 2267-2273.

Mei, L. Y., McClements, D. J., Wu, J. N., & Decker, E. A. (1998). Iron-catalyzed lipid oxidation in emulsion as affected by surfactant, pH and NaCl. *Food Chemistry*, 61 (3), 307-312.

Menchicchi, B., Fuenzalida, J. P., Bobbili, K. B., Hensel, A., Swamy, M. J. Goycoolea, F. M. (2014). Structure of chitosan determines its interactions with mucin. *Biomacromolecules*, 15, 3550-3558.

Menchicchi, B., Fuenzalida, J. P., Hensel, A., Swamy, M. J., David, L., Rochas, C., Goycoolea, F. M. (2015). Biophysical analysis of the molecular interactions between polysaccharides and mucin. *Biomacromolecules*, 16, 924-935.

Metcalf, K. L., & Vickers, Z. M. (2002). Taste intensities of oil-in-water emulsions with varying fat content. *Journal of Sensory Studies*, 17, 379–390.

Methven, L., Rahelu, K., Economou, N., Kinneavy, L., Ladbrooke-Davis, L., Kennedy, O. B., ... & Gosney, M. A. (2010). The effect of consumption volume on profile and liking of oral nutritional supplements of varied sweetness: Sequential profiling and boredom tests. *Food Quality and Preference*, 21(8), 948-955.

Meyer, D., Vermulst, J., Tromp, R. H., & de Hoog, E. H. A. (2011). The Effect of inulin on tribology and sensory profiles of skimmed milk. *Journal of Texture Studies*, 42, 387–393.

Miettinen, S.-M., Tuorila, H., Piironen, V., Vehkalahti, K., & Hyvonen, L. (2002). Effect of emulsion characteristics on the release of aroma as detected by sensory evaluation, static headspace gas chromatography, and electronic nose. *Journal of Agriculture and Food Chemistry*, 50(15), 4232–4239.

Monteleone, E., Condelli, N., Dinnella, C., & Bertuccioli, M. (2004). Prediction of perceived astringency induced by phenolic compounds. *Food Quality and Preference, 15*(7), 761-769.

Moreno, F. J., Mackie, A. R., & Mills, E. N. C. (2005). Phospholipid interactions protect the milk allergen alpha-lactalbumin from proteolysis during in vitro digestion. *Journal of Agricultural and Food Chemistry*, 53(25), 9810–9816.

Nikogeorgos, N., Madsen, J. B., & Lee, S. (2014). Influence of impurities and contact scale on the lubricating properties of bovine submaxillary mucin (BSM) films on a hydrophobic surface. *Colloids and Surfaces B: Biointerfaces*, 122, 760–6.

Nordman, H., Davies, J. R., Lindell, G., de Bolos, C., Real, F.,& Carlsted, I. (2002). Gastric MUC5AC and MUC6 are large oligomeric mucins that differ in size, glycosylation and tissue distribution. *Biochemical Journal*, 364, 191–200.

Ofokansi, K. C., Okore, V. C., & Adikwu, M. U. (2009). Biodegradable Microspheres Based on Gelatin–Porcine Mucin Admixtures: in Vitro and in Vivo Delivery Studies. *Biological and Pharmaceutical Bulletin*, 32(10), 1754-1759.

Ofokansi, K. C., Adikwu, M. U., & Okore, V. C. (2007). Preparation and evaluation of mucin-gelatin mucoadhesive microspheres for rectal delivery of ceftriaxone sodium. *Drug Development and Industrial Pharmacy*, 33(6), 691-700.

Pascal, C., Poncet-Legrand, C., Cabane, B., & Vernhet, A. (2008). Aggregation of a proline-rich protein induced by epigallocatechin gallate and condensed tannins: Effect of protein glycosylation. *Journal of Agricultural and Food Chemistry*, 56(15), 6724–6732.

Pearson, J. P., Allen, A., & Hutton, D. A. (2000). Rheology of mucin. *Glycoprotein Methods and Protocols: The Mucins*, 99-109.

Peppas, N. A., & Robinson, J. R. (1995). Bioadhesives for optimization of drug delivery. *Journal of Drug Targeting*, 3(3), 183-184.

Prakash, S., Tan, D. D. Y., & Chen, J. (2013). Applications of tribology in studying food oral processing and texture perception. *Food Research International*, 54, 1627–1635.

Qaqish, R., & Amiji, M. (1999). Synthesis of a fluorescent chitosan derivative and its application for the study of chitosan–mucin interactions. *Carbohydrate Polymers*, 38(2), 99-107.

Raikos, V. (2010). Effect of heat treatment on milk protein functionality at emulsion interfaces. A review. *Food Hydrocolloids*, 24(4), 259-265.

Rijnkels, M., Elnitski, L., Miller, W., & Rosen, J. M. (2003). Multispecies comparative analysis of a mammalian-specific genomic domain encoding secretory proteins. *Genomics*, 82(4), 417-432.

Rossi, S., Ferrari, F., Bonferoni, M.C., & Caramella, C. (2000). Characterization of chitosan hydrochloride–mucin interaction by means of viscosimetric and turbidimetric measurements. *European Journal of Pharmaceutical Science*, 10, 251–257.

Sakurai, K., & Goto, Y. (2002). Manipulating monomer-dimer equilibrium of bovine β-lactoglobulin by amino acid substitution. *Journal of Biological Chemistry*, 277(28), 25735-25740.

Sakurai, K., Konuma, T., Yagi, M., & Goto, Y. (2009). Structural dynamics and folding of β-lactoglobulin probed by heteronuclear NMR. *Biochimica et Biophysica Acta (BBA)-General Subjects*, 1790(6), 527-537.

Sakurai, K., Oobatake, M., & Goto, Y. (2001). Salt-dependent monomer–dimer equilibrium of bovine β-lactoglobulin at pH 3. *Protein Science*, 10(11), 2325-2335.

Sandberg, T., Blom, H., Caldwell, K. D. (2009). Potential use of mucins as biomaterial coatings. I. Fractionation, characterization, and model adsorption of bovine, porcine, and human mucins. *Journal of Biomed Materials Research A*, 91, 762-772.

Sano, H., Egashira, T., Kinekawa, Y., & Kitabatake, N. (2005). Astringency of bovine milk whey protein. *Journal of Dairy Science*, 88(7), 2312-2317.

Sarkar, A., Goh, K. K. T., & Singh, H. (2010). Properties of oil-in-water emulsions stabilized by b-lactoglobulin in simulated gastric fluid as influenced by ionic strength and presence of mucin. *Food Hydrocolloids*, 24, 534-541.

Sarkar, A., Goh, K. K. T., Singh, R. P., & Singh, H. (2009). Behaviour of an oil-in-water emulsion stabilized by b-lactoglobulin in an in vitro gastric model. *Food Hydrocolloids*, 23, 1563-1569.

Selway, N., & Stokes, J. R. (2013). Insights into the dynamics of oral lubrication and mouth feel using soft tribology: Differentiating semi-fluid foods with similar rheology. *Food Research International*, 54, 423–431.

Senapati, S., Das, S., & Batra, S. K. (2010). Mucin-interacting proteins: from function to therapeutics. *Trends in Biochemical Sciences*, *35*(4), 236–45.

Shi, L., Ardehali, R., Caldwell, K. D., & Valint, P. (2000). Mucin coating on polymeric material surfaces to suppress bacterial adhesion. *Colloids and Surfaces B: Biointerfaces*, *17*, 229–239.

Shrivastava, H. Y., & Nair, B. U. (2003). Structural modification and aggregation of mucin by chromium(III) complexes. *Journal of Biomolecular Structure & Dynamics*, 20(4), 575–87.

Silletti, E., Vingerhoeds, M. H., Norde, W., & Van Aken, G. A. (2007). The role of electrostatics in saliva-induced emulsion flocculation. *Food Hydrocolloids*, 21(4), 596-606.

Silletti, E., Vingerhoeds, M. H., Norde, W., & van Aken, G. A. (2007). Saliva-induced emulsion flocculation: role of droplet charge. In Food Colloids (pp. 463-472).

Silletti, E., Vitorino, R. M., Schipper, R., Amado, F. M., & Vingerhoeds, M. H. (2010). Identification of salivary proteins at oil–water interfaces stabilized by lysozyme and β-lactoglobulin. A*rchives of Oral Biology*, 55(4), 268-278.

Singh, H. (2011). Aspects of milk-protein-stabilised emulsions. *Food Hydrocolloids*, 25(8), 1938-1944.

Singh, H., & Ye, A. (2013). Structural and biochemical factors affecting the digestion of protein-stabilized emulsions. *Current Opinion in Colloid & Interface Science*, 18(4), 360-370.

Soares, R. V., Siqueira, C. C., Bruno, L. S., Oppenheim, F. G., Offner, G. D., & Troxler, R. F. (2003). MG2 and lactoferrin form a heterotypic complex in salivary secretions. *Journal of Dental Research*, 82(6), 471-475.

Sotres, J., & Arnebrant, T. (2013). Experimental Investigations of biological lubrication at the nanoscale: the cases of synovial joints and the oral cavity. *Lubricants*, 1(4), 102-131.

Steijns, J. M., & van Hooijdonk, A. C. M. (2000). Occurrence, structure, biochemical properties and technological characteristics of lactoferrin. *British Journal of Nutrition*, 84, 11-17

Taulier, N., & Chalikian, T. V. (2001). Characterization of pH-induced transitions of beta-lactoglobulin: ultrasonic, densimetric, and spectroscopic studies. *Journal of Molecular Biology*, 314(4), 873–89.

Taylor, C., Pearson, J. P., Draget, K. I., Dettmar, P. W., & Smidsrød, O. (2005). Rheological characterisation of mixed gels of mucin and alginate. *Carbohydrate Polymers*, 59(2), 189-195.

Teng, Z., Luo, Y., Li, Y., & Wang, Q. (2016). Cationic beta-lactoglobulin nanoparticles as a bioavailability enhancer: effect of surface properties and size on the transport and delivery in vitro. *Food Chemistry*, 204, 391-399.

Tokle, T., Lesmes, U., & McClements, D. J. (2010). Impact of electrostatic deposition of anionic polysaccharides on the stability of oil droplets coated by lactoferrin. *Journal of Agricultural and Food Chemistry*, 58(17), 9825-9832.

Uhrínová, S., Uhrín, D., Denton, H., Smith, M., Sawyer, L., & Barlow, P. N. (1998). Complete assignment of 1H, 13C and 15N chemical shifts for bovine beta-lactoglobulin: secondary structure and topology of the native state is retained in a partially unfolded form. *Journal of Biomolecular NMR*, 12(1), 89–107.

Van Aken, G. A. (2013). Acoustic emission measurement of rubbing and tapping contacts of skin and tongue surfaces in relation to tactile perception. *Food Hydrocolloids*, 31, 325–331.

van Aken, G.A., Vingerhoeds, M.H., & de Hoog, E.H.A. (2005). Colloidal behaviour of food emulsions under oral conditions. In E. Dickinson (Ed.), Food colloids 2004: interactions, microstructure and processing.

van Klinken, B. J. W., Einerhand, A. W. C., Bu¨ller, H. A., & Dekker, J. (1998). Strategic biochemical analysis of mucins. *Analytical Biochemistry*, 265, 103–116.

van Ruth, S. M., & Roozen, J. P. (2000a). Influence of mastication and saliva on aroma release in a model mouth system. *Food Chemistry*, 71, 339–345.

van Ruth, S. M., & Roozen, J. P. (2000b). Aroma compounds of oxidised sunflower oil and its oil-in water emulsion: Volatility and release under mouth conditions. *European Food Research and Technology*, 210, 258–262.

van Ruth, S. M., Roozen, J. P., & Cozijnsen, J. L. (1995). Changes in flavour release from rehydrated diced bell peppers (Capsicumannuum) by artificial saliva components in three mouth model systems. *Journal of the Science of Food and Agriculture*, 67, 189–196.

van Ruth, S., King, C., & Giannouli, P. (2002). Influence of lipid fraction, emulsifier fraction, and mean particle diameter of oil-in water emulsions on the release of 20 aroma compounds. *Journal of Agriculture and Food Chemistry*, 50, 2365–2371.

Vardhanabhuti, B., & Foegeding, E. A. (2010). Evidence of interactions between whey proteins and mucin: their implication on the astringency mechanism of whey proteins at low pH. In P. A. Williams, & G. O. Phillips (Eds.), Gums and stabilisers for the food industry 15 (pp. 137-146). Cambridge, UK: The Royal Society of Chemistry.

Vardhanabhuti, B., Cox, P. W., Norton, I. T., & Foegeding, E. A. (2011). Lubricating properties of human whole saliva as affected by β-lactoglobulin. *Food Hydrocolloids*, 25(6), 1499-1506.

Vardhanabhuti, B., Kelly, M. A., Luck, P. J., Drake, M. A., & Foegeding, E. A. (2010). Roles of charge interactions on astringency of whey proteins at low pH. *Journal of dairy science*, *93*(5), 1890-1899.

Vingerhoeds, M. H., Blijdenstein, T. B., Zoet, F. D., & van Aken, G. A. (2005). Emulsion flocculation induced by saliva and mucin. *Food Hydrocolloids*, 19(5), 915-922.

von Hippel, P. H. (2007). From “simple” DNA-protein interactions to the macromolecular machines of gene expression. *Annual Review of Biophysics and Biomolecular Structure*, 36, 79-105.

Wang, J., Tabata, Y., Bi, D., & Morimoto, K. (2001). Evaluation of gastric mucoadhesive properties of aminated gelatin microspheres. *Journal of Controlled Release*, 73, 223–231.

Wang, J., Tauch, Y., Deguchi, Y., Morimoto, K., Tabata, Y., & Ikada, Y. (2000) Positively charged gelatin microspheres as gastric mucoadhesive drug delivery system for clearance of H. pylori. *Drug Delivery*, 7, 237–243

Wirth, M., Gerhardt, K., Wurm, C., & Gabor, F. (2002). Lectin-mediated drug delivery: influence of mucin on cytoadhesion of plant lectins in vitro. *Journal of controlled release*, 79(1), 183-191.

Withers, C. A., Cook, M. T., Methven, L., Gosney, M. A., & Khutoryanskiy, V. V. (2013). Investigation of milk proteins binding to the oral mucosa. *Food & Function*, 4(11), 1668-1674.

Withers, C. A., Lewis, M. J., Gosney, M. A., & Methven, L. (2014). Potential sources of mouth drying in beverages fortified with dairy proteins: A comparison of casein-and whey-rich ingredients. *Journal of Dairy Science*, 97(3), 1233-1247.

Yakubov, G. E., McColl, J., Bongaerts, J. H., & Ramsden, J. J. (2009). Viscous boundary lubrication of hydrophobic surfaces by mucin. *Langmuir*, 25, 2313–2321.

Yan, Y., Hu, J., & Yao, P. (2009). Effects of casein, ovalbumin, and dextran on the astringency of tea polyphenols determined by quartz crystal microbalance with dissipation. *Langmuir*, 25, 397–402.

Ye, A., Streicher, C., & Singh, H. (2011). Interactions between whey proteins and salivary proteins as related to astringency of whey protein beverages at low pH. *Journal of Dairy Science*, 94(12), 5842-5850.

Ye, A., Zheng, T., Jack, Z. Y., & Singh, H. (2012). Potential role of the binding of whey proteins to human buccal cells on the perception of astringency in whey protein beverages. *Physiology & Behavior*, 106(5), 645-650.

Zalewska, A., Zwierz, K., Zo´ lkowski, K., & Gindzienski, A. (2000). Structure and biosynthesis of human salivary mucins. *Acta Biochimica Polonica*, 47(4), 1067–1079.

Zhang, R., Zhang, Z., Zhang, H., Decker, E.A., & McClements, D. J. (2010). Influence of emulsifier type on gastrointestinal fate of oil-in-water emulsions containing anionic dietary fiber (pectin). *Food Hydrocolloids*, 45, 175-185.

Zhao, Q., Barclay, M., Hilkens, J., Guo, X., Barrow, H., Rhodes, J. M., & Yu, L. G. (2010). Interaction between circulating galectin-3 and cancer-associated MUC1 enhances tumour cell homotypic aggregation and prevents anoikis. *Molecular Cancer*, 9(1), 154.

Zúñiga, R. N., Tolkach, A., Kulozik, U., & Aguilera, J. M. (2010). Kinetics of formation and physicochemical characterization of thermally-induced beta-lactoglobulin aggregates. *Journal of Food Science*, 75(5), 261–268.

CHAPTER 2

Spectroscopic studies of the interactions between β-lactoglobulin and bovine submaxillary mucin

(Paper I)

Food Hydrocolloids 50 (2015) 203–210

Contents lists available at ScienceDirect

Food Hydrocolloids

journal homepage: www.elsevier.com/locate/foodhyd

Spectroscopic studies of the interactions between β-lactoglobulin and bovine submaxillary mucin

Hilal Y. Çelebioğlu [a], María Gudjónsdóttir [a, *], Sebastian Meier [b], Jens Ø. Duus [b], Seunghwan Lee [c], Ioannis S. Chronakis [a, **]

[a] Technical University of Denmark, National Food Institute, Division of Industrial Food Research, Søltofts Plads, Building 227, 2800 Kongens Lyngby, Denmark
[b] Technical University of Denmark, Department of Chemistry, Building 201, 2800 Kongens Lyngby, Denmark
[c] Technical University of Denmark, Department of Mechanical Engineering, Building 425, 2800 Kongens Lyngby, Denmark

ARTICLE INFO

Article history:
Received 3 November 2014
Received in revised form
14 April 2015
Accepted 24 April 2015
Available online 7 May 2015

Keywords:
β-Lactoglobulin
Bovine submaxillary mucin
pH
NMR
CD
DLS

ABSTRACT

The structural changes occurring during the interaction between β-lactoglobulin (BLG), the major whey protein, and bovine submaxillary mucin (BSM), a major salivary protein, were studied using high and low field Nuclear Magnetic Resonance (NMR), Dynamic Light Scattering (DLS), and Circular Dichroism (CD) spectroscopy. The zeta potentials of the proteins were also measured to provide information on the role of electrostatic forces in the interaction. The ratio between BLG and BSM was 1:1, and pH was adjusted to 3.0, 5.0 and 7.4 at room temperature. These spectroscopic results suggested that the interaction between BSM and BLG led to a compact aggregation. DLS results of the mixture showed a size distribution which is intermediate between that of BLG (215 nm) and BSM (200 nm). While no particular changes in the secondary structure were observed in either BSM or BLG, a weak tertiary structure, observed in BLG only, was further weakened upon interaction with BSM. High field NMR results for the BSM-BLG mixture indicated that spectral differences were mostly observed for solvent exposed groups, especially the mucin glycan chains, while hydrophobic core residues were less affected. The interaction between the two proteins can thus be concluded to be mostly of hydrophilic origin. Moreover, low field NMR measurements showed a decrease in transverse relaxation times in the mixture compared to the pure BLG and buffer solutions. This is possibly connected to fewer hydrophilic binding sites available in the BLG–BSM mixtures for water–protein interaction after aggregation of the two proteins.

© 2015 Elsevier Ltd. All rights reserved.

1. Introduction

Proteins are important ingredients for food products in terms of providing desirable textural, sensory, and nutritional properties. In oral processing, food products are continuously mixed with saliva. Thus, on a molecular level, protein–protein interactions from food and saliva are highly expected. For this reason, it is likely that aggregates of these proteins, rather than pure food proteins, are ultimately interacting with the human body during consumption. Thus, it is necessary to clarify these protein–protein interactions to understand the functions of food proteins. Moreover, understanding protein–protein interaction would provide a new insight for further studies to determine their effects on perceived sensory attributes of foods.

Mucin is one of the major salivary proteins, which accompanies all food in digestion throughout the oral and gastrointestinal organs. Among several mucin types involved, submaxillary mucin is the one most related to oral processing. Bovine submaxillary mucin (BSM), used as a model mucin in this study, is a glycoprotein consisting of a linear polypeptide core with a highly glycosylated central part accounting for up to 80% of the proteins molecular weight (Shi, Ardehali, Caldwell, & Valint, 2000), which ranges between 0.5 and 20 MDa (Bansil & Turner, 2006). Due to the abundance of negatively charged groups, arising mainly from sialic acid residues and sulphated sugars, mucins generally have low isoelectric points, estimated to be between 2 and 3 (Durrer, Irache, Duchene, & Ponchel, 1995; Lee, Müller, Rezwan, & Spencer, 2005). The presence of many charged groups also

* Corresponding author. Tel.: +45 71706470.
** Corresponding author. Tel.: +45 40206413.
E-mail addresses: maguj@food.dtu.dk (M. Gudjónsdóttir), ioach@food.dtu.dk (I.S. Chronakis).

http://dx.doi.org/10.1016/j.foodhyd.2015.04.026
0268-005X/© 2015 Elsevier Ltd. All rights reserved.

results in pH-dependent physicochemical properties of the mucin molecules. Mucin molecules are amphiphilic due to alternating arrays of negatively charged, hydrophilic glycosylated regions (enriched with serine, threonine, and proline residues) and hydrophobic unglycosylated patches (enriched with cysteine residues). Monomeric mucin molecules can be linked with each other, for example via disulfide bonds by cysteine residues to form larger aggregates. Mucin's cysteine residues are capable of forming intermolecular bonds with other proteins as well (Mehrotra, Thornton, & Sheehan, 1998; Zalewska, Zwierz, Zółkowski, & Gindzieński, 2000). Additionally, mucins can also form aggregates with other proteins via non-covalent interactions by involving unglycosylated regions or oligosaccharide side chains (Senapati, Das, & Batra, 2010). However, not much attention has previously been paid to the interactions of mucins with food proteins.

β-Lactoglobulin (BLG) is one of the most important and extensively studied proteins of dairy food systems. Various attempts have been reported in literature to designate the effect of saliva/mucin to the milk protein especially by using the BLG-stabilized emulsions (Sarkar, Goh, & Singh, 2009; Sarkar, Goh, & Singh, 2010; Silletti, Vingerhoeds, Norde, & van Aken, 2007; Vingerhoeds, Blijdenstein, Zoet, & van Aken, 2005). Nevertheless, no literature is available for BLG and BSM interactions, which could be crucial to understand the critical points affecting the structure of mucin and sensory properties of BLG-contained-food products. BLG is the major whey protein constituting of >50% of the total whey proteins in bovine milk. BLG is a typical globular protein with molecular weight of 18.3 kDa and a radius of approximately 2 nm (Zúñiga, Tolkach, Kulozik, & Aguilera, 2010). According to its amino acid sequence and three-dimensional structure, BLG belongs to the lipocalin family, which can bind to small hydrophobic ligands and may thus act as specific transporters (Kontopidis, Holt, & Sawyer, 2004). BLG contains many charged groups and its structure and properties therefore depend strongly on the pH and ionic strength (Fang & Dalgleish, 1997). Taulier and Chalikian (2001) mentioned six pH-dependent structural states of BLG depending on solution conditions and characterized the acid- and base-induced conformational transitions between these structural states over the pH range from 1 to 13. This pH-dependent system may indicate that one of BLG functions is to bind to non-polar molecules and transport them through the acidic environment (stomach) into the basic environment (intestine). This strong pH dependency suggests that electrostatic interactions could play a significant role in interactions of BLG with other molecules. The electrostatic attractions even enhance the protein aggregation due to BLG–BLG interaction (Majhi et al., 2006). An association between peptides and BLG due to electrostatic attraction was recently observed in the study of Kosters, Wierenga, de Vries, and Gruppen (2013). They also observed stronger binding or even the formation of a covalent interaction between the free sulfhydryl group of the peptides and a cysteine residue of the BLG.

In the present study, we have focused on the interactions of BSM with BLG at different pH values in order to understand the protein–protein interactions in a food-saliva model system. In order to establish a basis to understand food oral processing of the two proteins on the molecular level, we have selected 1:1 ratio in the present study. Dynamic light scattering (DLS) was employed to investigate the changes in hydrodynamic radius of proteins. High and low field Nuclear Magnetic Resonance (NMR) techniques were employed to characterize interactions by monitoring changes on the chemical shifts of proteins residues. Finally, secondary and tertiary structures of proteins were studied using circular dichroism (CD) spectroscopy.

2. Materials and methods

2.1. Sample preparation

BLG from bovine milk and BSM (Type I–S) were purchased from Sigma–Aldrich (Sigma–Aldrich A/S, Brøndby, Denmark), and were used as received. Protein solutions with concentrations of 1 and 10 mg/mL were prepared by dissolving proteins in 10 mM phosphate buffered saline (PBS) solutions. The pH values of the buffer solutions were adjusted to 7.4, 5.0, and 3.0 by addition of HCl or NaOH as appropriate. For the mixture of BSM and BLG, the two protein solutions were mixed directly at the ratio of 1:1 (v:v).

2.2. Zeta potential and dynamic light scattering (DLS) measurements

Zeta-potential and DLS measurements were performed on the BLG, BSM and their mixtures with varying pH with a Zetasizer Nano ZS instrument (Malvern Instruments Ltd, Worcestershire, UK) to determine the charge and the particle size distribution of the proteins. Dispersions of 1 mL samples (10 mg/mL) were examined with a 10 mm path–length disposable polystyrene cuvette at 25 °C using a He–Ne Laser light source at 633 nm for DLS measurements, whereas the disposable cuvette with model DTS 1070 were used for zeta potential. During the DLS analysis the instrument used the backscattering configuration where detection was conducted at a scattering angle of 173°, thus reducing multiple scattering effects. The principle of hydrodynamic size distribution analysis by DLS is to measure the diffusion of the particles which are moving under Brownian motion and to convert the diffusion measurements to size and size distribution, using the Stokes–Einstein relationship. The number distribution was calculated from the intensity distribution by the installed software (Zetasizer software version 7.02) as shown below;

$$\frac{Ni}{\sum Ni} = \frac{Ii/Ri^{2x}}{\sum Ii/Ri^{2x}}$$

where N is the number concentration, I is the scattering intensity of the particles, R is the radius, and x is a shape parameter equal to 3 for spheres and 2 for coils. The number distribution is useful to prevent any shift towards higher values as a consequence of the higher scattering of the larger particles. The measurements were conducted at least in triplicate.

2.3. High field NMR measurements

Samples of BLG and BSM were produced at concentrations of 10 mg/mL in aqueous 50 mM PBS buffers of pH 3, 5 or 7.4. Buffers were prepared as aqueous solutions prior to freeze drying and redissolution in deuterium oxide (D_2O) (99.9%; Sigma–Aldrich A/S, Brøndby, Denmark). In addition to individual samples of BSM and BLG, 1:1 mixtures of BSM and BLG were prepared at the three different pH values. In the absence of isotope-enriched material, the BLG and BSM were assayed for interactions using ^{1}H NMR spectroscopy as follows. Samples of BLG and BSM in isolation were subjected to high-resolution ^{1}H NMR spectroscopy. Sum spectra of the BLG and BSM component spectra were constructed, and these sum spectra were then compared to the mixture spectra recorded on 1:1 (v:v) mixtures of BLG and BSM. To correct for the dilution effect on the concentrations by mixing the two pure solutions the intensity of the mixture spectra was multiplied by 2 before being compared to the sum spectra. All high-field NMR spectra were recorded at 25 °C on a 600 MHz Bruker (Bruker, Fällanden,

Switzerland) Avance spectrometer equipped with a TXI SmartProbe, by sampling 16,386 complex data points during an acquisition time of 1.7 s. Spectra were recorded and processed with extensive zero filling in Topspin 3.0 (Bruker, Rheinstetten, Germany), and a standard pre-saturation sequence was used to suppress residual water signals in the spectra of all samples.

2.4. Low field NMR measurements

A MARAN Magnetic Resonance spectrometer (Resonance Instruments, Witney, UK) with a magnetic field strength of 0.5 T and a proton frequency of 23.4 MHz was used for low field NMR measurements. The protein solutions (4 mL of 10 mg/mL concentration) were placed in sample cells with an inner diameter of 13 mm. These sample cells were placed in the sample tubes (18-mm-diameter). All samples were kept in a water bath in order to reach a stable temperature of 25 °C before the measurements. Measurements were conducted in triplicate. A Carr–Purcell–Meiboom–Gill (CPMG) pulse sequence was applied to measure the proton transversal (T_2) relaxation times (Carr & Purcell, 1954; Meiboom & Gill, 1958). The inter-pulse spacing τ was set to 1500 μs, the 90° pulse length was 9.4 μs and the number of data points acquired was 2048. A recycle delay of 6 s was used and each sample was scanned eight times. The obtained relaxation data was maximum normalized and fitted to an exponential curve, as expressed by the equation:

$$I = \sum_{i=1}^{n} A_i exp\left(-\frac{t}{T_{2i}}\right) + \xi$$

where I is the intensity of the signal, T_{2i} is the proton relaxation time of proton population i in the sample, A_i is the corresponding amount of protons in that same population i, n is the number of proton populations and ξ is the model error. The Low Field NMR Toolbox for Matlab (The Mathworks Inc., Natick, Mass., U.S.A.) was used for the data fitting as described by Pedersen, Bro, and Engelsen (2002). Residual model fitting analysis was used to assess the number of water pools present in the samples.

2.5. Circular dichroism (CD) spectroscopy

CD spectra were recorded at 25 °C using a Chirascan spectrophotometer (Applied Photophysics Ltd., Surrey, UK). The far UV CD spectra were recorded from 280 to 185 nm using a 1 mm path-length cuvette with a step size of 1 nm and bandwidth of 1 nm. The near UV CD spectra were recorded from 450 to 260 nm using a 1 mm path-length cuvette with the step size of 2 nm and bandwidth of 0.8 nm. The protein concentration was 1 mg/mL and 10 mg/mL for far UV CD and near UV CD measurements, respectively. The protein solutions were scanned three times and the scans were averaged to reduce the noise. The spectra obtained were subtracted from the spectrum of the solvent.

3. Results and discussion

3.1. Zeta potential of the proteins

Zeta potential measurements were performed to estimate the surface charge characteristics of the proteins. As the surface charge characteristics of both proteins are subject to change according to pH change, zeta potential can provide useful information on the molecular level interaction of the two proteins. In Table 1 the zeta potential of BLG, BSM and BLG–BSM mixture are presented as a function of the solution pH. A zeta potential of near 0 mV was observed at pH 5 for the BLG, which is indicative for almost zero net charge and consequently the isoelectric point (IEP) of BLG. When the pH was shifted away from the IEP of BLG, the absolute value of the zeta potential increased substantially. As expected, positive and negative zeta potentials were measured at pH 3 and 7.4, respectively, which is also in a close agreement with the study of Engelhardt et al. (2013). A gradual decrease in the absolute value of negative zeta potential (from −12.64 to −7.01) of BSM with decreasing pH (from pH 7.4 to pH 3.0) indicated a decrease in total net charge, which is expected with approaching the IEP. Despite these changes, the zeta potentials of both BLG and BSM remained negative at pH 7.4 and 5, whereas they are oppositely charged at pH 3. Thus, electrostatic attraction between BLG and BSM can more readily occur at pH 3 than at other pH conditions. The zeta potentials of the BLG–BSM mixture followed the trend of BSM; that is, the lower pH gave lower absolute negative zeta potential. The BSM dominated the surface charge characteristics of the BLG–BSM mixture and it can be assumed that the BLG is placed inside of the BSM molecules after binding and forming entangled BSM.

Table 1
Zeta potential of BSM, BLG and BLG–BSM mixture at pH 7.4, 5.0, and 3.0.

pH	Sample	Zeta potential (mV)	
		Mean	Stdev
7.4	BSM	−12.64	0.57
	BLG	−12.00	0.72
	BLG–BSM mixture	−11.10	0.79
5.0	BSM	−10.70	0.64
	BLG	−1.14	0.69
	BLG–BSM mixture	−9.28	0.56
3.0	BSM	−8.69	0.45
	BLG	2.18	0.59
	BLG–BSM mixture	−6.36	0.55

3.2. Hydrodynamic size distribution by DLS

Fig. 1 demonstrates the size distribution plots of BLG, BSM and the mixture, respectively, at 10 mg/mL concentration. At all three pHs, BLG showed an average hydrodynamic diameter of 6.5 nm which is consistent with the studies of Zúñiga et al. (2010), Martinez, Sánchez, Patino, and Pilosof (2009) and Rullier, Novales, and Axelos (2008), each of who reported a BLG diameter of 6.7, 6.5 and 6 nm, respectively. The size vs. number curves did not show any significant changes in the average hydrodynamic radius of BLG, BSM or the mixture with changing pH in the present study. Therefore, the size distribution of the proteins at pH 7.4 only was shown in Fig. 1 for clarity. The full DLS data, including the size distribution of the proteins at pH 3 and 5, are provided in Supplementary Information. In this study, we have analyzed the size distribution of the molecules according to the number than intensity because of substantially different sizes of the two proteins. For the intensity-based DLS plots the light scattered from larger particles (BSM) was dominant in the multi-dispersed system,

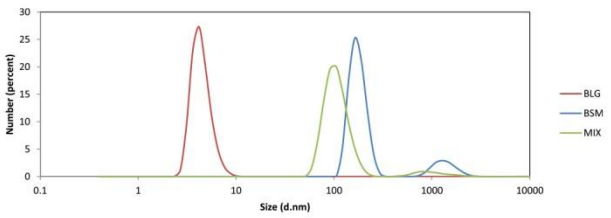

Fig. 1. Size distribution curves of β-lactoglobulin (BLG), bovine submaxillary mucin (BSM), BSM and BLG mixture (1:1) at pH 7.4.

so that the much smaller populations (BLG) could be undetectable in the presence of the larger BSM molecules. Accordingly, the populations of the small and large particles tend to be under- and overestimated, respectively. Meanwhile, as number-based DLS plots are obtained from numerical data processing of intensity-based plots, the accuracy of the data can be inferior to intensity plots.

For BSM, one large peak with the maximum at around 165 nm, and one small peak between 700 nm and 2000 nm were observed (Fig. 1) The bimodal distribution of the BSM molecules, as characterized by DLS in this study, was consistent with previous studies (Bastardo, Claesson, & Brown, 2002; Drug et al., 2011), while a multi-modal population of BSM is often reported. Notably, the size distribution of BSM in this study was significantly influenced by the high concentration of BSM, i.e. 10 mg/mL, which was employed in order to have a high relevance with physiological conditions (Bansil, Stanley, & LaMont, 1995). Furthermore, the high concentration increases the possibility of the molecules clustering together. For example, a control DLS experiment at 1 mg/mL showed only molecules smaller than 100 nm in number-weighted plots (data not shown). DLS results showed that there was no further pH-induced clustering or aggregation of the BSM within the pH range of 3.0–7.4 (the data at other pH values than 7.4 are available in Supplementary Information), presumably because the concentration-driven aggregation was already dominant. As the difference in size distribution of BSM and BLG was clear, a simple overlay of the two populations of the proteins was expected from the mixed sample if no interactions between the two proteins would occur. However, the size distribution of the mixture (Fig. 1) indicated that the BLG peak (corresponding to ca. 6 nm) completely disappeared in the mixture, while new peaks, indicating the presence of molecules with a smaller size than BSM were formed. The vanishing BLG peak, weakening of larger BSM peaks, and the formation of new peaks, which were located between those of the BLG and the BSM in size distribution, suggested attractive interaction between the two proteins. One possible explanation is that the BLG molecules bind to the BSM molecules resulting in a more compact conformation of the BSM molecules.

3.3. High-resolution NMR probing of BLG–BSM interactions

Owing to its high spectral resolution and rich information content, high-field NMR spectroscopy is a suitable method to characterize the BLG–BSM binding in more detail. Fig. 2 shows the sum spectrum (simply the addition of the BLG and BSM spectra), the mixture spectrum (the spectrum of the BLG–BSM mixture) and the difference of the sum spectrum and the mixture spectrum of BLG and BSM, in order to observe spectral changes upon mixing of BLG and BSM at the three different pH values. All spectra contained a residual water peak, at a chemical shift of approximately 4.7 ppm, which was removed from the spectra shown in Fig. 2. Spectra of the pure BLG and BSM as well as the mixture solution at pH 3 are furthermore shown in Appendix 1 to serve as an example for detailed presentation of the chemical shifts of the basic solutions. A complete assignation of ^{1}H chemical shifts for bovine BLG have previously been performed by Uhrínová et al. (1998) and will not be repeated here. A complete chemical shift assignment for BSM is not available from literature. However, Gerken (1986) performed a complete ovine submaxillary mucin (OSM) proton peak assignment and similarities between the two mucin types eased interpretation of the high field NMR results. Since it is known that the polypeptide backbone of BSM has a repeated amino acid sequence (GTTVAPGSSNT), as well as the composition of the highly glycosylated regions is known (Strous & Dekker, 1992), the appropriate

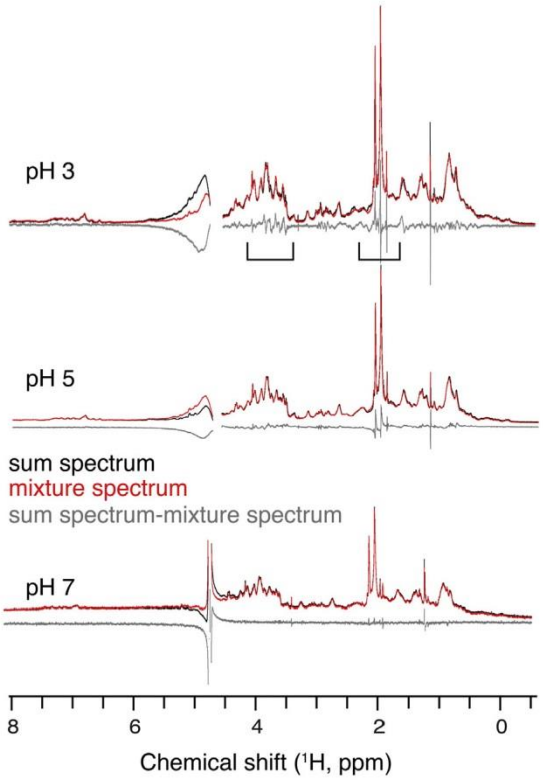

Fig. 2. High field ^{1}H NMR spectra of BLG and BSM sum spectra (black), mixture (1:1) spectra (red) and the calculated difference spectra between the sum and mixture spectra (grey) at pH 3.0, 5.0 and 7.4. (For interpretation of the references to colour in this figure legend, the reader is referred to the web version of this article.)

chemical shifts for the BSM could be estimated (Appendix 1–2). However, due to the large size and heterogeneity of the BSM protein, as well as a high degree of resonance overlapping in the present amino acids, a simplified approach was chosen for peak assignation. The focus was placed on the characterizing changes in the spectra before and after interaction of the two solutions by studying the differences between the mixture solution and generated sum spectrum of the pure solutions (Fig. 2). According to these spectra the most likely places of interaction between the two proteins were be found in the chemical shift intervals between 1.6 and 2.4 ppm and from 3.1 to 4.4 ppm. The present interacting residues of the BSM in these chemical shifts intervals are presented in Appendix 2. However one can appeal to the study of Uhrínová et al. (1998) to see the amino acids of the BLG in the suggested interacting intervals.

At pH 7.4, there was no detectable sign of interaction according to the spectral similarity of the sum and the mixture spectrum. In contrast, the high-resolution NMR assay yielded spectral differences between the mixture and sum spectra at pH 5 and even more so at pH 3. As expected, spectral differences were mostly observed for solvent exposed groups, especially the mucin glycan chains, while hydrophobic core residues (chemical shift near 0 ppm) were less affected by the mixing of BLG and BSM. Likewise, no significant changes in ^{1}H NMR spectral appearance were observed in the aromatic region, indicating that the aromatic amino acids did not play a significant role in the interaction between the two proteins (Fig. 2).

The trend towards stronger interactions at lower pH (Fig. 2) could be rationalized as follows. At pH 7.4, both the BSM and the BLG had a higher negative charge than at pH 5 and pH 3 as shown by zeta-potential results (Table 1) giving an impression that the electrostatic repulsion was preventing the interaction at pH 7.4. However, the electrostatic repulsion could not be the main factor that prevented the interaction at pH 7.4; instead, carboxyl groups (e.g. sialic acids) in the mucin molecule could have important effects on the interaction, as suggested by Svensson, Thuresson, and Arnebrant (2008). A stronger interaction at acidic pH in Fig. 2 could also be explained by that the carboxyl groups of mucin are protonated at a higher fraction at pH 5 and pH 3 than at pH 7.4, and more hydrogen bonds can be formed with the oxygen in the BLG molecules. Efremova, Huang, Peppas, and Leckband (2002) also suggested a stronger interaction of bovine submaxillary mucin with poly (ethylene oxide) at lower pH due to hydrogen bonding in their study. In addition, more signal reduction and the shifts of the peaks at pH 3 compared to pH 5 in Fig. 2 could be attributed to stronger interactions between amino groups in the BLG molecule and negatively charged groups in the mucin molecule; BLG (pI: 5.2) has a higher amount of protonated amino groups that can form electrostatic attraction with negatively charged groups in the BSM at pH 3. Electrostatic interaction of mucins with positively charged molecules, such as chitosan, has also been suggested in several earlier studies (Shrivastava & Nair, 2003; Sinha et al., 2004; Svensson, Lindh, Cárdenas, & Arnebrant, 2006; Takeuchi, Yamamoto, & Kawashima, 2001;). The higher hydrophilic interaction between the proteins at lower pH supports the pH dependent activity of both BLG and BSM. Furthermore, the positively charged groups of BLG, especially at acidic pHs, as shown by the zeta potential analysis (Table 1), neutralize negatively charged groups of BSM and cause the BSM to coil or contract into a smaller hydrodynamic volume, as suggested by Shrivastava and Nair (2003). In fact, even a weak hydrogen bonding between BLG and BSM brings about aggregation of mucin into a more compact structure at pH 7.4 as well according to our DLS results. The NMR results implied that negatively charged BLG has a tendency to interact with negatively charged mucin via secondary interactions (hydrogen bonding and hydrophobic effects), where the electrostatic interactions are unlikely to be the main reason of the binding. Furthermore the studies of Withers, Cook, Methven, Gosney, and Khutoryanskiy (2013) and Ye, Zheng, Ye, and Singh (2012) showed the binding of BLG to the mucosa at neutral pH, which agrees with our results.

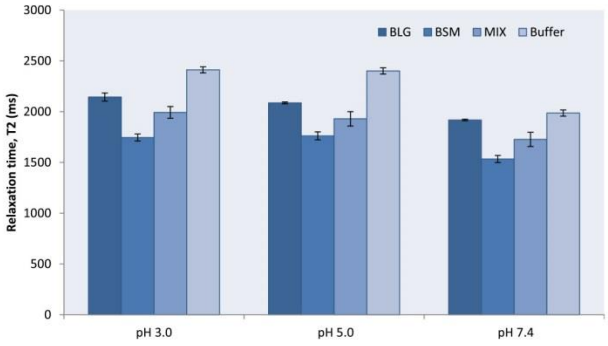

Fig. 3. Low field NMR T_2 transversal relaxation times of the BLG, BSM, BLG–BSM mixture and buffer solutions at pH 3.0, 5.0, and 7.4.

3.4. T_2 relaxation time assignment by low field NMR

Fig. 3 demonstrates the transverse T_2 relaxation times of the protein and buffer solutions (10 mg/mL) at the different pH values. A mono-exponential transverse T_2 relaxation time was observed for all solutions. Differences in the relaxation time were thus a measure of the exchange of hydrogen protons (from water) with the solute and how this exchange was affected by the different proteins present at the various pH environments.

Shorter relaxation times were observed at neutral pH than at the acidic pH values for all solutions. This is believed to be partly caused by the buffer characteristics at each pH, as different concentrations of HCl and NaOH were used to adjust the pH of the buffer solutions as appropriate. These buffer solutions were then used to prepare the protein solutions, explaining the shorter T_2 relaxation times observed in all solutions at neutral pH compared to the acidic pH values. In addition, Kontopidis et al. (2004) stated that BLG dissolves best in neutral, dilute salt solutions (similar to the buffer solution used in this study), while BSM starts to be protonated at acidic conditions, leading to the loss of solubility in water (Svensson et al., 2008). Granizo, Reuhs, Stroshine, and Mauer (2007) successfully used low field NMR relaxometry to monitor changes in solubility and hydration of food powders, such as purified BLG, zein, glucose and cellulose over time. As the degree of solubility of the proteins is connected to protein-water interference, it is also possible that this pH-induced effect on the molecules solubility was reflected in the obtained relaxation times.

The relaxation behavior of the protein solutions at varying pH conditions showed a similar trend between the three protein solutions at each pH values studied. The obtained relaxation times for BLG were in the range from 1918 to 2143 ms, which is similar to the values obtained by Indrawati, Stroshine, and Narsimhan (2007) and Kumosinski and Pessen (1982) for similar concentrations of BLG. A significantly shorter T_2 relaxation time was obtained for the BSM, indicating a stronger protein-water interaction and more "restricted" water structure in the BSM solutions compared to the BLG solutions. Haque, Bhandari, Gidley, Deeth, and Whittaker (2011) investigated the changes in water–protein interactions related to protein conformational modifications and solubility changes in milk protein concentrates. Their study indicated that water molecules can interact with the protein surface to a greater extent as the proteins unfolded and that the water molecules ordered themselves into layers around the charged groups on the protein surface. In the mixture of BLG and BSM, a longer T_2 relaxation time was observed at all pH values compared to the pure BSM, indicating an increase in the bulk water mobility. This is in agreement with the high field NMR results in the sense that the main interaction between BSM and BLG appeared in the hydrophilic parts of the proteins, thus leaving fewer charged groups on the proteins surfaces available for protein-water interaction. Moreover, according to the DLS results, the interaction between the two proteins caused a more compact molecular configuration, which might also affect the protein and bulk water exchange rates due to changes in the availability of charged groups on the protein surface. This is in agreement with the observations of Indrawati et al. (2007), which stated that the transverse relaxation time was inversely correlated to the hydrodynamic radius of the BLG solutions studied.

3.5. Protein conformation by CD spectroscopy

The far-UV CD spectra of the BLG solutions (1 mg/mL) at pH 3, 5, and 7.4 are shown in Fig. 4(a). A lower protein

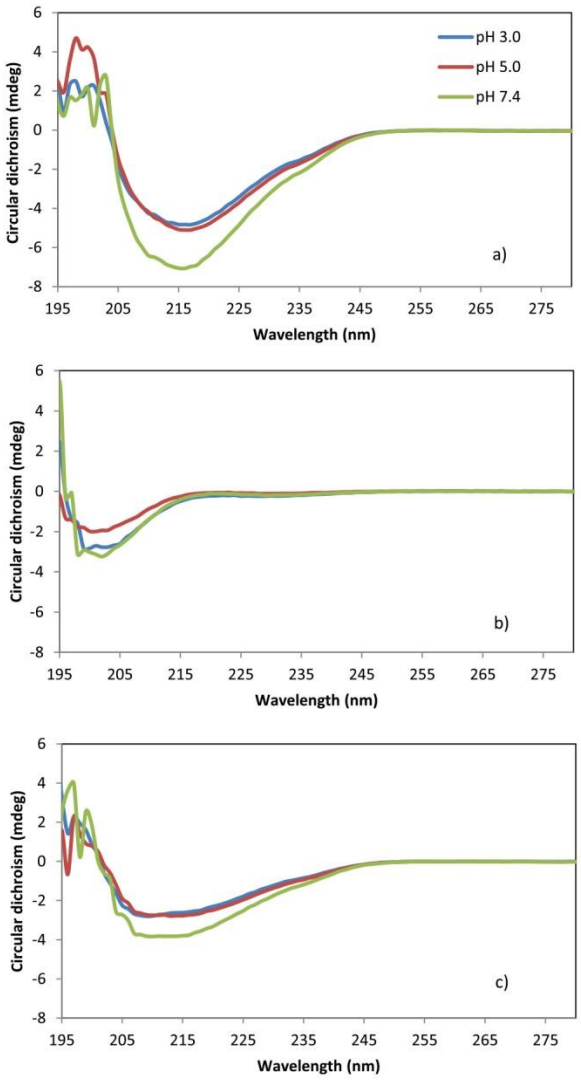

Fig. 4. Far-UV CD spectra of (a) BLG (b) BSM (c) BLG–BSM mixture at pH 3.0, 5.0 and 7.4.

concentration was used for far-UV CD spectroscopy in order to avoid too high light scattering and consequent poor signals obtained with 10 mg/mL solutions. In general, the far-UV CD spectra of BLG were in agreement with those reported by Taulier and Chalikian (2001). The spectra of Fig. 4(a) revealed that, at each pH, the protein exhibited a broad negative peak at around 218 nm, which is characteristic of a protein with well-defined antiparallel β-pleated sheets (β-helices) (Greenfield, 2006). The reduction in the intensity of the negative peak at pH 3 and pH 5 indicated a slight weakening of β-sheet structure, resulting from acid-induced aggregation or dimer-to-monomer transition. The far-UV CD spectra of BSM at all three pHs presented a very weak negative band near 200 nm, indicating a random coil conformation (Fig. 4(b)) in agreement with the observations of Madsen, Pakkanen, and Lee (2013). The absence of well-ordered α-helix or β-pleated sheet structure of BSM presumably is a consequence of the high glycosylation of the majority of the BSM surface. Unlike BLG, BSM showed a clear reduction in the peak intensity only at pH 3, which might be related to that BSM has a lower pI (2–3) (Perez & Proust, 1987) than BLG (5.2) (Leo, Pecquet, Rojas, Couvreur, & Fattal, 1998). The far-UV CD spectra of the BLG–BSM mixture showed an intermediate peak between those of the two proteins spectra; the negative peak minimum of the mixture was observed at around 210 nm, which is intermediate between that of BLG (215 nm) and BSM (200 nm). Furthermore, the peak intensity was weaker for the mixture than for BLG, but stronger than for BSM. This finding could be due to the concentration of the BLG, the chief resource of the negative peak intensity, being half in the mixture compared to the concentration of the BLG solution alone. Thus, the changes in the far UV CD spectra for the mixture of BLG and BSM could be simply due to an overlay of the spectra of the two proteins (Fig. 4(c)). But, in connection with the DLS data (Fig. 1), it can be argued that the changes indicate the interaction between the two proteins. Near-UV CD spectra of BLG, BSM and the mixture at 10 mg/mL concentration were also obtained in order to characterize the tertiary structures (Fig. 5). The spectrum of Fig. 5(a) showed two sharper and pronounced peaks at 285 and

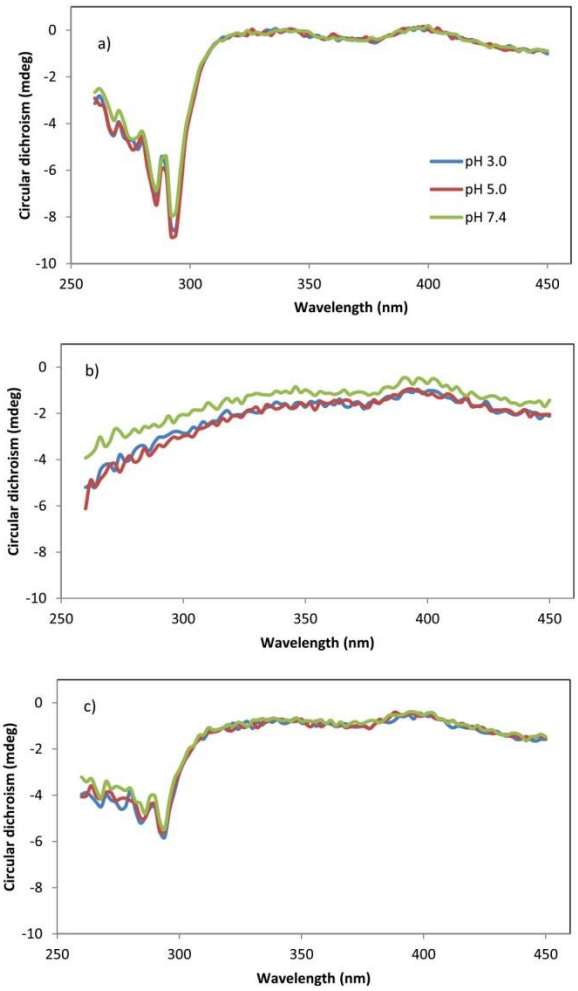

Fig. 5. Near- UV CD spectra of (a) BLG (b) BSM (c) BLG–BSM mixture at pH 3.0, 5.0 and 7.4.

293 nm for BLG, while a broad negative peak was observed from 260 nm to 310 nm with an intermediate intensity. No significant acid-induced changes in the tertiary structure were detected. The near-UV spectra were consistent with previous reports (Matsuura & Manning, 1994; Sakurai & Goto, 2006; Taulier & Chalikian, 2001). Near-UV CD spectra for BSM, as shown in Fig. 5(b), indicated that a stable tertiary structure could not be detected, except for the weakly and broadly developing negative signals with lowering wavelength. The near UV CD spectra of the mixture also revealed an intermediate feature of the two protein solutions, as shown by a broad negative peak from 260 nm to 310 nm, yet with a much reduced intensity (Fig. 5(c)). No interaction effects were visible in the CD spectra of the BLG–BSM mixture. Since carbohydrates do not contribute to the CD signal, this finding supports the observation from the high field NMR analysis that the interaction primarily took place on the glycosylated part of the mucin without significantly involving hydrophobic contacts.

While CD spectroscopy data are not conclusive about the interaction of the two proteins by themselves, they are supportive for both the DLS and NMR results in proposing the interaction between the two proteins.

4. Conclusion

The interaction between BSM and BLG was studied in dilute solutions with various spectroscopy methods and zeta potential measurements. The zeta potentials of the proteins showed that the surface charge characteristics of the BLG–BSM mixture were dominated by the BSM. Results from DLS measurements suggested that the interaction between the proteins caused a more compact conformation of BSM as the BLG integrated into the BSM. Far UV and near UV CD spectroscopy studies of the mixture of the two proteins showed intermediate spectra compared to each protein alone for both secondary and tertiary structure of the proteins, which may support the interaction theory proposed between them. High field NMR measurements are consistent with polar interactions at pH 5 and pH 3, whereas no significant interaction was detected at pH 7.4. Longer T_2 relation times were observed for the BLG–BSM mixture, especially at acidic pH, attributing to higher water mobility. The higher water mobility may indicate that fewer charged groups on the proteins surfaces were available for protein-water interaction due to interactions between the hydrophilic parts of BLG and BSM compared to BSM alone. The overall conclusion is that the interaction between BLG and BSM is mostly of hydrophilic origin and pH-dependent. This finding could provide a critical basis for the further studies about mucin functions and properties in the presence of food proteins.

Acknowledgements

The authors would like to thank to the Turkish Government for a PhD scholarship, European Research Council (Funding scheme: ERC Starting Grant 2010, project 261152), and the Danish Strategic Research Council (DSF-10-93456, FENAMI Project) for financial support.

Appendix A. Supplementary data

Supplementary data related to this article can be found at http://dx.doi.org/10.1016/j.foodhyd.2015.04.026.

Appendix 1

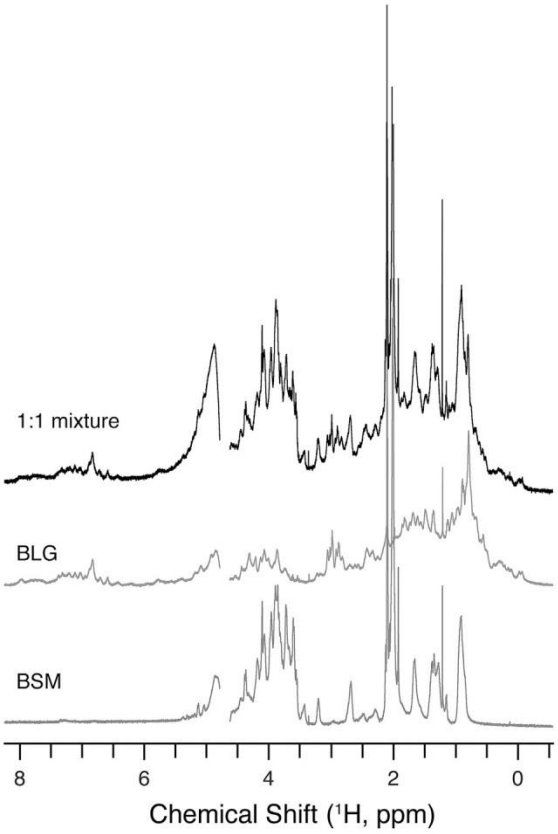

Fig. Appendix 1. High field ^{1}H NMR spectra of the pure BLG and BSM solutions, and their mixture (1:1) at pH 3.

Appendix 2. Identification of suggested interacting BSM residues.

Chemical shifts for BSM were estimated based on known approximate chemical shifts of the present amino acids (repeated [GTTVAPGSSNT] backbone sequence), as well as observed similarities between BSM and ovine submaxillary mucin (OSM) as studied by Gerken (1986). The suggested interacting BSM residues are presented in Table 2.

BSM residues within the 3.1–4.4 ppm interval were identified from similarities to OSM (Gerken, 1986). Furthermore, chemical shifts of the Ser and Thr amino acid protons were expected to shift slightly from their original position due to glycosylation and whether they were O-link to the protein backbone through Ser or

Table 2
The suggested interacting residues of BSM, when mixed (1:1) with BLG, based on their chemical shifts between 1.6 and 2.5 and from 3.1 to 4.4 ppm, where interaction is most likely to occur according to Fig. 2.

	Suggested interacting residues 1.6–2.5 ppm	Suggested interacting residues 3.1–4.4 ppm
BSM	GalNAc and sialic acid $-CH_3$ protons (narrow peaks, ~2.1 ppm)	Thr H_α and H_β
	Asn H_β (2.3, 2.5 ppm)	Ser H_α and H_β
		Sialic acid H4–H9, H9′
		GalNAc H2–H6, H6′

Thr residues. However, the exact assignation of the peaks within the 3.1–4.4 ppm interval was not performed and assessed to be outside the scope of this study, due to a high degree of overlapping of peaks within the interval and the lack of further analyzing tools/methods to fulfil this task with acceptable precision. The above mentioned intervals also contain some residues (i.e. H_α protons from the present amino acids all have resonances around 4–5 ppm) which are not believed to take part in the interaction. These were omitted from this table.

A complete assignation of peaks for BLG was performed by Uhrínová et al. (1998), which will not be repeated in this paper. Most amino acids present in the BLG contribute to signals within these chemical shift areas (i.e. various CH and CH_2 protons from the present amino acids within the broad peak at 1.6–1.8 ppm). Therefore, it was not possible to identify exact points of interaction between the BLG molecules to the BSM within this study.

References

Bansil, R., Stanley, E., & LaMont, J. T. (1995). Mucin biophysics. *Annual Review of Physiology, 57*, 635–657.

Bansil, R., & Turner, B. S. (2006). Mucin structure, aggregation, physiological functions and biomedical applications. *Current Opinion in Colloid & Interface Science, 11*(2–3), 164–170.

Bastardo, L., Claesson, P., & Brown, W. (2002). Interactions between mucin and alkyl sodium sulfates in solution. A light scattering study. *Langmuir, 18*(10), 3848–3853.

Carr, H. Y., & Purcell, E. M. (1954). Effects of diffusion on free precession in nuclear magnetic resonance experiments. *American Journal of Physiology, 94*, 630–638.

Drug, E., Landesman-Milo, D., Belgorodsky, B., Ermakov, N., Frenkel-Pinter, M., Fadeev, L., et al. (2011). Enhanced bioavailability of polyaromatic hydrocarbons in the form of mucin complexes. *Chemical Research in Toxicology, 24*(3), 314–320.

Durrer, C., Irache, J. M., Duchene, D., & Ponchel, G. (1995). Mucin interactions with functionalized polystyrene latexes. *Journal of Colloid and Interface Science, 170*(2), 555–561.

Efremova, N. V., Huang, Y., Peppas, N. A., & Leckband, D. E. (2002). Direct measurement of interactions between tethered poly (ethylene glycol) chains and adsorbed mucin layers. *Langmuir, 18*(3), 836–845.

Engelhardt, K., Lexis, M., Gochev, G., Konnerth, C., Miller, R., Willenbacher, N., et al. (2013). pH effects on the molecular structure of β-lactoglobulin modified air – water interfaces and its impact on foam rheology. *Langmuir, 29*(37), 11646–11655.

Fang, Y., & Dalgleish, D. (1997). Conformation of beta-lactoglobulin studied by FTIR: effect of pH, temperature, and adsorption to the oil-water interface. *Journal of Colloid and Interface Science, 196*(2), 292–298.

Gerken, T. A. (1986). The solution structure of mucous glycoproteins: proton NMR studies of native and modified ovine submaxillary mucin. *Archives of Biochemistry and Biophysics, 247*(2), 239–253.

Granizo, D. P., Reuhs, B. L., Stroshine, R., & Mauer, L. J. (2007). Evaluating the solubility of powdered food ingredients using dynamic nuclear magnetic resonance (NMR) relaxometry. *LWT – Food Science and Technology, 40*(1), 36–42.

Greenfield, N. J. (2006). Using circular dichroism spectra to estimate protein secondary structure. *Nature Protocols, 1*(6), 2876–2890.

Haque, E., Bhandari, B. R., Gidley, M. J., Deeth, H. C., & Whittaker, A. K. (2011). Ageing-induced solubility loss in milk protein concentrate powder: effect of protein conformational modifications and interactions with water. *Journal of the Science of Food and Agriculture, 91*(14), 2576–2581.

Indrawati, L., Stroshine, R. L., & Narsimhan, G. (2007). Low-field NMR: a tool for studying protein aggregation. *Journal of the Science of Food and Agriculture, 87*, 2207–2216.

Kontopidis, G., Holt, C., & Sawyer, L. (2004). Invited review: beta-lactoglobulin: binding properties, structure, and function. *Journal of Dairy Science, 87*(4), 785–796.

Kosters, H. A., Wierenga, P. A., de Vries, R., & Gruppen, H. (2013). Protein-peptide interaction: study of heat-induced aggregation and gelation of β-lactoglobulin in the presence of two peptides from its own hydrolysate. *Journal of Agricultural and Food Chemistry, 61*, 4218–4225.

Kumosinski, T. F., & Pessen, H. (1982). A deuteron and proton magnetic resonance relaxation study of β-lactoglobulin A association: some approaches to the scatchard hydration of globular proteins. *Archives of Biochemistry and Biophysics, 218*(1), 286–302.

Lee, S., Müller, M., Rezwan, K., & Spencer, N. D. (2005). Porcine gastric mucin (PGM) at the water/poly (dimethylsiloxane) (PDMS) interface: influence of pH and ionic strength on its conformation, adsorption, and aqueous lubrication properties. *Langmuir: The ACS Journal of Surfaces and Colloids, 21*, 8344–8353.

Leo, E., Pecquet, S., Rojas, J., Couvreur, P., & Fattal, E. (1998). Changing the pH of the external aqueous phase may modulate protein entrapment and delivery from poly (lactide-co-glycolide) microspheres prepared by a w/o/w solvent evaporation method. *Journal of Microencapsulation, 15*(4), 421–430.

Madsen, J. B., Pakkanen, K. I., & Lee, S. (2013). Investigation of the thermostability of Bovine Submaxillary Mucin (BSM) and its impact on lubrication. *APCBEE Procedia, 7*, 21–26.

Majhi, P. R., Ganta, R. R., Vanam, R. P., Seyrek, E., Giger, K., & Dubin, P. L. (2006). Electrostatically driven protein Aggregation: β-lactoglobulin at low ionic strength. *Langmuir, 22*(22), 9150–9159.

Martinez, M. J., Sánchez, C. C., Patino, J. M. R., & Pilosof, A. M. R. (2009). Interactions in the aqueous phase and adsorption at the air-water interface of casein-oglycomacropeptide (GMP) and beta-lactoglobulin mixed systems. *Colloids and Surfaces B: Biointerfaces, 68*(1), 39–47.

Matsuura, J. E., & Manning, M. C. (1994). Heat-induced gel formation of fl-lactoglobulin: a study on the secondary and tertiary structure as followed by circular dichroism spectroscopy. *Journal of Agricultural and Food Chemistry, 42*, 1650–1656.

Mehrotra, R., Thornton, D., & Sheehan, J. (1998). Isolation and physical characterization of the MUC7 (MG2) mucin from saliva: evidence for self-association. *Biochemical Journal, 334*, 415–422.

Meiboom, S., & Gill, D. (1958). Modified spin-echo method for measuring nuclear relaxation times. *Review of Scientific Instruments, 29*(8), 688.

Pedersen, H. T., Bro, R., & Engelsen, S. B. (2002). Towards rapid and unique curve resolution of low-field NMR relaxation data: trilinear SLICING versus two-dimensional curve fitting. *Journal of Magnetic Resonance, 157*(1), 141–155.

Perez, E., & Proust, J. E. (1987). Forces between mica surfaces covered with adsorbed mucin across aqueous solution. *Journal of Colloid and Interface Science, 118*(1), 182–191.

Rullier, B., Novales, B., & Axelos, M. A. V. (2008). Effect of protein aggregates on foaming properties of β-lactoglobulin. *Colloids and Surfaces A: Physicochemical and Engineering Aspects, 330*, 96–102.

Sakurai, K., & Goto, Y. (2006). Dynamics and mechanism of the tanford transition of bovine beta-lactoglobulin studied using heteronuclear NMR spectroscopy. *Journal of Molecular Biology, 356*(2), 483–496.

Sarkar, A., Goh, K. K. T., & Singh, H. (2009). Colloidal stability and interactions of milk-protein-stabilized emulsions in an artificial saliva. *Food Hydrocolloids, 23*(5), 1270–1278.

Sarkar, A., Goh, K. K. T., & Singh, H. (2010). Properties of oil-in-water emulsions stabilized by β-lactoglobulin in simulated gastric fluid as influenced by ionic strength and presence of mucin. *Food Hydrocolloids, 24*(5), 534–541.

Senapati, S., Das, S., & Batra, S. K. (2010). Mucin-interacting proteins: from function to therapeutics. *Trends in Biochemical Sciences, 35*(4), 236–245.

Shi, L., Ardehali, R., Caldwell, K. D., & Valint, P. (2000). Mucin coating on polymeric material surfaces to suppress bacterial adhesion. *Colloids and Surfaces B: Biointerfaces, 17*, 229–239.

Shrivastava, H. Y., & Nair, B. U. (2003). Structural modification and aggregation of mucin by chromium(III) complexes. *Journal of Biomolecular Structure & Dynamics, 20*(4), 575–587.

Silletti, E., Vingerhoeds, M. H., Norde, W., & van Aken, G. A. (2007). The role of electrostatics in saliva-induced emulsion flocculation. *Food Hydrocolloids, 21*(4), 596–606.

Sinha, V. R., Singla, A. K., Wadhawan, S., Kaushik, R., Kumria, R., Bansal, K., et al. (2004). Chitosan microspheres as a potential carrier for drugs. *International Journal of Pharmaceutics, 274*, 1–33.

Strous, G. J., & Dekker, J. (1992). Mucin-type glycoproteins. *Critical reviews in biochemistry and molecular biology, 27*(1–2), 57–92.

Svensson, O., Lindh, L., Cárdenas, M., & Arnebrant, T. (2006). Layer-by-layer assembly of mucin and chitosan–Influence of surface properties, concentration and type of mucin. *Journal of Colloid and Interface Science, 299*, 608–616.

Svensson, O., Thuresson, K., & Arnebrant, T. (2008). Interactions between drug delivery particles and mucin in solution and at interfaces. *Langmuir: The ACS Journal of Surfaces and Colloids, 24*(6), 2573–2579.

Takeuchi, H., Yamamoto, H., & Kawashima, Y. (2001). Mucoadhesive nanoparticulate systems for peptide drug delivery. *Advanced Drug Delivery Reviews, 47*(1), 39–54.

Taulier, N., & Chalikian, T. V. (2001). Characterization of pH-induced transitions of beta-lactoglobulin: ultrasonic, densimetric, and spectroscopic studies. *Journal of Molecular Biology, 314*(4), 873–889.

Uhrínová, S., Uhrín, D., Denton, H., Smith, M. H., Sawyer, L., & Barlow, P. N. (1998). Complete assignment of ^{1}H, ^{13}C and ^{15}N chemical shifts for bovine beta-lactoglobulin: secondary structure and topology of the native state is retained in a partially unfolded form. *Journal of Biomolecular NMR, 12*(1), 89–107.

Vingerhoeds, M. H., Blijdenstein, T. B. J., Zoet, F. D., & van Aken, G. A. (2005). Emulsion flocculation induced by saliva and mucin. *Food Hydrocolloids, 19*(5), 915–922.

Withers, C. A., Cook, M. T., Methven, L., Gosney, M. A., & Khutoryanskiy, V. V. (2013). Investigation of milk proteins binding to the oral mucosa. *Food & Function, 4*, 1668–1674.

Ye, A., Zheng, T., Ye, J. Z., & Singh, H. (2012). Potential role of the binding of whey proteins to human buccal cells on the perception of astringency in whey protein beverages. *Physiology & Behavior, 106*(5), 645–650.

Zalewska, A., Zwierz, K., Zółkowski, K., & Gindzieński, A. (2000). Structure and biosynthesis of human salivary mucins. *Acta Biochimica Polonica, 47*(4), 1067–1079.

Zúñiga, R. N., Tolkach, A., Kulozik, U., & Aguilera, J. M. (2010). Kinetics of formation and physicochemical characterization of thermally-induced beta-lactoglobulin aggregates. *Journal of Food Science, 75*(5), 261–268.

Appendix: Supplementary data

Supplementary data related to this article can be found at

http:// dx.doi.org/10.1016/j.foodhyd.2015.04.026.

Appendix 1

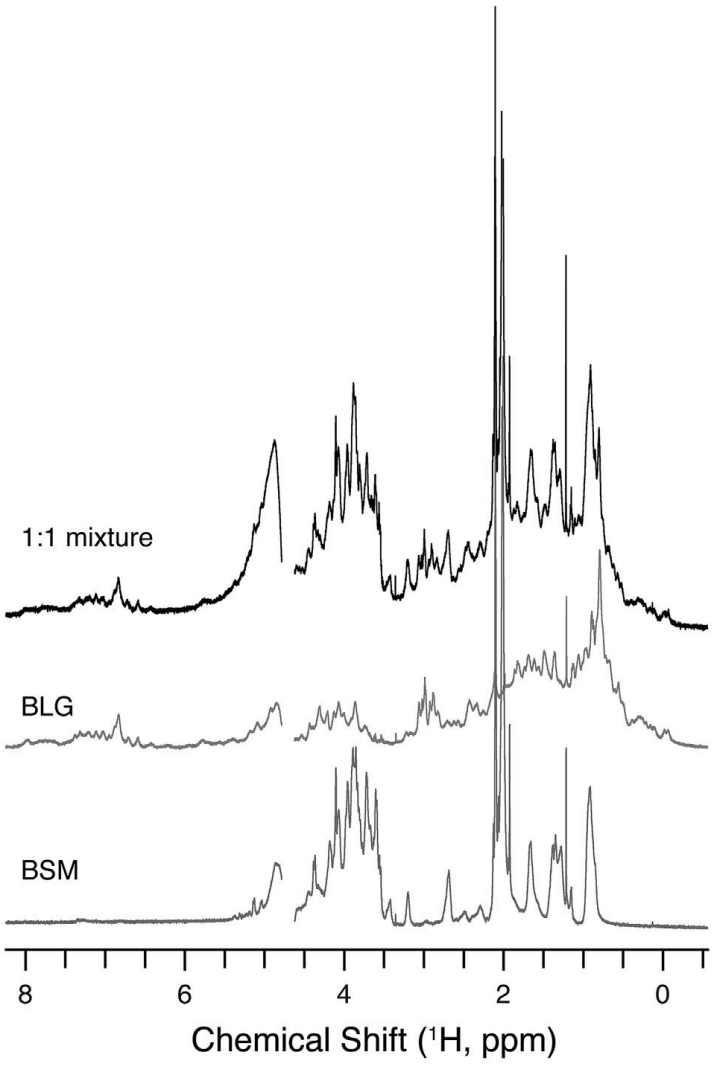

Fig. Appendix 1. High field 1H NMR spectra of the pure BLG and BSM solutions, and their mixture (1:1) at pH 3.

Appendix 2. Identification of suggested interacting BSM residues.

Chemical shifts for BSM were estimated based on known approximate chemical shifts of the present amino acids (repeated [GTTVAPGSSNT] backbone sequence), as well as observed similarities between BSM and ovine submaxillary mucin (OSM) as studied by Gerken (1986). The suggested interacting BSM residues are presented in Table 2. BSM residues within the 3.1 - 4.4 ppm interval were identified from similarities to OSM (Gerken, 1986). Furthermore, chemical shifts of the Ser and Thr amino acid protons were expected to shift slightly from their original position due to glycosylation and whether they were O-link to the protein backbone through Ser or Thr residues. However, the exact assignation of the peaks within the 3.1 - 4.4 ppm interval was not performed and assessed to be outside the scope of this study, due to a high degree of overlapping of peaks within the interval and the lack of further analyzing tools/ methods to fulfil this task with acceptable precision.

Table 2

The suggested interacting residues of BSM, when mixed (1:1) with BLG, based on their chemical shifts between 1.6 and 2.5 and from 3.1 to 4.4 ppm, where interaction is most likely to occur according to Fig. 2.

	Suggested interacting residues 1.6– 2.5 ppm	**Suggested interacting residues 3.1– 4.4 ppm**
BSM	GalNAc and sialic acid $-CH_3$ protons (narrow peaks, ∼2.1 ppm) Asn H_β (2.3, 2.5)	Thr H_α and H_β Ser H_α and H_β Sialic acid H4-H9, H9' GalNAc H2-H6, H6'

The above mentioned intervals also contain some residues (i.e. H_α protons from the present amino acids all have resonances around 4 - 5 ppm) which are not believed to take part in the interaction. These were omitted from this table. A complete assignation of peaks for BLG was performed by Uhrínova et al. (1998), which will not be repeated in this paper. Most amino acids present in the BLG contribute to signals within these chemical shift areas (i.e. various CH and CH_2 protons from the present amino acids within the broad peak at 1.6 - 1.8 ppm). Therefore, it was not possible to identify exact points of interaction between the BLG molecules to the BSM within this study.

CHAPTER 3

Investigation of the Interaction between Mucins and β-Lactoglobulin under Tribological Stress

(Paper II)

Food Hydrocolloids 54 (2016) 57–65

Contents lists available at ScienceDirect

Food Hydrocolloids

journal homepage: www.elsevier.com/locate/foodhyd

Investigation of the interaction between mucins and β-lactoglobulin under tribological stress

Hilal Y. Çelebioğlu [a], María Gudjónsdóttir [a, 1], Ioannis S. Chronakis [a], Seunghwan Lee [b, *]

[a] Nano-BioScience Research Group, DTU-Food, Technical University of Denmark, Søltofts Plads, Building 227, 2800 Kgs. Lyngby, Denmark
[b] Department of Mechanical Engineering, Technical University of Denmark, DK-2800 Kgs. Lyngby, Denmark

ARTICLE INFO

Article history:
Received 22 June 2015
Received in revised form
11 September 2015
Accepted 13 September 2015
Available online 18 September 2015

Keywords:
Tribology
Beta-lactoglobulin
Bovine submaxillary mucin
Porcine gastric mucin
pH

ABSTRACT

The interaction characteristics between mucins and beta-lactoglobulin (BLG) under tribological stress were investigated by comparing the lubricity of mixed solutions of mucin–BLG with that of neat protein solutions at compliant hydrophobic interfaces. Surface adsorption properties of the proteins as characterized by bicinchoninic acid (BCA) assay revealed that both bovine submaxillary mucin (BSM) and porcine gastric mucin (PGM) showed distinctly higher adsorbed masses compared to BLG onto polydimethylsiloxane (PDMS) or polystyrene (PS) surfaces. The adsorbed masses of the mixed protein solutions, namely BLG–BSM and BLG–PGM, reduced significantly, and BLG appeared to dominate the surface adsorption event, presumably due to the reduced concentration of mucins and the Vroman effect. While pin-on-disk tribometry and mini-traction machine (MTM) were employed to provide the tribological contacts with varying contact pressure, speed range, and slide/roll ratio, the dominant lubrication mechanism of the protein solutions was boundary lubrication. BLG–BSM mixture showed the highest level of degradation in the lubricity of BSM at pH 5, although BLG–saliva interaction is known to degrade the lubricity most rapidly at more acidic pH, such as at pH 3.5. More importantly, pH dependent lubricating properties of BLG–BSM mixed solutions appeared to be determined by competitive adsorption of the two proteins onto the substrates, which suggests that they do not form as strong aggregates as BLG–saliva, especially under tribological stress.

© 2015 Elsevier Ltd. All rights reserved.

1. Introduction

There has been growing interest in understanding food oral processing and digestion by applying various techniques to achieve desired designing of food and pharmaceuticals with new ingredients and interfacial structures (Lundin, Golding, & Wooster, 2008; McClements, Decker, & Park, 2009; Singh & Ye, 2013; Singh, Ye, & Horne, 2009). A few studies have investigated food oral processing by focusing on the interaction of food emulsions with saliva in the oral environment (Vingerhoeds, Blijdenstein, Zoet, & van Aken, 2005; Van Aken, Vingerhoeds, & de Hoog, 2007; Silletti, Vingerhoeds, Norde, & van Aken, 2007; Sarkar, Goh, & Singh, 2009). These studies have shown that either electrostatic interaction or hydrophobic forces causes emulsion flocculation, aggregation, or aroma releasing, which are related to sensory perception. Due to complexity of both food and saliva, the details of food–saliva interactions still require further explanations. In particular, little information is available in literature on the molecular-level interaction between constituents of food–saliva systems.

Recently, tribology has emerged as a new instrumental approach to investigate oral processing of food emulsions in simulated oral environment (Meyer, Vermulst, Tromp, & de Hoog, 2011; Vardhanabhuti, Cox, Norton, & Foegeding, 2011; Chojnicka-Paszun, de Jongh, & de Kruif, 2012; Chen & Stokes, 2012; Van Aken, 2013; Selway & Stokes, 2013; Prakash, Tan, & Chen, 2013; Chen, Liu, & Prakash, 2014; Joyner Melito, Pernell, & Daubert, 2014). In turn, this is often correlated with food's sensory perception (Meyer et al. 2011; Vardhanabhuti et al. 2011; Chojnicka-Paszun et al., 2012; Selway & Stokes, 2013; Prakash et al., 2013). Tribology is particularly useful for understanding the behavior of thin films formed between two opposing surfaces where rheological and structural/mechanical properties of food may no longer explain their behavior sufficiently.

* Corresponding author.
E-mail address: seele@mek.dtu.dk (S. Lee).
[1] University of Iceland, Faculty of Food Science and Nutrition, Vínlandsleið 14, 113 Reykjavík, Iceland.

http://dx.doi.org/10.1016/j.foodhyd.2015.09.013
0268-005X/© 2015 Elsevier Ltd. All rights reserved.

In the present study, we attempted to apply tribological techniques to investigate the interaction of β-lactoglobulin (BLG) with mucins under tribological stress and how it affects their lubricating properties. BLG is the major whey protein constituting >50% of the total whey proteins in bovine milk (Zúñiga, Tolkach, Kulozik, & Aguilera, 2010). BLG contains many charged groups, therefore, its structure and properties are highly pH-dependent (Fang & Dalgleish, 1997). Mucins are a family of large, extracellular glycoproteins (Bansil, Stanley, & LaMont, 1995; Svensson & Arnebrant, 2010) and are known to be chiefly responsible for the slipperiness of saliva (Berg, Lindh, & Arnebrant, 2004; Tabak, Kevine, Mandel, & Ellison, 1982). Apart from its functions in biological systems, previous studies have shown facile adsorption and effective lubrication on various engineering materials too (Lee, Müller, Rezwan, & Spencer, 2005; Nikogeorgos, Madsen, & Lee, 2014; Yakubov, McColl, Bongaerts, & Ramsden, 2009). The importance of understanding the interaction characteristics between BLG and mucins is related to an ongoing discussion on the origin of astringency. One of the most prevailing models is that astringents interact with saliva to form aggregates to deplete the lubricant (saliva) from the tribological contacts in the mouth (Rossetti, Bongaerts, Wantling, Stokes, & Williamson, 2009; Vardhanabhuti et al., 2011). Recent applications of tribological techniques allowed for quantitative characterization of the lubricating properties of the fluids involving saliva and BLG or other astringents. For example, Vardhanabhuti et al. (2011) showed that addition of BLG into a soft tribological interface increased the interfacial friction forces, yet at varying rates depending on pH. Aggregation of macromolecules (BLG) with hydrogel (saliva) is, however, a complex process influenced by a number of parameters. For example, among many types of proteins in saliva, which one(s) are involved in the aggregation with BLG is not clear. Thus, it would be important and meaningful to investigate the molecular-level interaction to deepen the understanding the interaction of saliva with whole food. Moreover, despite relatively more active studies addressing the interactions of mucins with polysaccharides (Menchicchi et al., 2014, 2015; Qaqish & Amiji, 1999), the studies for the interaction of mucins with food proteins are much more limited.

We have chosen two types of mucins, namely, bovine submaxillary mucin (BSM) and porcine gastric mucin (PGM), purchased from a commercial manufacturer (Sigma–Aldrich). The fact that both mucins are highly relevant to food digestion process, yet to different organs, is the first reason for comparing them. Additionally, in parallel with common structural features of the two mucins (Bansil et al., 1995; Sandberg, Blom, & Caldwell, 2009), reported differences in their biophysical properties, especially the lubricating properties (Lee et al., 2005; Nikogeorgos et al., 2014), may lead to different interaction with BLG and alteration in the lubricating properties.

2. Materials and methods

2.1. Sample preparation

BLG from bovine milk, BSM (Type I–S), and PGM (Type III) were purchased from Sigma–Aldrich (Brøndby, Denmark), and were used as received. Protein solutions with the concentration of 1 mg/mL were prepared by dissolving in 10 mM phosphate buffered saline (PBS) solutions and were used throughout the study. The pH values of the buffer solutions were adjusted to 7.4, 5, and 3 by addition of HCl or NaOH. For the mixture of BLG and mucins, the two protein solutions were mixed directly at the ratio of 1:1 (v:v) and the total protein concentrations were remained at either 1 mg/mL. Due to relatively weaker lubricating capabilities of PGM at 1 mg/mL (Lee et al., 2005), PGM, BLG, and PGM–BLG mixed solutions were studied at 10 mg/mL too.

2.2. Zeta potential measurements

The zeta potential of the protein solutions was characterized with a laser (633 nm) Doppler electrophoresis instrument (LDE; Zetasizer Nano ZS, Malvern, UK). Disposable cuvettes (model DTS 1070) were used. At least five measurements were performed for each protein solution to acquire statistically valid data.

2.3. Bicinchoninic acid (BCA) assay

Surface adsorption properties of the proteins onto hydrophobic substrates were characterized by means of BCA protein qualification assay. This technique is based on the reduction of Cu^{2+} to Cu^{+} in the presence of peptide bonds, and subsequent complex formation with BCA to form a purple-colored end product (Smith et al. 1985). The assay has been established to quantify proteins in bulk solution, and recently, it was further customized to estimate the protein amount adsorbed on surfaces (Pakkanen, Madsen, & Lee, 2015; Sandberg, Mellina, Gelius, & Caldwell, 2009). An important assumption in this modified approach is that surface adsorbed proteins (peptide bonds) have the same reduction reactivity of converting Cu^{2+} to Cu^{+} with those in bulk solution. Thus, the light absorbance by Cu^{+}–BCA complex is proportional to the amount of the proteins even if the proteins are surface-localized. Detailed procedures to acquire standard curves and the areal mass of the sample proteins are provided in the Supplementary information (Figure S1.) In this study, standard curves were prepared not only for bovine serum albumin (BSA) as a general test protein, but also for all the proteins or protein mixtures at each condition, including concentration, pH, and the choice of microtiter materials (see below). The absorbance of each protein sample was measured at 540 nm with an absorbance microplate reader (BioTek, ELx800 model). The measurements were repeated three times for each sample for statistical evaluation. The microtiter wells (GMBH + CO KG, Wertheim, Germany) were made of polystyrene (PS). While PS was not used as a tribopair material, we assume that protein adsorption properties of the proteins onto PS would be similar with those onto polyoxymethlylene (POM), which was used as a tribopair material. For the relevance of surface adsorption properties to tribological interfaces of poly(dimethylsiloxane) (PDMS), some microtiter wells were coated with a thin layer of PDMS. To this end, a two-component silicone kit (Sylgard 184, Dow Corning) was employed. Base fluid and crosslinker were mixed at the ratio of 10:1 (w/w). A small drop (ca. 20 μL) was added to each well and cured in an oven at 80 °C overnight. It is noted that as standard curves were independently obtained for PDMS-coated wells too, thin PDMS coating on the absorbance does not affect the adsorbed mass estimation.

2.4. Pin-on-disk tribometry

Lubricating properties of the protein solutions at sliding contacts were characterized by pin-on-disk tribometry (CSM, Peseux, Switzerland). In this approach, a loaded spherical pin is allowed to form a contact on a plane disk. The motor-driven rotation of the disk generates interfacial friction forces between the pin and the disk. The applied load is controlled by dead weight and the friction forces generated during sliding contact are monitored by a strain gauge. The coefficient of friction, μ, is defined from the relationship, $\mu = F_{friction}/F_{load}$.

PDMS was chosen as the tribopair for both pin (6 mm in diameter) and disk (30 mm in diameter and 5 mm in thickness).

The pin and disk from PDMS were prepared with the PDMS kit mentioned above as described by Nikogeorgos et al. (2014). To ensure that the lubricated contacts were in the boundary lubrication regime, a low sliding speed (5 mm/s) was selected under a 5 N or 2 N load, corresponding to the apparent maximum Hertzian contact pressure of 0.6 or 0.4 MPa, respectively. The friction force data were collected for 100 rotations at room temperature (25 °C) and the tests were repeated multiple times for statistical evaluation. For each measurement, a tribopair of PDMS–PDMS was used only once and discarded to avoid cross contamination between measurements. As a control, a POM pin (6 mm in diameter) was employed to form a POM/PDMS interface under 5 N (apparent maximum Hertzian contact pressure of 0.9 MPa). The basic mechanical and surface properties of the tribopair materials are presented in Table 1.

2.5. Mini traction machine (MTM)

Lubrication properties of the protein solutions were characterized at mixed/rolling contacts in the higher speed regime by means of a mini-traction machine (MTM, PCS Instruments Ltd., UK) too. Mixed rolling/sliding contacts are provided with MTM by independent rotation of ball and disk. The mean speed is defined as $[|speed_{ball} - speed_{disk}|/2]$. The slide/roll ratio (SRR) is defined as $SRR = (|speed_{ball} - speed_{disk}|)/[(speed_{ball} + speed_{disk})/2] \times 100\%$, where 0% SRR represents pure rolling and 200% SRR represents pure sliding. In this study, SRR of 20% was employed in all measurements with varying mean speed between 10 mm/s to 1200 mm/s. Tests were conducted at room temperature (25 °C) with the tribopair consisting of a POM ball and a PDMS disk. The PDMS disks were prepared from the aforementioned two-component silicone kit (Sylgard 184, Dow Corning) as well. A thick PDMS slab (ca. 5 mm) was cast on top of a steel disk (ca. 5 mm) for each sample. POM balls were purchased from a supplier (19.05 mm (¾ inch) in diameter, Precision Plastic Ball Co., IL) and were used as received. For each measurement, a new PDMS disk was employed, whereas the same POM ball was used after cleaning with distilled water, ethanol, and sonication in distilled water for 5 min. A fixed load (2 N) was applied with the estimated Hertzian contact pressure of 0.3 MPa. Tests were repeated three times and the friction data were averaged.

3. Results and discussion

3.1. Zeta potentials

In Fig. 1, the zeta potentials of the protein solutions are presented as a function of pH. A zeta potential of near 0 mV was observed at pH 5 for BLG, which is indicative of near-zero net charge and being close to the isoelectric point (IEP) of BLG. As expected, positive and negative zeta potentials were measured when the pH was shifted to 3 and 7.4, respectively in agreement with the study of Engelhardt et al. (2013). It is noted that despite a gradual decrease in the magnitude of negative charges with decreasing pH, the zero zeta potentials of the mucins were not reached even at pH 3, indicating that the IEPs of both mucins are lower than pH 3 (Lee et al., 2005; Sotres, Madsen, Arnebrant, & Lee, 2014). It is further to note that BSM displayed more negative zeta potentials than PGM at all pH values due to higher abundance of negatively charged moieties in BSM, such as sialic acids (bound sialic acid 9–17% for BSM Type I–S and 0.5–1.5% for PGM Type III, Sigma Aldrich).

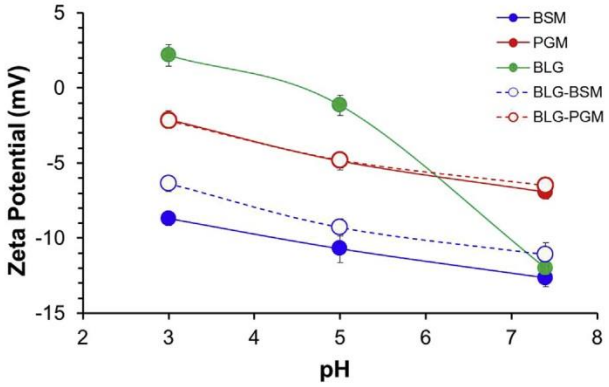

Fig. 1. Zeta potentials of the protein solutions as a function of pH.

For the BLG–BSM mixture, the trend of the zeta potential changes according to pH change appears to be similar to that of BSM itself, except for slightly less negative values. However, as the absolute values of the zeta potential of BLG at pH 3 and 5 are much smaller than those of BSM at these pHs, and as the zeta potentials of BLG and BSM are very similar to each other at pH 7.4, the interaction nature between BSM and BLG cannot be judged based on zeta potential data alone. The seemingly ignorable contribution of BLG to the zeta potential of BLG–PGM mixture at pH 5 could be also discussed in the same context. At pH 3 and 7.4, however, despite fairly different zeta potentials of BLG and PGM, their mixture showed nearly the same zeta potentials of PGM rather than intermediate ones, which signifies the dominance of the electrophoretic mobility of PGM in the mixed protein solutions.

3.2. Surface adsorption properties

The adsorbed masses of the proteins per unit area, denoted as Γ, of the PDMS-coated microtiter well surfaces are presented in Fig. 2. It is noted that Fig. 2(a) is for the data obtained from 1 mg/mL (all protein solutions) and Fig. 2(b) is for those from 10 mg/mL (PGM, BLG, and BLG–PGM mixture solutions only). The results for the PS microtiter wells were very similar and the results are shown in Supplementary information (Figure S3). A few noticeable features of the adsorption behavior of mucins, BLG, and their mixtures are discussed as follows.

Firstly, the adsorbed masses of mucins were clearly higher than those of BLG under the same conditions (concentration and pH). For instance, the Γ_{PGM} was ca. 3 mg/m^2 and Γ_{BSM} ranged ca. 2.0–4.5 mg/m^2 from 1 mg/mL solutions for all pH values, whereas Γ_{BLG} ranged ca. 0.4–1.0 mg/m^2 only (Fig. 3). While the experimental approach employed in this study was markedly different from more conventional optical approaches, the Γ values for mucins (Lee et al., 2005; Nikogeorgos et al., 2014; Shi & Caldwell, 2000) and BLG

Table 1
Mechanical and surface properties of the materials employed for tribological measurements in this study (Røn & Lee, 2014).

	Young's modulus (MPa)	Poisson ratio	Surface roughness (nm)	Static water contact angle (°)
PDMS	2	0.5	1.6 ± 0.3	105.6 ± 0.2
POM	3100	0.35	659 ± 179	84.8 ± 2.9

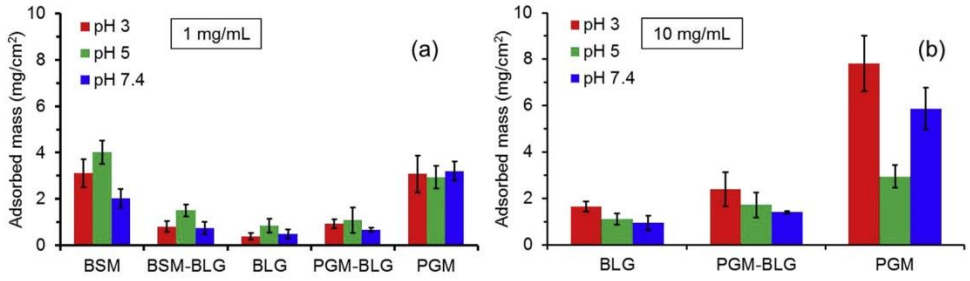

Fig. 2. Adsorbed masses of the proteins on PDMS-covered-well surfaces as characterized with BCA assay (a) from the 1 mg/mL solutions (b) from the 10 mg/mL solutions.

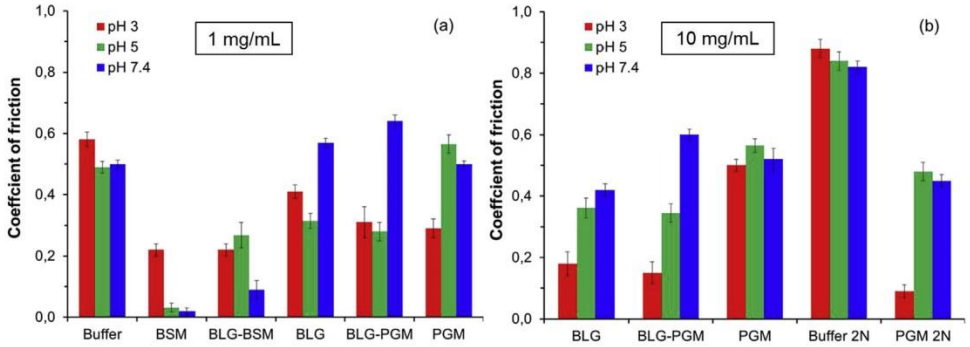

Fig. 3. Coefficients of friction from the sliding contacts of PDMS–PDMS pair lubricated with the protein solutions (a) at 1 mg/mL or (b) 10 mg/m, at pH 3.0, 5.0, and 7.4, as characterized by pin-on-disk tribometry (load = 5 N or 2 N, sliding speed = 5 mm/s).

(Krisdhasima, McGuire, & Sproull, 1992) onto hydrophobic surfaces are roughly in the same range, which supports the validity of BCA as a quantitative surface adsorption characterization technique. Given the adsorbed mass per unit area and the molecular weight of BSM (1.6 MDa, Shi & Caldwell, 2000), PGM (1.25 MDa, Davies & Viney, 1998), and BLG (18 kDa, Zúñiga et al., 2010), the number of protein molecules per unit area, or conversely, the surface area occupied per single molecule could be estimated. If we further assume that this area is circular, its diameter, D_s, can be compared with the hydrodynamic diameter, D_h, of the proteins in a bulk solution from literature (Çelebioğlu et al., 2015; Durrer, Irache, Duchene, & Ponchel, 1995). The results (Table 2) showed that the $D_{s,\ BLG}$, is comparable to $D_{h,\ BLG}$ or smaller, whereas the $D_{s,\ BSM}$ or $D_{s,\ PGM}$ is approximately only ca. 10–25% of their D_h in bulk solution. This means that mucins are not only higher than BLG in the adsorbed masses, but also adsorb onto the surfaces in a more compact conformation due to a high flexibility of mucins to accommodate themselves in a narrow space or a possibility to form multilayers.

Secondly, pH was observed to have an influence on the surface adsorption of both mucins and BLG. For instance, BSM showed higher adsorbed masses at acidic pHs than pH 7.4, in consistent with a recent study by Sotres et al. (2014). This behavior is readily expected from polyanionic characteristics of BSM and nonpolar characteristics of PDMS surface; adsorption of polyanionic species onto nonpolar surfaces from aqueous environment inevitably leads to the accumulation of charges on the surface and it acts as a barrier to hamper further adsorption (Sotres et al., 2014). With decreasing pH, BSM starts to be protonated and the barrier can be diminished. The pH dependence of PGM for the adsorption onto PDMS at 1 mg/mL is much weaker, and this is consistent with the fact that PGM carries less charged moieties as shown by the zeta potential measurements (Fig. 1). However, at 10 mg/mL, PGM also showed the highest adsorbed mass at pH 3 than at lower pHs, presumably due to the activation of the electrostatic repulsion mechanism mentioned above. Adsorption of BLG onto PDMS surfaces showed a higher Γ_{BLG} values at pH 5 compared to pH 3 and 7.4, which could

Table 2
Area per molecule, A, distance between protein molecule, D_s, and the ratio between D_s/D_h*. *The adsorbed masses of the protein solutions at 1 mg/mL only were analyzed. The area per molecules were obtained by assuming the molecular weight of BSM as 1.6 MDa (Shi & Caldwell, 2000), of PGM as 1.25 MDa (Davies & Viney, 19987), and of BLG as 18 kDa (Zúñiga et al., 2010). The distance between protein molecule on surface, D_s, was obtained by further assuming that the area per protein molecule is circular ($A = \pi (d/2)^2$, and thus $D_s = d$, diameter of the circle). D_h is hydrodynamic diameter of the proteins in bulk solution and the values were quoted from the literature: $D_{h,\ BSM} = 165$ nm at all pHs (Çelebioğlu et al., 2015), $D_{h,\ PGM} = 220$, 230, and 300 nm at pH 3, 5, and 7.4, respectively (Durrer et al., 1995), $D_{h,\ BLG} = 6.5$ nm at all pHs (Çelebioğlu et al., 2015)). While fairly different D_h values are also available for BSM and PGM in literature, those for the same commercial sources (Sigma Aldrich) are approximately in the same range.

Samples	Adsorbed mass (mg/m²)			A, Area per protein molecule (nm²)			D_s, Distance between protein molecule on surface (nm)			D_s/D_h		
pH	3	5	7.4	3	5	7.4	3	5	7.4	3	5	7.4
BSM	2.03	4.54	2.11	1307.6	585.2	1258.0	40.8	27.3	40.0	0.25	0.17	0.24
PGM	2.81	2.94	3.07	737.3	706.9	674.5	30.6	30.0	17.0	0.14	0.13	0.10
BLG	0.49	1.10	0.38	62.0	27.7	79.8	62.0	27.7	79.8	1.37	0.91	1.55

also be explained by the electrostatic repulsion model, as the zeta potential of BLG is nearly zero at pH 5 (Fig. 1).

Thirdly, and most importantly, mixed protein solutions showed much lower Γ values than those of respective mucins and comparable to BLG at each condition. While only a half of the mucin concentration in the mixed protein solutions can be a first reason, this behavior could be ascribed also to the Vroman effect too (Vroman & Adams, 1969; Lassen & Malmsten, 1997; Latour, 2008); as BLG is much smaller and lighter than the mucins, it is more mobile and can reach the surface faster than the mucins in the early stage of adsorption (≤1 h in this study). Furthermore, as the weight/volume concentration of BLG and mucins were equal in the mixed protein solutions, the number of BLG molecules overwhelms that of mucins due to much smaller molecular weight of BLG. Thus, BLG can readily dominate the initial surface adsorption.

More importantly, the dominance of BLG in the surface adsorption from the BLG–mucin mixture mentioned above implies that there is a large portion of "free" BLG molecules in the mixed protein solutions, and that they participate in the surface adsorption process in competition with the mucins. This is contradicting with a recent spectroscopic study on the interaction between BLG and BSM (Çelebioğlu et al., 2015), in which the DLS measurements of the BLG–BSM mixture led to a complete disappearance of the peak corresponding to free BLG molecules. This may be caused by the substantially different light scattering sensitivity for the two types of molecules, i.e. BLG molecules are not readily detectable when they are present together with much larger BSM molecules in a solution. It may also simply reflect a very weak interaction nature between BLG and BSM even if they may form loose aggregates.

3.3. Lubricating properties

In this study, two types of hydrophobic interfaces, namely PDMS–PDMS and POM–PDMS, were employed for the lubrication studies. Hydrophobic substrates were chosen as they may potentially mimic an oral mucosa membrane underneath mucus layers and facile adsorption of mucins onto the substrate can complete an in-vitro oral mucosa model. More importantly, in order to assess the boundary lubricating properties of the proteins, the substrates should effectively attract them onto the surface in the first place, and thus hydrophobicity is a first demanded attribute as the tribopair. POM and PDMS are though very different in their mechanical properties and surface roughness (Table 2). Thus, without substantial changes in the tribological parameters, e.g. external load, these two sliders provide significantly different contact pressure regimes on the opposing substrate.

3.3.1. Sliding contacts of soft–soft and smooth interface; pin-on-disk tribometry

Fig. 3 shows the μ values obtained from the sliding contacts of PDMS–PDMS interface as lubricated by the protein solutions at (a) 1 mg/mL (all protein solutions) and (b) 10 mg/mL (PGM, BLG, and BLG–PGM mixture solutions only) as characterized by pin-on-disk tribometry. Buffers with three different pHs showed μ values of 0.5–0.6 (Fig. 3(a)). At 1 mg/mL concentration, the BSM solutions displayed exceedingly superior lubricity. This is consistent with previous studies showing effective boundary lubrication by BSM at a PDMS–PDMS interface, yet under much lower load (Nikogeorgos et al., 2014). BSM showed higher μ values at pH 3 ($\mu \approx 0.2$) compared to pH 5 and 7.4 ($\mu \approx 0.02$), for which the origin is not clearly understood yet. As the Γ_{BSM} values at pH 3 was comparable to those at pH 5 and higher than at pH 7.4 (Fig. 2), this behavior cannot be understood in view of surface coverage with BSM at varying pH. One possibility is that charged BSM at pH 7 may lubricate more effectively due to charge–charge repulsion between the opposing surfaces.

PGM solutions showed virtually ignorable lubricating effect, despite comparable adsorbed masses with BSM at the same concentration, 1 mg/mL (Fig. 2). While the lubricity of the PGM solution improved at pH 3, in consistent with a former study (Lee et al., 2005), the μ values were still somewhat higher than those of BSM at the same condition. It is also noticeable that the lubricity of the PGM solutions at 10 mg/mL is not improving or even inferior to that of PGM at 1 mg/mL at pH 3 (Fig. 3(b)). As a control, an experiment employing the 10 mg/mL PGM solution at pH 3 again showed low μ values under a reduced load of 2 N (Fig. 3(b)), the exceptionally high μ values of 10 mg/mL PGM solutions at pH 3 under 5 N appear to be related to pressure-induced phenomena, such as bridging of PGM molecules between the two opposing PDMS surfaces and consequently high adhesive contacts.

The lubricating efficacy of BLG solutions was also observed to be poor. Although some variation in μ values according to the pH change was observed, at both 1 mg/mL and 10 mg/mL concentrations, the absolute μ values were relatively high ($\mu > 0.2$), indicating that this dependence is of little importance. Insignificant lubricity of BLG is firstly resulting from the lack of distinct amphiphilicity, a structural feature required to stabilize the macromolecules on hydrophobic substrates in aqueous environment. Relatively lower adsorbed masses and larger intermolecular distances between BLG on PDMS surface (Table 2) suggest that a strong adhesion between PDMS surfaces may be still active when PDMS–PDMS sliding contact is lubricated with BLG solutions.

3.3.2. Sliding contacts of hard–soft and rough interface; pin-on-disk tribometry

Fig. 4 shows the μ values obtained from POM–PDMS interface as lubricated by BSM solution at pH 7.4 or buffer solution under otherwise the same conditions with Fig. 3. For a direct comparison, the μ values from the PDMS–PDMS counterpart (Fig. 3) are also presented. About two times higher μ values observed from the POM–PDMS than the PDMS–PDMS interface in the buffer solutions is ascribed to the substantially higher surface roughness of the POM surface and consequently high local contact pressures (Table 1). Nevertheless, BSM solution displayed consistently more effective lubrication than BLG or the BLG–BSM mixture solutions. The ineffective lubricity of the PGM solutions for the POM–PDMS interface was also consistent (data not shown).

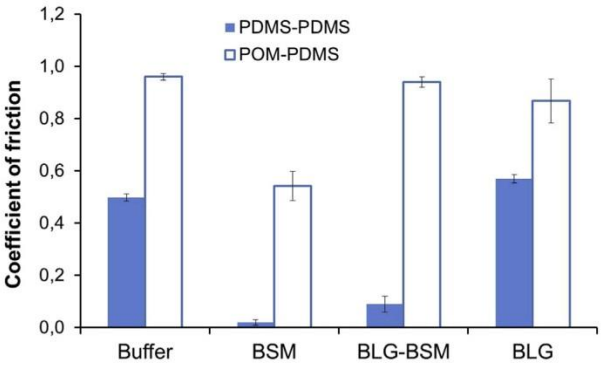

Fig. 4. Comparison of the coefficients of friction for PDMS–PDMS and POM–PDMS pairs lubricated by BSM solution as characterized by pin-on-disk tribometry (BSM solution = 1 mg/mL at pH 7.4, load = 5 N, sliding speed = 5 mm/s).

3.3.3. Mixed rolling–sliding contacts of hard–soft and rough interface; MTM

Fig. 5 shows the μ vs. speed plots obtained from the POM–PDMS tribopair lubricated with the protein solutions at 1 mg/mL (a) at pH 3, (b) pH 5, and (c) pH 7.4, as characterized with MTM. The results showed that all the protein solutions lowered the μ values compared to the respective buffer solutions (some missing μ data points in the low-speed regime for the buffer solutions > 1), even including PGM or BLG solutions, which were less lubricious in tribometer experiments. This is probably due to more favorable conditions for lubrication, including higher speed, higher rolling

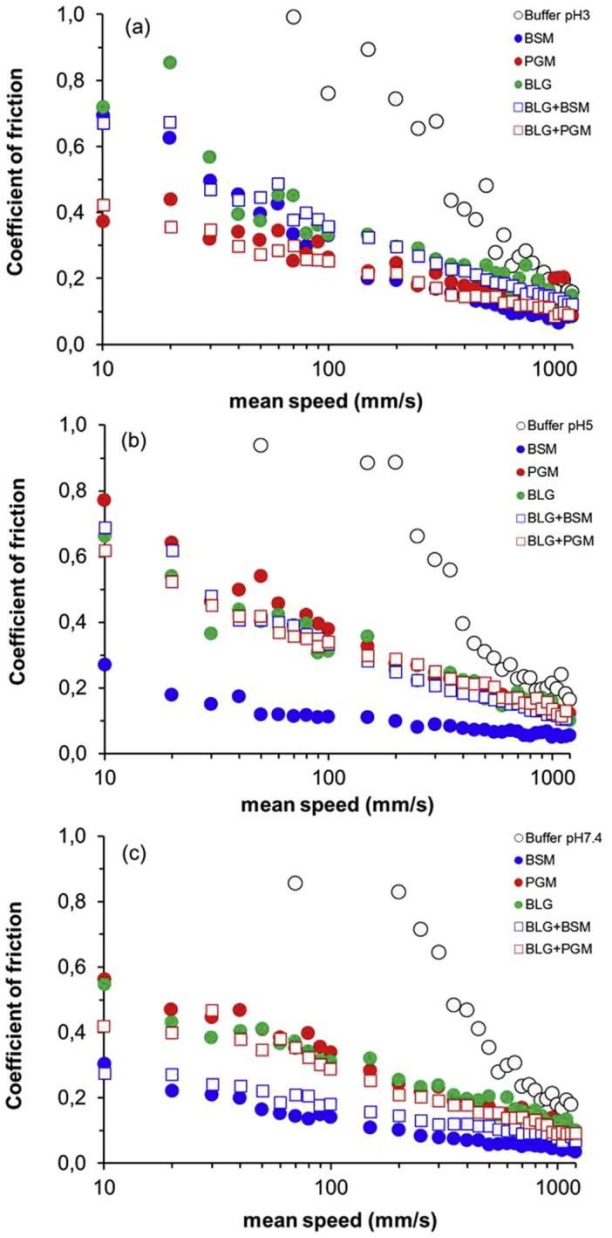

Fig. 5. Coefficient of friction vs. speed plots for POM–PDMS pair of the protein solutions at 1 mg/mL as characterized with MTM at (a) pH 3, (b) pH 5, and (c) pH 7.4 (load = 5 N, SRR = 20%).

characteristics, and lower apparent contact pressure (0.3 MPa) for the MTM experiments. With increasing mean speed, the μ values of all the samples started to decrease, reaching as low as 0.03 for the case of BSM at pH 7.4. However, even in the highest speed regime, no characteristic up-turn of μ values for elastohydrodynamic lubrication (EHL) (de Vincente, Stokes, & Spikes, 2005; Nalam, Clasohm, Mashaghi, & Spencer, 2010) was observed. Thus, the dominant lubrication mechanism is thought to be boundary and/or mixed lubrication without separation of the two opposing surfaces by the fluids. Inability to activate EHL mechanism for this contact is largely related to high surface roughness of the POM ball (Table 1), which was also attributed to as a main reason for higher friction forces for this pair in the pin-on-disk tribometry experiments (Fig. 4). The root-mean-square roughness (R_q) of the POM ball and PDMS disk is 659 ± 179 nm and 1.6 ± 0.3 nm, respectively. Therefore, the composite surface roughness of the POM–PDMS interface, $R_{q,c} = \sqrt{R_{q,POM}^2 + R_{q,PDMS}^2}$, is nearly identical with that of POM. Thus, for the activation of the EHL mechanism, the lubricating film thickness should be at least 3 times larger than $R_{q,c}$ (Røn & Lee, 2014), i.e. ca. 2 μm, which is not realistic, especially for aqueous lubrication.

Superior lubricity by the BSM solution to the other protein solutions, in particular at pH 7.4, was observed in consistent with the pin-on-disk tribometry results (Figs. 3 and 4). Due to the degraded lubricity of BSM at pH 3, however, the relative difference in μ values between the protein solutions became blurred, which also was consistent with the pin-on-disk tribometry data (Fig. 3). In fact, the μ values for the PGM solutions were slightly lower than those of BSM at pH 3, but this difference became much smaller in the high-speed regime. The data obtained from 10 mg/mL solutions of PGM or BLG–PGM (Supplementary information, Figure S2) were nearly indistinguishable from those obtained from 1 mg/mL in Fig. 5.

3.3.4. Surface adsorption properties and lubricity; BSM vs PGM

A strong contrast in the lubricity between BSM and PGM at PDMS–PDMS sliding interface remains elusive to be understood; both mucins are known to be large in molecular weight and comparable to each other (Sandberg, Blom, et al., 2009). Both are heavily glycosylated in the central region to similar extents, and are proposed to be adsorbing onto hydrophobic surfaces from water via hydrophobic interaction with unglycosylated C- and N-terminal regions. The adsorbed masses onto PDMS surface were also fairly comparable for BSM and PGM as shown from the same concentration, 1 mg/mL, in this study (Fig. 2).

It should be noted that the aqueous lubrication by adsorption of amphiphilic macromolecules onto hydrophobic surfaces is achieved essentially by hydration of the hydrophobic surfaces and removal of hydrophobic adhesion between the two opposing surfaces (Lee & Spencer, 2005). For mucins, this is achieved by respective role of unglycosylated terminal regions acting as an anchor onto the surface and the glycosylated central region acting to recruit water into the interface as mentioned above. Critically important for effective lubrication is to *sustain* the lubricating layer, i.e. mucin film, under persistently applied tribostress, not just to adsorb in high amount under initial tribostress-free condition. Thus, the adsorbed mass determined in the absence of tribostress (Fig. 2) provides only a first indication for lubricity. Another related point to note is that as the adsorption of mucins onto hydrophobic surfaces is achieved mainly via hydrophobic interaction, its binding strength is not strong enough to withstand the tribostress as a monolayer coating. For example, a recent study demonstrated that a monolayer coating of BSM on PDMS surface immersed in buffer solution, i.e. without excess BSM in solution, showed an immediate loss of lubricity upon sliding against a PDMS slider and a gradual increase of μ with increasing rotation on a sliding track

(Nikogeorgos et al., 2014). Thus, effective lubrication by a BSM solution at PDMS–PDMS or POM–PDMS interfaces is enabled by continuous re-establishment of the lubricating film under tribostress involving the cycles of adsorption–desorption–readsorption of BSM molecules. Thus, the superior lubricity of BSM to PGM should be related to many other factors than the adsorbed mass itself, such as BSM's superior binding strength onto the surface, more optimized conformation to hydrate the surface, as well as faster convection to the surface to re-form the lubricating films, or the combination thereof.

In order to visualize the relationship between the lubrication efficacy and the surface adsorption properties of the proteins in this study, their adsorbed masses, Γ, are plotted against μ values obtained from the pin-on-disk tribometry in Fig. 6. Because of somewhat extreme behavior of PGM and its mixture with BLG at 10 mg/mL, only the data obtained from 1 mg/mL protein solutions are displayed. In Fig. 6, as the BSM data set lies in the "right-bottom" quadrant, it reflects the case where high adsorbed mass is directly correlated with effective lubrication. The μ vs. Γ plots also display that the relatively higher friction of BSM at pH 3 is not due to the reduced adsorbed mass at that pH condition. PGM, being placed in the "right-upper" quadrant, clearly demonstrates the case where high adsorbed mass is not sufficient for effective boundary lubrication. Lastly, the location of BLG in the "upper-left" quadrant in the plot suggests that the poor adsorption onto PDMS surface is probably the primary reason for its poor boundary lubrication properties.

3.3.5. *Lubricating properties of BLG–mucin mixtures*

Distinctively different lubricating properties of BSM and BLG make it most interesting to explore the effect of mixing the two proteins. As mentioned earlier, this is interesting largely because a previous study by Vardhanabhuti et al. (2011) reported that the addition of a BLG solution to the PDMS–PDMS interface, lubricated by human saliva film, led to a rapid loss of lubricity at an acidic pH (3.5), but at a much slower pace at pH 7 or 5.

The relationship in the change of the adsorbed mass and lubricity upon mixing BLG and BSM could be clearly manifested in the μ vs. Γ plots in Fig. 6. Basically, as a group, the BLG–BSM data set is shifted leftwards, yet without shifting upwards with respect to the BSM data set, suggesting that the lubricity of BSM is generally maintained despite significantly reduced adsorbed masses upon mixing with BLG. In more detail, at pH 7.4, a substantial reduction in the adsorbed mass is accompanied with only a slight degradation of BSM's lubricity upon mixing with BLG. If the reduced surface adsorption is related to the competitive adsorption of BLG, this observation is surprising because, under persistently applied tribostress, molecules that adsorb quicker, i.e. BLG, should dominate the tribological interface. A fairly well sustained lubricity of the BLG–BSM mixture compared to the neat BSM solution suggests that BSM rather dominates the tribological properties of the mixture at this pH. One possible explanation is that as the adsorption of BLG onto PDMS surface tends to leave the ample PDMS surface uncovered (see the Section 3.2), BSM can readily overlay onto the surface that is pre-occupied with BLG at pH 7.4 and still effectively lubricate the tribological interface. At pH 5, however, a drastic reduction in both the adsorbed mass and lubricity of BLG–BSM mixture compared BSM is observed. This is related to more facile adsorption of BLG onto PDMS surface at pH 5 than at pH 3 or 7.4; the adsorbed mass of BLG at pH 5 was roughly twice those at pH 3 and 7.4 (Fig. 2). In turn, this can be attributed to the electrostatic neutrality of BLG at this pH (Fig. 1) and the absence of electrostatic repulsion between BLG molecules in the surface adsorption process. Thus, the dominance of BLG at the tribological interface, i.e. clearly degraded lubricity of BLG–BSM mixture compared to BSM, can be intensified at pH 5. At pH 3, a reduction in the adsorbed mass without degrading lubricity is observed upon mixing BSM with BLG, similarly with pH 7.4. However, as the μ values of BLG and BSM are similar to each other, the dominance of BLG at the tribological interface can be suggested only based on the significantly reduced adsorbed mass.

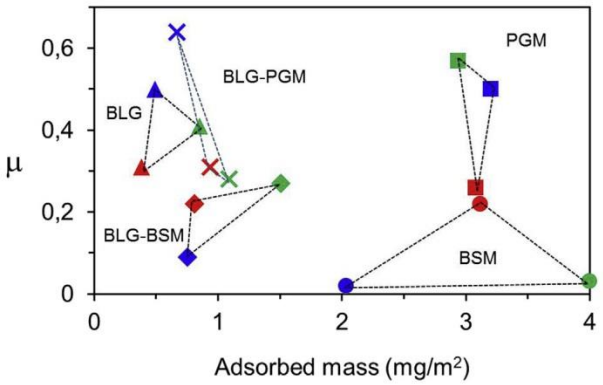

Fig. 6. Coefficient of friction, μ (PDMS–PDMS pair) vs. adsorbed mass, Γ (PDMS surface) of the protein solutions (1 mg/mL concentrations only). The color codes are for different pHs: red for pH = 3, green for pH = 5, and blue for pH = 7.4. Different symbols represent different protein or mixed protein solutions. (For interpretation of the references to color in this figure legend, the reader is referred to the web version of this article.).

Overall, a strong pH dependence of the lubricating properties of BLG–BSM at the PDMS–PDMS interface, which can be related to the reported pH dependence of the lubricating properties of BLG–saliva interaction, was confirmed even on a molecular level interaction. However, more detailed trends are very different in the interaction of BLG–saliva vs. BLG–BSM. Firstly, for the former, strong interaction of BLG with saliva (Vingerhoeds et al., 2005) or mucosa (Withers, Cook, Methven, Gosney, & Khutoryanskiy, 2013) has well been established and it formulates the ground for the rapid depletion of saliva films from the tribological interface at pH 3.5. Meanwhile, for the mixed BLG–BSM solution at 1 mg/mL concentration, competitive adsorption between them onto the tribological interface and its dependence on pH appears mainly responsible for varying lubricity according to pH change. This means, however, that BLG and mucins do not formulate tightly bound aggregates in the mixture solution. Secondly, while rapid degradation of lubricity was observed only at pH 3.5 for the BLG–saliva interaction, the degraded lubricity was most prominent at pH 5 for the BLG–BSM interaction, yet much weaker at pH 7.4 or pH 3. Again, this is due to that the main cause for the degrading lubricity of BLG–BSM mixed solution is competitive adsorption onto the tribological interface rather than strong aggregation between them.

For the mixtures of BLG–PGM, as the lubricity of BLG or PGM, as well as the mixed solution of BLG–PGM, is equally poor, the tribology data alone do not provide conclusive information on the interaction between BLG and PGM. Meanwhile, Fig. 6 shows that the net effect of mixing BLG and PGM is featured with substantially decreased adsorbed masses compared to the neat PGM solutions. Thus, it can be also suggested that BLG dominates the tribological interface for BLG–PGM mixture.

4. Conclusions

In this study, we have investigated the molecular-level interaction between mucins and BLG by means of tribological approaches according to mucin type, solution pH, and protein

concentration. Hydrophobic interfaces, namely PDMS–PDMS and POM–PDMS, were employed for feasible adsorption of the proteins and consequent possibility of assessment of the boundary lubricating properties. Surface adsorption properties of the proteins by BCA assay revealed that both mucins adsorbed onto the hydrophobic substrates in a large amount to form either highly compact layers or multilayers, whereas BLG appeared to adsorb without interfering with neighboring molecules or even by partly exposing bare substrates. This difference was firstly related to generally more effective lubricating properties of mucins, in particular BSM, compared to BLG. Nevertheless, nearly ignorable lubricating effect by PGM, despite its facile surface adsorption, suggests that other parameters than adsorbed masses play a significant role to impart superior lubricity of BSM to PGM or BLG. While both pin-on-disk tribometry and MTM were employed to provide the tribological contacts with different contact pressure, speed range, and slide/roll ratio, the dominating lubrication mechanism by the protein solution was boundary lubrication. Surface adsorption and lubricating properties of mixed protein solutions, such as BLG–BSM and BLG–PGM, with respect to neat protein solutions were of prime interest as it can be compared with the well-known role of BLG as astringency to form a complex with saliva and rapidly deplete from the tribological interface at acidic pH (3.5, for example). Even in the absence of tribostress, the adsorbed masses of the mixed protein solutions reduced significantly, and BLG appeared to dominate the surface adsorption event, presumably due to the reduced concentration of mucins as well as the Vroman effect. Nevertheless, excellent lubricity was still observed at pH 7.4 and BSM apparently dominated the tribological interface, which highlights the excellent lubricating capabilities of BSM. Although being still relatively more lubricious than the other proteins, the BLG–BSM mixture showed the highest level of degradation in the lubricity of BSM at pH 5, which contrasts the case of BLG–saliva interaction. This is due to that instead of strong aggregation, as in BLG–saliva, the lubricating properties of BLG–BSM are determined by competitive adsorption of the two proteins onto substrates. Most importantly, these observations further suggest that BLG and BSM molecules do not form strong aggregates, especially under tribological stress. PGM's intrinsically weaker lubricity remained largely unchanged even in the interaction with BLG.

Acknowledgments

The authors would like to thank to the Turkish Government for a PhD scholarship, European Research Council (Funding scheme: ERC Starting Grant 2010, project 261152), and the Danish Strategic Research Council (DSF -10-93456, FENAMI Project) for financial support.

Appendix A. Supplementary data

Supplementary data related to this article can be found at http://dx.doi.org/10.1016/j.foodhyd.2015.09.013.

References

Bansil, R., Stanley, E., & LaMont, J. T. (1995). Mucin biophysics. *Annual Review Physiology, 57*, 635–657.
Berg, I. C. H., Lindh, L., & Arnebrant, T. (2004). Intraoral lubricaiton of PRP-1, statherin, and mucin as studied by AFM. *Biofouling, 20*, 65–70.
Çelebioğlu, H. Y., Guðjónsdóttir, M., Meier, S., Duus, J.Ø., Lee, S., & Chronakis, I. S. (2015). Spectroscopic studies of the interactions between beta-lactoglobulin and bovine submaxillary mucin. *Food Hydrocolloids, 50*, 203–210.
Chen, J., Liu, Z., & Prakash, S. (2014). Lubrication studies of fluid food using a simple experimental set up. *Food Hydrocolloids, 42*, 100–105.
Chen, J., & Stokes, J. R. (2012). Rheology and tribology: two distinctive regimes of food texture sensation. *Trends in Food Science & Technology, 25*(1), 4–12.
Chojnicka-Paszun, A., de Jongh, H. H. J., & de Kruif, C. G. (2012). Sensory perception and lubrication properties of milk: influence of fat content. *International Dairy Journal, 26*, 15–22.
Davies, J. M., & Viney, C. (1998). Water-mucin phases: conditions for mucus liquid crystallinity. *Thermochimica Acta, 315*, 39–49.
Durrer, C., Irache, J. M., Duchene, D., & Ponchel, G. (1995). Mucin interactions with functionalized polystyrene latexes. *Journal of Colloid and Interface Science, 170*(2), 555–561.
Engelhardt, K., Lexis, M., Gochev, G., Konnerth, C., Miller, R., Willenbacher, N., et al. (2013). pH effects on the molecular structure of β-lactoglobulin modified air–water interfaces and its impact on foam rheology. *Langmuir, 29*, 11646–11655.
Fang, Y., & Dalgleish, D. (1997). Conformation of beta-lactoglobulin studied by FTIR: effect of pH, temperature, and adsorption to the oil-water interface. *Journal of Colloid and Interface Science, 196*, 292–298.
Joyner Melito, H. S., Pernell, C. W., & Daubert, C. R. (2014). Impact of formulation and saliva on acid milk gel friction behavior. *Journal of Food Science, 79*, 67–80.
Krisdhasima, V., McGuire, J., & Sproull, R. (1992). Surface hydrophobic influences on β-lactoglobulin adsorption kinetics. *Journal of Colloid and Interface Science, 154*, 337–350.
Lassen, B., & Malmsten, M. (1997). Competitive protein adsorption at plasma polymer surfaces. *Journal of Colloid and Interface Science, 186*, 9–16.
Latour. (2008). Molecular simulation of protein-surface interaction: Benefits, problems, solutions, and future directions (Review). *Biointerphases, 3*(3), FC2–FC12.
Lee, S., Müller, M., Rezwan, K., & Spencer, N. D. (2005). Porcine gastric mucin (PGM) at the water/poly(dimethylsiloxane) (PDMS) interface: influence of pH and ionic strength on its conformation, adsorption, and aqueous lubrication properties. *Langmuir, 21*, 8344–8353.
Lee, S., & Spencer, N. D. (2005). Aqueous lubrication of polymers: influence of surface modification. *Tribology International, 38*, 922–930.
Lundin, L., Golding, M., & Wooster, T. J. (2008). Understanding food structure and function in developing food for appetite control. *Nutrition & Dietetics, 65*, S79–S85.
McClements, D. J., Decker, E. A., & Park, Y. (2009). Controlling lipid bioavailability through physicochemical and structural approaches. *Critical Reviews in Food Science and Nutrition, 49*(1), 48–67.
Menchicchi, B., Fuenzalida, J. P., Bobbili, K. B., Hensel, A., Swamy, M. J., & Goycoolea, F. M. (2014). Structure of chitosan determines its interactions with mucin. *Biomacromolecules, 15*, 3550–3558.
Menchicchi, B., Fuenzalida, J. P., Hensel, A., Swamy, M. J., David, L., Rochas, C., et al. (2015). Biophysical analysis of the molecular interactions between polysaccharides and mucin. *Biomacromolecules, 16*, 924–935.
Meyer, D., Vermulst, J., Tromp, R. H., & de Hoog, E. H. A. (2011). The effect of inulin on tribology and sensory profiles of skimmed milk. *Journal of Texture Studies, 42*, 387–393.
Nalam, P. C., Clasohm, J. N., Mashaghi, A., & Spencer, N. D. (2010). Macrotribological studies of poly(L-lysine)-graft-poly(ethylene glycol) in aqueous glycerol mixtures. *Tribology Letters, 37*, 541–552.
Nikogeorgos, N., Madsen, J. B., & Lee, S. (2014). Influence of impurities and contact scale on the lubricating properties of bovine submaxillary mucin (BSM) films on a hydrophobic surface. *Colloids and Surfaces B: Biointerfaces, 122*, 760–766.
Pakkanen, K. I., Madsen, J. B., & Lee, S. (2015). Conformation of bovine submaxillary mucin layers on hydrophobic surface as studied by biomolecular probes. *International Journal of Biological Macromolecules, 72*, 790–796.
Prakash, S., Tan, D. D. Y., & Chen, J. (2013). Applications of tribology in studying food oral processing and texture perception. *Food Research International, 54*, 1627–1635.
Qaqish, R. B., & Amiji, M. M. (1999). Synthesis of a fluorescent chitosan derivative and its application for the study of chitosan-mucin interactions. *Carbohydrate Polymers, 38*, 99–107.
Røn, T., & Lee, S. (2014). Influence of temperature on the frictional properties of water-lubricated surfaces. *Lubricants, 2*(4), 177–192.
Rossetti, D., Bongaerts, J. H. H., Wantling, E., Stokes, J. R., & Williamson, A. (2009). Astringency of tea catechins: more than an oral lubrication tactile percept. *Food Hydrocolloids, 23*(7), 1984–1992.
Sandberg, T., Blom, H., & Caldwell, K. D. (2009). Potential use of mucins as biomaterial coatings. I. Fractionation, characterization, and model adsorption of bovine, porcine, and human mucins. *Journal of Biomedical Materials Research A, 91*, 762–772.
Sandberg, T., Mellina, L., Gelius, U., & Caldwell, K. D. (2009). Surface analysis of pure and complex mucin coatings on a real-type substrate using individual and combined mBCA, ELLA, and ELISA. *Journal of Colloid and Interface Science, 333* , 180–187.
Sarkar, A., Goh, K. K. T., & Singh, H. (2009). Colloidal stability and interactions of milk-protein-stabilized emulsions in an artificial saliva. *Food Hydrocolloids, 23*, 1270–1278.
Selway, N., & Stokes, J. R. (2013). Insights into the dynamics of oral lubrication and mouth feel using soft tribology: differentiating semi-fluid foods with similar rheology. *Food Research International, 54*, 423–431.
Shi, L., & Caldwell, K. D. (2000). Mucin adsorption to hydrophobic surfaces. *Journal of colloid and Interface Science, 224*, 372–381.
Silletti, E., Vingerhoeds, M. H., Norde, W., & van Aken, G. A. (2007). The role of electrostatics in saliva-induced emulsion flocculation. *Food Hydrocolloids, 21*, 596–606.
Singh, H., & Ye, A. (2013). Structural and biochemical factors affecting the digestion

of protein-stabilized emulsions. *Current Opinion in Colloid & Interface Science, 18*, 360–370.
Singh, H., Ye, A., & Horne, D. (2009). Structuring food emulsions in the gastrointestinal tract to modify lipid digestion. *Progress in Lipid Research, 48*, 92–100.
Smith, P. K., Krohn, R. I., Hermanson, A. K., Mallia, A. K., Gartner, F. H., Provenzano, E. K., et al. (1985). Measurement of protein using bicinchoninic acid. *Analytical Biochemistry, 150*, 76–85.
Sotres, J., Madsen, J. B., Arnebrant, T., & Lee, S. (2014). Adsorption and nanowear properties of bovine submaxillary mucin films on solid surfaces: influence of solution pH and substrate hydrophobicity. *Journal of Colloid and Interface Science, 428*, 242–250.
Svensson, O., & Arnebrant, T. (2010). Mucin layers and multilayers - physicochemical properties and applications. *Current Opinion in Colloid & Interface Science, 15*, 395–405.
Tabak, L. A., Kevine, M. J., Mandel, I., & Ellison, S. A. (1982). Role of salivary mucins in the protection of the oral cavity. *Journal of Oral Pathology, 11*, 1–17.
Van Aken, G. A. (2013). Acoustic emission measurement of rubbing and tapping contacts of skin and tongue surfaces in relation to tactile perception. *Food Hydrocolloids, 31*, 325–331.
Van Aken, G. A., Vingerhoeds, M. H., & de Hoog, E. H. A. (2007). Food colloids under oral conditions. *Current Opinion in Colloid & Interface Science, 12*(4–5), 251–262.
Vardhanabhuti, B., Cox, P. W., Norton, I. T., & Foegeding, E. A. (2011). Lubricating properties of human whole saliva as affected by β-lactoglobulin. *Food Hydrocolloids, 25*, 1499–1506.
de Vincente, J., Stokes, J. R., & Spikes, H. A. (2005). Lubrication properties of non-adsorbing polymer solutions in soft elastohydrodynamic (EHD) contacts. *Tribology International, 38*, 515–526.
Vingerhoeds, M. H., Blijdenstein, T. B. J., Zoet, F. D., & van Aken, G. A. (2005). Emulsion flocculation induced by saliva and mucin. *Food Hydrocolloids, 19*, 915–922.
Vroman, L., & Adams, A. L. (1969). Findings with the recording ellipsometer suggesting rapid exchange of specific plasma proteins at liquid/solid interfaces. *Surface Science, 16*, 438–446.
Withers, C. A., Cook, M. T., Methven, L., Gosney, M. a, & Khutoryanskiy, V. V. (2013). Investigation of milk proteins binding to the oral mucosa. *Food & Function, 4*, 1668–1674.
Yakubov, G. E., McColl, J., Bongaerts, J. H., & Ramsden, J. J. (2009). Viscous boundary lubrication of hydrophobic surfaces by mucin. *Langmuir, 25*, 2313–2321.
Zúñiga, R. N., Tolkach, A., Kulozik, U., & Aguilera, J. M. (2010). Kinetics of formation and physicochemical characterization of thermally-induced beta-lactoglobulin aggregates. *Journal of Food Science, 75*, 261–268.

Appendix: Supplementary data

<The procedure to obtain the adsorbed mass data from BCA assay>

1. Experiments

The schematic of the experimental procedure is shown in scheme 1.

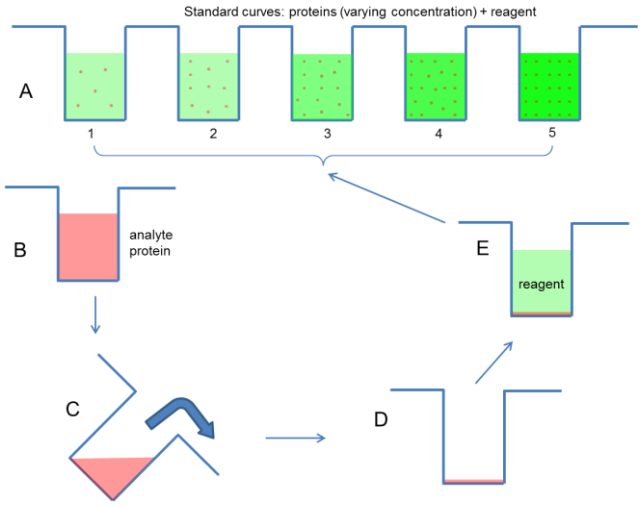

Scheme 1. The experimental procedure to obtain the standard curves (A) and to determine the adsorbed mass for an analyte protein on a microtiter well (B-E).

1. **STEP A**: Standard curves were firstly obtained according to the procedure provided by the manufacturer (Sigma Aldrich). The basic conditions include; sample:reagent = 1:8 (25 μL of the sample or standard at varying concentrations and 200 μL of the reagent) in each well, thoroughly mix for 30 seconds, incubate at room temperature for 2 hours, and measure the absorbance at 540 nm on a plate reader.

The results for the standard curves are as follows.

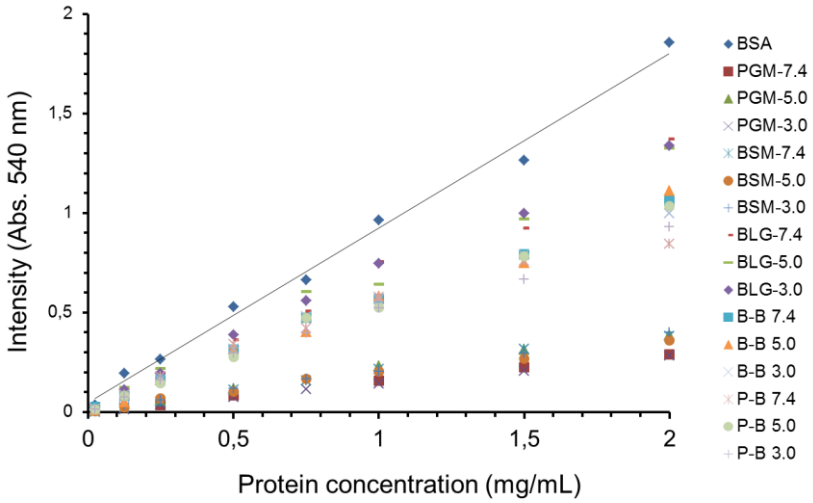

Figure S1. Standard curves for each protein or protein mixtures in the study: the numbers after the name of the protein acronyms represent the pH. For mixed proteins, B-B and P-B stand for BSM-BLG and PGM-BLG, respectively.

For clarity, the linear regression for BSA only is presented in this plot (Figure 1), but the same process applies to all proteins. Here, we stress that we did not rely on BSA as a universal protein for the standard curves, and in fact, we did not even use it for the calculations later. BSA was employed only for the validation of BCA technique in general. Instead, each protein or protein mixture, such as BSM, PGM, BSM-BLG, and PGM-BLG, at known concentrations (within the range between 25 μg/mL to 2,000 μg/mL) and varying pH (3, 5, and 7.4), were employed as standard proteins. This removes any potential errors that might be arising from different optical sensitivity of proteins in absorbance according to type, pH, and interaction between two proteins. It is already notable that the absorbance of BLG or BLG-mucin mixtures is much higher than that of pure mucins because of higher amount of peptide bonds for a given mass/volume. Thus, they provide fairly different standards curves.

2. **STEP B:** 100 μL of the protein sample solution ("analytes", in variation of the type (BSM, PGM, BSM-BLG, and PGM-BLG), concentration (1 or 10 mg/mL), and pH (3, 5, and 7.4)). For statistical evaluation, 3 wells were employed for each sample. 2 hours were provided to allow for the proteins to adsorb on the bottom surface of the wells.

3. **STEP C:** The protein solutions were discarded. Then, the wells were filled with respective buffers and emptied again a couple of times (rinsing). At this point, strongly bound proteins are assumed to remain on the bottom surface of the wells.

4. **STEP D:** The microtiter wells were filled with 225 μL of reagent. The complex formation between peptide bond and Cu^{+} is assumed to occur even though the proteins are localized on the bottom surface of the wells, and possibly in multilayers, because Cu^{+} ions are much smaller than the proteins in size.

4. **STEP E:** The absorbance was measured. For all samples studied, the intensity of the measured absorbance from the analyate sample fell within the full range of the standard curves.

2. Calculation of the adsorbed masses of proteins

A schematic to illustrate the calculation of the adsorbed mass of the proteins is provided below.

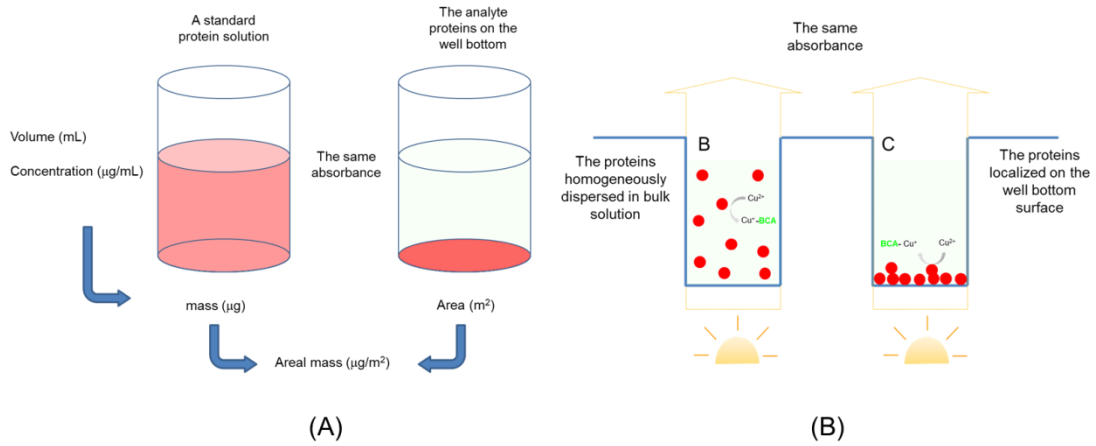

Scheme 2. (A) The calculation procedure to obtain the areal mass of the analyte proteins (B) An important assumption in this calculation is that the absorbance is the same as long as the protein amount in the cell is identical, whether the proteins are homogeneously dispersed or localized on the well bottom surface.

1. The concentration (c*) from the standard curve giving the same absorbance with the analyte is identified.

2. **(A, left):** From this c* (μg/mL) in the standard curve, and the volume of the well filled with the solution (= 225 μL), the total mass of the protein (μg) within the cell (the standard curves) can be obtained.

3. **(A. right):** Based on the area of the bottom well (m^2) and the total mass estimated in the previous step (μg) **(A, left)**, the adsorbed mass per unit area (μg/m^2) can be deduced.

CHAPTER 4

Interfacial Shear Rheology of β-Lactoglobulin – Bovine Submaxillary Mucin Layers Adsorbed at Air/Water Interface

(Paper III)

International Journal of Biological Macromolecules xxx (2017) xxx-xxx

Contents lists available at ScienceDirect

International Journal of Biological Macromolecules

journal homepage: www.elsevier.com

Interfacial shear rheology of β-lactoglobulin—Bovine submaxillary mucin layers adsorbed at air/water interface

Hilal Y. Çelebioğlu[a], Joanna Kmiecik-Palczewska[a, b], Seunghwan Lee[c], Ioannis S. Chronakis[a, *]

[a] Nano-BioScience Research Group, DTU-Food, Technical University of Denmark, Building 202, 2800, Kgs. Lyngby, Denmark
[b] Poznan University of Technology, Institute of Chemical Technology and Engineering, Department of Chemical Engineering and Equipment, ul. Berdychowo 4, 60-965 Poznan, Poland
[c] Department of Mechanical Engineering, Technical University of Denmark, DK-2800, Kgs. Lyngby, Denmark

ARTICLE INFO

Article history:
Received 16 February 2017
Received in revised form 25 March 2017
Accepted 15 April 2017
Available online xxx

Keywords:
Interfacial shear rheology
β-lactoglobulin
Bovine submaxillary mucin

ABSTRACT

The interfacial rheological properties of solutions of β-lactoglobulin (BLG), as a model food compound, mixed with bovine submaxillary mucin (BSM), a major salivary protein, have been investigated. Time, frequency, stress sweep and flow measurements have been performed at different pHs (7.4, 5.0 and 3.0), to investigate the air/water interfacial properties. All protein layers (BLG, BSM, and BLG-BSM mixtures) formed an elastic network at the air/water interface with low frequency dependence of the interfacial modulus. The results indicated that BLG moves faster as smaller molecule than mucin, and dominate the surface adsorption and the network formation for the BLG-BSM mixtures. Moreover, BLG-BSM protein mixtures exhibited interfacial properties with lower elastic and viscous moduli than BLG, as a result of competitive displacement of BLG proteins with BSMs from the interface. It is suggested that hydrophobic patches of BSM can be imbedded into the BLG monolayer as driven by a strong hydrophobic interaction with air and disrupt the cohesive assembly of BLG, whereas the hydrophilic (negatively charged) parts of the BSM chain are protruding from the interface towards the bulk water.

© 2016 Published by Elsevier Ltd.

1. Introduction

Beta-lactoglobulin (BLG) is a milk protein widely used as functional ingredient for the formation and stabilization of food emulsions and foams [1–3], due to its ability to adsorb rapidly at the surface and stabilize colloidal systems [4]. BLG is the major whey protein, constituting >50% of the total whey proteins in bovine milk, with a molecular weight of 18.3 kDa and a radius of approximately 2 nm [5]. On the other hand, bovine submaxillary mucin (BSM), used as a model mucin in this study, is a glycoprotein consisting of a linear polypeptide core with a highly glycosylated central part accounting for up to 80% of the proteins molecular weight [6] which ranges between 0.5 and 20 MDa [7]. Among several types of mucin involved, submaxillary mucin is the one most closely related to oral processing.

The interaction between a model food protein, BLG, and saliva protein, bovine submaxillary mucin (BSM), has been investigated by different techniques, including nuclear magnetic resonance, dynamic light scattering, circular dichroism, in our recent study [8]. The main findings are: (i) An attractive interaction between the two proteins was suggested. (ii) Higher hydrophilic interactions between the proteins at lower pH supported the pH dependent activity of both BLG and BSM. (iii) The positively charged groups of BLG, especially at acidic pHs, neutralized negatively charged groups of BSM and caused the BSM to coil or contract into a smaller hydrodynamic volume [8,9]. (iv) Even a weak hydrogen bonding between BLG and BSM, promotes aggregation of mucins into a more compact structure at pH 7.4. (v) NMR studies showed that negatively charged BLG has a tendency to interact with negatively charged mucin via secondary interactions (hydrogen bonding and hydrophobic effects), where the electrostatic interactions are unlikely to be the main reason of the binding.

Another recent study [10] based on bicinchoninic acid (BCA) protein qualification assay showed that mucins were not only higher than BLG in the adsorbed masses onto the solid hydrophobic surface, but also adsorb in a more compact conformation due to a high flexibility to accommodate themselves in a narrow space and/or possibly to form multilayers. However, BLG can readily dominate the initial stage of surface adsorption at the solid/water interface in the solution mixture of BSM and BLG, due to the ability of the smaller and lighter BLG molecules to reach the surface faster than mucins. For the adsorption of the BLG-BSM mixture onto hydrophobic solid surfaces, it was assumed that there is a large portion of "free" BLG molecules in the mixed protein solutions, and that they participate in the surface adsorption process in competition with the mucins. Consequently, the BLG, BSM and their mixtures showed an interesting interaction and different surface adsorption behavior at the solid/liquid interface. However, the interfacial properties of BLG, BSM, and their mixtures at air/liquid interface were not studied to date despite their high relevance and significance to the formation of emulsion and foams.

* Corresponding author.
Email address: ioach@food.dtu.dk (I.S. Chronakis)

http://dx.doi.org/10.1016/j.ijbiomac.2017.04.063
0141-8130/© 2016 Published by Elsevier Ltd.

UNCORRECTED PROOF

Furthermore, interfacial shear rheology provides valuable information on the intermolecular interaction processes and structural changes of interfacial layers at the air/liquid interface [11]. The interfacial shear rheology is based on the functional relationship between stress, deformation and the rate of deformation at an interface in terms of elastic modulus (G_i') and viscous modulus (G_i'') [12]. The interfacial rheological properties are less sensitive to Marangoni stresses and dynamic surface tension but more sensitive to intermolecular interactions between adsorbed molecules [13]. Hence, such properties are valuable to study protein interactions, in particular the adsorption of large molecular weight proteins (i.e. mucins) which have slow and irreversible adsorption process, and Marangoni stresses at which dynamic surface tension effects are suppressed [14]. It is to note that proteins at the interface interact through physical interactions such as electrostatic, hydrophobic as well as van der Waals forces.

The interfacial shear rheology of BLG has been studied as a function of heat treatment, pH dependence and ionic strength. For example, Jung et al. [15], Kim et al. [16], Roth et al. [17], and Rühs et al. [3] suggested that BLG is able to develop a strong and rapid viscoelastic layer at the air/water interface, which is strongest at its isoelectric point (pI 5.4) due to the lowest net charge and due to the presence of a more strongly cross-linked protein network at the interface. Meanwhile, to the best of our knowledge, only one study is available in the literature related to the interfacial rheological properties of saliva and astringent compounds by Rossetti et al. [13], who have studied the interfacial behavior of pig gastric mucin and bovine sub-maxillary gland mucin in comparison with the saliva. They have observed that these mucins do not form a strong protein network, as indeed shown by the human saliva at the air/water interface.

Moreover, it is important to understand the interfacial rheological properties of adsorbed BLG and BSM mucin layers and their network formation at the air/liquid interface, as this is relevant in understanding the interactions between (dairy) emulsions and saliva, and thus in understanding emulsion perception. In this study, the air/water interfacial rheological properties of solutions of BLG with a salivary BSM mucin protein, and their mixtures at different pHs, were investigated.

2. Materials and methods

2.1. Sample preparation

BLG from bovine milk and BSM (Type I-S) were purchased from Sigma Aldrich (Sigma Aldrich A/S, Brøndby, Denmark), and were used as received. Protein solutions with the concentration of 1 mg/mL were prepared by dissolving proteins in 10 mM phosphate buffered saline (PBS) solutions. The pH values of the buffer solutions were adjusted to 7.4, 5.0, and 3.0 by the addition of HCl or NaOH as appropriate. For the mixtures of BSM and BLG, the two protein solutions were mixed at the ratio of 1:1 (v:v), while the final concentrations of the total proteins were set at 1 mg/mL or 2 mg/mL. The concentration of 1 mg/mL was used for the first mixture (MIX 1) where each protein (BLG and BSM) has 0.5 mg/mL in concentration. The second mixture (MIX 2) was prepared with 1 mg/mL concentration of each proteins (BLG and BSM), hence with 2 mg/mL in total protein concentration.

2.2. Interfacial shear experiments

In the present study, a bi-conical disc was used, where the edge of the bi-cone bob was located at the interface of a liquid sample (air/liquid interface). The outer cup is stationary and the bi-conical geometry acts as "two-dimensional concentric cylinder geometry" [18]. Further details about the instrumental setup of the bi-cone rheometer can be found in the literature [19].

A Physica MCR 302 rheometer with a Peltier temperature device (P-PTD 200/80I) and the Interfacial Rheology System (IRS) accessory with the bi-cone (BiC68-5) geometry from Anton Paar (Graz, Austria) were used for all the experiments. The bi-cone geometry had a diameter of 68.32 mm and the angle was 10° (2 × 5°). Time sweep measurements were performed with a constant frequency (6.28 rad/s) and an amplitude gamma (strain) of 0.02% during 150 min. Then, G_i' and G_i'' were measured in angular frequency from initial 100 rad/s to final 0.01 rad/s with amplitude gamma of 0.02%. After that, strain sweeps were obtained using a constant frequency of 6.28 rad/s. Finally, flow measurements were performed while changing the shear rate from 0.1 s^{-1} to 300 s^{-1}. All measurements were performed at 20 °C.

3. Results & discussions

3.1. Time dependence of the interfacial modulus

Initially, the interfacial linear viscoelastic properties of the proteins were measured as a function of time. The time dependencies of the interfacial shear elastic modulus G_i' and viscous modulus G_i'' for BLG, BSM and for the BSM-BLG mixtures at different pH values are shown at Fig. 1. The results indicate that all the proteins adsorbed immediately and formed a stable viscoelastic network at the air/water interface with $G_i' > G_i''$ with a formation of a plateau within 50 min.

Clearly, BLG molecules had higher elastic modulus than the BSM and the BLG-BSM mixtures, indicating that the BLG formed a stronger viscoelastic adsorption layer at all pH conditions. The elastic modulus of BLG was about 0.02, 0.2, and 0.035 Pa.m at pH 3.0, 5.0, and 7.4, respectively. Thus, BLG had relatively higher values of G_i' and G_i'' at the pH close to the isoelectric point of the protein (pH = ~5.2). This is in agreement with previous studies for BLG and for other proteins, suggesting that in the absence of electrostatic repulsive interactions at their isoelectric pH, the proteins experience mainly attractive interactions at the interface leading to aggregation and network formation [17,20–23]. The increase of the electrostatic repulsions of the protein at pH 7.4 and pH 3 could be responsible for the lower viscoelastic interactions and lower interfacial modulus in comparison with the modulus of the protein at pH 5, as also suggested in previous studies [24,25,3].

BSM molecules formed weak viscoelastic networks immediately; the elastic and viscous modulus values remain nearly constant regardless of pH changes (Fig. 1). This weak viscoelastic network was destroyed easily even at low strain values (≥0.03%, see below). The lack of strong interfacial viscoelasticity of BSM was also shown in the study Rossetti et al. [13]. They have compared commercial mucins (pig gastric mucin and bovine sub-maxillary gland type I mucin from Sigma Aldrich) with the human whole saliva and concluded that the commercial mucin did not fully mimic the interfacial properties of human whole saliva, possibly due to the degradation of the gel-like structure occurred during the isolation process.

The interfacial rheological properties of the BLG and BSM mixtures are also shown in Fig. 1. The values of the elastic and viscous modulus for both BLG-BSM mixtures (MIX 1 and MIX 2) were between those of neat BLG and BSM. Both G_i' and G_i'' of the MIX 1 and MIX 2 at pH 5 and pH 3 were decreased during the first 60 min to reach a plateau, while they were almost stable at pH 7.4 during 150 min of time (Fig. 1). These results indicate that the interfacial layer of the protein mixtures is formed mainly through the adsorption of the interfacial active BLG molecules, with the additional incorporation of BSM molecules within the surface layer, which retard and diminish the interfacial

UNCORRECTED PROOF

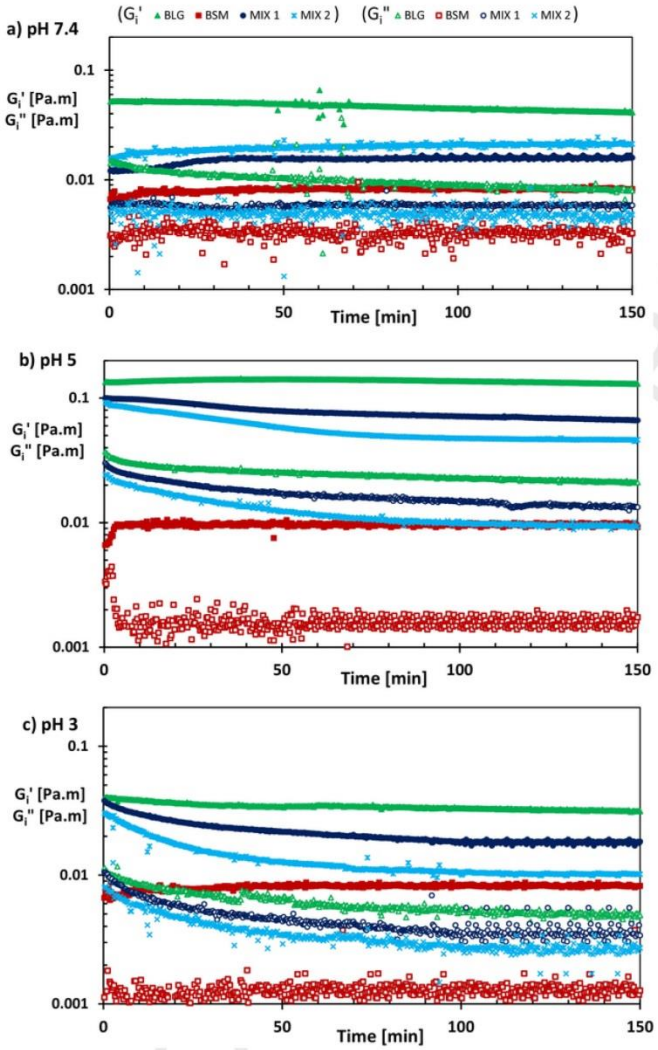

Fig. 1. Time sweep for 1 mg/mL BLG, BSM and the BLG-BSM mixtures at (a) pH 7.4, (b) pH 5.0, and (c) pH 3.0. Two different concentrations for the mixture were used. MIX 1 and MIX 2 represent 1 mg/mL and 2 mg/mL concentration, respectively.

network modulus. Note that MIX 2 has slightly higher modulus at pH 7.4, but lower modulus at pH 5.0 and pH 3.0, than the MIX 1.

The pH dependent changes of the elastic modulus (G_i') of BLG, BSM and BLG-BSM mixtures with different protein concentrations is shown at Fig. 2a. In particular, the values of the elastic modulus were utilized for the evaluation of the interaction between the BLG and BSM [26], by using the interaction term $\Delta G_i'$

$$G_{i\,mix}' = G_{i\,BLG}' + G_{i\,BSM}' + \Delta G_i' \quad (1)$$

where $G_{i\,mix}'$ is the elastic modulus of the mixture and $G_{i\,BLG}'$ and $G_{i\,BSM}'$ represent the elastic modulus of BLG and BSM, respectively (Fig. 2a).

The above results showed that BSM caused a decrease of the elastic modulus of the BLG-BSM mixtures, and that the interfacial properties of the protein mixtures have similar pH-dependent properties with the BLG. Consequently, for the BLG-BSM mixtures it is reasonable to suggest that BLG is the dominant interfacial active molecule due to its capability to adsorb fast and form an interfacial network, while the presence of long BSM chains rather disrupts it. This is in agreement with a previous study by Dickinson [27] where in the case of the competitive adsorption between proteins, the adsorbed layer is dominated by the protein that adsorbed first to the interface. In our recent tribology study, we have also observed that BLG dominates the surface adsorp-

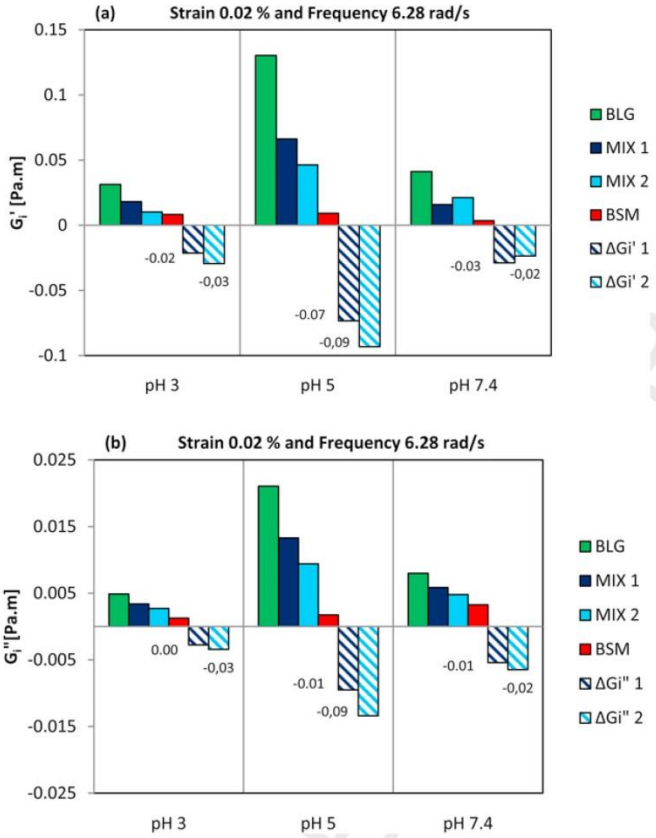

Fig. 2. (a) Elastic modulus and (b) viscous modulus of BLG, BSM, the BLG-BSM mixtures, and calculated interaction terms $\Delta G_i'$ and $\Delta G_i''$ Two different concentrations for the mixture were used. MIX 1 and MIX 2 represent 1 mg/mL and 2 mg/mL concentration, respectively. All samples were prepared in phosphate buffer. Values shown correspond to the frequency of 6.28 rad/s and strain of 0.02%.

tion at water/hydrophobic (solid surface) interfaces, and at pH 5.0 the adsorbed amount is roughly double to those at pH 3.0 and 7.4 [10]. Hägerström et al. [26] also found that bovine submaxillary gland mucin destroyed the interfacial network structure of the absorbed deacetylated gellan gum. Danov et al. [28] observed the same phenomena for the interfacial properties of active globular protein hydrophobin (HFBII) and the disordering protein β-casein. They showed that the disordering protein decreases the rigidity of the HFBII adsorption layers, due to the penetration of long hydrophobic chains of β-casein between the adsorbed HFBII molecules, as driven by the favorable hydrophobic interaction between the chains and air.

The negative interaction term $\Delta G_i'$ at each pH values denotes the extent of the reduction of the interfacial network of the protein mixtures (Fig. 2a). Note that the values of $\Delta G_i'1$ and $\Delta G_i'2$ were similar at each pH despite that the protein concentration was two times higher for the MIX 2. This could be due to that the large molecular weight BSM effectively disrupts the viscoelastic layer of BLG and limit the stability of the interfacial network even at lower concentrations (e.g. that of MIX 1). Moreover, the values of $\Delta G_i'$ showed maxima at pH 5.0, which indicates that the disruption of BLG layer by BSM is most effective at this pH condition. This is readily understandable for the case of pH 7.4, where both BLG and BSM were negatively charged, and thus BSM molecules may be repelled in approaching to the interface. However, at pH 3.0, BLG and BSM molecules are oppositely charged and even hydrogen bonding were observed to be activated [8]. Thus, BSM molecules may have a stronger attraction with the BLG layer formed at pH 3 than that at pH 7.4. Nevertheless, since both electrostatic and hydrogen bonding are hydrophilic characteristics, it would be predominantly the hydrophilic moieties, (e.g. central glycosylated regions of BSM), that are interacting with the BLG layer and the interaction would be limited within the water phase. Moreover, the increase of the electrostatic repulsions of the BLG molecules at pH 7.4 and pH 3 could be responsible for the lower interfacial modulus of BLG and the lower viscoelastic interactions of BLG with BSM, in comparison with the interactions found at pH 5 (Fig. 3). Thus, disruption of the BLG layer would be limited accordingly. On the contrary, at pH 5, the interaction of the hydrophobic patches of BSM with the BLG layer maybe particularly facilitated due to the non-polar characteristics of the BLG layer. Such interactions can be further extended at the air/water interphase and disrupt effectively the BLG layer, as illustrated at Fig. 3.

Similar trends of the interfacial properties were also observed for the viscous modulus $G_i''_{mix}$ of the mixture when correlated with $G_i''_{BLG}$

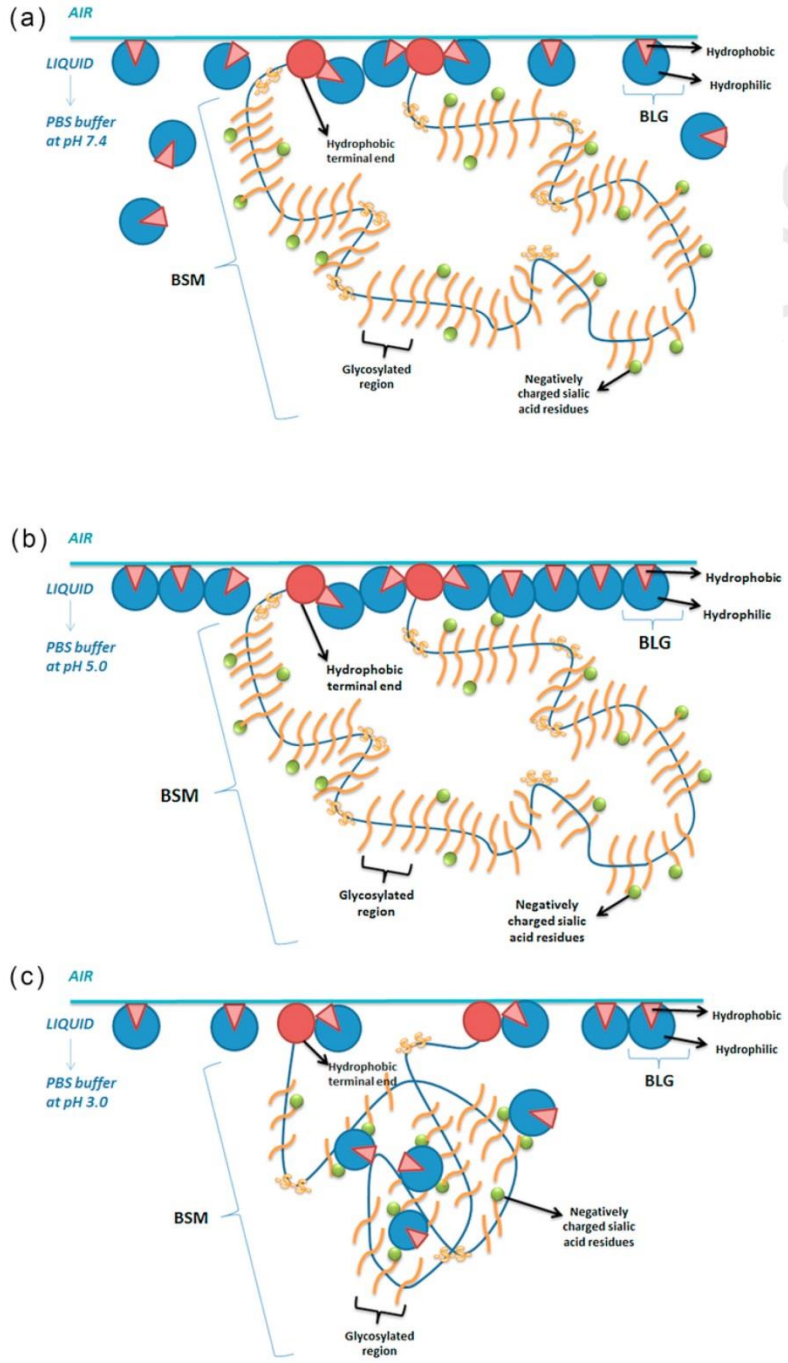

Fig. 3. Illustration of the interactions of hydrophobic patches of BSM with the adsorbed BLG layer at (a) pH 7.4, (b) pH 5.0 and (c) pH 3.0.

and $G_i''_{BSM}$ (the viscous modulus of BLG and BSM) and the term $\Delta G_i''$ (Fig. 2b).

3.2. Frequency dependence of the interfacial modulus

Fig. 4 shows the changes of the G_i' and G_i'' as a function of angular frequency for BLG, BSM, MIX 1 and MIX 2 at different pH values. The values of the elastic modulus G_i' were greater than the viscous modulus G_i'' for all the protein samples suggesting that they exhibited mainly elastic-like behavior within a frequency range from 0.01 rad/s to 10 rad/s. Moreover, the interfacial modulus were increased with the frequency, with different slopes and both moduli were described by the power law equation:

$$G_i' = k'\omega^{m'} \quad (2)$$

$$G_i'' = k''\omega^{m''} \quad (3)$$

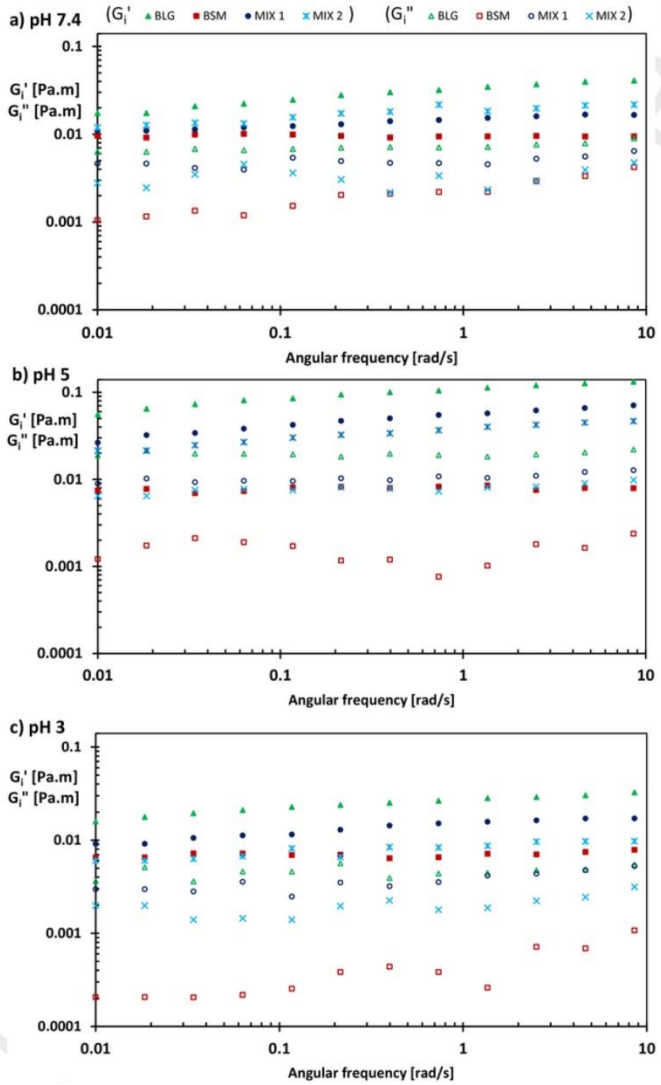

Fig. 4. Frequency dependence of BLG, BSM, and BLG-BSM mixtures at (a) pH 7.4, (b) pH 5.0, and (c) pH 3.0. Two different concentrations for the mixture were used. MIX 1 and MIX 2 represent 1 mg/mL and 2 mg/mL concentration, respectively. The data fit to power law equation: $G_i' = k'\omega^{m'}$ and $G_i'' = k''\omega^{m''}$ where the values of constants k' and $k''$and slopes m' and $m''$are shown in Table 1.

The values of constants k' and $k''$and slopes m' and $m''$are shown in Table 1.

The elastic modulus G_i' of BSM had lower slopes than the elastic modulus G_i' of BLG at each pH values (Table 1), i.e. BSM molecules were less frequency dependent and with low elastic modulus. The slopes (m') of BLG-BSM mixtures showed similar values at pH 7.4 and 3.0 and were low, while the slopes at pH 5.0 were higher and close to the slope of BLG. The similarities of the frequency sweeps of the BLG-BSM mixtures with that of BLG also support the above suggestion that BLGs move faster as smaller molecules than mucins, and dominate the surface adsorption, the network formation and stability in the BLG-BSM mixtures.

Frequency dependent changes in the interfacial complex (η_i^*) and interfacial steady-shear (η_i) viscosities of all protein samples at pH 7.4, pH 5.0 and pH 3.0 are shown in Fig. 5. Clearly the interfacial complex viscosity of the MIX 2 was significantly higher than the interfacial steady-shear viscosity at each pH values; this suggests that the protein samples deviate from the Cox-Merz rule (at which the complex dynamic viscosity (η^*) and the steady-shear viscosity (η) superimpose at equivalent numerical values of frequency and shear rate). The higher values of the interfacial complex viscosity in comparison with the interfacial steady-shear viscosity, indicates that the interfacial structure of the BLG-BSM mixture was easier to be deformed in the steady state flow than in the oscillatory shear. This type of behavior is characteristic for high-density entangled or aggregated structures [29] and provides additional evidences that an associated BLG-BSM interfacial network was formed.

3.3. Strain dependence of the interfacial modulus

Fig. 6 shows the results of strain sweeps for BLG, BSM and the mixtures at pH 7.4, 5.0 and 3.0. The both moduli were described by the power law equation:

$$G_i' = c'\gamma^{n'} \quad (4)$$

$$G_i'' = c''\gamma^{n''} \quad (5)$$

Table 1
The rate of frequency dependent change in viscoelastic moduli of BLG, BSM and the BLG-BSM mixture at pH 7.4, 5.0, and 3.0. Two different concentrations for the mixture were used. MIX 1 and MIX 2 represent 1 mg/mL and 2 mg/mL concentration, respectively. The data fit to power law equation: $G_i' = k'\omega^{m'}$ and $G_i'' = k''\omega^{m''}$ where the values of constants k' and k'' and slopes m' and m''. Frequency range was from 0.01 to 10 rad/s.

		constant		slope	
pH	sample	k'	k''	m'	m''
7.4	BLG	0.033	0.008	0.136	0.042
	BSM	0.010	0.002	[a]0.081	0.196
	MIX 1	0.015	0.005	0.072	0.041
	MIX 2	0.018	0.004	0.077	0.062
5.0	BLG	0.108	0.020	0.122	0.004
	BSM	0.008	0.002	0.013	0.210
	MIX 1	0.055	0.011	0.139	0.042
	MIX 2	0.037	0.009	0.116	0.060
3.0	BLG	0.027	0.005	0.100	0.030
	BSM	0.007	0.001	0.016	0.228
	MIX 1	0.015	0.004	0.060	0.087
	MIX 2	0.008	0.002	0.070	0.117

[a] Slope was calculated in frequency range of 0.02–0.06 rad/s.

The values of constants c' and $c''$and slopes n' and $n''$are shown in Table 2. In addition, Table 3 shows the crossover points of each sample.

According to Fig. 6a, BLG at pH 7.4 has a well-established linear viscoelastic region up to 3% of strain with 0.03 Pa.m of elastic modulus and 0.007 Pa.m of viscous modulus. At 25% of strain, the crossover point for the BLG samples was observed and each modulus started to decrease. The decrease of $G_i'$of BLG was rapid with a slope of −1.22, while the decrease of G_i'' was slower with a slope of −0.51. At pH 5.0, the BLG had higher values of G_i' (ca. 0.11 Pa.m) and G_i'' (ca.0.019 Pa.m) than at pH 7.4, however the crossover point was reached at 6% of strain with higher slopes (−2.06 for $G_i'$and −0.81 for G_i''). On the other hand, a lower modulus (0.02 Pa.m and 0.005 Pa.m for G_i' and G_i'' , respectively) and weak elastic properties were observed at pH 3.0, with similar crossover strain as at pH 5.0 (Table 3). In contrast to BLG, BSM lost its weak linear viscoelastic network properties rapidly with increasing strain beyond 0.003% and then exhibited viscous behavior (Fig. 6).

In the case of the protein mixtures (MIX 1 and MIX 2), despite the presence of large BSM molecules, they exhibited a viscoelastic strain sweep behavior similar to BLG. The crossover point for the MIX 1 mixture was observed at ca. 37%, 8%, and 12% strain at pH 7.4, 5.0, and 3.0, respectively. The slopes of the decrease of G_i' was −1.16, −1.86, −1.95, similar to BLG, while the decrease of G_i'' was lower than BLG with slopes of −0.32, −0.72, −0.42 at pH 7.4, 5.0 and 3.0, respectively.

These results also indicate that the BLG protein dominated the network formation and network stability for the BLG-BSM mixtures at 1 mg/mL. The strain sweep of the MIX 2 (Fig. 6 and Tables 2 and 3) showed similar elastic and viscous modulus and slopes with MIX 1 at pH 7.4; however, the modulus of the MIX 2 was decreasing with a lower slope at pH 5.0 than MIX 1. For instance, the slopes of $G_{i'}$ of MIX 2 were −1.29 and −1.27, while they were −1.17 and −1.86 for MIX 1 at pH 7.4 and pH 5.0, respectively. At pH 3.0 both the elastic and viscous moduli of the MIX 2, as well as the linear viscoelastic region were very narrow, close to BSM, with the crossover point at 0.40% of strain. This may suggest that the MIX 2 at pH 3.0 had a disrupted, non-stable interfacial network formation and lower modulus than MIX 1 due to the higher content of BSM (Table 3). The higher hydrophilic interaction between the proteins at pH 3.0, as well as the increased electrostatic attraction between positively charged BLG and negatively charged BSM, as suggested at our previous study [8], most probably caused the BSM to be imbedded into the assembled BLG layer and destabilize the interfacial network.

Fig. 7 shows the *tan* δ_i values as a function of strain for BSM, BLG and the mixtures of BSM-BLG. *Tan* δ_i is the ratio of G_i''/G_i', providing a convenient index of the proportion of the viscous-like character. The higher *tan* δ_i values indicate a more viscous-like behavior while the lower values indicate a more elastic-like behavior. At all pH values, BLG showed lower *tan* δ_i values with increased strain than the MIX 1 and MIX 2. BSM showed low *tan* δ_i values below the strain of 0.02% where the interfacial network disrupted suddenly. Moreover, MIX 2 exhibited higher *tan* δ_i values at pH 3.0, indicating the relative viscous-like behavior in comparison with the interfacial network at pH 7.4 and 5.0. The increased electrostatic interaction between protein (positively charged BLG and negatively charged BSM) at pH 3.0 resulted in the formation of a complex protein interfacial network with dominating BSM viscoelasticity.

UNCORRECTED PROOF

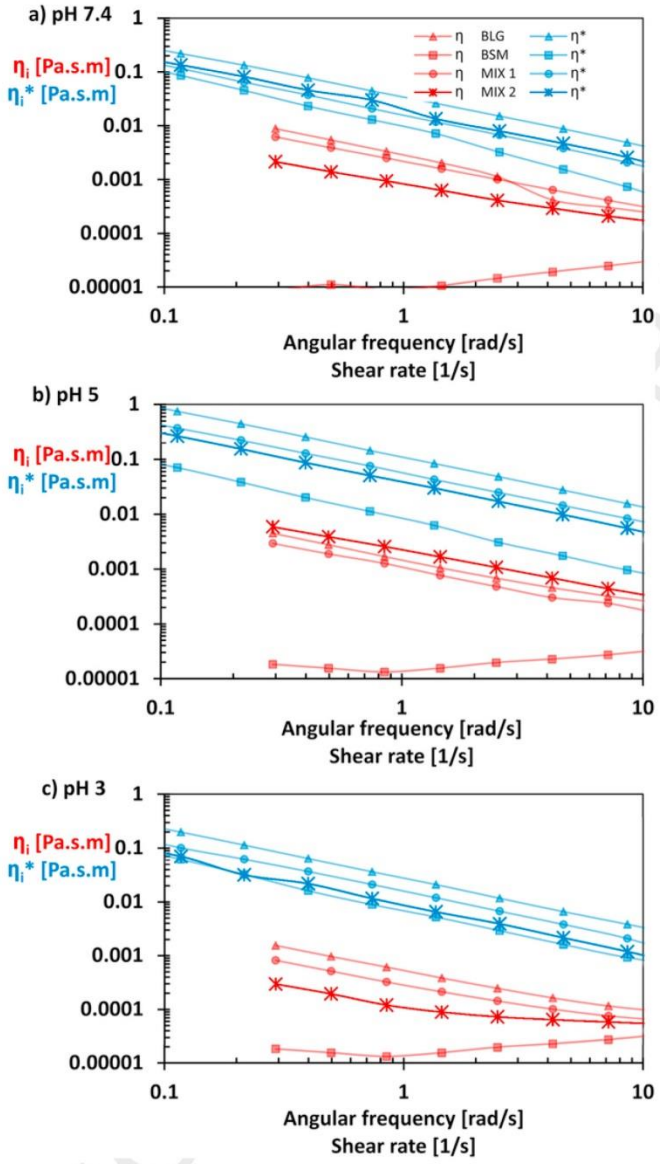

Fig. 5. Interfacial complex viscosity (blue) and interfacial steady-shear viscosity (red) of BLG, BSM, and the BLG-BSM mixtures (a) pH 7.4, (b) pH 5.0, and (c) pH 3.0. Two different concentrations for the mixture were used. MIX 1 and MIX 2 represent 1 mg/mL and 2 mg/mL concentration, respectively. (For interpretation of the references to colour in this figure legend, the reader is referred to the web version of this article.)

4. Conclusions

We have studied the interfacial rheological properties of solutions of BLG (as a model food compound) with a salivary mucin protein BSM and their mixtures, at different pHs. All protein layers (BSM, BLG, MIX1 and MIX2) formed at air/water interface has some similarities such as a rapidly developed elastic interfacial network and low frequency dependence of the interfacial modulus.

The BSM protein with the high molecular weight formed a weak viscoelastic interfacial network (lower modulus) compared to BLG at all pHs, which is destroyed even at a low strain (0.003%). The pH has a significant effect on the surface density of adsorbed BLG proteins, as it determines the net charges and the modulus of the interfacial net-

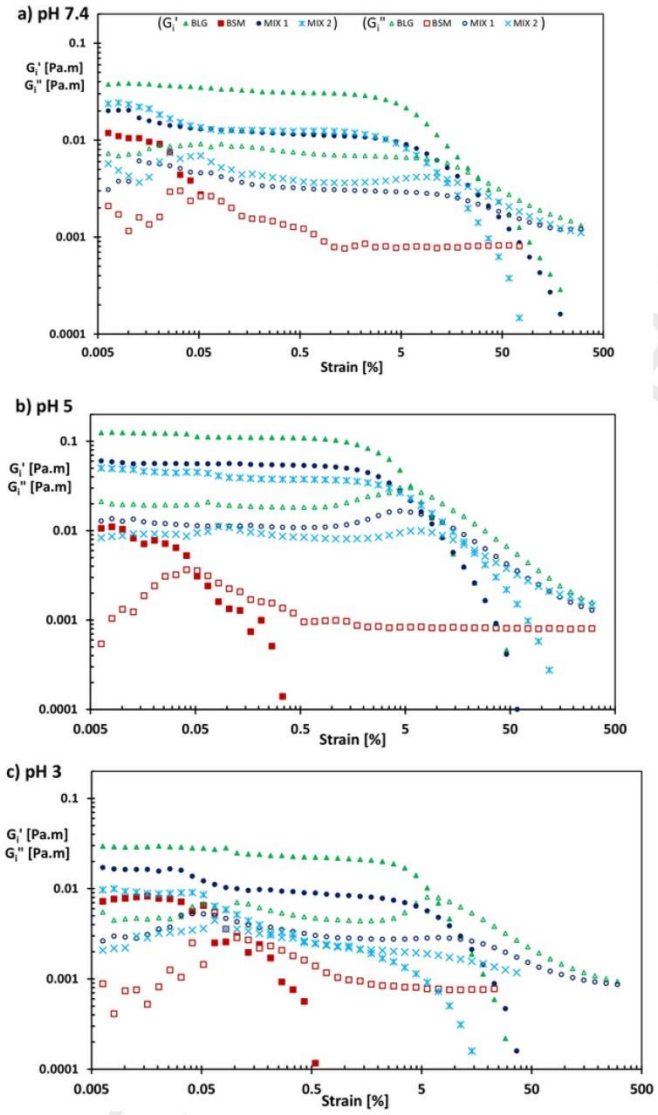

Fig. 6. Strain sweep for 1 mg/mL BLG, BSM and the BLG-BSM mixtures at (a) pH 7.4, (b) pH 5.0, and (c) pH 3.0. Values shown correspond to the frequency of 6.28 rad/s. Two different concentrations for the mixture were used. MIX 1 and MIX 2 represent 1 mg/mL and 2 mg/mL concentration, respectively. The rate of strain dependent decrease in viscoelastic moduli of protein samples after the breaking of the sample structure fit to power law equation: $G_i' = c'\gamma^{n'}$ and $G_i'' = c''\gamma^{n''}$ where the values of constants c' and c'' and slopes n' and n'' are shown in Table 2.

work. At pH close to the isoelectric point, electrostatic repulsions between the adsorbed BLG molecules at the interface are minimized, promoting the formation of a stable adsorbed layer with a high elastic modulus.

Furthermore, BLG molecules move faster due to their smaller size/mass than mucins, and dominate the surface adsorption and the network formation of the BLG-BSM mixtures. However, BLG-BSM protein mixtures exhibited interfacial properties with lower elastic and viscous moduli than BLG, as a result of competitive displacement of BLG proteins with BSM molecules at the interface.

We propose that BSMs decreased the surface viscoelasticity and the rigidity of the BLG layers through the penetration of the hydrophobic parts of BSM between the adsorbed BLG molecules and disorder their cohesive assembly, which was most pronounced at pH 5.0. Moreover, it is to note that the facile attraction of BSM molecules towards BLG layer within water phase is not sufficient to activate this mecha-

Table 2
The rate of strain dependent decrease in viscoelastic moduli of BLG and the BLG-BSM mixture at pH 7.4, 5.0, and 3.0 after the breaking of the sample structure. Two different concentrations for the mixture were used. MIX 1 and MIX 2 represent 1 mg/mL and 2 mg/mL concentration, respectively. The data fit to power law equation: $G_l' = c'\gamma^{n'}$ and $G_l'' = c''\gamma^{n''}$ where the values of constants c' and c'' and slopes n' and n''.

		constant		slope	
pH	sample	c'	c''	n'	n''
7.4	BLG	0.220	0.023	−1.223	−0.514
	MIX 1	0.113	0.006	−1.165	−0.316
	MIX 2	0.098	0.013	−1.297	−0.450
5.0	BLG	1.181	0.144	−2.062	−0.806
	MIX 1	0.594	0.070	−1.862	−0.724
	MIX 2	0.223	0.037	−1.265	−0.593
3.0	BLG	0.297	0.035	−1.986	−0.714
	MIX 1	0.307	0.008	−1.953	−0.415
	MIX 2	0.001	0.003	−0.666	−0.201

Table 3
Crossover points.

	Crossover point	
pH	sample	Strain (%) (ca.)
7.4	BLG	25.00
	BSM	0.05
	MIX 1	37.00
	MIX 2	13.00
5.0	BLG	6.00
	BSM	0.06
	MIX 1	8.00
	MIX 2	19.00
3.0	BLG	6.00
	BSM	0.06
	MIX 1	12.00
	MIX 2	0.40

nism. At pH 3.0, for example, despite the electrostatic attraction between the oppositely charged BSM and BLG layers, the reduction in the viscoelasticity and rigidity of the network is weaker compared to that at pH 5.0.

Acknowledgments

The authors would like to thank to the Turkish Government for a PhD scholarship, the European Research Council (Funding Scheme: ERC Starting Grant, 2010, Project Number 261152), and the Danish Strategic Research Council (DSF −10-93456) for financial support. We also thank to Anton Paar Nordic AB Malmö, Sweden (Parastoo Salavati and Jan B Petersen) for providing access to the interfacial Physica MCR 302 rheometer and for valuable discussions.

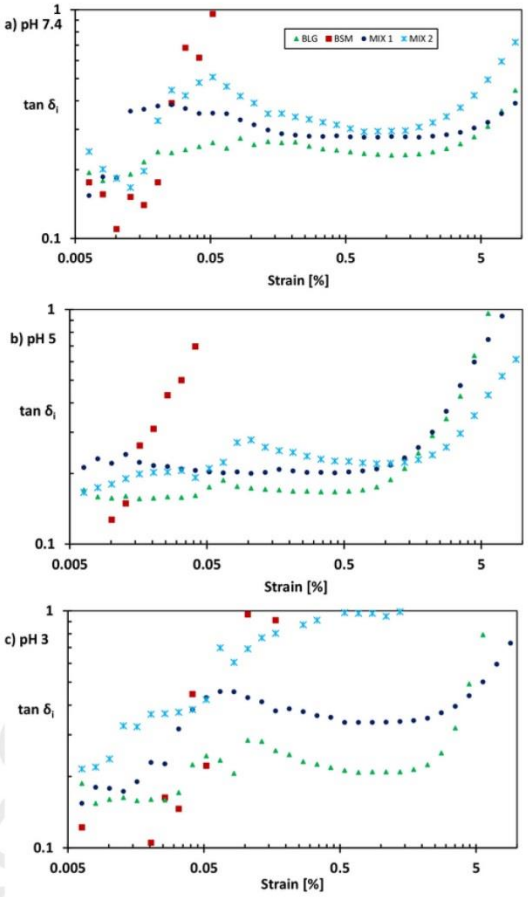

Fig. 7. Strain dependence of loss tangent ($tan\ \delta_l$) of BLG, BSM, and BLG-BSM mixtures at (a) pH 7.4, (b) pH 5.0, and (c) pH 3.0. Two different concentrations for the mixture were used. MIX 1 and MIX 2 represent 1 mg/mL and 2 mg/mL concentration.

References

[1] J.T. Petkov, T.D. Gurkov, B.E. Campbell, R.P. Borwankar, Dilatational and shear elasticity of gel-like protein layers on air/water interface, Langmuir 16 (2000) 3703–3711.
[2] P. Cicuta, E.M. Terentjev, Viscoelasticity of a protein monolayer from anisotropic surface pressure measurements, Eur. Phys. J. E 16 (2005) 147–158.
[3] P.A. Rühs, N. Scheuble, E.J. Windhab, P. Fischer, Simultaneous control of pH and ionic strength during interfacial rheology of β—lactoglobulin fibrils adsorbed at liquid/liquid interfaces, Langmuir 28 (2012) 12536–12543.
[4] E. Dickinson, Adsorbed protein layers at fluid interfaces: interactions, structure and surface rheology, Colloids Surf. B Biointerfaces 15 (1999) 161–176.
[5] R.N. Zúñiga, A. Tolkach, U. Kulozik, J.M. Aguilera, Kinetics of formation and physicochemical characterization of thermally-inducedbeta-lactoglobulin aggregates, J. Food Sci. 75 (2010) 261–268.
[6] L. Shi, R. Ardehali, K.D. Caldwell, P. Valint, Mucin coating on polymeric material surfaces to suppress bacterial adhesion, Colloids Surf. B Biointerfaces 17 (2000) 229–239.
[7] R. Bansil, B.S. Turner, Mucin structure aggregation, physiological functions and biomedical applications, Curr. Opin. Colloid Interface Sci. 11 (2006) 164–170.

UNCORRECTED

[8] H.Y. Çelebioğlu, M. Gudjónsdóttir, S. Meier, J.O. Duus, S. Lee, I.S. Chronakis, Spectroscopic studies of the interactions betweenbeta-lactoglobulin and bovine submaxillary mucin, Food Hydrocoll. 50 (2015) 203–210.
[9] H.Y. Shrivastava, B.U. Nair, Structural modification and aggregation of mucin by chromium(III) complexes, J. Biomol. Struct. Dyn. 20 (2003) 575–587.
[10] H.Y. Çelebioğlu, M. Gudjónsdóttir, I.S. Chronakis, S. Lee, Investigation of the interaction between mucins and beta-lactoglobulin under tribological stress, Food Hydrocoll. 54 (2016) 57–65.
[11] J. Krägel, S.R. Derkatch, Interfacial shear rheology, Curr. Opin. Colloid Interface Sci. 15 (2010) 246–255.
[12] E.H. Lucassen-Reynders, D.T. Wasan, Interfacial viscoelasticity in emulsions and foams, Food Struct. 12 (1993) 1–12.
[13] D. Rossetti, G.E. Yakubov, J.R. Stokes, A.-M. Williamson, G.G. Fuller, Interaction of human whole saliva and astringent dietary compounds investigated by interfacial shear rheology, Food Hydrocoll. 22 (2008) 1068–1078.
[14] J. Maldonado-Valderrama, J.M.R. Patino, Interfacial rheology of protein-surfactant mixtures, Curr. Opin. Colloid Interface Sci. 15 (2010) 271–282.
[15] J.-M. Jung, D.Z. Gunes, R. Mezzenga, Interfacial activity and interfacial shear rheology of native β-lactoglobulin monomers and their heat-induced fibers, Langmuir 26 (2010) 15366–15375.
[16] D.A. Kim, M. Cornec, G. Narsimhan, Effect of thermal treatment on interfacial properties of beta-lactoglobulin, J. Colloid Interface Sci. 285 (2005) 100–109.
[17] S. Roth, , , B.S. Murray, , E. Dickinson, Interfacial sheer rheology of aged and heat-treated beta-lactoglobulin films: displacement by nonionic surfactant, J. Agric. Food Chem. 48 (2000) 1491–1497.
[18] J. Läuger, P. Heyer, Interfacial shear rheology of coffee samples, AIP Conf. Proc. (2008) 1057–1059, http://dx.doi.org/10.1063/1.2964465.
[19] P. Erni, P. Fischer, E.J. Windhab, V. Kusnezov, H. Stettin, J. Läuger, Stress- and strain-controlled measurements of interfacial shear viscosity and viscoelasticity at liquid/liquid and gas/liquid interfaces, Rev. Sci. Instrum. 74 (2003) 4916–4924.
[20] J. Krägel, S.R. Derkatch, R. Miller, Interfacial shear rheology of protein-surfactant layers, Adv. Colloid Interface Sci. 144 (2008) 38–53.
[21] R. Wüstneck, J. Krägel, R. Miller, V.B. Fainerman, P.J. Wilde, D.K. Sarker, D.C. Clark, Dynamic surface tension and adsorption properties of β -casein and β -lactoglobulin, Food Hydrocoll. 10 (1996) 395–405.
[22] J. Krägel, M. Bree, R. Wüstneck, A.V. Makievski, D.O. Grigoriev, O. Senkel, R. Miller, V.B. Fainerman, Dynamics and thermodynamics of spread and adsorbed food protein layers at the water/air interface, Mol. Nutr. Food Res. 42 (1998) 229–231.
[23] R. Miller, J. Kragel, R. Wustneck, P.J. Wilde, J.B. Li, V.B. Fainerman, G. Loglio, A. W. Neumann, Adsorption kinetics and rheological properties of food proteins at air/water and oil/water interfaces, Mol. Nutr. Food Res. 42 (1998) 225–228.
[24] H. Pessen, J.M. Purcell, H.M. Farrell, Proton relaxation rates of water in dilute solutions of beta-lactoglobulin. Determination of cross relaxation and correlation with structural changes by the use of two genetic variants of a self-associating globular protein, Biochim. Biophys. Acta (BBA)/Protein Struct. Mol. 828 (1985) 1–12.
[25] N. Taulier, T.V. Chalikian, Characterization of pH-induced transitions of beta-lactoglobulin: ultrasonic, densimetric, and spectroscopic studies, J. Mol. Biol. 314 (2001) 873–889.
[26] H. Hägerström, M. Paulsson, K. Edsman, Evaluation of mucoadhesion for two polyelectrolyte gels in simulated physiological conditions using a rheological method, Eur. J. Pharm. Sci. 9 (2000) 301–309.
[27] E. Dickinson, Faraday research article. Structure and composition of adsorbed protein layers and the relationship to emulsion stability, J. Chem. Soc. Faraday Trans. 88 (1992) 2973.
[28] K.D. Danov, P.A. Kralchevsky, G.M. Radulova, E.S. Basheva, S.D. Stoyanov, E.G. Pelan, Shear rheology of mixed protein adsorption layers vs their structure studied by surface force measurements, Adv. Colloid Interface Sci. 222 (2015) 148–161.
[29] J.F. Steffe, Rheological Methods in Food Process Engineering, Freeman press, 1996.

UNCORRECTED PROOF

CHAPTER 5

Spectroscopic studies of the interactions of β-Lactoglobulin (BLG) with bovine submaxillary mucin (BSM) vs. porcine gastric mucin (PGM): the role of hydrophobic and hydrophilic residues as studied by fluorescence and nuclear magnetic resonance (NMR) spectroscopies

(Paper IV)

Hilal Y. Çelebioğlu,[1] María Gudjónsdóttir,[2] Ioannis S. Chronakis,[1] and Seunghwan Lee[3]*

[1]Nano-BioScience Research Group, DTU-Food, Technical University of Denmark, Søltofts plads, building 227, 2800 Kgs. Lyngby, Denmark.

[2]University of Iceland, Faculty of Food Science and Nutrition, Vínlandsleið 14, 113 Reykjavík, Iceland

[3]Department of Mechanical Engineering, Technical University of Denmark, DK-2800 Kgs. Lyngby, Denmark

*__Corresponding author__: Seunghwan Lee, Tel: +45 4525 2193, e-mail: seele@mek.dtu.dk

Keywords: fluorescence, nuclear magnetic resonance (NMR), beta-Lactoglobulin, bovine submaxillary mucin, porcine gastric mucin, pH

This manuscript was submitted to "Food Chemistry" in February 2017.

Abstract

Molecular level interactions of food proteins and salivary proteins are critical to understand the textural, sensory, and nutritional properties of food products in digestion. The aim of this study was to investigate binding interactions between β-Lactoglobulin (BLG) and two different mucins, bovine submaxillary mucins (BSM) and porcine gastric mucin (PGM), using fluorescence and high field nuclear magnetic resonance (HF-NMR) spectroscopies. Intrinsic fluorescence spectra showed that mixing of BLG with PGM led to enhanced decrease of fluorescence intensity of BLG at all pH conditions compared to when BLG was mixed with BSM. This indicated stronger hydrophobic interactions of BLG with PGM than with BSM, which was further supported by extrinsic fluorescence spectroscopy. Stronger interactions of BLG with PGM also suggest a more abundant presence of hydrophobic moieties in PGM than BSM. Furthermore, HF-NMR studies indicated that the hydrophilic interaction also contributed to the interactions with both mucins, especially at acidic conditions.

Introduction

Proteins are important ingredients for food products to provide desirable textural, sensory, and nutritional properties. To optimize the utilization of proteins in food science and engineering, an in-depth understanding is needed of the various interrelated parameters that influence aggregation, adsorption, and structural behavior of proteins. For instance, the interactions of β-Lactoglobulin (BLG), a major whey protein, and mucins, as the major component in saliva or gastric fluids, are drawing increasing attentions in the context of understanding the oral processing or digestion of dairy food on the molecular level. Bovine β-Lactoglobulin (BLG) has been one of the most extensively studied proteins (Pervaiz and Brew 1985; Godovac-Zimmermann 1988; Hambling et al. 1992; Sawyer and Kontopidis 2000: Sakurai et al. 2009), mainly due to its abundance in cow's milk. The concentration of BLG in milk is about 0.2 g/100 ml, which is second highest after the concentration of casein (2.9 g/100 ml) (Cerbulis and Farrell 1975). BLG molecules exist mainly as dimers at neutral pH and room temperature, whereas they dissociate into monomers at pH < 3, and partly exist as octamers at its isoelectric point (pI~5.2) (Liang and Subirade 2012; Engelhardt et al. 2013; He et al. 2016). BLG has a nonpolar interior region and two Tryptophan (Trp) residues (Fugate and Song et al. 1980), i.e. Trp-19, which is located in the more hydrophobic environment at the bottom of the calyx formed by the antiparallel β-strands, while Trp-61 is positioned adjacent to the strand involved in antiparallel interaction of the dimer (Papiz et al. 1986; Brownlow et al. 1997). Extensive studies regarding the structure and functions of BLG have provided important information about pH-dependent conformational transitions (Tanford and Nozaki 1959) and binding with various hydrophobic and amphiphilic ligands (Fugate and Song 1980).

Mucin, on the other hand, is one of the major proteins in saliva or gastric fluids, which accompany all food bolus in digestion throughout the oral and gastrointestinal organs. Mucins from different organs have some common features, such as a high degree of glycosylation, high

molecular weights ranging from 0.5 to 40 MDa (Bansil and Turner 2006; Svensson and Arnebrant 2010), amphiphilic character, and low isoelectric points, estimated to be between 2 and 3 (Durrer et al. 1995; Bansil et al. 1995; Sandberg et al. 2009). Meanwhile, different mucins with different origins show important differences in their composition, structure, and biophysical properties too. These differences are reported to be originated from both hydrophobic terminal domains, as well as the central regions, where the types, amount, and position of negatively charged moieties are different (Bansil and Turner 2006, Lee et al. 2005; Nikogeorgos et al. 2014; Madsen et al. 2016).

Our recent spectroscopy study based on dynamic light scattering (DLS), circular dichroism (CD) spectroscopy, and nuclear magnetic resonance (NMR) spectroscopy suggested pH-dependent hydrophilic interactions between BLG and bovine submaxillary mucin (BSM) (Çelebioğlu et al. 2015). However, there has been no study specifically designed to probe hydrophobic interaction between the BLG and mucins or any role of hydrophobic residues of these proteins yet. In this context, fluorescence spectroscopy can be considered as an optimal technical approach to investigate the hydrophobic interaction between proteins. Fluorescence spectroscopy is based on the presence of intrinsic fluorophores, e.g. Trp residues, in which the emission spectra (both intensity and max. peak position) are sensitive to the local environment of the Trp residues, and can thus provide useful information on both conformational and structural changes of proteins (Lakowicz 1999, Kanakis et al. 2011, and Mensi et al. 2013). Hence, the changes in the intrinsic Trp fluorescence of Trp-61 and Trp-19 in BLG (Busti et al. 1998; Renard et al. 1998; Muresan et al. 2001; Liang & Subirade, 2010; He et al. 2016) while interacting with mucins may provide valuable information on their binding patterns/mechanisms where Trp resides are involved. Furthermore, extrinsic fluorescence spectroscopy, e.g. by employing aromatic fluorescent dyes, such as 8-anilino-1-naphthalene sulfonate (ANS), is broadly used to monitor the conformational changes of proteins (Ptitsyn and Bychkova 1995, Uversky et al. 1996), especially for those that lack strong intrinsic

fluorophores. ANS shows particular affinity to hydrophobic domains (Daniel and Weber 1966) of native and partially unfolded proteins (Cattoni et al. 2009). Conformational transitions, binding properties, pH and temperature dependence of BLG have been studied for years (Laligant et al. 1991, D'Alfonso et al. 1999, Collini et al. 2000, Alizadeh-Pasdar and Li-Chan 2000, Vetri and Militello 2005, Santambrogio and Grandori 2008). There are, however, only a few fluorescence studies (both intrinsic and extrinsic) available for mucins (Smith and LaMont 1984; Qaqish and Amiji 1998; Liao et al. 2016). Moreover, no literature information is available for the interaction of BLG and mucin specifically based on fluorescence technique to date.

Thus, the objectives of the present study were to elucidate the interaction mechanisms of BLG and two types of mucins, namely bovine submaxillary mucin (BSM) and porcine gastric mucin (PGM), specifically focusing on the role of hydrophobic residues of the proteins at different pH conditions in the context of understanding the food digestion process along the gastrointestinal organs. Intrinsic fluorescence spectroscopy and the fluorescent dye ANS techniques were used to assay conformal modifications of the proteins, as induced by binding interactions between the proteins, by focusing on changes in their hydrophobic residues. As recently shown by Brandão et al. (2017), fluorescence quenching and NMR are two complementary techniques, by together providing information about the modification of protein structure induced by binding and the structural features of the ligand involved in the interaction. Hence, HF-NMR spectroscopy was also used to obtain further details about the structural differences between the two mucins and their interaction properties, both hydrophobic and hydrophilic, with BLG.

Materials and methods

Intrinsic fluorescence spectroscopy

All intrinsic fluorescence measurements were carried out using a Varian Cary Eclipse Fluorescence Spectrophotometer (Varian, Mulgrave, Australia) using a 10 mm quartz cuvette cell with the cell compartment set at 25 °C. The excitation wavelength range (λ_{ex}) was from 230 to 320 nm (measured every 5 nm) and the emission wavelength range was from 230 to 450 nm (measured every 2 nm). Other settings of the instrument were; a slit width of 5 nm (for both excitation and emission), a scan rate of 1200 nm/min and a photomultiplier (PMT) detector voltage of 600 V. The protein solutions were scanned three times and the spectra were averaged to reduce the noise. The spectra obtained were subtracted from the spectrum of the solvent. The BLG, BSM, and PGM solutions had a 0.5 mg/mL concentration, while the mixtures had a 1 mg/mL concentration, so that in the 1:1 BLG-mucin mixtures each protein had a 0.5 mg/mL concentration.

Extrinsic fluorescence spectroscopy

ANS fluorescence spectra were recorded at 25 °C using a Chirascan spectrophotometer (Applied Photophysics Ltd., Surrey, UK). The ANS spectra were recorded from 350 to 600 nm, using a 10 mm path length cuvette with a step size of 1 nm and a bandwidth of 1 nm. ANS was prepared as a 100 μM stock solution in a 10 mM phosphate buffered saline (PBS) solution at pH 3, 5, and 7.4. The protein concentration was 1 mg/mL. The protein solutions were scanned three times and the spectra were averaged to reduce the noise. The spectra were obtained by subtracting the spectrum of the solvent (PBS buffer with ANS).

High field NMR spectroscopy

Samples of BLG, BSM, and PGM were produced at concentrations of 1 mg/mL in aqueous 50 mM PBS of pH 3, 5 or 7.4, respectively. Buffers were prepared as aqueous solutions prior to freeze drying and dissolution in deuterium oxide (D_2O) (99% isotopic enrichment, Sigma Aldrich) containing 5.8 mM TSP-d_4 [the sodium salt of 3-(trimethylsilyl)propionic-2,2,3,4-d_4 acid, Sigma Aldrich]. Thus, all obtained spectra in this study included a strong peak at 0 ppm related to the internal TPS-d_4 in D_2O standard solution. In addition to individual samples, 1:1 mixtures of BSM-BLG and PGM-BLG were prepared at the three different pH values. NMR spectroscopy was carried out using a Bruker Avance DRX-500 (11.7 T) spectrometer (Bruker Biospin, Rheinstetten, Germany) operating at a Larmor frequency of 500.13 MHz for ^1H. All experiments employed a sample temperature of 25 °C, using a double-tuned BBI (Broad Band Inverse detection) probe equipped for 5 mm (o.d.) NMR tubes. The ^1H experiments were performed using the zgcppr pulse sequence (pre-saturation of water followed by a composite 90° pulse), employing a recycle delay of 5 s, 64 scans, a spectral width of 10 kHz, and an acquisition time of 1.639 s. Chemical shifts were referenced to the internal standard of TSP-d4 in D_2O solution, giving rise to a peak at 0 ppm.

Results and discussion

Effect of pH on the intrinsic fluorescence intensity of BLG, BSM, and PGM

Multiple intrinsic fluorescence emission spectra were obtained in the range from 230 to 450 nm, each with increasing excitation wavelength from 320 to 240 nm in 5 nm intervals to find optimum conditions of all relevant excitation wavelengths (data not shown). For the resultant fluorescence emission spectra, as shown in Fig. 1 (i.e. excitation at 280 nm and emission in 335 – 340 nm), the major fluorophores are Trp residues in BLG (Lakowicz 1999). For the two mucins, the intensities of the emission fluorescence spectra were relatively weaker compared to BLG and nearly

independent of pH, presumably due to that there are very few Trp residues in the mucins and the numbers of mucin molecules were also small at the same concentration due to their large molecular weights.

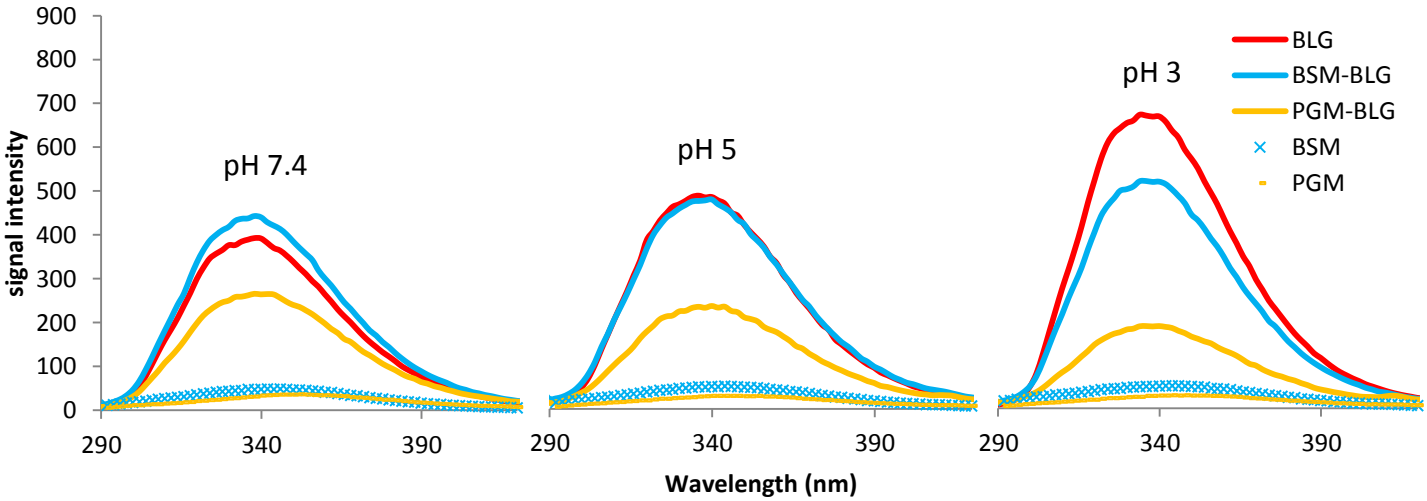

Fig. 1. Intrinsic fluorescence emission spectra of protein solutions (BLG, BSM and PGM solution with 0.5 mg/mL concentration and BSM-BLG and PGM-BLG mixtures with 1 mg/mL concentration) at λ_{ex}=280 nm showing the changes in fluorescence signal intensity (in particular the Trp fluorescence emission intensity) before and after the mixing/interaction of BLG and mucins at pH 7.4, pH 5, and pH 3.

The intensity of the intrinsic fluorescence emission signals of the BLG solution (0.5 mg/mL) at its maximum wavelength (F_{max}) decreased with increasing pH , with intensities of 673, 489, and 393 (in arbitrary units) at pH 3, 5 and 7.4, respectively (Fig. 1). For more visualized comparison, the relative intensities of F_{max} of each spectrum at each pH are displayed in Fig. 2. The changes in the FI of BLG were accompanied by the shifts in the maximum peak position of the emission

spectra according to the pH change. The maximum peak position showed gradual red shifts by 2 nm each upon changing the pH from 3 to 5, and again to pH 7.4, respectively. The red shift can be accounted for by the increased exposure of Trp and tyrosine (Tyr) residues to the solvent (Lakowicz 2013). Hence, the trend in the FI of BLG, as a function of pH (Fig. 2. *a*), can be explained primarily by the varying extent of exposure of hydrophobic residues (mainly Trp residues) to the aqueous solvent in the different protein solutions. At pH 3, even though BLG is overall positively charged, it becomes more hydrophobic in the sense that nonpolar solutes are more effectively shielded from aqueous solvents and a more compact configuration is formulated (Cardamone and Puri, 1992). Hence, BLG shows a higher FI at pH 3 due to the preserved Trp residues within "hydrophobic pockets" (Fritz et al. 2004; Gibbons et al. 2005). BLG at pH 5 is almost uncharged (the isoelectric point of BLG is approximately 5 (Engelhardt et al. 2013) and Trp residues have a higher chance to be exposed to the solvent. This can account for the reduced FI of BLG at pH 5 compared to the FI at pH 3. It is also proposed that Trp-61 can be quenched in the native protein (around pH 5), possibly by the nearly Cysteine 160–66 disulfide bond (Mills and Creamer, 1975). At pH 7.4, BLG molecules associate to dimers and unfolding starts due to the Tanford transition (Tanford et al. 1959). Between pH 6 and pH 8, BLG undergoes the Tanford transition involving a displacement of loop EF (residues 85 to 90), which acts as a lid to close the interior/binding sites of BLG (Qin et al. 1997). The Tanford transition may also involve the transition accompanied by a change in the microenvironment of Tyrosine, Tyr-42 (Oliveira et al. 2001), and causes an alteration in the relative orientation of monomers in the dimer (Brownlow et al. 1997). Since BLG molecules have more access to the quenchers at pH 7.4, a reduced intrinsic fluorescence signal intensity was observed. Lakowicz (1999) also observed a reduction of FI of BLG due to the transition-induced change in the local microenvironment of aromatic residues.

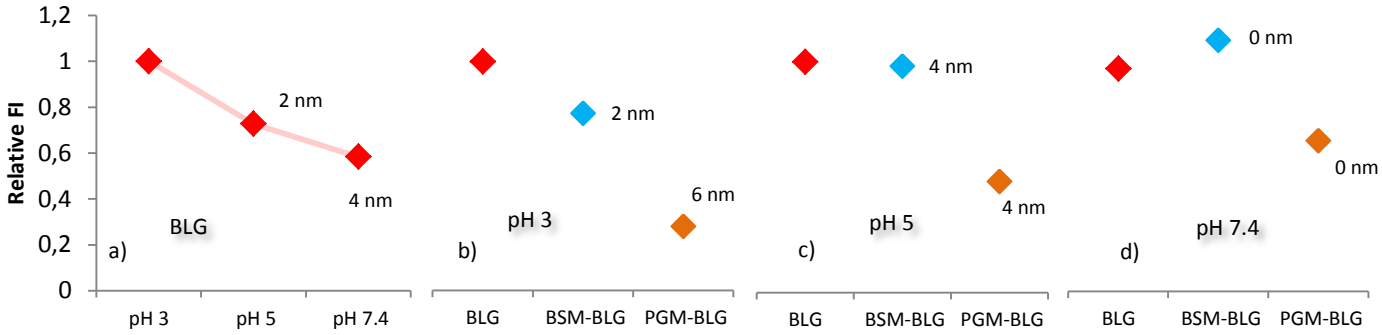

Fig. 2. Relative maximum intrinsic fluorescence intensities (F_{max}) and the total shifts on corresponding maximum fluorescence emission wavelength (λ_{max}) of BLG-mucin mixtures over pure BLG (0.5 mg/mL). For instance, for BLG (a), intensities and total shifts were relative to at pH 3; however, all mixtures were relative to BLG at corresponding pH (b, c, d).

Secondly, pH dependent changes in the FI of BLG can also be explained by monomer-dimer transitions. Close to pH 3, BLGs are known to be mainly monomeric, yet mainly dimeric at a neutral pH (Busti et al. 1998). Mills and Creamer (1975) reported that Trp fluorescence of BLG was reduced in intensity by association of the monomeric proteins into dimers, which is consistent with the trend shown in Fig. 1. It is to note that dimerization is driven mainly by hydrophobic interactions between two BLG molecules. In this process, exposure of hydrophobic patches to aqueous solvents is likely to occur, as shielding of them by only two amphiphilic molecules is much less effective compared to, for example, micelles. Thus, the reduced FI of BLG at pH 5 compared to pH 3 is closely related to the formation of dimers.

Effect of mucins (BSM and PGM) on the intrinsic fluorescence intensity of BLG

The influence of mixing BLG with mucins on the FI, as well as on the maximum peak position, was highly dependent on the solvent pH and the type of mucin present. For example, mixing with BSM resulted in a decrease of the FI of BLG by 23% at pH 3, yet no change at pH 5,

and finally an increase by 13% at pH 7.4 (Fig. 1 and Fig. 2). Meanwhile, mixing with PGM led to a decrease of the FI of BLG at all pH conditions (by 72%, 52%, and 32% at pH 3, pH 5, and pH 7.4, respectively). Moreover, the magnitudes of the decrease were much higher when mixing the BLG with the PGM than during the case of mixing BLG with BSM. Here, the concentrations of the total proteins (BLG + mucin) in the mixed solutions (1 mg/mL) were twice as high as those of the neat BLG or mucin solutions (0.5 mg/mL). Given that the changes in the FI are an indication for the conformational changes of Trp residues of BLG, this observation suggests that the presence of mucins surrounding BLG could be a source for such changes, but the pattern/magnitude is highly dependent on the type of mucins and pH. For example, if the Trp residues of BLG are left intact in the course of mixing with mucin molecules, and thus no related conformational changes are induced, the resultant FI would be a simple arithmetic summation of the two. It is proposed that this is the case of the BLG-BSM mixture at pH 7.4. This can be readily understood by considering that both BLG and BSM are negatively charged at pH 7.4, and thus may the Trp residues of BLG well remain preserved and thus no significant conformational changes involving hydrophobic domains are expected. This is, in fact, consistent with an earlier NMR study (Çelebioğlu et al, 2015) that reported the dominance of hydrophilic characteristics in BLG-BSM interactions. In turn, this also means that in all other cases, the interaction between BLG and mucin molecules involves significant conformational changes of Trp residues and their surrounding in a direction to lower the FI. In other words, the presence of mucins surrounding BLG tends to enhance the exposure of Trp residues. Similarly with the process of dimerization of BLG molecules, interaction between BLG and mucins can induce an exposure of hydrophobic patches of BLG containing Trp residues to the aqueous solvent when further shielding of them by hydrophilic moieties is not complete. It is important to note that while fluorescence spectroscopy is focused on probing the hydrophobic interaction between BLG and mucin molecules, it can occur via electrostatic attraction too, for

instance, at pH 3 where BLG and mucins are oppositely charged. Further discussion on the overall interaction mechanisms between BLG and mucin molecules will be provided in the section 3.5 below. More enhanced reductions were observed in the FI of BLG upon mixing with PGM than BSM at all pH conditions, which suggests that hydrophobic moieties that can interact with BLG via hydrophobic interaction, and possibly cause conformational changes of Trp residues in BLG, are more available in PGM than BSM. This may explain that even at pH 7.4, mixing of BLG with PGM led to a reduction in FI, in contrast to the case of mixing with BSM.

In addition to the variation in FI, mixing of BLG with mucins led to shifts of the peak maxima in a similar pattern too. For instance, mixing of BLG with both mucins at pH 7.4 led to nearly no further shift in the peak maximum compared to BLG alone, but at pH 5 and 3, the red shift of BLG was further enhanced. Moreover, further red shifts were relatively more distinct upon mixing with PGM than BSM. Overall, the observed changes in the FI and shifts in peak maximum of BLG upon mixing with mucins indicated a quenching effect of mucins on the fluorescence emission of Trp residues of BLG, chiefly based on hydrophobic interaction, with generally stronger effects by PGM than BSM.

ANS binding of BLG, BSM, and PGM and effect of pH on their ANS fluorescence intensity

Extrinsic dye ANS-based fluorescence is independent of the presence and position of a fluorophore within the target proteins; hence, it is a valuable addition to understanding the interaction behavior between BLG and mucins. Moreover, minor changes in surface hydrophobicity of the proteins can be monitored by ANS fluorescence, which are not necessarily probed by the tryptophan and tyrosine fluorescence method (Hawe et al. 2007). In Fig. 3, emission fluorescence

spectra of ANS in the presence of BLG, BSM and PGM acquired at different pH values are presented. The spectra shown in Fig. 3 were obtained by subtracting the corresponding spectra of the solvent (ANS in respective buffer) at each pH. Emission fluorescence spectra of ANS in an aqueous solvent alone was nearly featureless (data not shown) as it is quickly quenched when directly exposed to the aqueous solvent. But the quenching can be suppressed in the presence of amphiphilic molecules, such as proteins, if hydrophobic interactions result in shielding of ANS from exposure to the aqueous solvent (Gasymov and Glasgow 2007). In this process, the conformation of the neighboring amphiphilic molecules is a determining factor, which is, in turn, highly dependent on the solvent pH. Among the three types of proteins, BLG showed the highest enhancement of fluorescence intensity of ANS at pH 7.4, where the FI increased by 76 % in the presence of BLG, whereas it increased only by 31 % and 21 % when accompanied by BSM and PGM, respectively. At pH 5, ANS-BLG slightly lost its FI compared to that at pH 7.4, whereas both ANS-BSM and ANS-PGM increased the FI compared to at pH 7.4. Nevertheless, the FI of ANS-BLG was still higher than those of the ANS-mucin solutions. At pH 3, the FI increased most substantially for all the ANS-proteins samples, although the difference in the relative intensities between the different ANS-protein samples was ignorable. Lastly, the maximum peak positions (λ_{max}) of the three different ANS-protein spectra were in the order of PGM < BSM < BLG with increasing emission wavelengths. It is well known that gastric mucin undergoes a conformational change from a random coil conformation at pH ≥ 4 to an anisotropic, extended conformation at pH < 4 (Cao et al. 1999). Hong et al. (2005) also mentioned a conformational transition at pH < 4, where mucin molecules cluster together. The increased ANS fluorescence intensity with decreasing pH, therefore, indicated increased binding of the hydrophobic ANS molecules to the mucins due to conformational transitions, accompanied by increased exposure of hydrophobic binding sites at the mucins. Smith and LaMont (1984) also observed an incremental effect of decreasing pH on mucin-

induced ANS fluorescence using bovine gallbladder mucin and suggested that the ANS binding domain becomes more accessible in an acidic environment due to that the negatively charged groups of ANS are protonated and thus facilitate the hydrophobic interaction.

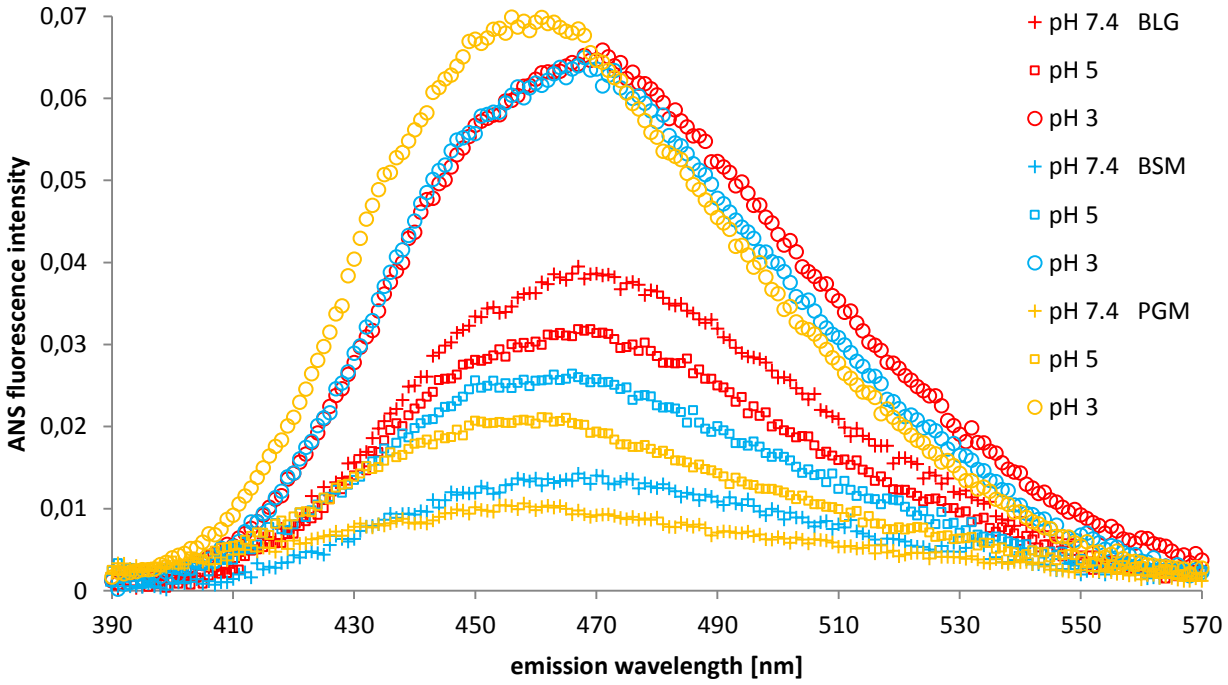

Fig. 3. pH dependent fluorescence emission spectra of ANS binding proteins (BLG, BSM, PGM) at pH 7.4, pH 5, and pH 3. (Excitation wavelength: 365.5 nm)

ANS binding to BLG is stronger at pH 3 than at pH 7.4 and the minimum value is observed near the isoelectric point (pH 5.2), which is in agreement with previous studies in the literature (D'Alfonso et al. 1999, Collini et al. 2000). They also reported that the highest ANS fluorescence signal intensity was observed at the most acidic state, while the lowest intensity was observed at pH 5.2. In short, the intensity of ANS fluorescence increased as the pH shifted away from the isoelectric point (IEP) of the BLG. Mucins (pI~2), however, have decreasing fluorescence intensity

as the pH is shifted away from the IEP (with increasing pH). The reason is that the increasing electronegative charges of mucins with increasing pH causes a strong repelling effect to the negatively charged probe ANS. Laligant et al. (1991) also explained the low affinity of ANS to BLG in its negative state in view of electrostatic repulsion between them. Similarly, higher ANS fluorescence intensity of BLG at pH 3 compared to pH 7.4 can be explained by the electrostatic attraction, i.e. positively charged BLG at pH 3 are more accessible to the negatively charged probe ANS, and thus they can bind to each other more at pH 3. A contribution of electrostatic interactions in the measurement of surface hydrophobicity of proteins using anionic fluorescent probes has already been discussed by Alizadeh-Pasdar and Li-Chan (2000). They used one uncharged probe, namely (6-propionyl-2-(N,N dimethylamino)-naphthalene, "PRODAN"), and two negatively charged probes, namely (cis-parinaric acid, "CPA") and ANS, for surface hydrophobicity measurements of BLG and bovine serum albumin. Generally, higher emission intensities observed at acidic pH, compared to neutral and alkaline pH by using ANS and CPA, were explained by more effective affinity via electrostatic attraction.

Effect of pH and BLG-mucin interaction on ANS binding and ANS fluorescence intensity

ANS fluorescence spectra of the BLG-mucin mixtures are more complicated as they may reflect not only the interaction of ANS with BLG or the mucins, respectively, but also the interaction between BLG and the mucins or their aggregates. In order to analyze the ANS fluorescence spectra of the BLG-mucin mixtures, the measured intensities of the mixtures (i.e. ANS in BLG + mucin mixture solution) were compared with the numerical sum of ANS fluorescence intensities of the two respective proteins (i.e. ANS in BLG solution + ANS in mucin solution). The

BLG-mucin mixtures had a 1 mg/mL concentration with 1:1 w/w ratios, which means that each protein had 0.5 mg/mL concentration in the mixture. Therefore, an observed decrease in the signal intensity of ANS in the mixtures compared to in the neat BLG (1 mg/mL) solution could simply be a concentration effect. To clarify this, a simple calculation was carried out as follows:

$$Average\ (concentration\ based) signal\ intensity\ = \frac{FI\ of\ Protein\ 1}{2} + \frac{FI\ of\ Protein\ 2}{2}$$

These numerical averages of the signals were then compared with the measured values (Fig. 4). Thus, if there is no interaction between two proteins, i.e. BLG and mucin, the experimentally determined spectra should be overlapped with the calculated ones, as shown in a previous study by the authors on NMR and circular dichroism (CD) spectroscopy (Çelebioğlu et al., 2015).

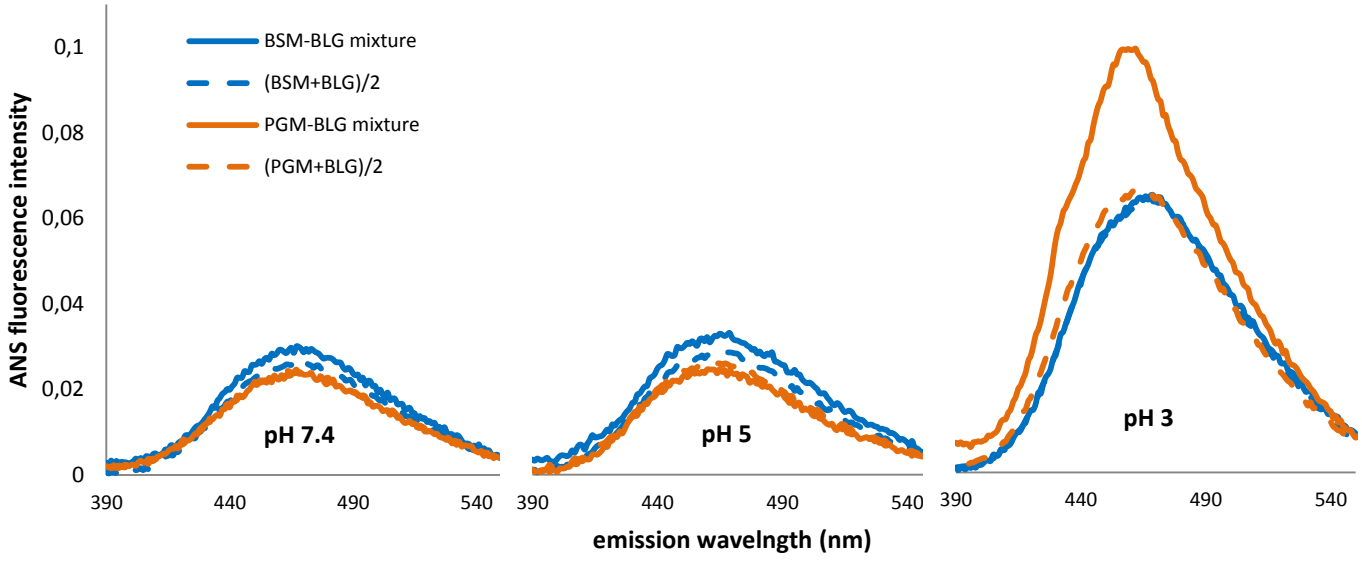

Fig. 4. The comparison of the external fluorescence spectra of the BSM-BLG and PGM-BLG mixtures with their calculated spectra (mucin + BLG)/2 using the spectra of pure BLG and mucins

At pH 5 and pH 7.4, the two spectra were similar to each other and nearly overlapped for both BLG-mucin mixtures (Fig. 4). This trend was also observed in the BLG-BSM mixture at pH 3. However, for the BLG-PGM mixture at pH 3, the experimentally determined ANS fluorescence intensity was much higher than the numerical average of the two spectra. In other words, compared to when ANS was exposed to either BLG or PGM molecules alone, there was a synergetic effect between BLG and PGM in the binding affinity with ANS. This can be closely correlated to the most outstanding associative interaction of BLG with PGM at pH 3, as mentioned in the previous section. Moreover, it is also noted that the maximum peak position of the PGM-BLG mixture at pH 3 (experimentally determined spectra) showed a shift to a shorter wavelength (i.e. blue shift) compared to the numerical average of the two spectra and other BLG-mucin mixtures (PGM-BLG mixtures at pH 5 and pH 7.4 and BSM-BLG mixtures at each pH values). This effect can be interpreted as further support for the synergetic hydrophobic interaction of the mixture of BLG and PGM at pH 3. Even though the interaction of BLG-PGM at pH 3 might result in a more exposure of the Trp residues of BLG to water, as discussed above, it might have generated more effective "hydrophobic pockets" to host ANS from water instead. This is possible because ANS is much smaller than BLG, not to speak of the mucins, in size. It should be also noted that hydrophilic interaction of the proteins with ANS might also be a contributing factor to the higher ANS intensity of the experimentally determined spectra. At pH 3, ANS (negatively charged probe) can easily bind to the positively charged BLG and the protonated sides of the PGM in addition to the hydrophobic binding. Moreover, this electrostatic interaction between ANS and the proteins can facilitate refolding of the proteins at low pH (Ali et al. 1999). Accordingly, the unfolded terminal regions of PGM at pH 3 (Cao et al. 1999, Madsen et al. 2016) may undergo folding again after binding with BLG, ANS or a BLG-ANS complex. Thus, ANS can be buried in the hydrophobic protein matrix.

After all, it can be concluded that ANS can be buried within the PGM-BLG protein complex most effectively at pH 3 in addition to its higher hydrophilic and hydrophobic binding capacity at pH 3.

High-resolution NMR probing of proteins

While fluorescence spectroscopy showed a particular sensitivity to probe the hydrophobic interaction between BLG and mucins as addressed above, high field ^{1}H spectra can be an alternative to probe both hydrophilic and hydrophobic interactions between BLG and mucins. HF-NMR spectra of the neat solutions of BLG, BSM and PGM at the various pH conditions are shown in Fig. 5.

Uhrínová et al. (1998) performed a detailed assignment of proton NMR peaks for bovine BLG, and identified the peaks in the range from approximately 1.2 to 4.0 ppm mostly due to β-protons in BLG, with some overlap of peaks in the range from 3.6 to 5.7 ppm related to α-protons in the protein. Chemical shifts below or around 1 ppm were related to γ and/or δ-protons from the present amino acids, while protons in close relation to nitrogen (HN protons) showed a chemical shift in the range from approximately 7 to 9 ppm, along with δ-protons from phenylalanine (Phe). The BLG spectra obtained in the current study (Fig.5) was in excellent agreement with the study by Uhrínová et al. (1998) and will therefore not be discussed in greater detail here.

Although no detailed assignment of peaks exists on BSM and PGM, to the best knowledge of the authors, some NMR studies have been made on the structure of other mucins. Gerken (1986) performed a complete peak assignment of ovine submaxillary mucin (OSM). Similarities between the mucin types eased interpretation of the high field NMR results of the BSM solutions, as presented by Çelebioğlu et al. (2015). Furthermore, Fontenot et al. (1993) identified the peaks in the range from 1.3 ppm to 3.7 ppm as characteristic for β-protons of the amino acid side chains of

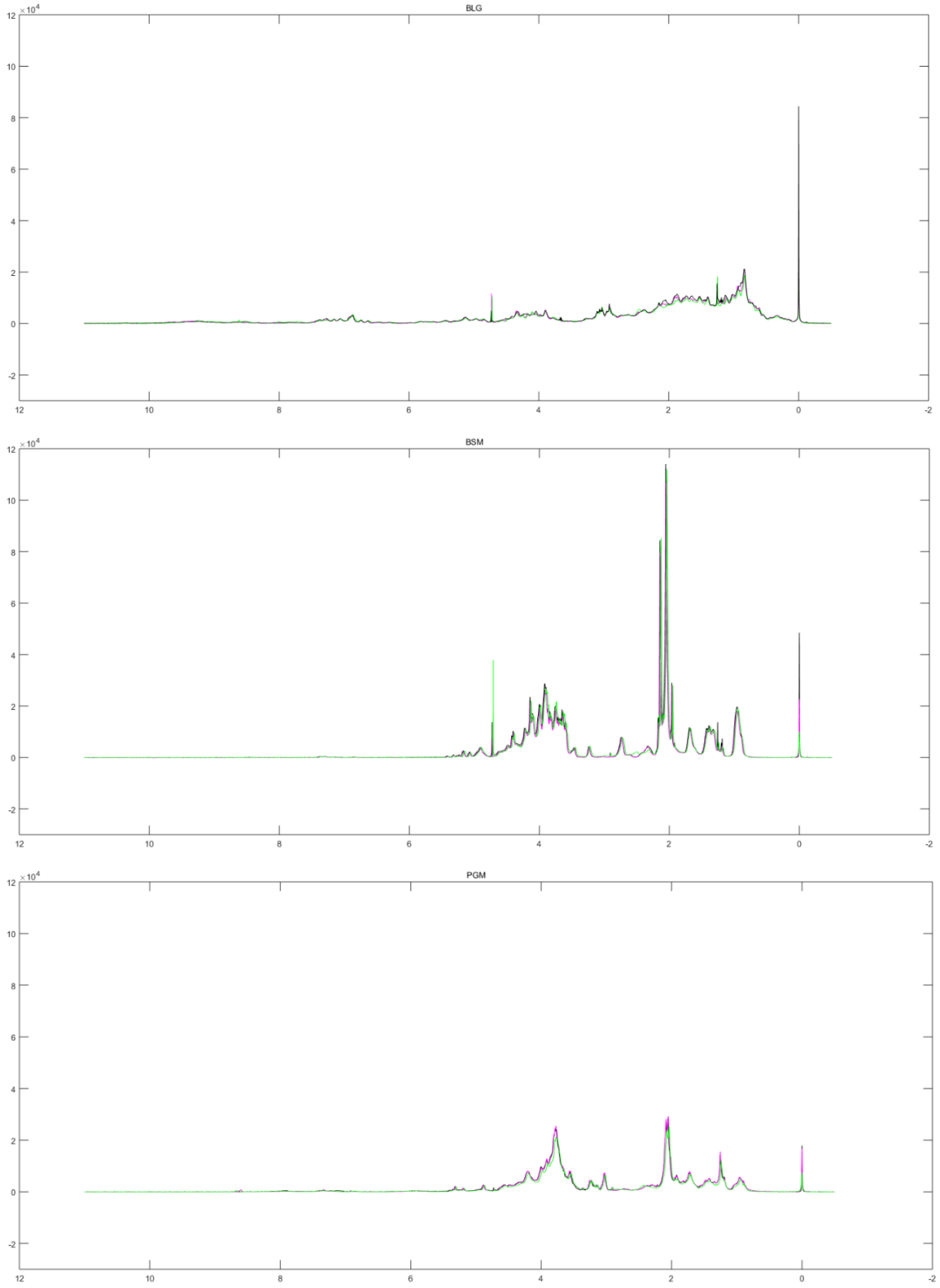

Fig. 5. High field water suppressed ^{1}H NMR spectra of BLG (top), BMS (middle) and PGM (bottom) each at pH 3 (green), pH 5 (pink) and pH 7.4 (black), respectively.

human mucin MUC-1, and proposed that changes in chemical shifts and numbers of peaks within this peak range were a result of structural changes and folding of the peptide backbone with added tandem repetitions in the mucin.

However, due to the complex and large structure of the proteins in the solutions a detailed assignment of peaks to their representative amino acids or other components of the present proteins was not attempted in the present study. Instead, a simplified approach was used to identify the differences between the BSM and PGM and to understand their different interaction features with BLG. ^{1}H NMR spectra were measured both for the BLG and mucin mixtures, as well as of each compound individually (BLG, BSM and PGM) at each analyzed pH, as mentioned before. The sum spectra were then calculated (BLG spectra + mucin spectra) for each mucin and each pH. The differences in the measured spectra of the mixtures and the calculated sum spectra then reveal which components take part in the interaction and/or where any conformal changes of the proteins occur at the various conditions.

The mixture, sum and difference spectra of the solutions are presented in Fig. 6. These results revealed that the most likely place of interaction between BLG and BSM was in the chemical shift range from 1.2 to 2.5 ppm, as well as from 3.5 to 4.5 ppm. This is in good agreement with the study of Çelebioğlu et al. (2015), which suggested that the dominant interacting residues of BSM were likely due to the interaction of N-acetyl methyl of the GalNAc residues and sialic acid $–CH_3$ protons (narrow peaks around 2.1 ppm), and Asn β-protons (2.3 and 2.5 ppm), as well as from α- and β-protons from serine (Ser) and threonine (Thr), sialic acid H4-H9 and H9‘ protons, as well as the GalNAc H2-H6 and H6‘ protons, giving rise to peaks in the range from 3.1-4.4 ppm. In agreement with the observations of Fontenot et al. (1993), the small changes observed in the difference spectra of the PGM-BLG and BSM-BLG solutions in the chemical shift region from 1-4.5 ppm are believed to represent conformal changes in the proteins due to the change in pH. Little to no

changes were observed in the difference spectra for chemical shifts above 4.5 ppm, indicating that aromatic protons or protons in relation with nitrogen (HN protons) were not influencing the interaction between BLG and the two mucins to any extent.

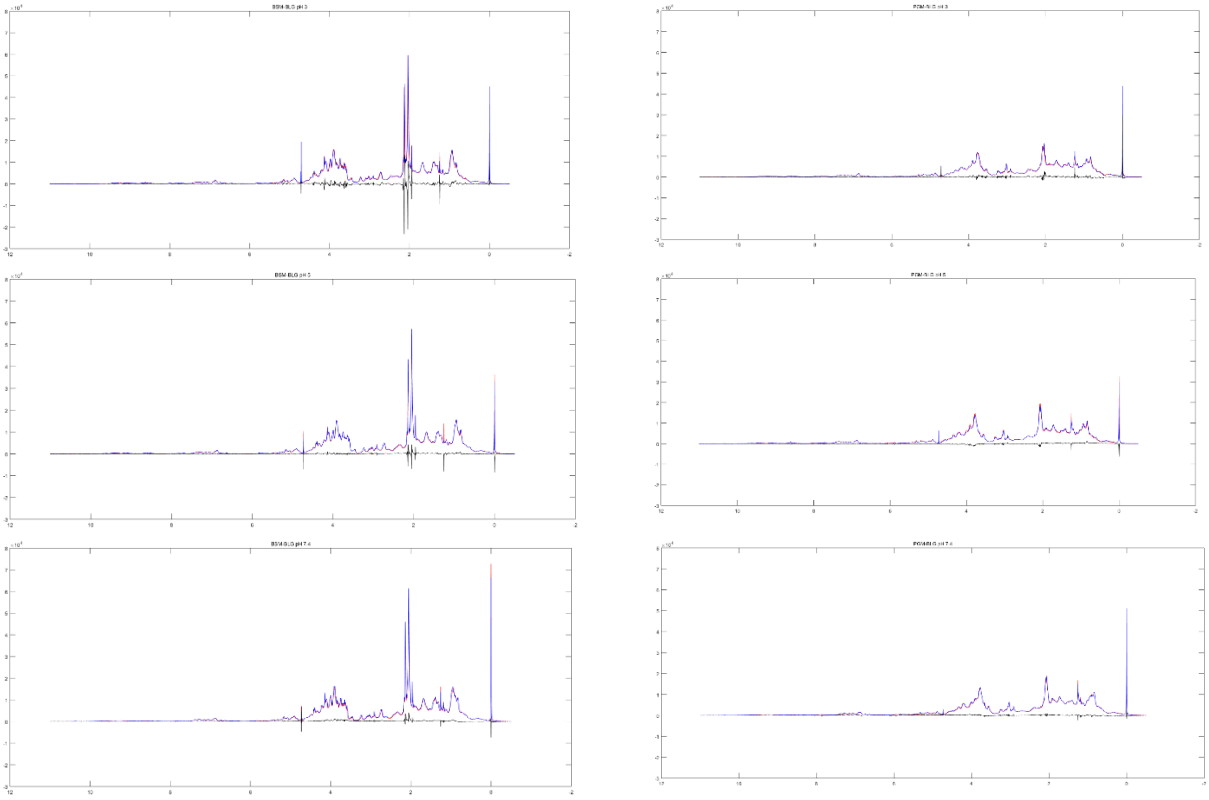

Fig. 6. High field water suppressed ^{1}H NMR spectra of 1:1 solutions of BSM-BLG (left) and PGM-BLG at pH 3 (top), pH 5 (middle) and pH 7.4 (bottom), respectively. Red spectra represent the analyzed mixtures (BSM-BLG or PGM-BLG), blue spectra are the sum spectra of the pure BLG and BSM or PGM solution, respectively, and the black spectra are the difference spectra (mixture spectrum – sum spectrum) of the solutions at each pH.

The indicated interaction is, however, somewhat different in the PGM-BLG solutions due to the absence of a GalNAc and sialic acid $–CH_3$ protons interaction peak in the PGM, which was represented by a strong narrow peak at 2.1 ppm in the BSM samples, as mentioned before. However the strongest interaction was observed at a chemical shift of approximately 2 ppm, indicating that the α- and β-protons of serine and threonine in the repeated strands of the PGM were still likely to contribute to the interaction between PGM and BLG in a similar manner as shown earlier for BSM and BLG (Çelebioğlu et al., 2015). Furthermore, higher NMR peak intensities of the difference spectra at pH 3 indicated that the strongest protein interactions occurred at acidic conditions for both BLG-mucin solutions, in agreement with the obtained fluorescence results.

To put the NMR results in better relation to the fluorescence analysis, a closer look was taken at the characteristic peaks of Trp in the samples. The $\boldsymbol{\alpha}$-proton in Trp gives rise to a peak at approximately 4.5 ppm, the β-protons at approximately 2.9 and 3.1 ppm, while the ring C-H protons were detected in the range from approximately 6.5 to 7.9. However, no clear detection was made of the HN protons (peaks around 10 ppm), possibly due to their low abundance or that they are generally found deeper into the protein structure and thus not as easily detected as protons on the protein surface. Generally, the Trp peaks were stronger in BLG compared to the mucins, and the peak strength was pH dependent (strongest at acidic conditions). The intensity of the peaks mentioned before were, however, lower in all cases in the mixtures, compared to the neat protein solutions. This can possibly be interpreted as that the environment of the Trp residues were changed, and thus not detected to the same degree due to changed nearby atoms, when BLG was interacting with the mucins. This is in good agreement with the lowered FI of the BLG when interacting with the mucins, especially PGM.

Conclusions

In this study, fluorescence and NMR spectroscopic studies were carried out in order to understand the interaction behavior between BLG and the two mucins, namely BSM and PGM. It can be concluded from the fluorescence analysis that the presence of mucins surrounding BLG tends to enhance the solvent exposure of Trp residues in BLG. More enhanced reduction in FI, together with the red shift of peak maximum of BLG upon mixing with PGM than BSM, suggested that hydrophobic moieties, which can effectively interact with BLG, are more abundantly present in PGM than BSM. This may explain that even at pH 7.4, mixing of BLG with PGM led to a reduction in FI, in contrast to the case of mixing with BSM. In this sense, a quenching effect of mucins on the fluorescence emission of Trp residues of BLG is suggested, chiefly based on hydrophobic interaction, with generally stronger effects by PGM than BSM. Even though the initial interaction between BLG and the mucin molecules can occur via hydrophobic interaction, the results indicated that the interaction can also be facilitated by electrostatic attraction, which was especially evident at pH 3 where BLG and the mucins are oppositely charged. HF-NMR showed the strongest interaction between the BLG and mucins at acidic pH too, supporting this observation. Moreover, increased ANS fluorescence when BLG and PGM were mixed at pH 3 supported that the PGM-BLG mixture synergistically enhances the hydrophobic interaction with ANS, and that ANS can be buried in the PGM-BLG complex. Not only the enhanced hydrophobic interaction, but also the electrostatic interaction of the proteins with ANS might be the reason of higher ANS intensity by facilitating refolding of proteins and helping to bury ANS in the hydrophobic protein matrix at low pH. The study thus confirmed that NMR provided valuable information about the interaction and structural changes within the proteins upon mixing, while fluorescence provided complimentary data on the conformal changes and quenching resulting from those protein-protein interactions. Since the molecular-level interactions of food proteins and salivary proteins can be critical to understand the

textural, sensory, and nutritional properties of food products in digestion, the findings have great potential for understanding oral processing and digestion related applications of BLG. Further studies about the quenching potential of mucins would be interesting to observe more detailed and optimized quenching mechanism of mucins on proteins.

References

Ali, V., Prakash, K., Kulkarni, S., Ahmad, A., Madhusudan, K. P., & Bhakuni, V. (1999). 8-anilino-1-naphthalene sulfonic acid (ANS) induces folding of acid unfolded cytochrome c to molten globule state as a result of electrostatic interactions. Biochemistry, 38(41), 13635-13642.

Alizadeh-Pasdar, N., & Li-Chan, E. C. (2000). Comparison of protein surface hydrophobicity measured at various pH values using three different fluorescent probes. Journal of Agricultural and Food Chemistry, 48(2), 328-334.

Bansil, R., & Turner, B. S. (2006). Mucin structure, aggregation, physiological functions and biomedical applications. Current Opinion in Colloid & Interface Science, 11(2-3), 164-170.

Bansil, R., Stanley, E., & LaMont, J. T. (1995). Mucin biophysics. Annual Review Physiology, 57, 635-657.

Brandão, E., Silva, M. S., García-Estévez, I., Mateus, N., de Freitas, V., & Soares, S. (2017). Molecular study of mucin-procyanidin interaction by fluorescence quenching and Saturation Transfer Difference (STD)-NMR. Food Chemistry, 228, 427-434.

Brownlow, S., Cabral, J. H. M., Cooper, R., Flower, D. R., Yewdall, S. J., Polikarpov, I., ... & Sawyer, L. (1997). Bovine β-lactoglobulin at 1.8 Å resolution—still an enigmatic lipocalin. Structure, 5(4), 481-495.

Busti, P., Gatti, C. A., & Delorenzi, N. J. (1998). Some aspects of β-lactoglobulin structural properties in solution studied by fluorescence quenching. International journal of biological macromolecules, 23(2), 143-148.

Cao, X., Bansil, R., Bhaskar, K. R., Turner, B. S., LaMont, J. T., Niu, N., & Afdhal, N. H. (1999). pH-dependent conformational change of gastric mucin leads to sol-gel transition. Biophysical journal, 76(3), 1250-1258.

Cardamone, M.; Puri, N. Spectrofluorimetric assessment of the surface hydrophobicity of proteins. Biochem. J. 1992, 282, 589-593.

Cattoni, D. I., Kaufman, S. B., & Flecha, F. L. G. (2009). Kinetics and thermodynamics of the interaction of 1-anilino-naphthalene-8-sulfonate with proteins. Biochimica et Biophysica Acta (BBA)-Proteins and Proteomics, 1794(11), 1700-1708.

Çelebioğlu, H. Y., Gudjónsdóttir, M., Chronakis, I. S., & Lee, S. (2016). Investigation of the interaction between mucins and β-lactoglobulin under tribological stress. Food Hydrocolloids, 54, 57–65.

Çelebioğlu, H. Y., Gudjónsdóttir, M., Meier, S., Duus, J. Ø., Lee, S., & Chronakis, I. S. (2015). Spectroscopic studies of the interactions between β-lactoglobulin and bovine submaxillary mucin. Food Hydrocolloids, 50, 203–210.

Cerbulis, J., & Farrell, H. M. (1975). Composition of milks of dairy cattle. I. Protein, lactose, and fat contents and distribution of protein fraction. Journal of Dairy Science, 58(6), 817-827.

Collini, M., D'Alfonso, L., & Baldini, G. (2000). New insight on β-lactoglobulin binding sites by 1-anilinonaphthalene-8-sulfonate fluorescence decay. Protein Science, 9(10), 1968-1974.

D'Alfonso L, Collini M, Baldini G. (1999). Evidence of heterogeneous 1- anilinonaphthalene-8-sulfonate binding to b-lactoglobulin from fluorescence spectroscopy. Biochim Biophys Acta 1432:194–202.

Daniel, E., & Weber, G. (1966). Cooperative Effects in Binding by Bovine Serum Albumin. I. The Binding of 1-Anilino-8-naphthalenesulfonate. Fluorimetric Titrations*. Biochemistry, 5(6), 1893-1900.

Engelhardt, K., Lexis, M., Gochev, G., Konnerth, C., Miller, R., Willenbacher, N., et al. (2013). pH effects on the molecular structure of β-lactoglobulin modified air water interfaces and its impact on foam rheology. Langmuir, 29(37), 11646-11655.

Fritz, T. A., Hurley, J. H., Trinh, L.-B., Shiloach, J. Tabak, L. A. (2004) The beginnings of mucin biosynthesis: The crystal structure of UDP-GalNAc:polypeptide α-Nacetylgalactosaminyltransferase-T1. PNAS, 101(43), 15307–15312.

Fugate, R. D., & Song, P. S. (1980). Spectroscopic characterization of β-lactoglobulin-retinol complex. Biochimica et Biophysica Acta (BBA)-Protein Structure, 625(1), 28-42.

Gerken, T. A. (1986). The solution structure of mucous glycoproteins: proton NMR studies of native and modified ovine submaxillary mucin. Archives of Biochemistry and Biophysics, 247(2), 239-253.

Gibbons, J. A., Weiser, D. C., Shenolikar, S. (2005). Importance of a surface hydrophobic pocket on protein phosphatase-1 catalytic subunit in recognizing cellular regulators. Journal of Biological Chemistry, 280, 15903-15911.

Godovac-Zimmermann, J. (1988). The structural motif of ß-lactoglobulin and retinol-binding protein: a basic framework for binding and transport of small hydrophobic molecules?. Trends in biochemical sciences, 13(2), 64-66.

Hambling, S. G., McAlpine, A. S., Sawyer, L., & Fox, P. F. (1992). β-Lactoglobulin. Advanced dairy chemistry-1: Proteins., (Ed. 2), 141-190.

He, Z., Zhu, H., Xu, M., Zeng, M., Qin, F., & Chen, J. (2016). Complexation of bovine β-lactoglobulin with malvidin-3-O-glucoside and its effect on the stability of grape skin anthocyanin extracts. Food chemistry, 209, 234-240.

Hong, Z., Chasan, B., Bansil, R., Turner, B. S., Bhaskar, K. R., & Afdhal, N. H. (2005). Atomic force microscopy reveals aggregation of gastric mucin at low pH. Biomacromolecules, 6(6), 3458-3466.

Kanakis CD, Hasni I, Bourassa P, Tarantilis PA, Polissiou MG, Tajmir-Riahi H (2011) Milk β-lactoglobulin complexes with tea polyphenols. Food Chem 127:1046–1055

Lakowicz, J. R. (1999). Instrumentation for fluorescence spectroscopy. In Principles of fluorescence spectroscopy (pp. 25-61). Springer US.

Laligant, A., Dumay, E., Casas Valencia, C., Cuq, J. L., & Cheftel, J. C. (1991). Surface hydrophobicity and aggregation of beta-lactoglobulin heated near neutral pH. Journal of Agricultural and food Chemistry, 39(12), 2147-2155.

Lee, S., Müller, M., Rezwan, K., & Spencer, N. D. (2005). Porcine gastric mucin (PGM) at the water/poly(dimethylsiloxane) (PDMS) interface: influence of pH and ionic strength on its conformation, adsorption, and aqueous lubrication properties. Langmuir, 21, 8344-8353.

Liang L, Subirade M (2012) Study of the acid and thermal stability of β-lactoglobulin- ligand complexes using fluorescence quenching. Food Chem 132:2023–2029

Liang, L., & Subirade, M. (2010). b-Lactoglobulin/folic acid complexes: Formation, characterization, and biological implication. J. Phys. Chem. B, 114, 6707–6712.

Liao, X., Yuan, D., Tang, J., Yang, H., Liang, B., Cheng, Q., and Li, H. (2016). Probing into the Interaction of Nicotine and Bovine Submaxillary Mucin: NMR, Fluorescence, and FTIR Approaches. Journal of Spectroscopy, 2016, 1-9

Madsen, J. B., Sotres, J., Pakkanen, K. I., Efler, P., Svensson, B., Hachem, M. A., Arnebrant, T., & Lee, S. (2016). Structural and Mechanical Properties of Thin Films of Bovine Submaxillary Mucin versus Porcine Gastric Mucin on a Hydrophobic Surface in Aqueous Solutions. Langmuir,32 (38), 9687-9696

Mensi A, Choiset Y, Rabesona H, Haertlé T, Borel P, Chobert J(2013) Interactions of β-lactoglobulin variants A and B with vitaminA. Competitive binding of retinoids and carotenoids. J Agric Food Chem 61:4114–4119

Mills, O. E., & Creamer, L. K. (1975). A conformational change in bovine β-lactoglobulin at low pH. Biochimica et Biophysica Acta (BBA)-Protein Structure, 379(2), 618-626.

Muresan, S., A. van der Bent, and F. A. de Wolf. (2001). Interaction of β-lactoglobulin with small hydrophobic ligands as monitored by fluorometry and equilibrium dialysis: Nonlinear quenching effects related to protein-protein association. J. Agric. Food Chem. 49:2609–2618.

Nikogeorgos, N., Madsen, J. B., & Lee, S. (2014). Influence of impurities and contact scale on the lubricating properties of bovine submaxillary mucin (BSM) films on a hydrophobic surface. Colloids and Surfaces B: Biointerfaces, 122, 760–6.

Papiz, M. Z., Sawyer, L., Eliopoulos, E. E., North, A. C. T., Findlay, J. B. C., Sivaprasadarao, R., ... & Kraulis, P. J. (1986). The structure of b-lactoglobulin and its similarity to plasma retinol-binding protein. Nature, 324(6095), 383-385.

Pervaiz, S., & Brew, K. (1985). Homology of beta-lactoglobulin, serum retinol-binding protein, and protein HC. Science, 228(4697), 335-337.

Ptitsyn, O. B., Bychkova, V. E., & Uversky, V. N. (1995). Kinetic and equilibrium folding intermediates. Philosophical Transactions of the Royal Society B: Biological Sciences, 348(1323), 35-41.

Qaqish, R., & Amiji, M. (1999). Synthesis of a fluorescent chitosan derivative and its application for the study of chitosan–mucin interactions. Carbohydrate Polymers, 38(2), 99-107.

Qin, B. Y., Bewley, M. C., Creamer, L. K., Baker, E. N. & Jameson, G. B. (1997). Functional implications of structural differences between variants A and B of bovine b-lactoglobulin. Protein Sci. 8, 75-83.

Renard, D., Lefebvre, J., Griffin, M. C. A., & Griffin, W. G. (1998). Effects of pH and salt environment on the association of β-lactoglobulin revealed by intrinsic fluorescence studies. International Journal of Biological Macromolecules, 22(1), 41-49.

Sakurai, K., Konuma, T., Yagi, M., & Goto, Y. (2009). Structural dynamics and folding of β-lactoglobulin probed by heteronuclear NMR. Biochimica et Biophysica Acta (BBA)-General Subjects, 1790(6), 527-537.

Sandberg, T., Blom, H., & Caldwell, K. D. (2009). Potential use of mucins as biomaterial coatings. I. Fractionation, characterization, and model adsorption of bovine, porcine, and human mucins. Journal of Biomedical Materials Research A, 91, 762-772

Santambrogio, C., & Grandori, R. (2008). Monitoring the Tanford transition in β-lactoglobulin by 8-anilino-1-naphthalene sulfonate and mass spectrometry. Rapid communications in mass spectrometry, 22(24), 4049-4054.

Sawyer, L., & Kontopidis, G. (2000). The core lipocalin, bovine β-lactoglobulin. Biochimica et Biophysica Acta (BBA)-Protein Structure and Molecular Enzymology, 1482(1), 136-148.

Smith, B. F., & LaMont, J. T. (1984). Hydrophobic binding properties of bovine gallbladder mucin. Journal of Biological Chemistry, 259(19), 12170-12177.

Svensson, O., & Arnebrant, T. (2010). Mucin layers and multilayers – physicochemical properties and applications. Current Opinion in Colloid & Interface Science, 15, 395-405

Tanford, C., & Nozaki, Y. (1959). Physico-chemical comparison of β-lactoglobulins A and B. Journal of Biological Chemistry, 234(11), 2874-2877.

Tayeh, N., Rungassamy, T., & Albani, J. R. (2009). Fluorescence spectral resolution of tryptophan residues in bovine and human serum albumins. J. Pharm. Biomed. Anal., 50, 107–116.

Uhrínova, S., Uhrín, D., Denton, H., Smith, M. H., Sawyer, L., & Barlow, P. N. (1998). Complete assignment of 1H, 13C and 15N chemical shifts for bovine betalactoglobulin: secondary structure and topology of the native state is retained in a partially unfolded form. Journal of Biomolecular NMR, 12(1), 89-107.

Uversky, V. N., Winter, S., & Löber, G. (1996). Use of fluorescence decay times of 8-ANS-protein complexes to study the conformational transitions in proteins which unfold through the molten globule state. Biophysical chemistry, 60(3), 79-88.

Vetri, V., & Militello, V. (2005). Thermal induced conformational changes involved in the aggregation pathways of beta-lactoglobulin. Biophysical chemistry, 113(1), 83-91.

CHAPTER 6

Lubrication studies of β-lactoglobulin-stabilized emulsions mixed with bovine submaxillary mucin

Introduction

Recently, tribology has started to be employed as a new approach to investigate oral processing of food emulsions in simulated oral environment (Meyer, Vermulst, Tromp, & de Hoog, 2011; Vardhanabhuti, Cox, Norton, & Foegeding, 2011; Chojnicka- Paszun, de Jongh, & de Kruif, 2012; Chen & Stokes, 2012; Van Aken, 2013; Selway & Stokes, 2013; Prakash, Tan, & Chen, 2013; Chen, Liu, & Prakash, 2014; Joyner Melito, Pernell, & Daubert, 2014). Traditionally, viscosity data have been correlated with some aspects of perceived texture in the mouth. However, bulk rheological properties alone do not represent all the in-mouth sensory properties for many soft-solid foods (Malone, Appelqvist, & Norton, 2003). Tribology (or thin film rheology), the science of adhesion, friction and lubrication, can provide an important information on the properties of materials in thin films that cannot be deduced from bulk properties. Since food hydrocolloids and emulsions are often squeezed between moving surfaces such as the tongue and palate (or food substrate and palate) during eating, the texture or oral perception of food is related to its thin film rheological behaviour as well as to its bulk properties (Malone, Appelqvist, & Norton, 2003; Meyer et al. 2011; Vardhanabhuti et al. 2011; Chojnicka-Paszun et al., 2012; Selway & Stokes, 2013; Prakash et al., 2013). Recent applications of tribology techniques also allowed for quantitative characterization of the lubricating properties of the fluids involving saliva and BLG (Vardhanabhuti et al. 2011; Celebioglu et al. 2016), where saliva–emulsion interactions is anticipated to play an important role in understanding emulsion perception (van Aken, Vingerhoeds, & de Hoog, 2007).

We have recently investigated the structure and molecular-level interaction of BLG and mucins, representing major components of the dairy products and saliva systems, respectively, in spectroscopy, rheology, adsorption, and tribology point of views (Celebioglu et al, 2015, 2016, in press). In the present study, the tribological and physicochemical properties of a model mucus compound, namely highly concentrated bovine submaxillary mucin solution (BSM), with the negatively charged BLG-stabilized emulsion (at pH 6.8) were determined as an attempt to understand the physicochemical basis of BLG-stabilized emulsion in the oral environment. In this chapter, a preliminary set of experimental results is presented. The detailed interpretation and analysis of them, in-depth discussion on the results, as well as further experiments, if necessary, are presently under progress.

Materials and methods

Sample preparation

BLG from bovine milk was purchased from Sigma-Aldrich (Sigma-Aldrich A/S, Brøndby, Denmark) and BSM was purchased from Merck Millipore (Merck KGaA, Darmstadt, Germany) and both were used as received.

A protein stock solution (1 wt%) was prepared by dispersing BLG in 10 mM phosphate buffered saline (PBS) solutions at pH 6.8 and stirring for 30 min at room temperature. Sodium azide (0.02 wt%) was added to avoid microbial growth. Sunflower oil was then added to the protein solution slowly by mixing with Ultra-Turrax homogenizer (DI 25 basic; IKA-WERKE, Staufen, Germany) at low speeds (6,000 min^{-1}) to form final emulsions containing 20 wt%, 30 wt% or 40 wt% sunflower oil. After an aliquot of sunflower oil was added to BLG solution, the mixture was homogenized for 30 min with Ultra-Turrax at high speed (20,000 min^{-1}). To prevent uncontrolled

changes in temperature, water bath was used during mixing. The final emulsions were denoted as "emulsion 2:8", "emulsion 3:7", or "emulsion 4:6" according to their oil:water phase ratios (w/w). The BLG-stabilized emulsions of 2:8, 3:7, and 4:6 had BLG:oil ratios of 1:25, 1:43, and 1:67, respectively. Another emulsion, denoted as "emulsion 3:7*" was prepared with the oil:water phase ratio at 3:7, but the BLG:oil ratio at 1:25 (instead of 1:43 as in "emulsion 3:7") by increasing the concentration of BLG. This was a control to compare with the emulsion 2:8 at the same BLG:oil ratio, yet with different oil:water ratio. In addition, 1 wt% and 5 wt% oil content emulsions were also prepared to observe the effect of low amount of oil for lubrication.

To prepare emulsion-mucin mixtures, stock emulsions were mixed gently with model mucus containing 3 wt% concentrations of BSM for 5 min; the final mixture contained 1 wt% mucin and thus the BLG:BSM ratio was 1:1.

In order to track the emulsifier properties of mucin, a reference emulsion, stabilized by mucin, was also prepared with the same emulsion preparation method mentioned above. Moreover, 1 wt% BLG and 1 wt% BSM solutions with and without homogenization step were prepared as reference samples for emulsion and emulsion-mucin mixtures in tribology analysis.

Tribology

Pin-on-disk tribometry

Lubricating properties of the emulsions, emulsion-mucin mixtures, and protein solutions at sliding contacts were characterized by pin-on-disk tribometry (CSM, Peseux, Switzerland). In this approach, a loaded spherical pin is allowed to form a contact on a plane disk. The motor-driven rotation of the disk generates interfacial friction forces between the pin and the disk. The applied

load is controlled by dead weight and the friction forces generated during sliding contact are monitored by a strain gauge. The coefficient of friction, μ, is defined from the relationship;

$\mu = F_{friction}/F_{load}$

Initially, PDMS was chosen as the tribopair for both pin (6 mm in diameter) and disk (30 mm in diameter and 5 mm in thickness). The pin and disk from PDMS were prepared with the PDMS kit (Sylgard 184, Dow Corning) according to a procedure described by Nikogeorgos, Madsen, & Lee (2014). In addition to PDMS-PDMS tribopair, HDPE pin and PDMS disk, roughened PDMS pin and disk, and steel pin and PDMS disk were used as tribopairs. Roughened PDMS pins and disks were prepared by roughening the corresponding templates by means of sandblasting. To investigate the speed dependent and load dependent behavior of emulsions, a sliding speed range of 0.25 – 100 mm/s and loads of 1, 2, 5, 7, and 10 N were selected, respectively. The friction force data were collected for 100 rotations at room temperature (25 °C) and the tests were repeated multiple times. For each measurement, a tribopair of PDMS-PDMS (or any PDMS surface) was used only once and discarded to avoid cross contamination between measurements. However, HDPE and steel pins were used again after cleaning. HDPE and steel pins were cleaned by means of ultrasonication in ethanol for 15 min. Steel pins/balls were further cleaned with a plasma cleaner (2 min, high power) and used immediately after plasma treatment.

Mini traction machine (MTM)

Lubrication properties of the emulsions were characterized at mixed rolling/sliding contacts in higher speed regime by means of a mini-traction machine (MTM, PCS Instruments Ltd., UK) too. Mixed rolling/sliding contacts are provided with MTM by independent rotation of ball and disk. The mean speed is defined as [$|speed_{ball} - speed_{disk}|/2$]. The slide/roll ratio (SRR) is defined as SRR

= ($|speed_{ball} - speed_{disk}|$)/[($speed_{ball} + speed_{disk}$)/2] × 100%, where 0% SRR represents pure rolling and 200% SRR represents pure sliding. In this study, SRR of 20% was employed in all measurements with a varying mean speed between 10 mm/s to 1200 mm/s. Tests were conducted at room temperature (25 °C) with the tribopair consisting of HDPE ball – PDMS disk, steel ball – PDMS disk, and PDMS ball – PDMS disk. The PDMS disks were prepared from the aforementioned two-component silicone kit (Sylgard 184, Dow Corning) as well. A thick PDMS slab (ca. 5 mm) was cast on top of a steel disk (ca. 5 mm) for each sample. HDPE balls were purchased from a supplier (19.05 mm (¾ inch) in diameter, Precision Plastic Ball Co., IL) and were used as received. For each measurement, a new PDMS disk was employed, whereas the same HDPE and steel balls were used after cleaning as described above. A fixed load (2 N) was applied with the estimated Hertzian contact pressure of 0.3 MPa. Tests were repeated three times and the friction data were averaged.

Contact angle – goniometer

Contact angle measurements were performed with a goniometer (Model Raméhart 200, Succasunna, NJ) and running software version 2.4.11. Static contact angles by distilled water were measured by applying a 5 µL droplet onto surfaces.

Rheology

The viscosity of the samples was examined using a controlled stress HAAKE™ MARS™ rheometer (Thermo Scientific Inc., Germany). Flow measurements using a coaxial cylinder set-up

were performed in which the shear rate was increased from 10 to 100 s^{-1}. All measurements were carried out at room temperature (25 °C) in triplicate for each sample.

Droplet size and distribution

Droplet size distributions of the emulsions and emulsion-mucin mixtures were characterized using a light scattering analyzer (Mastersizer, Zetamaster, Malvern Instruments Ltd.). Measurements of droplet size were carried out at least in duplicate.

The distribution of oil droplet of emulsion before and after mixing with mucin was analyzed by light microscopy.

Results

Boundary lubricating properties: pin-on-disk tribometry

Load dependent lubricating behavior of different emulsions

Figure 1 shows the COFs for the sliding contacts of PDMS-PDMS in the emulsion 2:8, emulsion 3:7, BLG and sunflower oil (as control) by means of pin-on-disk tribometer at three different speeds (1, 5, and 10 mm/sec) and different loads (2, 4, 6, 8, and 10 N). All emulsions demonstrated no significant dependence on load, except for the emulsion 2:8 at 10 mm/s. Although Fig. 1 was plotted mainly for load dependence, the COF values obtained at 1 mm/sec are clearly higher than those obtained at two other speeds for both emulsions. Lastly, the COFs were virtually not dependent on load for sunflower oil, but showed a decreasing trend with increasing load for the reference BLG solution with relatively higher values. This is an indication of superior lubricating properties of sunflower oil than BLG solution.

Influence of model mucus on the speed dependent lubricating properties of emulsions

The COFs of PDMS-DPMS tribopair in the emulsions, emulsion-mucin mixture systems, and control fluids with varying speeds (0.25, 0.5, 1, 2.5, 5, 10, 25, 50, and 100 mm/sec) under 1 N load are illustrated in Fig. 2. Prior to mucin addition, the COFs for the case of emulsion 3:7 (with BLG:oil ratio is 1:25) showed a similar trend with those for sunflower oil. Emulsion 2:8 showed somewhat lower COFs than those of the emulsion 3:7 (both have the same BLG:oil ratio) in low-speed regime, however they showed similar COF values with increasing speed. Decrease of the BLG content within the same emulsion (3:7) created a fluctuation of COF values at lower speeds. Addition of mucin increased the COF values, especially in low-speed regime, but they start to decrease at high speeds, and very much alike to emulsions without mucin at the highest speed. It is interesting to note that the emulsion-mucin mixtures show a similar trend with mucin-stabilized emulsion. Moreover, emulsions with 1 % and 5 % oil content showed similar frictional behavior with emulsion-mucin mixture or with mucin-stabilized emulsion. No important difference in COFs was observed between 1% emulsion and 5% emulsion as the speed increased. However, they all displayed a decreasing trend in COF with increasing speed (Appendix 1).

Influence of contact interfaces

In order to investigate the influence of different tribopairs, the PDMS pin was switched with HDPE first. The load and speed were identical to those for PDMS-PDMS interface. At HDPE-PDMS interface, all emulsions and emulsion-mucin mixtures behaved similarly to sunflower oil in the sense that the COF values were much closer to each other (Fig. 3). They did not show any strong speed dependence either. The COFs for buffer and BLG solution were distinctly higher and show increasing trend with increasing speeds.

Another tribopair was the interface composed of self-mated, surface-roughened PDMS. As shown in Fig. 4, for roughened PDMS pairs, buffer and 1% BLG solutions showed exceptionally higher COF values compared to the other samples, although buffer and 1% BLG solutions showed an increasing and decreasing COFs values with increasing the speed, respectively. Sunflower oil, mucin emulsion, and all the other emulsion samples showed almost the same COF values with slightly deceasing trend with increasing speed.

Since emulsion 2:8 and emulsion 3:7 showed very similar COFs for all the tribopairs investigated so far, namely PDMS-PDMS, HDPE-PDMS and roughened PDMS interfaces, some of forthcoming experiments were conducted with the emulsion 2:8 only.

Steel-PDMS tribopair was further employed to investigate the friction behavior of the emulsion 2:8 at hydrophilic-hydrophobic contact interface (Fig. 5). In contrast to the other tribopairs, addition of mucin to emulsion 2:8 did not make significant changes in COFs. It is also notable that both the emulsion and emulsion-mucin mixture showed very low COFs (≤ 0.05) over the entire speed range.

In order to visualize the influence of tribopairs on the addition effect of mucins to emulsions more clearly, the results for emulsion 2:8 and its mucin mixture obtained from different tribopairs are displayed together in Fig. 6. No clear difference in COFs was found for steel-PDMS pair between emulsion 2:8 and its mucin mixture. Moreover, the COF values were the lowest among all tribopairs. For HDPE-PDMS pair, the COF values were slightly higher for both emulsion 2:8 and its mucin mixture compared to those from steel-PDMS pair. At HDPE-PDMS interface, the COF values were generally independent from the speed in low-to-medium speed regime, but clearly increased at high speeds for the emulsion-mucin mixture. At roughened PDMS-PDMS interface, the COF values were somewhat higher than those at HDPE-PDMS interface. No significant difference in COFs was found between emulsion 2:8 and its mucin mixture. Lastly, for PDMS-PDMS interface, emulsion 2:8 displayed relatively high COF values in low-speed regime (≤ 1 mm/s), but

started to show very low values (ca. 0.05), similar to those at steel-PDMS surface. In contrast, emulsion-mucin mixture yielded much higher COFs in low-to-medium speed regime, although the COF values became very low again in high-speed regime.

In summary, the order of COF of emulsion-mucin mixture was observed to be as follow,

- Relative frictions at speed 50 mm/sec: HDPE > ROUGH PDMS > PDMS = STEEL
- Relative frictions at speed 5.0 mm/sec: ROUGH PDMS > HDPE > PDMS = STEEL
- Relative frictions at speed 0.5 mm/sec: PDMS > ROUGH PDMS > HDPE > STEEL

Wettability of emulsion-mucin systems on different contact surfaces

The boundary lubricating properties of fluids are often related to the wettability on tribopair surfaces (Table 1). Static contact angles of emulsions and emulsion-mucin mixtures are presented in Table 1. As expected, the lowest contact angle values were obtained on steel surface for emulsion 2:8. Among three hydrophobic surfaces, the contact angle was generally in the order of HDPE < PDMS ≈ rough PDMS. Addition of mucin to emulsion 2:8 tends to increase the contact angles slightly except for HDPE, where rather a slight reduction was observed. For emulsion 3:7, the contact angles were somewhat larger (i.e. less wetting) on steel, PDMS, and roughened PDMS surfaces, although somewhat lower (i.e. more wetting) on HDPE compared to emulsion 2:8. Upon addition of mucin, the contact angles became lower for all the surfaces, although the magnitude of reduction was different for each surface. The shape of the emulsions droplets and emulsion-mucin mixtures on each contact surfaces can be seen in Appendix 2.

Fluid-lubrication properties: Mini-traction machine (MTM)

Lubrication properties of the emulsions at mixed rolling/sliding

The lubricating properties of emulsion 2:8 and its mixture with mucin were further investigated at a mixed rolling/sliding contact by employing HDPE ball–PDMS tribopair on MTM. As the highest speed was increased to 1 m/s and the dominant contact characteristic was rolling than sliding, a possibility to form fluid film lubricant at the interface is expected to be much higher than pin-on-disk tribometry shown in the previous section. The results for emulsion 2:8 and its mixture with mucin are presented in Fig. 7. In general, emulsion 2:8-mucin mixture showed somewhat higher COF values than emulsion 2:8, except for very high-speed regime (ca. > 500 mm/s) where both samples showed similar COF values. The COF values for emulsion 2:8 in low-speed regime were similar to those of sunflower oil, although the latter showed clearly lower COF values at higher speeds (> ca. 200). On the contrary, buffer and 1 % BLG solutions showed distinctly higher COF values compared to other samples, similarly with the results from PoD experiments, and they revealed an increasing trend with increasing speed.

Fig. 8 shows the results for the same experiments with Fig. 7, yet from steel ball-PDMS tribopair. Due to hydrophilic characteristics of steel ball, the COF values were much lower than those from HDPE-PDMS tribopair for both emulsion 2:8 and its mixture with mucin. But, the emulsions containing mucins displayed even lower COF values than the emulsion without mucin at low speeds. At speeds beyond 10 mm/s, COFs of emulsion and emulsion-mucin mixture showed similar values with each other as well as with the reference samples, i.e. buffer and sunflower oil.

The lubricating behavior of emulsion 2:8 at different tribopairs as characterized with MTM are compared more explicitly in Appendix 3. For simplicity, the trend lines connecting data points only are displayed (both Appendix 3 and 4 below). In this plot, the results from PDMS-PDMS are also added. The results of PDMS-PDMS pair displayed a strong dependence on speed in the changes of COF, for instance, a fluctuated rise of COF with increasing speed. Roughly, the COF values were in the order of PDMS-PDMS > HDPE-PDMS > steel-PDMS pairs. In addition to the emulsion 2:8,

two more types of emulsions with different oil:water ratio (3:7 and 4:6) were characterized at HDPE-PDMS pair as a function of speed (1-1200 mm/s at 2 N load 20% SRR) and the results are shown in Appendix 4. For all three emulsions, the COF values showed a decreasing trend with increasing speed and the COF values were similar to each other in low-to-medium speed regime. At high speeds (> 100 mm/s) though, the COF values for the emulsions 3:7 and 4:6 were slightly lower than those of emulsion 2:8.

Rheological properties of model mucus

Fluid-film lubrication properties are often correlated to the rheological properties of fluids in question. As shown in Fig. 9, both samples showed a Newtonian behavior within the shear rate range of 10 to 100 s^{-1}. More importantly, the apparent viscosity of the emulsion 2.8 with mucin was nearly twice than that of the emulsion 2.8.

Droplet size and microstructure of emulsions and emulsion-mucin mixtures

Hydrodynamic sizes of oil-protein droplets in emulsions with and without mucin were assessed with Mastersizer, and the results are presented in Fig. 10. For both emulsion samples with different oil:water ratios, two major peaks, one in ca. 0.05-1.00 μm range, and the other in ca. 10-200 μm range, were observed. The "small-sized droplets" (0.05-1.00 μm with a local peak max. at around 0.1 μm) were observed from the emulsion 2:8 and emulsion 3:7 without mucins and the peak for emulsion 2:8 was somewhat higher than that of emulsion 3:7. Upon addition of mucins, the small-sized droplets disappeared and "large-sized droplet" (10-200 μm with a local peak max. at around 100 μm) emerged instead. Both emulsion samples showed similar local max. peaks at around 100 μm, but the distribution was somewhat narrower for the emulsion 2:8-mucin mixture than the emulsion 3:7-mucin mixture.

In order to compare with the observations with Mastersizer particle size analyzer, the microscopy images of the emulsion 2:8 and its mixture with mucin were collected. Fig. 11 shows enhanced emulsion flocculation induced by mucin (model mucus) and higher population of "large-sized droplets" (D ~ 100 μm). Overall, addition of mucin clearly increased the droplet size of the emulsions 2:8 and emulsion 3:7.

Summary of the results for future discussion

The lubricating properties of emulsions were characterized with both PoD and MTM. Experiments with PoD were expected to provide the information on the boundary lubricating properties. Experiments with MTM were designed to increase the likelihood of formation of fluid film lubricants. But, whether a fluid-film lubricant was indeed formed or not at the tribological interface is not conclusive based on MTM data alone, and it should be further studied either experimentally and/or in comparison with theoretical modelling in the future. A main focus of this study was to investigate the influence of the composition of emulsions, in particular, the oil:water ratio, BLG:oil ratio, and the contribution of mucin. A unique feature of tribological study was to vary the contacting interface in terms of hydrophilicity, hardness, and surface roughness by performing experiments at different tribopairs. Future discussion will be made to unravel the influence of all these parameters on the lubricating properties of the emulsion samples. Lastly, given the fluid lubricants in this study are emulsions, a primary interest is to understand the relationship between the droplet sizes and the lubricating properties. The droplet sizes of the BLG-stabilized emulsions were significantly increased by the addition of BSM with notable flocculation and coalescence. The net effect of mucins on the lubricating properties of emulsions was significantly different for different tribopairs and speed of the moving surfaces.

References

Çelebioğlu, H. Y., Gudjónsdóttir, M., Chronakis, I. S., & Lee, S. (2016). Investigation of the interaction between mucins and β-lactoglobulin under tribological stress. Food Hydrocolloids, 54, 57-65.

Çelebioğlu, H. Y., Gudjónsdóttir, M., Meier, S., Duus, J. Ø., Lee, S., & Chronakis, I. S. (2015). Spectroscopic studies of the interactions between β-lactoglobulin and bovine submaxillary mucin. Food Hydrocolloids, 50, 203-210.

Chen, J., & Stokes, J. R. (2012). Rheology and tribology: Two distinctive regimes of food texture sensation. Trends in Food Science & Technology, 25(1), 4–12.

Chen, J., Liu, Z., & Prakash, S. (2014). Lubrication studies of fluid food using a simple experimental set up. Food Hydrocolloids, 42, 100–105.

Chojnicka-Paszun, A., de Jongh, H. H. J., & de Kruif, C. G. (2012). Sensory perception and lubrication properties of milk: Influence of fat content. International Dairy Journal, 26, 15–22.

Joyner Melito, H. S., Pernell, C. W., & Daubert, C. R. (2014). Impact of formulation and saliva on acid milk gel friction behavior. Journal of Food Science, 79, 67–80.

Lee, S., Müller, M., Rezwan, K., & Spencer, N. D. (2005). Porcine gastric mucin (PGM) at the water/poly (dimethylsiloxane)(PDMS) interface: influence of pH and ionic strength on its conformation, adsorption, and aqueous lubrication properties. Langmuir, 21(18), 8344-8353.

Malone, M. E., Appelqvist, I. A. M., & Norton, I. T. (2003). Oral behaviour of food hydrocolloids and emulsions. Part 1. Lubrication and deposition considerations. Food Hydrocolloids, 17(6), 763-773.

Meyer, D., Vermulst, J., Tromp, R. H., & de Hoog, E. H. A. (2011). The Effect of inulin on tribology and sensory profiles of skimmed milk. Journal of Texture Studies, 42, 387–393.

Prakash, S., Tan, D. D. Y., & Chen, J. (2013). Applications of tribology in studying food oral processing and texture perception. Food Research International, 54, 1627–1635.

Selway, N., & Stokes, J. R. (2013). Insights into the dynamics of oral lubrication and mouth feel using soft tribology: Differentiating semi-fluid foods with similar rheology. Food Research International, 54, 423–431.

van Aken, G. A. (2013). Acoustic emission measurement of rubbing and tapping contacts of skin and tongue surfaces in relation to tactile perception. Food Hydrocolloids, 31, 325–331.

van Aken, G. A., Vingerhoeds, M. H., & de Hoog, E. H. (2007). Food colloids under oral conditions. Current Opinion in Colloid & Interface Science, 12(4), 251-262.

Vardhanabhuti, B., Cox, P. W., Norton, I. T., & Foegeding, E. A. (2011). Lubricating properties of human whole saliva as affected by β-lactoglobulin. Food Hydrocolloids, 25(6), 1499-1506.

Vingerhoeds, M. H., Blijdenstein, T. B., Zoet, F. D., & van Aken, G. A. (2005). Emulsion flocculation induced by saliva and mucin. Food Hydrocolloids, 19(5), 915-922.

Tables

Table 1. Contact angles of different emulsion droplets and their mucin mixtures on different tribopair surfaces

Surface	Sample	mean
PDMS	E-2:8	87.1
	E-2:8 + mucin	92.0
	E-3:7	91.0
	E-3:7 + mucin	79.8
HDPE	E-2:8	61.0
	E-2:8 + mucin	54.8
	E-3:7	56.3
	E-3:7 + mucin	54.5
Rough PDMS	E-2:8	87.5
	E-2:8 + mucin	89.4
	E-3:7	91.9
	E-3:7 + mucin	82.7
Steel	E-2:8	3.7
	E-2:8 + mucin	12.1
	E-3:7	28.0
	E-3:7 + mucin	27.1

Figures

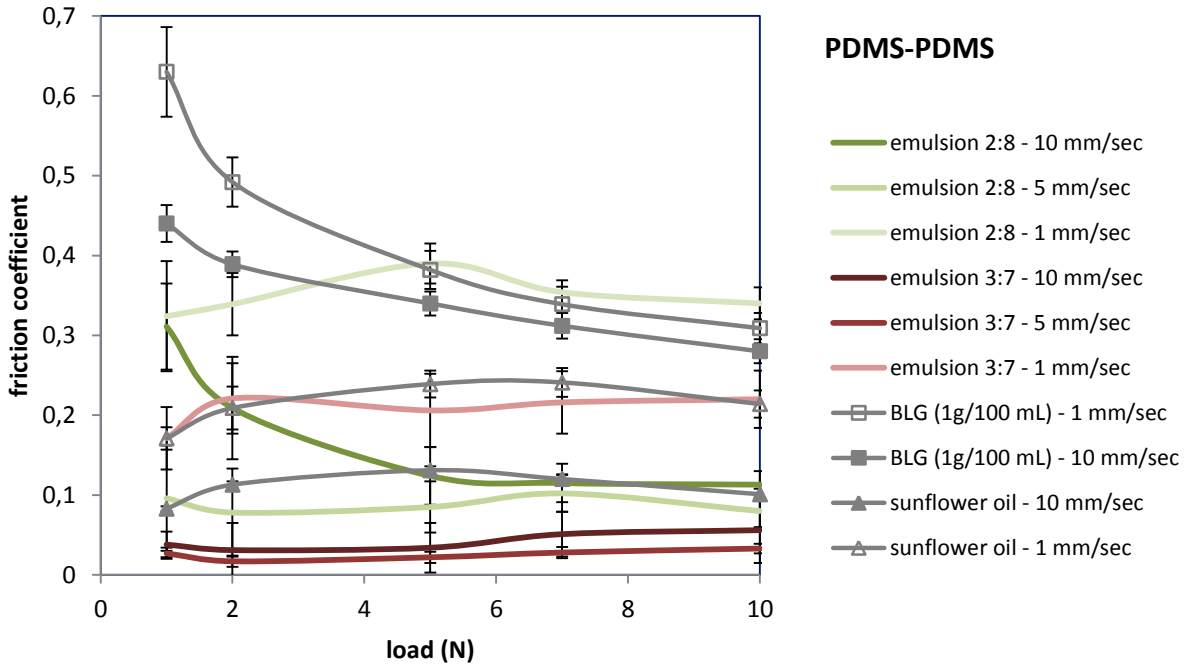

Fig. 1. Load dependent friction coefficient measurement of different BLG-stabilized emulsions at PDMS-PDMS interface with Pin-on-Disk (PoD) tribometry.

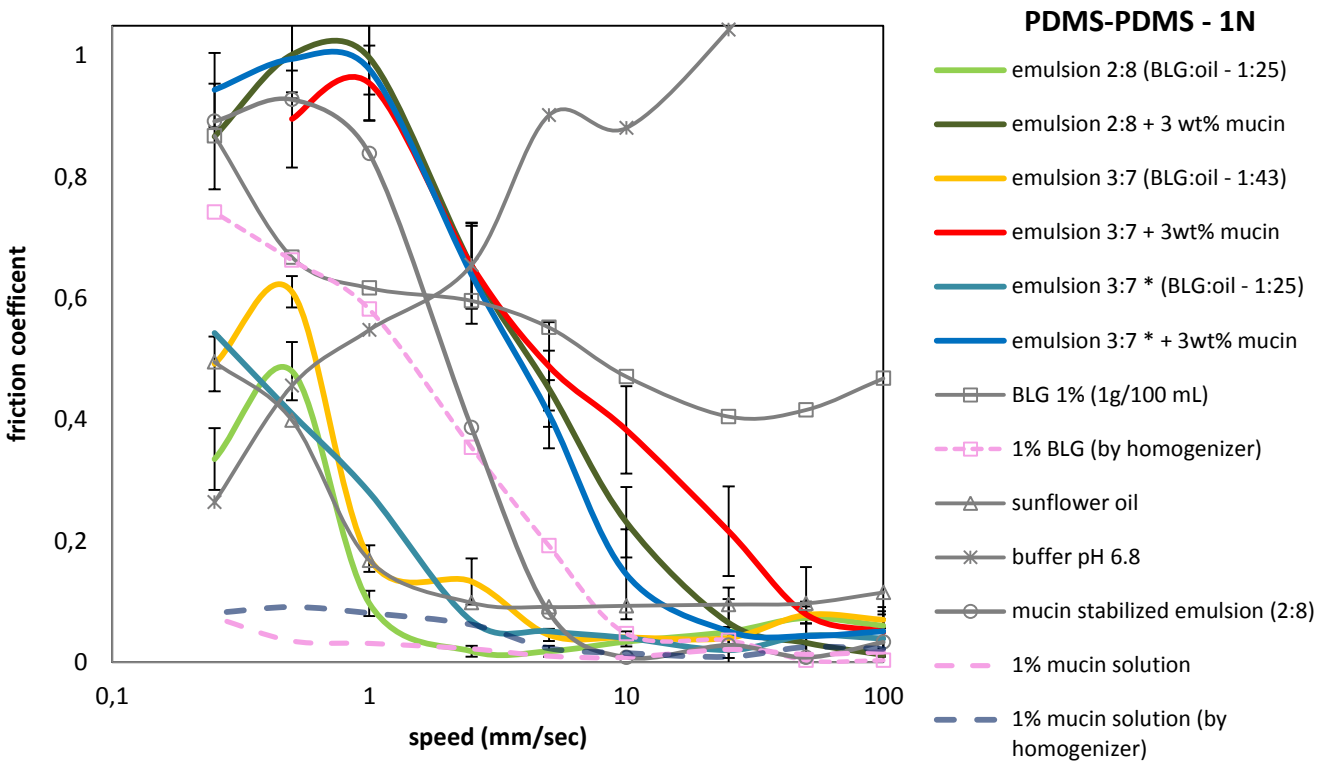

Fig. 2. Speed dependent friction coefficient measurement of different BLG-stabilized emulsions-with/without mucin solution at PDMS-PDMS interface with Pin-on-Disc (PoD) tribometry (1 N load)

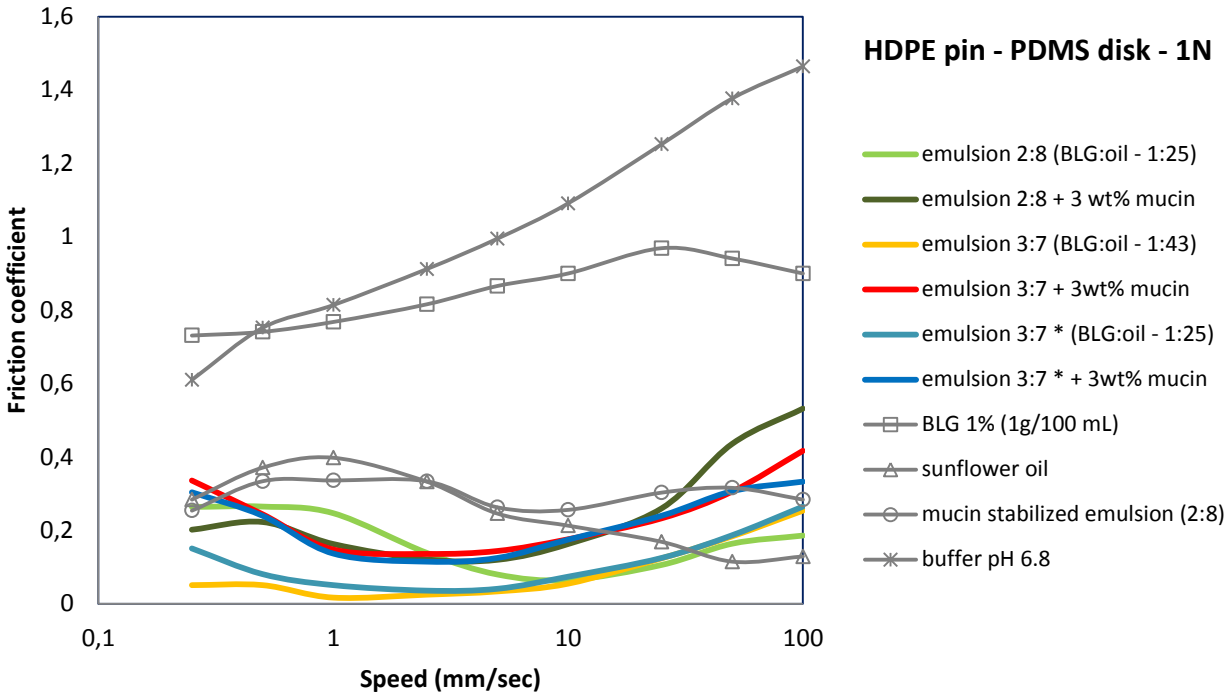

Fig. 3. Speed dependent friction coefficient measurement of different BLG-stabilized emulsions - with/without mucin at HDPE-PDMS interface with Pin-on-Disk (PoD) tribometry (1 N load)

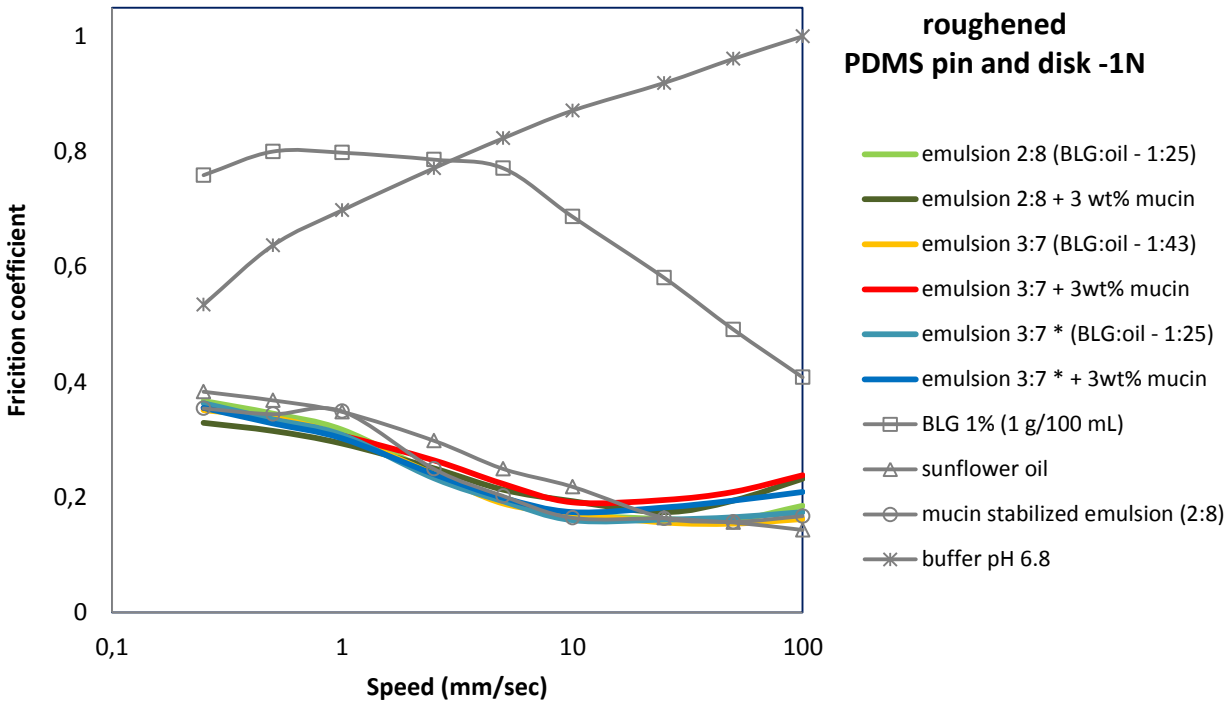

Fig. 4. Speed dependent friction coefficient measurement of different BLG-stabilized emulsions - with/without mucin at roughened PDMS-PDMS interface with Pin-on-Disk (PoD) tribometry (1 N load)

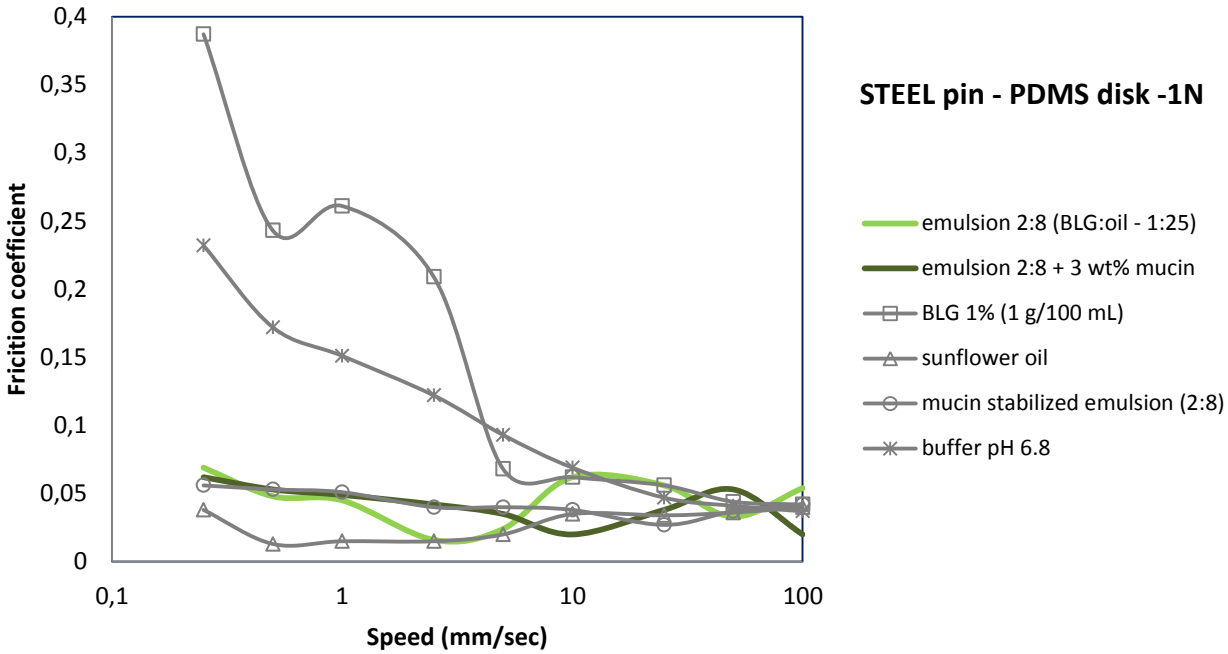

Fig. 5. Speed dependent friction coefficient measurement of emulsion 2:8 - with/without mucin at steel-PDMS interface with Pin-on-Disk (PoD) tribometry (1 N load)

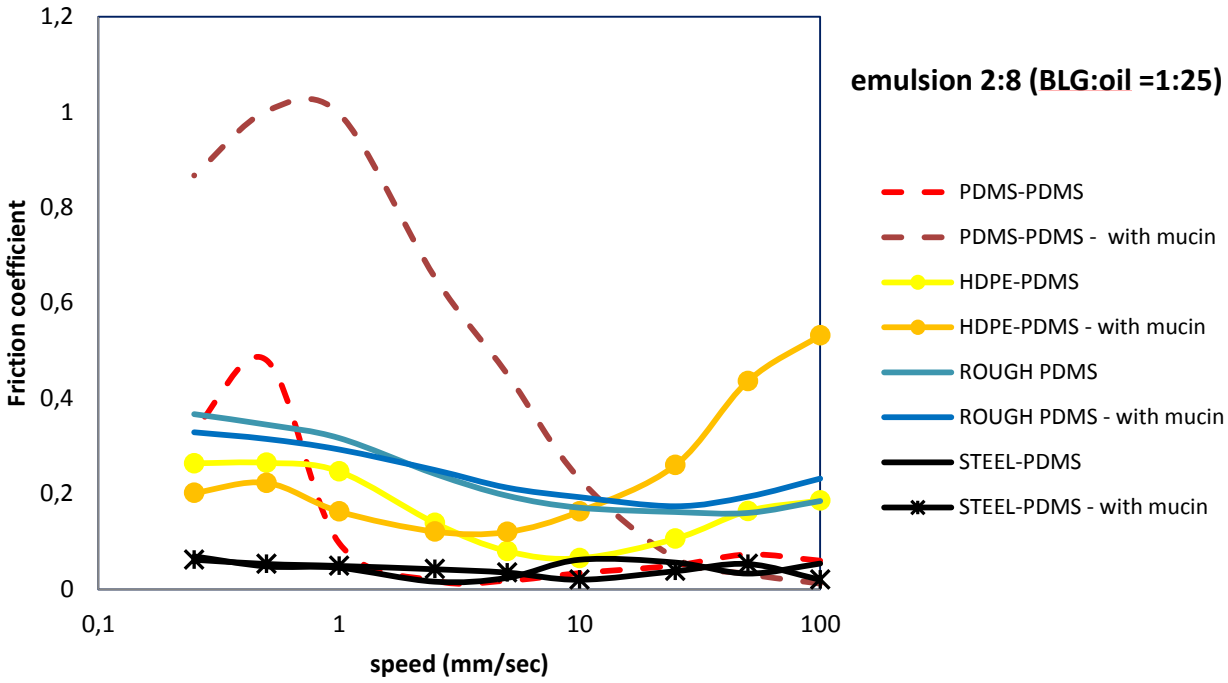

Fig. 6. Speed dependent friction coefficient measurement of emulsion 2:8 - with/without mucin with at various interfaces with Pin-on-Disk (PoD) tribomety (1 N load)

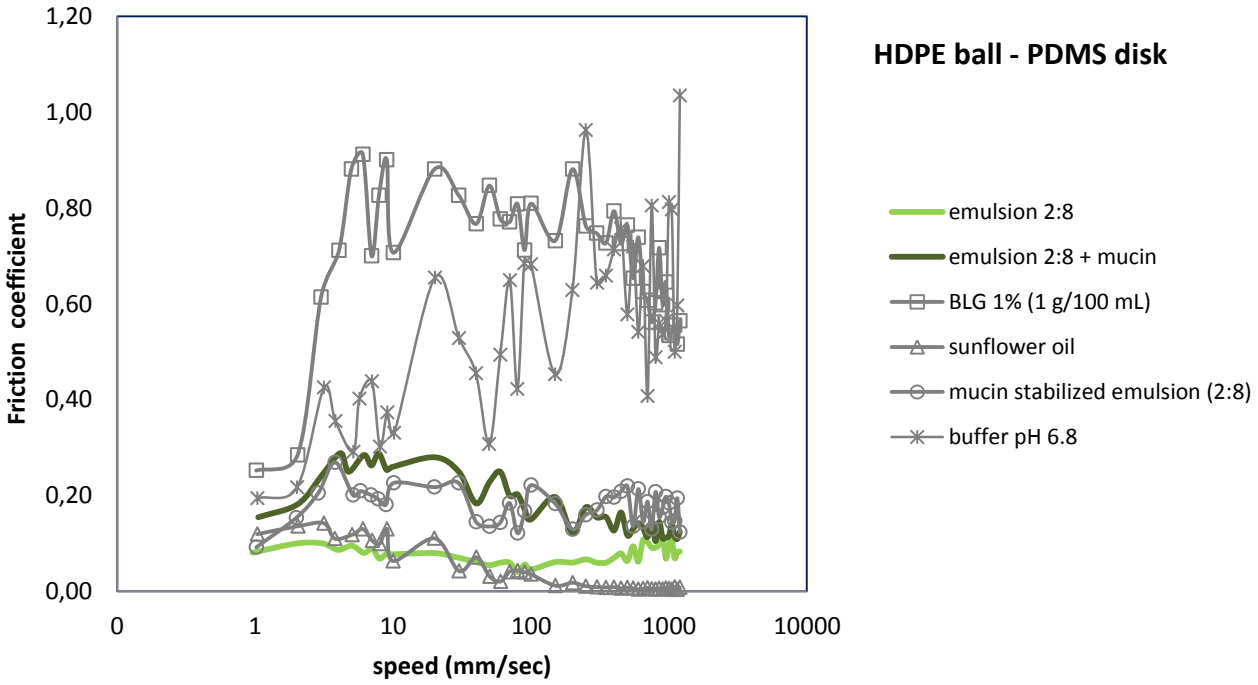

Fig. 7. Speed dependent friction coefficient measurement of emulsion 2:8 - with/without mucin at HDPE-PDMS interface with Mini Traction Machine (MTM) (2 N load)

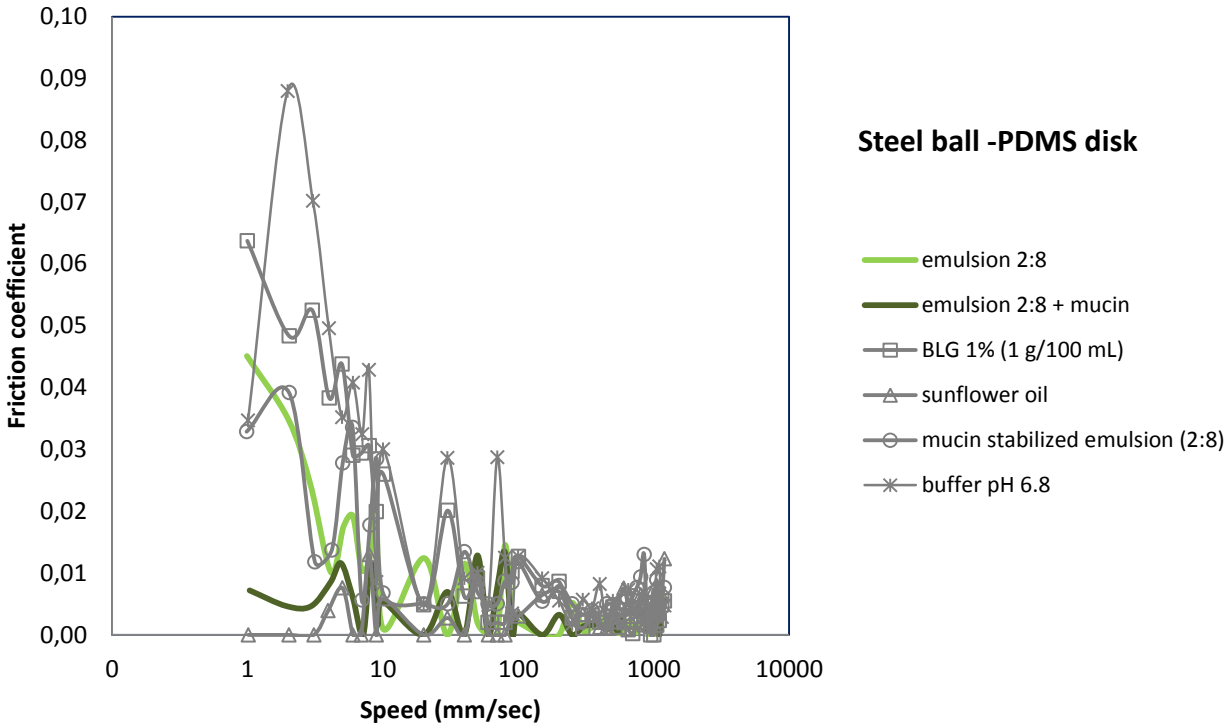

Fig. 8. Speed dependent friction coefficient measurement of emulsion 2:8 - with/without mucin at steel-PDMS interface with Mini Traction Machine (MTM) (2 N load)

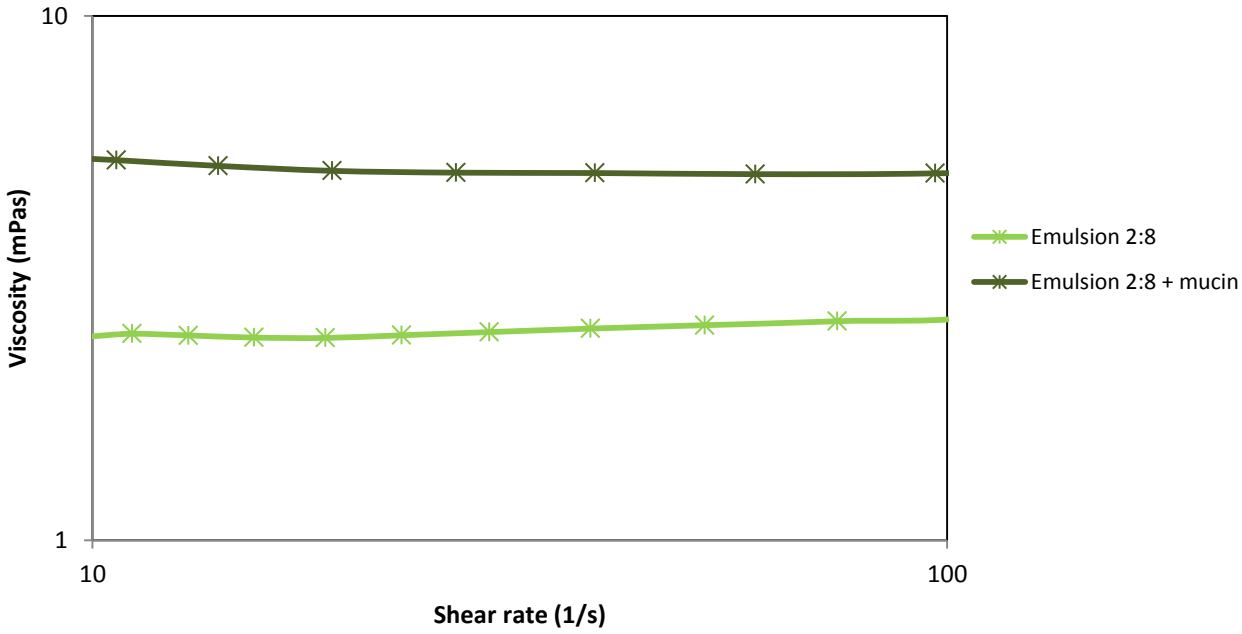

Fig. 9. Effect of the shear rate on the apparent viscosity of the emulsion 2:8 with/without mucin

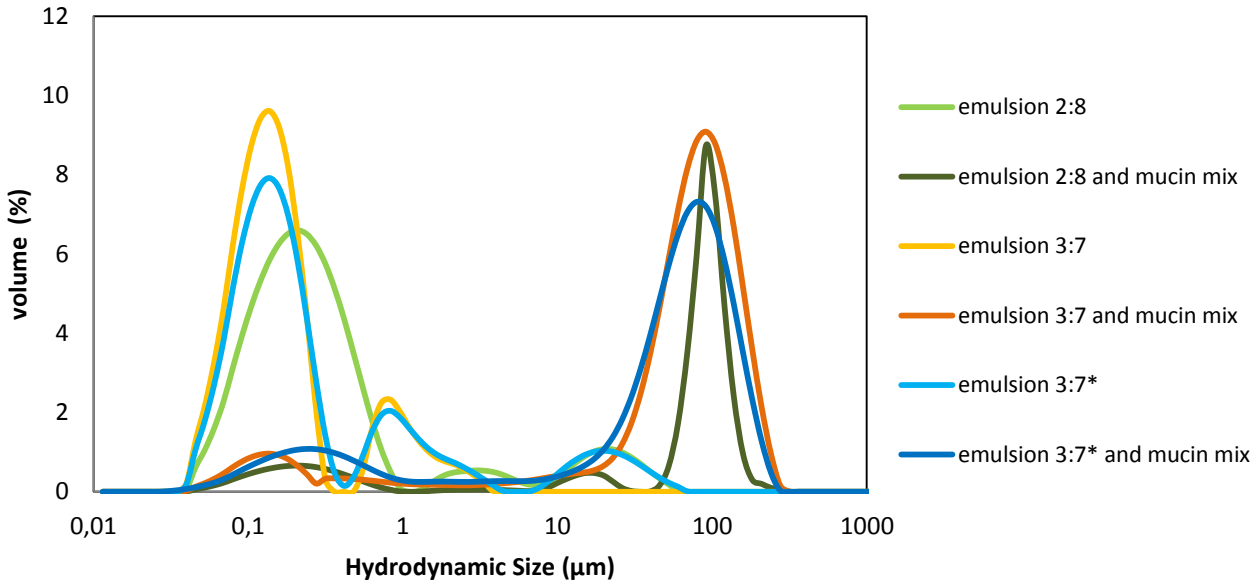

Fig. 10. Volumetric percentage of hydrodynamic size distribution of emulsion-mucin systems

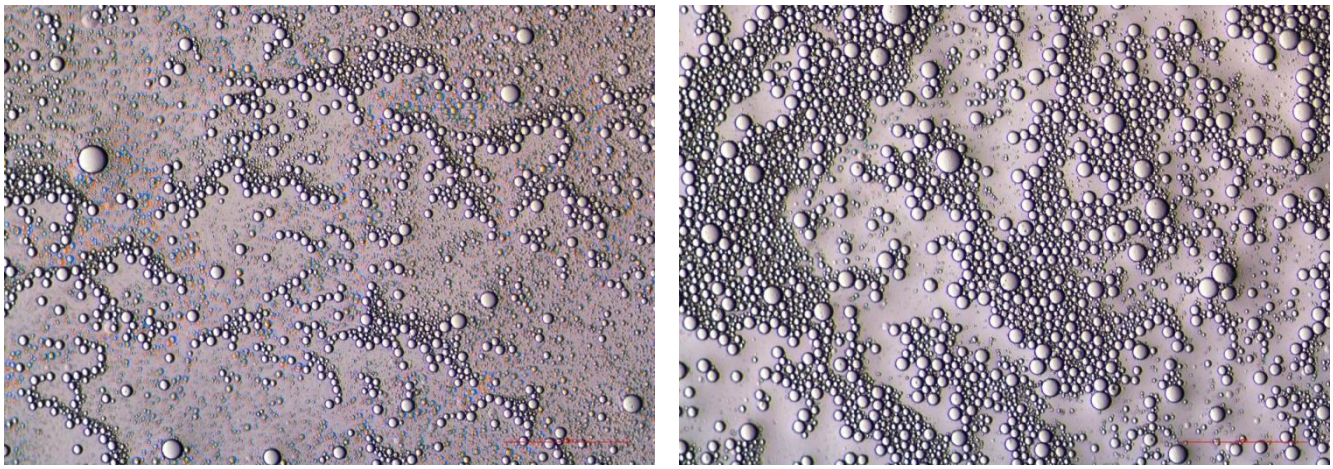

Fig. 11. Optical light microscopy images of emulsion 2:8 after 30 min from the emulsion preparation (left) and emulsion-mucin mixtures after 5 minutes from mucin addition (right)

Appendix

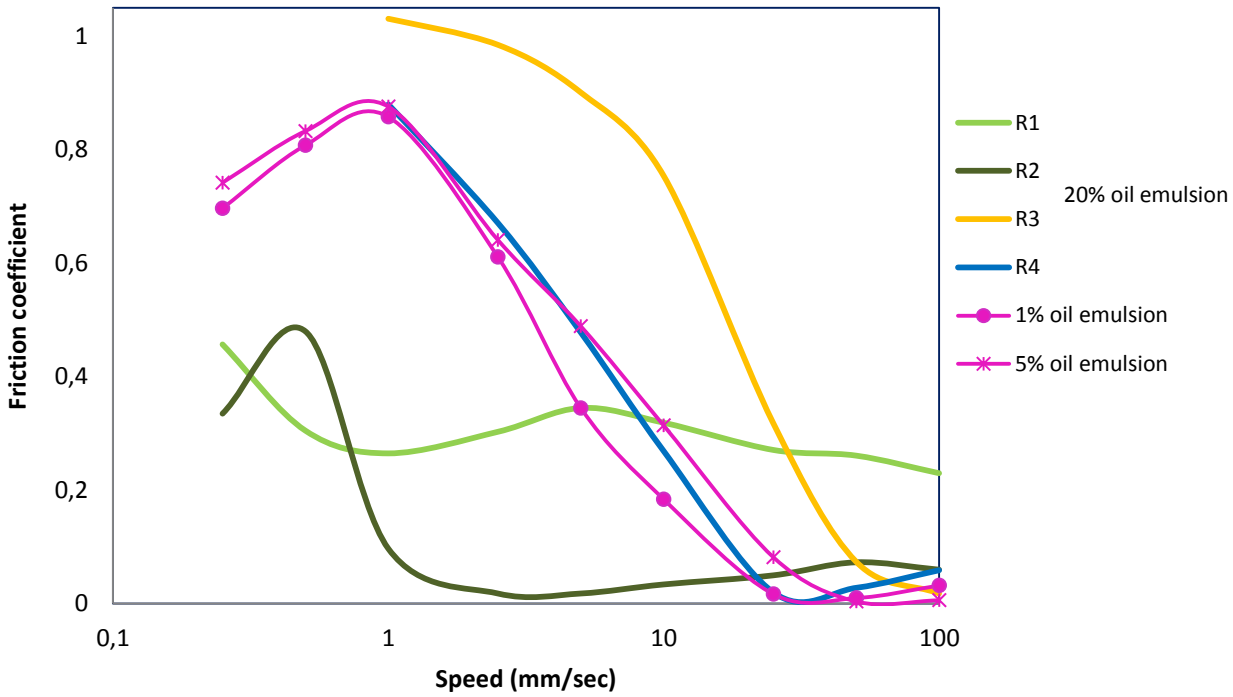

Appendix 1. Speed dependent friction coefficient measurement of 1%, 5% and 20% oil content emulsions with Pin-on-Disk (PoD) tribomety using PDMS pin and disk under 1 N load. Various replications of the measurements for 20% oil content emulsion were compared as R1, R2, R3, and R4

Surface	Sample		Surface	Sample	
PDMS	E-2:8	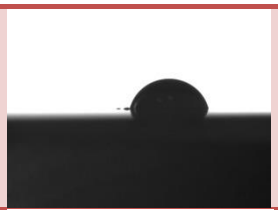	Rough PDMS	E-2:8	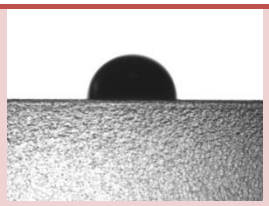
	E-2:8 + mucin	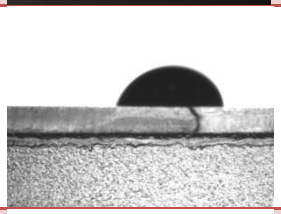		E-2:8 + mucin	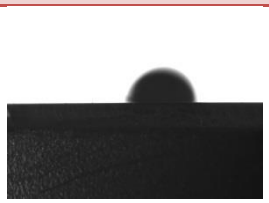
	E-3:7	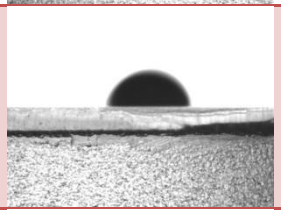		E-3:7	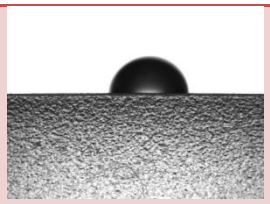
	E-3:7 + mucin	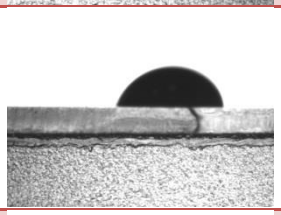		E-3:7 + mucin	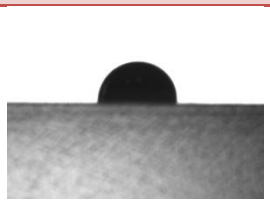
HDPE	E-2:8	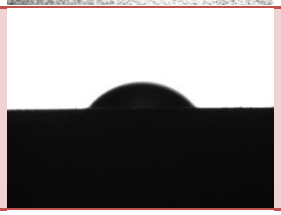	Steel	E-2:8	
	E-2:8 + mucin			E-2:8 + mucin	
	E-3:7			E-3:7	
	E-3:7 + mucin	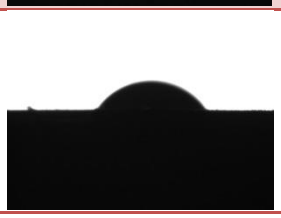		E-3:7 + mucin	

Appendix 2. Droplet images of different oil content BLG-stabilized emulsions - with/without mucin solution on different surfaces during contact angle measurements

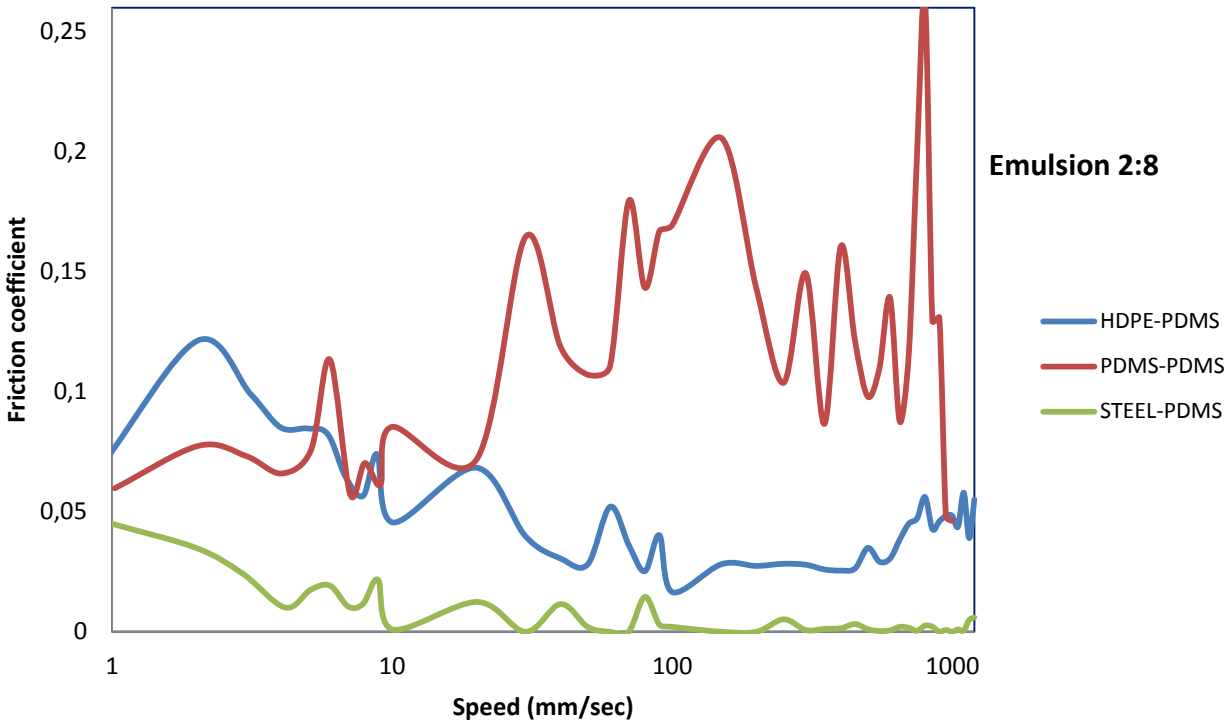

Appendix 3. Speed dependent friction coefficient measurement of emulsion 2:8 - with/without mucin with Mini Traction Machine (MTM) by comparing different tribopairs under 2 N load

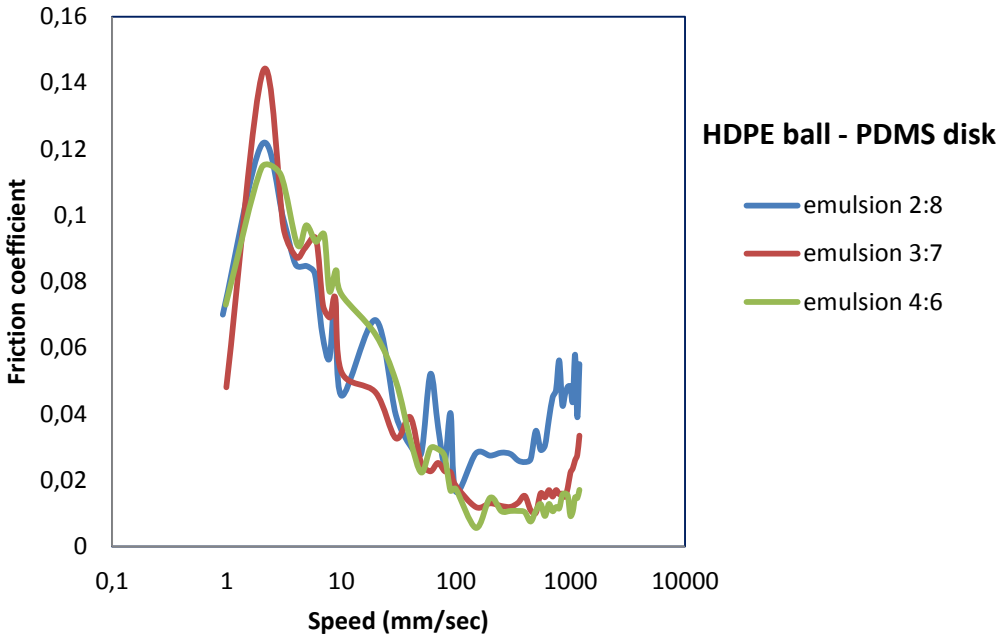

Appendix 4. Speed dependent friction coefficient measurement of emulsions 2:8, 3:7, and 4:6 with oil content of 20%, 30%, and 40%, respectively with Mini Traction Machine (MTM) using HDPE ball and PDMS disk under 2 N load